DISS. ETH NO. 29306

Economic Development, Risk Management, and Climate Policy

A thesis submitted to attain the degree of
Doctor of Sciences
(Dr. sc. ETH Zurich)

presented by
CLÉMENT RENOIR

Master Models and Methods of Quantitative Economics (QEM),
Université Paris 1 Panthéon-Sorbonne,

born on 16.11.1994,

accepted on the recommendation of
Prof. Dr. Lucas Bretschger
Prof. Dr. Antoine Bommier

2023

Acknowledgments

I want to start by thanking my supervisor Prof. Dr. Lucas Bretschger, for allowing me to pursue this degree. He offered excellent working conditions, support, and research opportunities. I am also grateful to my co-examiner Prof. Dr. Antoine Bommier, for the time he devoted to my thesis and to Prof. Dr. Hans Gersbach for chairing my defense committee. I also thank Prof. Dr. Lint Barrage, who kindly invited me to visit the University of California Santa Barbara during Spring 2022.

I also thank my co-authors: Alexandra Brausmann, Lucas Bretschger, Jere Lehtomaa, Alena Miftakhova, and Aleksei Minabutdinov, for all their support, discussions, and patience. I am grateful to them as they helped me grow as a researcher; I wish them the success they deserve.

It is time to thank my friends who supported me in this adventure. I thank Leonard, Loris, Ouriel, and Valentin for their regular visits and continuous support from abroad. I thank Elisa, Emanuele, and Sara for their warm welcome in Zürich. Again, I thank Alena, Aleksei, and Jere, together with Chiara, Florian, Noe, Vanessa, and Veronika, for their friendship and support in and out of the office. I am also grateful for the help and support from all the other researchers I met at the Chair of Economic and Resource Economics. At last, thank you, Beatrice, for your endless support and the strength you give me daily.

Clément Renoir
Zürich, April 2023

Je dédie cette thèse à ma ma famille, pour son soutien indéfectible.

Contents

List of Figures

List of Tables

Thesis Summary

This thesis uses numerical, statistical, and theoretical approaches to explore the relationship between economic development, risk management, and climate policy. It identifies and quantifies some of the risks of economic development. It provides insights into how countries can develop and implement policies that support growth, mitigate risks, and contain climate change. Ultimately, this research contributes to the global conversation on achieving sustainable and inclusive economic development in the face of climate change and other environmental challenges.

The first chapter introduces the themes of the thesis. It takes a historical approach to economic development from before the industrial revolution to today. This chapter leads us to assess the risks and benefits from economic development and question the balance between economic development and the externalities it creates. It also proposes prospects of future growth with climate and environmental policies.

The second chapter presents a new framework for estimating the long-run economic impacts of natural disasters. The approach combines a disaster impact model with a general equilibrium model. This chapter focuses on the effects of tropical cyclones in the United States, the Caribbean islands, Japan, China, and the Philippines. Results show that the post-disaster recovery after a single shock can take several decades, with notable cumulative adverse effects for frequently affected regions. This chapter also shows extensions of the model with two additional scenarios. The first scenario considers endogenous economic productivity gains from specialization, and the second scenario includes climate change that alters the intensity and frequency of future disasters. The extensions modify the quantitative results but do not change the qualitative conclusions.

The third chapter examines the macro drivers of adaptation to river flood risk

worldwide. It is the first study to use the sub-national features of a publicly available database on disasters in combination with the output of a global hydrological model measuring river flooding. The chapter specifies adaptation by estimating the elasticity of damages and fatalities to income, population density, and long-run average flood depth in the areas affected. The analysis concludes with evidence of adaptation as income and population density increase. But results also show recurring signs of maladaptation to intense and less frequent events. Policymakers may be interested in identifying such vulnerability in light of climate change.

The fourth chapter explores the risk and management of chain disasters. Following the recent COVID-19 pandemic, governments worldwide implemented disaster mitigation efforts only after the gravity of the pandemic became evident instead of taking preventive measures ahead of time. The chapter questions the optimality of such a "reactive" approach to disaster management by studying disaster prevention and growth policies in an environment where a primary economic shock may provoke future calamities through contagion effects. It exposes a novel dynamic stochastic framework where disasters follow a Hawkes process. The best policy response, which devotes a stochastic fraction of the output to disaster mitigation, is an increasing function of the Hawkes intensity and essentially tracks disaster arrivals. The latter implies that the optimal policy is indeed reactive.

The fifth chapter studies the role of the anticipation of climate policies on equity and economic growth in a numerical model of general equilibrium. The presence of an anticipation period allows the agents to adjust their choices before policy implementation. This period might change the equilibrium dynamics and impact the redistribution of wealth in the economy. In this chapter, the Swiss economy is a basis to exemplify and analyze these anticipation effects. The economy's supply side adjusts by redirecting the investments to "cleaner" sectors with a lower tax burden and higher profitability. On the demand side, welfare impacts by households vary according to their principal source of income. Households with a high share of their income from capital rents benefit more from the policy's announcement than others. The main conclusion of the chapter is that for the most stringent climate policies, the effect of anticipation is strongly positive but also regressive.

Résumé

Cette thèse utilise des méthodes numériques, statistiques et théoriques afin d'explorer les relations entre le développement économique, la gestion des risques et la politique climatique. La thèse identifie et quantifie certains des risques liés à la croissance économique et donne un aperçu de la manière dont les pays peuvent élaborer et mettre en œuvre des politiques qui soutiennent le développement tout en atténuant les risques qui y sont liés, l'un d'entre eux étant le changement climatique. En fin de compte, cette recherche contribue au débat sur la réalisation d'un développement économique durable et inclusif face au changement climatique et autres défis environnementaux.

Le premier chapitre présente les thèmes de la thèse. Il adopte une approche historique du développement économique, revenant brièvement sur les conditions de vie et de production avant la révolution industrielle, jusqu'à aujourd'hui. Ce chapitre nous amène à évaluer les risques et les bénéfices du développement économique et à nous interroger sur l'équilibre entre ce dernier et les externalités qu'il engendre. Ce chapitre propose également des perspectives de croissance future avec des politiques climatiques et environnementales.

Le deuxième chapitre présente un nouveau cadre pour l'estimation des impacts économiques à long terme des catastrophes naturelles. L'approche combine un modèle d'impact des catastrophes naturelles et un modèle économique en équilibre général. Ce chapitre se concentre sur les effets des cyclones tropicaux aux États-Unis, dans les îles des Caraïbes, au Japon, en Chine et aux Philippines. Les résultats montrent que la reprise économique suite à une catastrophe naturelle peut prendre plusieurs décennies. Les effets négatifs sont d'autant plus notables qu'ils s'accumulent dans les régions fréquemment touchées. Ce chapitre présente également deux extensions possibles à la nouvelle méthodologie présentée. La première exten-

sion consiste à prendre en compte les gains de productivité économique endogènes résultant de la spécialisation de la production. La seconde extension inclut le changement climatique dans l'analyse, ce qui modifie l'intensité et la fréquence des catastrophes futures. Ces possibles apports modifient les résultats quantitatifs mais ne changent pas les conclusions qualitatives établies plus tôt dans le chapitre.

Le troisième chapitre examine les moteurs macroéconomiques de l'adaptation au risque d'inondation fluviale dans le monde. Il s'agit de la première étude à utiliser les caractéristiques infranationales d'une base de données publique sur les catastrophes naturelles en combinaison avec les résultats d'un modèle hydrologique mesurant les inondations fluviales à travers le monde. Ce chapitre identifie l'adaptation en estimant l'élasticité des dommages et des décès par rapport au revenu, à la densité de population et à la profondeur moyenne des inondations dont les zones touchées font face sur long terme. Les résultats de l'analyse montrent des preuves d'adaptation à mesure que le revenu et la densité de population augmentent. Mais les résultats montrent également des signes récurrents d'inadaptation aux événements intenses et moins fréquents. Les conclusions de l'étude indiquent qu'il serait judicieux pour les décideurs publics de se pencher sur cette vulnérabilité aux évènements intenses qui sera d'autant plus mise en lumière par le changement climatique dans les années qui viennent.

Le quatrième chapitre explore la gestion du risque de catastrophes en chaîne. Suite à la récente pandémie de COVID-19, les gouvernements du monde entier n'ont mis en œuvre des mesures d'atténuation de la pandémie qu'une fois que la gravité de cette dernière est devenue évidente, plutôt que de prendre des mesures préventives plus importantes durant les mois et années qui précédaient. Ce chapitre questionne l'optimalité d'une telle approche "réactive" de la gestion des catastrophes en étudiant les politiques de prévention des catastrophes et de croissance dans un environnement où un choc économique primaire peut provoquer de futures calamités par effet de contagion. Pour ce faire, ce travail présente un nouveau cadre dynamique stochastique dans lequel les catastrophes suivent un processus de Hawkes. La meilleure réponse en termes de politique publique consacre une fraction stochastique de la production à l'atténuation des catastrophes. La politique d'atténuation est une fonction croissante de l'intensité du processus de Hawkes et suit essentiellement l'arrivée des catastrophes. Cela implique que la politique optimale est effectivement

réactive.

Le cinquième chapitre étudie le rôle de l'anticipation des politiques climatiques sur l'équité et la croissance économique dans un modèle numérique d'équilibre général. La présence d'une période d'anticipation permet aux agents d'ajuster leurs choix avant la mise en œuvre de la politique. Cette période peut modifier la dynamique de l'équilibre et avoir un impact sur la redistribution de la richesse dans l'économie. Dans ce chapitre, l'économie suisse sert de base pour illustrer et analyser ces effets d'anticipation. L'offre de l'économie s'ajuste en réorientant les investissements vers des secteurs plus "verts" où la charge fiscale est plus faible et la rentabilité plus élevée. Du côté de la demande, l'impact sur le bien-être des ménages varie en fonction de leur principale source de revenus. La principale conclusion de ce chapitre est que pour les politiques climatiques les plus strictes, la période d'anticipation contribue à améliorer le bien-être des ménages ; cependant elle bénéficie d'avantage aux ménages les plus riches pour lesquels la majeure partie des revenus provient du capital.

Chapter 1

Introduction

For thousands of years, income per capita and population remained relatively constant. Yearly population growth rates were between null and 0.09% worldwide between year 0 and 1000 (Common Era). GDP per capita grew by at most 0.01% yearly during the same period. Between the year 1000 and 1820, annual average compound growth rates of population and GDP per capita were about 0.17% and 0.05% respectively (Maddison, 2001).

During these times, famine was a regular concern for most people. Mistakes in land and crop management or bad weather could quickly lead to starvation. In Finland, a famine caused by weather conditions in the years 1694-1697 killed 25-33% of the population. The granaries in France were empty in 1694 due to consecutive poor harvests, leading to the death of about 2.8 million people, or 15% of the population (Neumann and Lindgrén, 1979). Historians even speculate that poor harvests due to a drought in 1788 in France contributed to the French Revolution (Neumann, 1977). The vulnerability of agriculture to weather and the exposures to famine were in part due to the little technological and methodological means of the time. Sée (1958) reports about french farms: "The farm buildings were poorly arranged, and the implements were unsatisfactory and quite primitive, being hardly superior to those employed during the Middle Ages. Intensive cultivation was practically unknown everywhere."[1]

After the famine, infectious diseases and plagues were the second great enemy

[1] In Greenlaw (1958, p. 51-52).

of humanity. The Black Death began in the 1330s in central or east Asia, spread through rats and fleas, and quickly reached Europe, Africa, and the rest of Asia. It arrived in Europe in the Mediterranean area around the 1350s. Historians estimate the mortality rate from the Black Death and its collateral effects to be about 60% of the European population, some 50 million people, with a lethality rate, the proportion of those who died after contracting the virus, of 80% (Benedictow, 2004). Many other disastrous epidemics affected America, Australia, and the Pacific islands when European explorers and settlers discovered these territories. Smallpox, measles, typhus, cholera, tuberculosis, syphilis, and flu, killed tens of millions of people native to these territories and who had no immunity (Crosby, 2003; Nunn and Qian, 2010).

The Spanish Flu pandemic of 1918 was particularly devastating, killing between 50 and 100 million people worldwide in about a year (Taubenberger and Morens, 2006). The flu was carried worldwide on boats loaded with food and commercial goods. Soldiers in the trenches of northern France were amongst the first Europeans to succumb to the virus, brought to Europe in Brest, one of the main ports of France serving the needs of the war (Patterson and Pyle, 1991; Potter, 2001). In comparison, the First World War killed about 20 million people from 1914 to 1918 (Héran, 2014). The global spread of the Spanish flu was much faster than previous epidemics, aided by the greatly enhanced pace and volume of human movement of the last decades (Patterson and Pyle, 1991).

The industrial revolution triggered a rapid change in manufacturing organization, science, and innovation, fundamentally transforming human societies. It began in England in the late 1700s and spread worldwide, flaring economic growth and urbanization. The economic growth that accompanied the industrial revolution also brought about population growth. The worldwide annual average compound growth rates of population and GDP per capita reached 0.98% and 1.21% respectively, between 1820 and 1998 (Maddison, 2001). Population growth initially posed a problem, as some feared that the world would be unable to feed the growing population. The Malthusian school of thought, named after economist Thomas Malthus, predicted that population growth would outstrip the food supply, leading to widespread famine and poverty (Malthus, 1798). However, they were proven wrong by technological progress, which enabled more efficient and productive agri-

culture, among other advancements. The shift from an agricultural to an industrial economy significantly increased productivity and efficiency as machines replaced manual labor (Maddison, 2001). The invention of the steam engine, for example, revolutionized transportation and manufacturing, allowing goods to be produced faster and transported more easily.

According to the unified growth theory, the transition from economic stagnation to growth is an inevitable consequence of the development process (Galor and Weil, 1999, 2000; Galor and Moav, 2002; Galor, 2005a). This transition stems from the interaction between the level of technology and the size and composition of the population, which accelerates technological progress and increases the importance of human capital in production. During the second phase of industrialization, the demand for human capital increased, leading to improvements in human capital formation and the beginning of the demographic transition. The increase in the population's level of education led to significant technological advances and reduced fertility rates and population growth. As a result, economies have allocated more of the benefits of factor accumulation and technological progress to per capita income growth rather than population growth (Galor, 2005b).

The technological revolution and the increase in per capita income that accompanied it brought significant progress in reducing the incidence of famine and other food-related issues. The growth of global trade networks has allowed the distribution of food and other resources to areas that otherwise lack access to them. Despite progress since the industrial revolution, hunger, and malnutrition remain prevalent issues in many parts of the world. But political instability, bad governance, and conflict became the main factors contributing to these problems, not weather (Sen, 1982; Macrae and Zwi, 1992; Devereux, 2009).

The growing interconnected nature of the world, the growing population, and the growing population concentration should have increased the frequency and intensity of epidemics. Yet, the deaths from infectious diseases have dropped since the Spanish flu, especially in rich countries and for vaccine-preventable diseases (Roush et al., 2007; Andre et al., 2008; van Wijhe et al., 2016). The technological progress in the continuity of the industrial revolution also brought tremendous achievements in medicine during the 20^{th} century. We now have the vaccination, antibiotics, hygiene norms, and better medical infrastructures. In the United States, Roush et al. (2007)

show a greater than 92% decline in cases and a 99% or greater decline in deaths due to diseases prevented by vaccines recommended before 1980 for diphtheria, mumps, pertussis, and tetanus. Smallpox has been eradicated worldwide (Fenner et al., 1988), substantial progress has been made in measles elimination (Andre et al., 2008), and a large part of the reduction in childhood mortality is attributed to the successful prevention of infectious diseases (van Wijhe et al., 2016).

The COVID-19 pandemic that began in 2020 reminded us of our vulnerability to infectious diseases; it caused significant disruptions to daily life and posed significant challenges for healthcare systems worldwide. For many, it also sounded like an alarm concerning the externalities generated by the economic development of the last 200 years, shedding light on the impact of human activity on ecosystems.

The Anthropocene is a term used to describe the geological age in which humans significantly impact the Earth's climate and biodiversity. Though there had already been ecological evolution and epoch changes, they were caused by natural forces such as tectonic plate movement, volcanic eruptions, and asteroid collisions (Lewis and Maslin, 2015). Over the past 300 years, over 85% of the planet's wetlands have been lost, mainly through drainage and land conversion (United Nations, 2022). Wildlife populations are also drastically declining. Since 1970, and despite growing ecological awareness, monitored populations of vertebrates (mammals, birds, amphibians, reptiles, and fish, 32,000 species in total) have seen a devastating 69% drop according to World Wildlife Fund (Almond et al., 2022). These changes are primarily due to humanity's impact on the global ecology, making it the single most important agent of change (Lewis and Maslin, 2015). Nowadays, there are about 200,000 wild wolves on Earth for 900 million dogs; less than 40,000 lions compared to 600 million cats; 600,000 African buffalo versus 1.5 billion cattle; 37.2 billion chickens for 50 billion wild birds (and at current trends, the total number of poultry will soon exceed the total number of wild birds (Morand, 2022)).[2] Although it is uncertain when the Anthropocene began, and the term still needs official recognition, there is little doubt that we are now fully entrenched in it (Lewis and Maslin, 2015).

[2]For the dogs, see Gompper (2014) and Lescureux and Linnell (2014); for cats, see https://www.worldatlas.com/; for wolves and lions, see Ripple et al. (2014); for the number of African buffaloes, see Cornélis et al. (2014); for the number of birds in the world, see Callaghan et al. (2021); for the cattle and chickens, see Morand (2022); I follow the insightful comparisons made by Harari (2016).

The significant increase in the utilization of fossil fuels since the industrial revolution slowly but surely led to the present-day climate predicament (Bernstein et al., 2008; Pachauri et al., 2014; IPCC, 2023). The ramping global warming prompts the question of whether we are observing the emergence of a new form of Malthusianism. The atmosphere's limited capacity to absorb emissions would replace the agricultural capabilities as the limiting factor in a Malthusian model. If there are no measures to decouple carbon emissions from economic development, there will be an escalation in climate-related harm and significant adverse environmental impacts (Bretschger, 2020).

Human-driven environmental changes bring back issues we thought humanity had solved, such as vulnerability to climate hazards and epidemics. In the foreword of the recent United Nations report taking stock of the advances to meet the sustainable development goals (SDGs), the Secretary-General of the United Nations declares:[3]

> As the world faces cascading and interlinked global crises and conflicts, the aspirations set out in the 2030 Agenda for Sustainable Development are in jeopardy. With the COVID-19 pandemic in its third year, the war in Ukraine is exacerbating food, energy, humanitarian and refugee crises—all against the background of a full-fledged climate emergency.

Before adding:

> [C]limate change [...] acts as a "crisis multiplier" [...] whose impacts are already being felt across the globe. Increased heatwaves, droughts and floods are affecting billions of people worldwide, contributing further to poverty, hunger and instability.

Already today, the impact of climate change on droughts, floods, and heatwaves, is causing additional strain on food production in numerous parts of the world. Several regions in Africa and Central and South America are already grappling with heightened, occasionally severe, food insecurity and malnutrition due to floods and droughts (United Nations, 2022). Additionally, ocean warming and acidification have negatively impacted food production from fisheries and shellfish aquaculture

[3]In the Sustainable Development Goals Report 2022 (United Nations, 2022).

in some oceanic regions (IPCC, 2023). The achievement of zero hunger by 2030, one of the 17 SDGs objectives, is being hindered by various factors such as climate variability and extremes, conflict, economic shocks, and increasing inequality. The number of individuals experiencing food insecurity and hunger has been rising since 2014 (United Nations, 2022; IPCC, 2023). Already today, the recent publication by the Intergovernmental Panel on Climate Change (IPCC, 2023) reports an increase in the occurrence of climate-related food-borne and water-borne diseases and the incidence of vector-borne diseases due to increases in extreme heat events.

The pace of progress and economic growth has put humankind in a double race between achieving middle-class standards of living for everyone and avoiding ecological collapse. This race becomes more challenging each year as bringing the world's poor closer to the American dream simultaneously pushes the planet toward the brink (Harari, 2016). Limiting the temperature increase to 1.5°C, as set in the Paris Agreement, requires rapid reductions in global emissions and reaching net zero by 2050. Yet, studies indicate that at current greenhouse gas emission rates, the remaining carbon budget for meeting the 1.5°C target will deplete before 2030. At current rates, we would also exhaust more than a third of the remaining carbon budget for a 2°C warming target (IPCC, 2023).

Tomorrow, as global temperatures continue to rise, the risks associated with climate change will become more intricate and challenging to handle. Various climatic and non-climatic risk factors will intertwine, leading to an overall increase in risk, with risks cascading across multiple sectors and regions. Global warming is expected to cause more powerful cyclones, greater coastal storm surges, and increased frequency and severity of flooding (Pörtner et al., 2022). In 2050, there could be additional 31-450 million people, 59 to 430 thousand km^2 of cropland, and between -9 and +376% of asset value exposed to river flood risk (Arnell and Gosling, 2016). By 2100, yearly mean damage from cyclones in the Philippines may increase by 126%, decrease consumption by 6%, and welfare by 4%, compared to a scenario without climate change (Lehtomaa and Renoir, 2023).

Climate-induced food insecurity and supply instability are also expected to rise as global temperatures increase, further amplified by non-climatic risk factors such as competition for land between urban expansion and food production, pandemics, and conflict (IPCC, 2023). Hasegawa et al. (2018) estimate the population at risk of

hunger in 2050 may increase by 24-100 million depending on warming and mitigation policies.[4]

Using recent estimates of the rate of increase in disease emergence from zoonotic reservoirs associated with environmental change, Marani et al. (2021) estimate the yearly probability of occurrence of extreme epidemics, such as COVID-19, can increase up to threefold in the coming decades. In the absence of CO_2 emission reductions, warming temperatures could expose an additional 76 million people to malaria transmission in Eastern and Southern Africa by the year 2080 (Ryan et al., 2020) and more than 1.3 billion new people worldwide to Zika virus risk by 2050 (Ryan et al., 2021).

Managing the double race requires a balance between economic growth and environmental concerns. Humanity risks financial ruin, political turmoil, and a fall in living standards if we don't find the right balance (Harari, 2016).

Economists have a role in finding solutions to the challenges of the Anthropocene. Our task is to identify and promote the conditions under which the interdependence of population, resources, and technology produces a transition from unsustainable resource-based economic development to sustainable knowledge-based growth (Bretschger, 2020; Peretto, 2021). We must look for ways to implement effective and equitable strategies and policies that can help mitigate the impact of human activities on the environment. The consequences of climate change and biodiversity loss will affect the poor more than the rich, even though the latter caused the problem (IPCC, 2023). We must develop risk management strategies and climate policies that promote social justice and equity.

Economic analysis and policies may also help find adaptation solutions to extreme heat and weather events, for example. The IPCC (2023) identifies as critical barriers to adaptation the limited amount of resources, lack of private sector and citizen engagement, insufficient mobilization of finance, low climate literacy, lack of political commitment, limited research, slow and low uptake of adaptation science, and low sense of urgency. Taxes, fees, tradable permits, insur-

[4]Hasegawa et al. (2018) even highlight the potentially increased risk of food insecurity due to climate mitigation. Despite moderate climate change, the increased food prices and decreased food consumption due to climate policies may outweigh the risk of hunger from crop yield declines without any climate policy. They use this result to stress the importance of carefully designing emissions mitigation policies.

ance schemes, environmentally-motivated subsidies, consumption and production nudges, and payments for environmental services schemes are all part of the economists' toolkit to promote long-term planning and implementation of adaptation actions.

These are daunting tasks, but it is critical for the survival of numerous species on the planet and the well-being of future generations. This thesis contributes to the global conversation on achieving sustainable and inclusive development and developing effective risk management strategies and policies in the face of climate change and other environmental challenges.

Outline of the thesis

This thesis consists of four research essays, all linked to the theme of economic development. The first two chapters relate to natural catastrophes, which may intensify due to the changing climate. The third chapter links the catastrophes literature and policy recommendations for risk management. It introduces the issue of the risk of chain disasters. The fourth and last chapter focuses on one type of policy: the carbon tax. In what follows, I present the main research questions and methods used in each chapter.

The economic impact of tropical cyclones

In Chapter 2, Jere Lehtomaa and I develop a framework for estimating the long-term impact of natural disasters.[5] We apply our methodology to study the impact of tropical cyclones on economic growth and welfare.

Our approach involves incorporating tools from both economics and climate science literature. Initially, we utilize a probabilistic model to assess the direct annual losses incurred by regional capital stocks resulting from natural disasters. These estimates integrate capital depreciation's calibration in a multi-sectoral, dynamic general equilibrium growth model. Using this economic model, we analyze the components of GDP, such as investments, consumption, import, and exports, to evaluate tropical cyclones' short-term and long-term effects on economic growth.

[5]Both authors contributed equally to the chapter.

By combining both models, we can provide globally consistent damage estimates for cyclones and generate new insights into their long-term general equilibrium impact on economic growth.

We collect data from various sources, including satellite data for modeling the cyclones' tracks and satellite imagery for estimating the spatial distribution of exposed assets based on nighttime light intensities. We calibrate the economic model with the Global Trade Analysis Project dataset. It provides a sectoral decomposition of economic activities, and bilateral trade flows for 129 world regions. We focus our analysis on the USA, the Caribbean islands, Japan, China, and the Philippines. These regions are regularly exposed to tropical cyclones and show considerable heterogeneity in size, economic structure, and overall cyclone exposure.

Our results highlight the dissimilarity between cyclone impacts on GDP and welfare. Since consumption is our model's sole determinant of welfare, the GDP changes alone fail to capture cyclones' full welfare effect. GDP, in this case, masks the opposite impacts cyclones have on individual GDP components, producing artificially small aggregate changes.

Since our analysis is on the long-run quantification of the effect of tropical cyclone shocks on the economy, we also consider i) the underlying mechanisms of economic growth and ii) climate change. The general equilibrium model allows us to consider growth dynamics based on either physical capital accumulation or knowledge creation with endogenous productivity gains from specialization. Compared to physical capital accumulation, the knowledge-based growth engine dampens the negative cyclone impacts due to higher productivity and additional incentives for investing in new capital varieties. Under this growth specification, in extreme cases, cyclones' long-run effect on GDP can even become positive due to very high investment levels. Finally, to study the role of climate change on future cyclone intensity and frequency, we recalibrate the regional cyclone damage distributions to simulate cyclone damage under two Representative Concentration Pathway (RCP) scenarios: RCP4.5 and RCP8.5.

Global adaptation to river flood risk

Chapter 3 is a single-author work.[6] I use statistical and geographic information system (GIS) methods to examine the factors that drive adaptation to river flood risk through a quantitative analysis of the damages and fatalities caused by individual river floods worldwide. The analysis is conducted at a sub-national level, focusing on three key dimensions: population concentration, GDP per capita, and flood experience of affected locations.

This approach identifies the macro drivers of adaptation to river floods by addressing three sub-questions. The first sub-question investigates whether wealthy areas experience fewer fatalities and damages than poor ones, given, for example, their potential access to better prevention and emergency plans, building standards, and river and sewage management. The second sub-question examines whether dense areas react differently to river floods than sparse areas. The difference may arise because of factors such as access to hospitals and the impact of population concentration on water evacuation, for example. The third sub-question investigates whether long-term flood exposure facilitates better preparation for this risk. Intuitively, regularly exposed areas may benefit from regular investment in protection measures. But they may also suffer from warning fatigue and over-reliance on a state or public insurance.

This study primarily uses two sources of data. On the one hand, the Inter-Sectoral Impact Model Intercomparison Project (ISIMIP2a) provides long-term flood exposure data. Such data is derived by reconstruction from reanalysis data, processed by global hydrological models that estimate river flooding. On the other hand, data that combines information on the flood type (e.g., coastal, flash, or river flood) and fatalities and damages caused by each flood is publicly available in the EM-DAT database. This chapter connects data on deaths, damages, disaster intensity, and the location of river floods with GDP, population, and long-term flood exposure data from 1,800 administrative regions globally from 1980 to 2020.

This chapter highlights the crucial role of long-term flood exposure in shaping adaptation capacities. Although regions are adapting to the risk of fatalities and

[6]This work is part of a project that has received funding from the European Union's Horizon 2020 research and innovation programme under the Marie Skłodowska-Curie grant agreement No. 870245.

damages caused by low-intensity floods, I have found that they exhibit maladaptation to rare and intense floods. This maladaptation to high-intensity, low-frequency floods is observed in both affluent and impoverished areas concerning the risk of fatalities. This analysis also reinforces the evidence of global adaptation to river flood risk as economies become wealthier. Yet, GDP per capita is less critical for the adaptation to the fatality risk of flooding in high-income provinces, which may induce a convergence in vulnerability between high and low-income regions. Additionally, when comparing adaptation between rural and urban areas, the findings suggest that, on average, urban areas experience roughly two times as many fatalities and four times as much damage as rural areas.

Managing the risk of chain disasters

Chapter 4 is a theoretical work in collaboration with Alexandra Brausmann, Aleksey Minabutdinov, and Lucas Bretschger.[7] An essential concern for policymakers is how a government should handle the prospect of disasters that could trigger cascades of economic shocks, significant financial losses, and hindrances to growth and development. Specifically, what are the most effective policies to mitigate disasters in the presence of contagion effects? In this study, we address these and comparable inquiries using a new approach that enables us to introduce contagion effects explicitly into a stochastic and dynamic macroeconomic framework.

One notable aspect of large-scale interconnected disasters that remains undiscovered in the literature is that measures aimed at mitigating their effects tend to have a reactionary rather than a preventive character. The recent COVID-19 pandemic provides an excellent example of this phenomenon. Although many countries had legislation requiring sufficient medical supplies to be in stock for emergencies such as a pandemic, when the pandemic occurred, even basic equipment such as surgical masks, protective suits, and hospital beds were in short supply. This outcome raises questions about whether incurring sunk costs to keep equipment stocks and maintain additional intensive care units as a precaution was justifiable, given the low historical probability of a pandemic. Nevertheless, once the pandemic occurred,

[7] My contribution was conceptualizing the research question, the first modeling and solution attempt, and drafting the work.

governments sometimes took draconian measures to contain the virus's spread, such as travel restrictions, multiple lockdowns, school closures, and business failures. As a result, governments worldwide had to deploy substantial financial aid packages to support at least parts of the population. For example, in Wuhan, China, the authorities built an entire hospital for up to 1000 patients in ten days. In 2020, China alone increased mask production by a staggering 450% compared to 2019.

We address the questions above and emphasize the complex and long-term nature of the issue by constructing a general equilibrium growth model that considers multiple interconnected risks. The model allows for endogenous investment decisions to accumulate a productive input such as capital, which is subject to damages from randomly occurring disasters. Additionally, one disaster may lead to a cascade of interlinked disasters, producing a contagion effect. We introduce contagion effects into the model through Hawkes processes, which have a self-exciting mechanism. The negative externality generated by economic activity, such as carbon emissions or intensive food production, exacerbates the damages caused by a disaster. To reduce the losses, society must allocate part of its output to mitigation measures, such as emissions reduction for climatic disasters, vaccination and healthy living promotion for health crises, or reserve requirements and incentive alignment for financial crises.

Our main result is that the presence of contagion among disasters calls for a specific type of disaster-management policy. Unlike the existing literature that assumes independent shocks, we find that the optimal mitigation propensity is not constant but stochastic, tracking the disaster arrivals. This result is consistent with the reactive policies observed during pandemics and major disaster-relief programs.

The anticipation of a climate policy

Chapter 5 is co-authored with Alena Miftakhova.[8] This chapter examines the repercussions of anticipating the carbon tax of various stringency levels for the Swiss economy in a numerical model of general equilibrium. Initially, we execute the typical expectation situation, in which the policymaker declares the carbon tax ahead

[8]Both authors contributed equally to the chapter. We gratefully acknowledge financial support from the Swiss Federal Office of Energy.

of its execution. Then, we replicate an unforeseen situation where members of the economy cannot adapt to the forthcoming carbon tax, as if no prior announcements had been made. In both the expected and unexpected scenarios, the policy objective (the cap on carbon emissions) is the same. Subsequently, we contrast the outcomes from the two situations and ascribe any disparities to the influence of anticipation.

To our knowledge, our research is the first examination of policy anticipation's impact on economic growth and the well-being of diverse households. Our findings indicate that the anticipation phase influences investment choices and that anticipating the carbon tax triggers early divestment from fossil fuels. Consequently, these decisions affect sectoral and overall growth and households' preferences regarding labor supply and consumption growth rates.

Policy announcements enable economic actors to align their investment decisions accordingly and reduce future compliance costs with the policy. However, our research reveals that the degree to which individuals can take advantage of early capital reallocation is not uniform and depends on their involvement in the capital market. Individuals who possess the majority of the capital in the economy and receive a large portion of their income from capital rents benefit the most from investment reallocation. Conversely, other individuals who rely primarily on labor income and government transfers must adjust their consumption and labor decisions to confront the new market circumstances. Therefore, an anticipation period has a regressive impact, regardless of the policy target's severity. The regressive effect of anticipation intensifies as the policy's stringency increases.

This chapter also explores the impacts of stringent climate policies on the economy's path to decarbonization. We simulate carbon emissions policies that target CO_2 up to 95% reductions from its current level by 2050. Our findings indicate that the policy's stringency has a non-linear impact on anticipation dynamics, both quantitatively and qualitatively. At a low carbon reduction target, households' consumption-smoothing precedes their consumption-investment decisions and negatively affects aggregate long-term welfare. In anticipation of more stringent carbon policies, the agents more actively redistribute their investments beforehand and achieve a more profitable allocation under the upcoming policies. Thus, the given opportunity to adjust in advance turns out beneficial on the aggregate level. But, due to the inherent inequality of the anticipation effect, wealthy households

that own most capital benefit more from the adaptation opportunity than poorer households.

Chapter 2

The Economic Impact of Tropical Cyclones: Case Studies in General Equilibrium[1]

Abstract

We present a new framework for estimating the long-run economic impacts of natural disasters. Our approach combines a disaster impact model with a general equilibrium model of the economy. We apply the methodology to study the effects of tropical cyclones in the United States, the Caribbean islands, Japan, China, and the Philippines. Our results show that the post-disaster recovery after a single shock can take several decades, with notable cumulative negative effects for frequently affected regions. For instance, cyclone activity reduces long-run aggregate consumption between 0.3 - 22 %, depending on the region. To evaluate the robustness of our results, we extend the model with two additional scenarios. First, we consider endogenous economic productivity gains from specialization. Second, we add a scenario where climate change alters the intensity and frequency of future disasters. The extensions slightly modify the numerical results but do not change the qualitative conclusions.

[1]This chapter is joint work with Jere Lehtomaa. This chapter is reprinted with minor edits from Lehtomaa and Renoir (2023). Lehtomaa and Renoir (2022) presents an overview of the methodology and partial results.

2.1 Introduction

Tropical cyclones are among the costliest natural catastrophe events, causing approximately $50 billion of damage per year on average since the year 2000 (EM-DAT, 2020). In addition to their direct effects through loss of lives and destruction of economic assets, tropical cyclones can permanently shape regional growth dynamics by causing prolonged reconstruction periods (Hsiang and Jina, 2014) and forced relocation (Deryugina et al., 2018). Future cyclone impacts might increase for two main reasons. First, the development of coastal regions increases the exposures (Gettelman et al., 2018). Second, climate change could increase cyclones' intensity and frequency (Masson-Delmotte et al., 2021). Yet, to our knowledge, there are few and sometimes inconclusive quantitative estimates of the general equilibrium dynamics and the long-term effects of cyclones' strikes on economic growth and its determinants.

We present a new framework for evaluating cyclones' effects on economic growth and welfare. We integrate tools from both the economics and climate science literature. First, we employ a probabilistic disaster impact model to quantify the direct annual losses to regional capital stocks using historical and synthetic cyclone tracks (Aznar Siguan and Bresch, 2019). Then, we feed the estimations of capital destruction into a dynamic, multi-sectoral general equilibrium growth model (Bretschger et al., 2017). With the economic model, we track the components of GDP (investments, consumption, import, and exports), explain the short-term, and appraise the long-term impacts of tropical cyclones on economic growth. Combining both models allows us to derive globally consistent cyclone damage estimates, providing new results on cyclones' long-run general equilibrium effects on economic growth.

We gather data from different sources. The disaster impact model uses satellite data from the International Best Track Archive for Climate Stewardship (IBTrACS) database to model the cyclones' tracks (Knapp et al., 2010). We also use satellite imagery for estimating the spatial distribution of exposed assets based on nighttime light intensities (Román et al., 2018). The spatial resolution of the data enables damage estimates on a detailed 10×10 km global grid. We calibrate the economic model with the Global Trade Analysis Project dataset. It provides a sectoral decomposition of economic activities and bilateral trade flows for 129 world regions.

We focus our analysis on the USA, the Caribbean islands, Japan, China, and the Philippines. These regions are regularly exposed to tropical cyclones and show considerable heterogeneity in size, economic structure, and overall cyclone exposure.

In our setting, the immediate economic response after a cyclone strike is a jump in aggregate investments and a consequent drop in consumption to replace the damaged capital stock. Hallegatte and Przyluski (2010) refer to this tradeoff as *"forced investment"* since the reconstruction efforts can spur economic activity while there is still an overall reduction in welfare. Although the reconstruction in our model is relatively quick, it can take several decades to catch up with the benchmark growth path where no shocks occur. For some economic variables, such as the aggregate output and consumption levels, the post-disaster trajectory remains below the reference path for the entire simulation period.

Our results also highlight the dissimilarity between cyclone impacts on GDP and welfare. Whereas the long-run average drop in consumption ranges from 0.3% in the U.S. to more than 20% in the Philippines, the respective GDP reductions are only 0.1% and 6%. Since consumption is our model's sole determinant of welfare, the GDP changes alone fail to capture the cyclones' full welfare effect. GDP, in this case, masks the opposite impacts cyclones have on individual GDP components, producing artificially small aggregate changes (Mohan et al., 2018).

A long-run quantification of the effect of tropical cyclone shocks on the economy ought to take into consideration *i)* the underlying mechanisms of economic growth and *ii)* climate change. The general equilibrium model allows us to consider growth dynamics based on either physical capital accumulation or knowledge creation with endogenous productivity gains from specialization. Compared to physical capital accumulation, the knowledge-based growth engine dampens the negative cyclone impacts due to higher productivity and additional incentives for investing in new capital varieties. Under this growth specification, in extreme cases, cyclones' long-run effect on GDP can even become positive due to very high investment levels. The long-run GDP loss that results from the cumulative effect of thirty years of cyclone activity is, on average, roughly 1.5-3 times smaller when knowledge is the driver of growth.

Finally, to study the role of climate change on future cyclone intensity and frequency, we recalibrate the regional cyclone damage distributions under two Repre-

sentative Concentration Pathway (RCP) scenarios. Under the intermediate RCP4.5 scenario, cyclone intensity increases in the North Atlantic basin (the U.S. Atlantic coast and Caribbean islands) with no changes in event frequency, driving up the total economic losses. On the other hand, cyclone frequency in the Northwestern Pacific basin (Japan, China, and the Philippines) falls with only a slight increase in intensity, leading to lower mean damages at the end of the century. Under the high-emissions RCP8.5 scenario, cyclone damages increase in all considered regions. In the US, for instance, the aggregate capital stock in 2100 under RCP8.5 is approximately 1% lower compared to the same year under constant climate conditions. The Philippines is the most affected region. Climate change could increase consumption losses from cyclones by an additional 11% under such severe warming scenario.

Related literature

The empirical evidence on the link between disasters and economic growth is inconclusive. For instance, Skidmore and Toya (2002) find a positive relationship between climatic disaster frequency and economic growth due to a shift from physical to human capital investments. On the other hand, Hsiang and Jina (2014), analyzing tropical cyclones, finds a negative long-run impact on output and long-run growth with no clear evidence of a rebound effect during the two decades following the catastrophe. Strobl (2012) focus their analysis on the Central American and Caribbean regions and estimate the average hurricane to reduce the output growth rate by roughly 0.84%.

Several works attempt to reconcile the diverging empirical evidence. One explanation is the difference between the *risk* of disasters occurring and the consequences after experiencing a disaster *strike* (Akao and Sakamoto, 2018; Bakkensen and Barrage, 2018). Whereas disaster strikes can cause output losses due to capital destruction and business interruptions, disaster risk might induce higher precautionary savings, thereby inflating the economy's growth rate. However, Douenne (2020) casts doubt on the possible role of precautionary savings in explaining the positive relationship between economic growth and disasters. A positive relationship would require unreasonably high values of intertemporal substitution elasticity and relative risk aversion when calibrating an endogenous growth model with U.S.

data.

Another explanation for the inconclusive empirical findings lies in the relative damages disasters might cause depending on the capital variety. As cyclones are particularly destructive to physical capital, frequent disasters might steer investments towards accumulating human capital instead, thereby enhancing productivity (Skidmore and Toya, 2002; Ikefuji and Horii, 2012; Akao and Sakamoto, 2018). Whether natural disasters mainly affect productive capital stocks or durable consumption goods might also play a role (Strulik and Trimborn, 2019). Losing productive capital harms economic performance, whereas only replacing damaged durable goods can boost output, potentially pushing GDP above the pre-disaster level.

A third possible explanation for positive tropical cyclone impacts is the process of creative destruction. As Akao and Sakamoto (2018, p.90) write, *"By destroying old factories and roads, disasters allow new and more efficient infrastructure to be built, providing an opportunity for the economy to transform itself into a more productive one in the long run."* Older capital vintages might also be more susceptible to disaster damages than newer variants, amplifying the effect (Okuyama et al., 2004). However, much depends on the affected region and the economic sector. For instance, Crespo Cuaresma et al. (2008) find that the creative destruction effect only occurs in sufficiently developed economies. According to Loayza et al. (2012), on the other hand, storms can cause significant damage to agriculture, while capital stock upgrades only boost industrial growth. Other mechanisms might also dampen the productivity gains from creative destruction. For instance, small firms might not afford the business interruptions and worker re-training that are often necessary when replacing lost capital goods with new variants (Hallegatte and Dumas, 2009; Hallegatte and Przyluski, 2010).

Several studies also highlight the role of institutions as a determinant of disaster impacts. Kahn (2005), for instance, finds that countries with higher-quality institutions suffer fewer disaster-related deaths. Education, trade openness, and financial system maturity also matter for disaster resilience (Toya and Skidmore, 2007; Felbermayr and Gröschl, 2013, 2014). The high institutional quality helps endure the initial catastrophe shock and enables faster deployment of resources for reconstruction, thus reducing negative disaster spillovers to the broader economy (Noy, 2009).

Specialized cyclone impact models provide another way to estimate the disasters' long-run economic consequences (Mendelsohn et al., 2012; Gettelman et al., 2018). In particular, future losses might increase as the value of exposed assets goes up with coastal development and as climate change alters the intensity and frequency of disasters. Although rich in spatial detail, these analyses frequently rely on predefined GDP projections to quantify long-term effects. However, as disasters become increasingly harmful, they are more likely to affect consumption, investment patterns, and the underlying growth trajectories. Models featuring fixed economic growth paths cannot – by design – capture these feedback mechanisms.

This chapter contributes to the literature by considering the impacts of cyclone strikes on long-run economic development. Empirical works such as Hsiang and Jina (2014) provide insight into the causal effect of cyclone shocks on GDP. However, they have to deal with several confounding factors and only analyze the effects in partial equilibrium. On the other hand, disaster impact models such as Gettelman et al. (2018) represent cyclone damages in great detail but typically do not capture the economic adjustments over time. Our general equilibrium approach uses the spatial detail of a full disaster impact framework while capturing the endogenous dynamics during the recovery period. All model components rely on global datasets, allowing us to consistently evaluate country-level impacts, incorporating direct damages and the secondary effects through trade linkages. Finally, through changes in a single elasticity parameter, the economic model can also capture different assumptions regarding the underlying determinants of growth, from a standard capital accumulation setting to an endogenous representation where gains from specialization drive growth.

2.2 Methodology

This section describes the disaster impact framework, the economic growth model, and the integration of the two systems. We focus our study on five regions: the US, the Caribbean islands, Japan, China, and the Philippines. These regions are frequently exposed to damages from tropical cyclones and vary drastically in the structure and size of their economies. All model components rely on globally consistent datasets, which makes extending the regional coverage of the analysis straight-

forward.

2.2.1 Disaster impact model

Quantifying the direct disaster impacts requires data describing the exposures (the spatial distribution of vulnerable physical assets) and the hazards (tracks and wind speeds of historical cyclones). We access both datasets and run the analysis using the open-source CLIMADA (CLIMate ADAptation) platform (Aznar Siguan and Bresch, 2019; Bresch and Aznar-Siguan, 2021).

Exposure

To estimate the annual disaster impacts, we first need to construct the spatial distribution of physical assets in all regions of our study. We use the *LitPop* model (Eberenz et al., 2019), which combines nighttime light satellite imagery with gridded population accounts to obtain a globally consistent estimate of the asset distribution.

Satellite imagery is convenient for its public availability, global spatial coverage, and frequent update schedule. Our nighttime light intensity data comes from NASA's Black Marble suite, available at a global resolution of approximately 500 meters (Román et al., 2018). Our base year for the nighttime light data is 2016. However, there are some known caveats in using satellite light intensities as a proxy for economic activity. These include, among others, high measurement errors in luminosity data, saturating pixel values, and bright pixels leaking light into their adjacent pixels, thus inflating their value (Chen and Nordhaus, 2011; Eberenz et al., 2019).

To overcome some of the above issues, the LitPop model supplements the nighttime light data with global population estimates from the Gridded Population of the World database (CIESIN, 2016). The database provides globally disaggregated population counts with a resolution of 1×1 km. We give equal weight to the light intensity (Lit) and population data (Pop) and compute the share of the physical assets (A_i) in each pixel i out of N total pixels for a given country as:

$$A_i = \frac{Lit_i^n Pop_i^m}{\Sigma_i^N (Lit_i^n Pop_i^m)},$$

where m and n denote the tuneable share parameters. We use an aggregated resolution of 10×10 km for the final asset exposures. Since we model cyclone damages as destroyed capital stock, we use the value of the produced capital stock from the World Bank wealth accounts as the region-specific indicator for aggregate physical asset value (World Bank, 2018). Hence, the value of physical capital per land area is the product of the country's total capital stock value and pixel-specific capital share. Figure 2.1 illustrates the resulting distribution of exposed capital stocks for the U.S. state of Florida.

Figure 2.1: Estimated distribution of capital stocks in the U.S. state of Florida

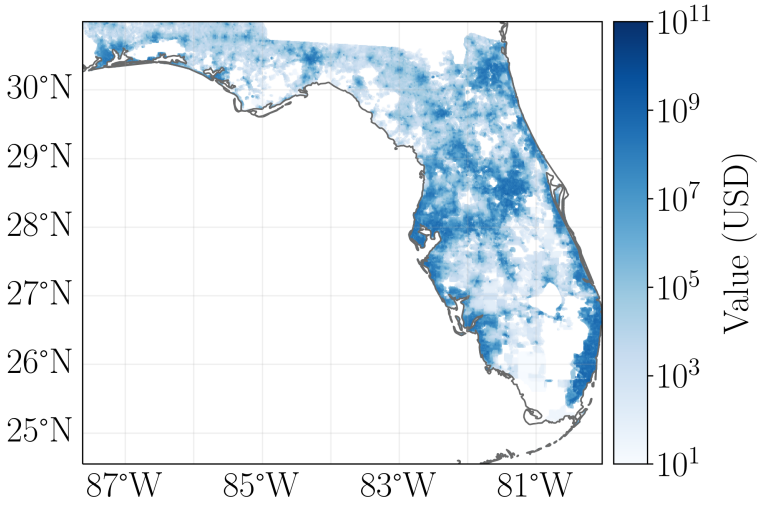

Notes: Each pixel is weighted according to its nighttime light intensity and population density. For each region in our sample, we distribute the aggregate capital stock value according to the pixel-specific shares.

Hazard

Next, we estimate the cyclone damages based on historical cyclone tracks. We obtain the path and the maximum sustained wind speed of each recorded cyclone from 1950 to 2019 from the International Best Track Archive for Climate Stewardship (IBTrACS) database (Knapp et al., 2010). That represents a set of 6,907 tropical cyclone tracks, illustrated in Figure 2.2. Among them, 1,079 happened in the North Atlantic basin (containing the Caribbean islands and the U.S. Atlantic

coast), and 2,040 in the Northwest Pacific Ocean basin (containing Japan, China, and the Philippines). For each historical cyclone in the IBTrACS database, we construct 50 synthetic cyclone tracks that are random walk processes under parameters controlling their distance from the original observations. The synthetic tracks inherit several features from their historical counterparts, such as changes in wind speeds on landfall —which are relevant for the damage computation. These additional synthetic data improve the probabilistic description of the annual cyclone activity compared to using only historical storm tracks. The augmented dataset contains 55,029 and 104,040 events for the North Atlantic and the Northwestern Pacific basin, respectively.

We use maximum wind speed to measure storm intensity as it is a common choice in the literature (Hallegatte, 2007; Pielke Jr., 2007; Narita et al., 2009; Nordhaus, 2010). The storm intensity allows us to construct a proxy for capital destruction caused by each cyclone. We use the damage function from Emanuel (2011) to translate cyclone wind speeds into capital destruction. The fraction of capital damaged by storm j at location i, and time t, $\delta_{i,j,t}$ varies with wind speeds exceeding a threshold value:

$$\delta_{i,j,t} = \frac{v_{i,j,t}^3}{1 + v_{i,j,t}^3}, \tag{2.1}$$

where,

$$v_{i,j,t} \equiv \frac{\max\{V - V_{thresh}, 0\}}{V_{half} - V_{thresh}}. \tag{2.2}$$

Similar to Emanuel (2011), we set the wind speed below which there are no damages at $V_{thresh} = 25.7m/s$. The parameter $V_{half} = 74.7m/s$ determines the wind speed that destroys 50% of the capital stock Sealy and Strobl (2017). We aggregate the output $\delta_{i,j,t}$ by the year of each event j to compute statistics such as the mean and the standard deviation of damage for all regions.

Ultimately, we want to represent cyclone damages as annual economic shocks. Although the synthetic cyclone tracks extend our pool of disaster events, our dataset still only contains estimates for seventy annual cyclone damages (from 1950 to 2019). The small number of data points in our sample may limit us from having a good overview of tropical cyclones' impact on the economy. To overcome this

Figure 2.2: Global tropical cyclone activity for 1950-2019 based on the IBTrACS database

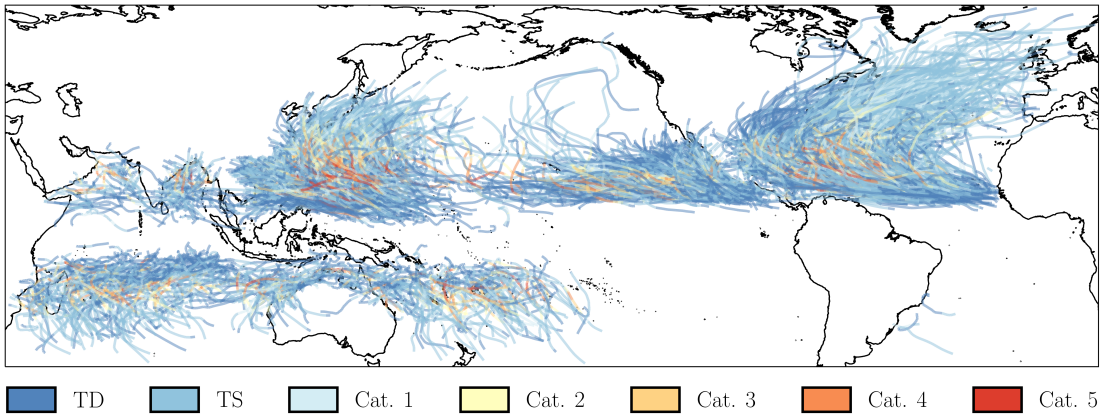

Notes: The intensity levels from lower to higher wind speeds are tropical depression (TD), tropical storm (TS), and hurricanes of category 1 to 5 (Cat. 1-5) on the Saffir-Simpson hurricane wind scale.

limitation, we enlarge our sample on annual damage estimates by creating a set of synthetic years. More specifically, we create 5,000 additional synthetic years of tropical cyclone activity by assuming the disaster frequency to follow a Poisson distribution Emanuel (2013); Bakkensen and Barrage (2018) and then resampling a corresponding number of random events from the collection of synthetic and historical cyclone tracks. Appendix A.1.5 provides additional details on the data generation process.

Table 2.1 summarizes the main damage statistics from the set of 5,070 years of damages for each region of our study. We detect no sign of systematic bias between the historical and the augmented sample. The three statistics we use to compare the two samples are roughly similar although the augmented sample has a much broader set of yearly damage estimates. Table 2.1 also highlights the considerable regional variation in relative cyclone-induced capital damages, ranging from an additional depreciation rate of 0.15% in the U.S. to 2.67% in the Philippines.

Table 2.1: Yearly cyclone damage statistics region

	USA	CAR	JPN	CHN	PHL
	Historical sample				
% of events that cause damages	29.84	13.07	19.41	33.28	22.21
Mean damage, $\bar{\delta}_{TC}$ (%)	0.15	0.59	1.10	0.40	2.67
Std. of damages, σ_{TC}	0.21	1.51	1.82	0.51	6.43
	Augmented sample				
% of events that cause damages	26.82	13.50	18.68	28.74	21.64
Mean damage, $\bar{\delta}_{TC}$ (%)	0.09	0.65	0.84	0.40	2.73
Std. of damages, σ_{TC}	0.14	1.67	1.51	0.50	5.67

Notes: The historical sample only contains the cyclone observations between 1950-2019. The augmented sample corresponds to the 5,070 years that we simulate from the historical tracks augmented by their 50 respective synthetic tracks.

2.2.2 Economic model

This section describes the main features of the economic growth model, as well as the datasets used for model calibration.

Numerical framework

We employ a dynamic, multi-regional and multi-sectoral numerical general equilibrium model based on Bretschger et al. (2011) and Bretschger et al. (2017). The production structure of the economy consists of *i*) final good producers, *ii*) producers of intermediate goods, and *iii*) producers of intermediate composites. The separation between intermediate goods and intermediate composites is one of the framework's key features. It enables switching on endogenous productivity gains from increasing capital varieties with a simple change of model parameters. The time horizon of the theoretical model formulation is infinite with discrete increments but approximated using a finite number of periods in the numerical implementation. A detailed technical description of the model is available in Appendix A.1.1.

Each regional economy consists of a forward-looking representative household, maximizing the discounted sum of utility from consumption. Households also own all firms and factors of production. Labor and capital are mobile across sectors, and

all countries are open to trade. We model international trade using the Armington (1969) assumption, which treats goods produced in different regions as imperfect substitutes. As opposed to an assumption of small open economies, our trade specification allows changes in regional production and demand patterns to affect world prices. Consequently, disaster impacts in one country can spill over to other regions via global supply chain links. The model consists of nested constant elasticity of substitution (CES) blocks that combine domestic and imported goods from various sectors into consumption aggregates and production input bundles.

Economic accounts and calibration

We calibrate the economic model using the Global Trade Analysis Project (GTAP) database (Narayanan et al., 2012). GTAP provides unified base-year economic accounts for 129 regions, 57 commodities, and five primary production factors. The dataset describes the flow of goods across sectors and regions and how the regional agents allocate them between final demand, intermediate production inputs, or trade. We use the GTAP data as a static snapshot of the economy and extrapolate —using a set of exogenous parameter assumptions— an initial balanced growth path on which all sectors grow at the same rate. The dataset also includes sectoral greenhouse gas emissions, which allows the construction of additional climate policy scenarios. Appendix A.1.2 contains details on the sectoral and regional aggregation of the raw GTAP data.

In addition to the dollar-valued economic accounts from GTAP, the model requires various sector- and region-specific elasticity values. The elasticity estimates for consumer demand and the substitution elasticities between different production inputs are among the most important determinants of our numerical results. We use estimates mainly from the MIT Economic Projection & Policy Analysis model (Paltsev et al., 2005a) and Narayanan et al. (2012). The numerical values are available in Appendix A.1.3.

2.2.3 Model integration

In summary, we can describe our modeling framework as follows. We generate data on cyclone activity in all five regions of our study based on historical and

synthetic cyclone tracks. By combining the cyclone tracks data with a damage function from wind and the spatial distribution of economic assets, we compute the capital destruction caused by each cyclone in the sample. We aggregate this capital destruction estimate by year and obtain a distribution over the annual capital depreciation due to cyclone exposure for each economy. We consider the region-specific cyclone shocks as a yearly and unexpected increase in the natural depreciation level of capital. We calibrate our economic growth model to a balanced growth path in the absence of cyclones. Finally, introducing the shocks, we can run counterfactual simulations and compare how the economic trajectories differ between the reference growth path and the one affected by cyclones.

Numerical general equilibrium models provide a flexible instrument for analyzing the multi-sectoral adjustment of prices after an economic shock. Their deterministic structure, however, imposes some limitations on modeling the impacts of rare natural disasters such as tropical cyclones. Introducing disaster impacts in an arbitrary time step t, without further adjustments, would imply that for the periods preceding t, all agents in the model have perfect information over the timing and magnitude of the upcoming event. Agents would then react to disasters with optimal precautionary savings, producing an overly optimistic description of disaster impacts.

We choose a solution algorithm that maintains the forward-looking nature over the model's economic variables but treats the disaster realizations as unanticipated shocks. To model an unanticipated disaster occurring at time τ, we first solve for a reference equilibrium path without shocks from the initial period t_0 to the terminal time T, such that $t_0 < \tau < T$. We then fix all the variables from the reference equilibrium until τ, and re-run the model with the shock. In other words, we only allow the agents to adjust their behavior in the period $t \geq \tau$. In the newly constructed sub-model, from τ to T, the shock occurs in the first period of the simulation. Agents have no chance of anticipating the shock. We combine the solution from the reference equilibrium and the one from the sub-model by using the reference equilibrium values for $t < \tau$ and the sub-model values for $t \geq \tau$. In the absence of shocks, this alternative method produces the same numerical results as only simulating the reference equilibrium path.

2.3 Results

We analyze the simulation results in four parts. First, we study the impulse response of the economy after a single year of cyclone activity. It illustrates the primary economic mechanisms and provides intuition for the recovery period dynamics under a single fixed-magnitude shock. Second, for the chapter's main results, we run the model with recurring probabilistic shocks to study the cumulative long-run disaster effects. We then provide two sensitivity scenarios to scrutinize the main long-run modeling assumptions. We first recalibrate the general equilibrium model to introduce endogenous productivity gains from specialized capital varieties. Finally, we alter the cyclone damage distribution to analyze how climate change might affect the intensity and frequency of future disasters. We present all numerical results as counterfactual simulations to a no-shock baseline economy.

2.3.1 Impulse response to a single cyclone shock

Consider first the effect of an individual cyclone shock. Figure 2.3 decomposes the general equilibrium response into expenditure-side GDP contributions. We simulate a shock at time $t = 5$ that increases capital depreciation compared to a year without disaster events. The magnitude of the shock for all countries is one standard deviation above the regional mean, as described in Table 2.1. [2] The overall picture is relatively similar for all regions. GDP falls on impact, followed by a catch-up period of faster growth and reinvestment. The higher depreciation increases the marginal productivity of capital, bringing greater returns on investment. Consequently, savings increase as a response to the reconstruction efforts. However, the increase in savings comes at the expense of lower consumption, reducing welfare. The magnitude of the investment jump ranges from 0.06% in the U.S. to more than 4% in the Philippines.

International trade linkages are another determinant of the recovery period's shape and duration. Following the disaster, the trade balance deteriorates in all regions. Countries use more imports to facilitate reconstruction efforts while exports suffer from the lost local production capacity and increased domestic investment

[2] The shock distributions have a strong positive skew, producing relatively low mean damages.

Figure 2.3: Impulse response to a single cyclone shock

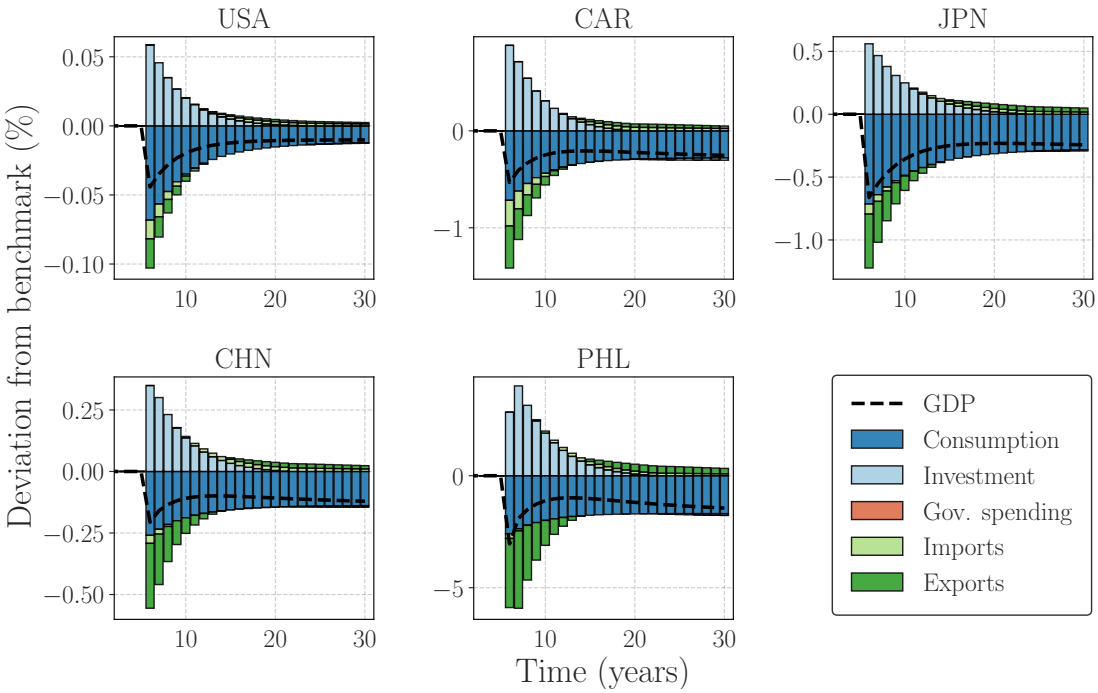

Notes: The magnitude of the shock for all countries is one standard deviation above the regional mean, as described in Table 2.1. The change in GDP is the sum of changes in aggregate investments, consumption, government expenditure, and the trade balance. All values are relative to a benchmark economy that grows on a balanced growth path without shocks.

demand. Thus, the trade channel highlights the additional flexibility that international openness can provide in the disaster aftermath. For most regions, the trade volumes converge relatively quickly to their original levels, closing the gap between the benchmark trajectory within a few years of the shock.

For the post-disaster periods, capital depreciation returns to its natural level, and the regional economies gradually return to their original steady-state path. Reconstruction is often relatively fast. For instance, reaching the pre-disaster capital stock level takes three years in the Philippines, whereas the U.S. already reinvests the lost capital amount in the first post-disaster period. However, compared to the benchmark economic trajectory that evolves without interruptions, the catch-up recovery period can take up to several decades. Although the aggregate capital

stock eventually reaches the reference trajectory, households spread the required additional investments over multiple years to avoid a drastic drop in consumption. As a result, the consumption (and GDP) levels remain permanently below the reference path in all regions. The long-run gap is 0.01% in the US, but up to 1.6% in the Philippines.

That the recovery back to the pre-disaster growth path can take decades might sound surprisingly slow. In reality, however, several factors can contribute to long recovery times. The first is the limited reconstruction capacity. With insufficient financial resources, a rapid reconstruction can only come with a sudden drop in consumption, prolonging the recovery. Technical limitations, such as the lack of a sufficient reconstruction workforce, are also possible. Moreover, business cycles can further amplify the effects, particularly if the disaster strikes during a high cycle where available resources are already scarce (Hallegatte and Przyluski, 2010). There can also be significant production factor rigidity, especially between-sector capital immobility, that complicates reconstruction efforts. The long recovery times are a common finding both in empirical works (Hsiang and Jina, 2014) and studies based on numerical general equilibrium simulations (Gertz et al., 2019).

Governments usually assume an active role in the disaster aftermath. Yet changes in public demand are absent from the results shown in Figure 2.3. Since the cyclone impacts in our framework occur solely through losses in capital stock, the primary recovery mechanism is reinvesting. However, our numerical model makes no distinction between the private sector and government investments. Therefore, the numerical results we present on post-disaster aggregate investment levels include the increased public investment demand. Although our framework is flexible enough to consider additional transfer schemes from the government to households (Gertz et al., 2019), we ignore them since the shock process does not automatically trigger any. Introducing these measures would require additional ad-hoc assumptions on government payouts. In reality, however, transfers such as medical payments and unemployment support can significantly increase in response to disaster events (Deryugina, 2017).

Finally, disasters' consequences unquestionably go beyond their impacts on physical assets and direct loss of lives. In addition, disasters can cause traumatic injuries, stress, or diseases that have long-lasting effects on welfare and productivity.

However, these effects are likely to vary depending on the local institutions and the type of disaster. As this chapter focuses on constructing a globally consistent modeling framework, we omit these effects from the numerical model but acknowledge that their unmeasured cost can be substantial.

2.3.2 Cumulative effect of recurring cyclone shocks

Whereas the previous section illustrated the model dynamics, we now turn to the chapter's main results of quantifying the long-run cumulative cyclone impacts. We randomly draw annual capital depreciation shocks from the augmented disaster event pool constructed in Section 2.2.1. We run 500 Monte Carlo simulations of the economic model for each region and provide aggregate results over a 30-year period.

When cyclone shocks are frequent and random, the economy is constantly adjusting to new conditions. Capital depreciation is therefore always above its natural level, hampering growth. Figure 2.4 shows the cumulative impact on the aggregate consumption levels. In the US, where direct cyclone damages typically only occur in specific regions, the cyclone-induced consumption drop is approximately 0.3% after 30 years of simulation. However, the reduction can be significantly greater for more thoroughly exposed regions. For instance, consumption in the Caribbean islands is more than 3% below the baseline level, whereas, in the Philippines, the long-run reduction exceeds 20%.

Compared to prior works, the magnitude of the results appears reasonable. For instance, Anttila-Hughes and Hsiang (2013) find that typhoon exposure in the Philippines leads to an approximately 7% drop in the next year's household expenditure. On the other hand, the U.S. Congressional Budget Office estimates the country's annual hurricane damages at 0.16% of GDP (CBO, 2016).

Appendix A.1.4 illustrates the results for additional economic variables. Investment levels are consistently above the no-disaster baseline trajectory for all regions, reflecting the dynamics explained in the stylized single-shock scenarios above. Similarly, industry output and capital intensity remain consistently below the reference values for the entire simulation horizon.

Notably, compared to the changes in aggregate consumption and investments, the impacts on GDP appear relatively small. For instance, the long-run GDP in

Figure 2.4: Change in aggregate consumption by region with recurring cyclone shocks

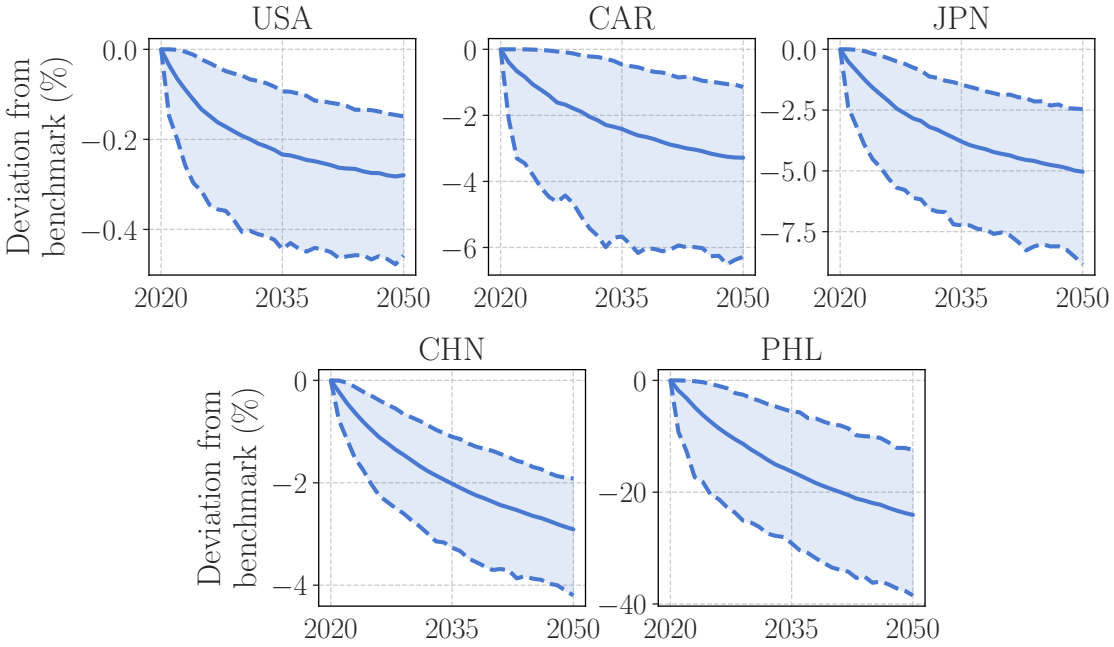

Notes: The solid lines represent the means of 500 Monte Carlo runs. The shaded areas denote simulations between the 5th and 95th percentiles. All values are relative to benchmark economies that grow on a steady-state path without shocks.

the U.S. is only 0.1% below the reference growth trajectory, compared to a drop of 0.3% in consumption. The difference highlights that the long-term welfare implications of tropical cyclones are likely to be higher than what the GDP impacts alone might suggest. Mohan et al. (2018) also find similar results, where collapsing the cyclone effects to only GDP masks the heterogeneous impacts they might have on macroeconomic activity through changes in consumption, investment, and trade patterns. Nevertheless, the unambiguous finding here is that cyclone activity negatively affects GDP, consumption, and welfare in all regions. In terms of equivalent variation, taking cyclone activity into account reduces welfare by 0.35% in the US, 4.25% in the Caribbean islands, 6.2% in Japan, 3.4% in China, and 30.3% in the Philippines.

2.3.3 Productivity gains from specialization

Our regional sample consists of heterogeneous countries in terms of size and economic structure. It is therefore important to consider alternative assumptions regarding the underlying drivers of growth as an explanation for varying disaster effects. Different growth mechanisms might allow, for instance, some countries to exhibit a post-disaster growth spurt due to "build back better" dynamics. In contrast, others may never recover to their original growth trend. [3] The capital structure is also likely to play a role. Richer economies might have a higher share of knowledge capital, less susceptible to natural disasters, attenuating the overall negative cyclone impacts.

We model the endogenous productivity gains with a simple model reparameterization. Instead of considering capital only as the physical stock, we make a broader interpretation of a capital composite that includes both the physical stock and the immaterial knowledge capital. Intermediate firms can invest in new sector-specific capital varieties. The varieties are imperfectly substitutable, such that the intermediate firms make positive profits due to a monopoly mark-up. Similarly to the growth dynamics in Romer (1990), firms investing in new varieties receive a perpetual blueprint for their product. Compared to the previous section, where growth is solely due to physical capital accumulation, there is now an additional incentive for conducting R&D investments. The positive spillovers from specialization, on the other hand, enhance the overall economic growth rate.

We simulate the economies with the same shock realizations as in the previous section but now turn on the endogenous gains from specialization. We again use 500 Monte Carlo runs and report the results after 30 years of simulation. The resulting growth trajectories vary significantly compared to the previous section, as summarized in Table 2.2. Overall, the endogenous growth engine substantially dampens the negative impacts of repetitive cyclone events. Under gains from specialization, post-disaster investments increase more than under the standard case. As a result, the capital stock, although damaged by the same amount, gets rebuilt faster, leading to lower capital losses in the long run. The existing capital stock is

[3] For a thorough discussion on the hypotheses regarding possible post-disaster growth trends, see Hsiang and Jina (2014).

Table 2.2: Change in mean tropical cyclone impacts after 30 years of simulation with endogenous gains from specialization

	USA	CAR	JPN	CHN	PHL
ΔConsumption	-23.18	-24.50	-26.30	-22.30	-17.21
ΔInvestments	0.60	7.72	24.60	14.80	51.73
ΔCap. intensity	-7.25	-4.22	-6.55	-5.73	-12.96
ΔCapital Stock	-15.45	-24.88	-25.20	-24.67	-44.90
ΔIndustry output	-45.54	-66.04	-63.01	-59.73	-84.22
ΔGDP	-45.03	-57.16	-56.73	-59.24	-87.95
ΔWelfare	-16.28	-20.40	-20.45	-17.87	-14.77

Notes: All values denote percentage change relative to the cyclone impacts in Section 2.3.2. For instance, compared to the scenario without productivity gains, aggregate long-term consumption drop in the U.S. is 23.18% *smaller, the reduction in capital stock* 15.45% *smaller, and the increase in investments is* 0.60% *larger. Welfare impacts are measured in terms of Hicksian equivalent variation.*

also more productive, affording a faster reconstruction and limiting the overall drop in consumption and welfare.

For most regions, the GDP reduction after 30 years of cyclone activity is more than 50% smaller than under the standard scenario. The consumption losses are between 17% to 26% smaller than before, depending on the region. For extreme shock realizations, GDP impacts under endogenous productivity gains can even become temporarily positive for the most affected regions, driven by the higher investment levels and increasing capital returns. However, even under these extreme realizations, the overall consumption impact remains negative. GDP only appears higher as the destroyed capital stocks are not measured in GDP, whereas the reconstruction efforts are. Even with gains from specialization, the long-run average GDP impacts remain negative for all regions.

2.3.4 Effects of climate change

Climate change likely increases the intensity and the frequency of weather-related extreme events (Pörtner et al., 2022). At the same time, economic growth and

coastal development can increase future cyclone impacts by increasing the value of exposed assets (Gettelman et al., 2018). For instance, the U.S. Congressional Budget Office estimates the country's hurricane damages to rise from the current levels of USD 28 billion per year to USD 39 billion by 2075, attributing half of the increase to climate change and another half to further coastal development CBO (2016). Therefore, in the final scenario, we study how our framework's main long-run economic variables react to the assumptions on future climate trajectories.

In the following, we extend our model horizon from 30 to 80 years and simulate up to the year 2100 for the climate change impacts to take effect. We run the model in ten-year increments to compensate for the resulting increase in computational cost. We consider two possible greenhouse gas concentration pathways: the RCP4.5 with intermediate emissions and the high-emission RCP8.5 scenario. We calibrate a new damage distribution for each region and concentration scenario by tuning the cyclone intensity and frequency values based on Knutson et al. (2015). Appendix A.1.6 documents the steps in more detail.

To ensure that the economic growth model is also consistent with the RCP scenarios, we implement a carbon tax on both the baseline economy and counterfactual simulations. As a result, the emissions from our simulated economic trajectories approximately match those used in the disaster impact estimation. That is, the percent change we show is the comparison between the value of an economic variable in 2100 under a growth scenario (without productivity gains from capital variety) with a carbon tax and the distribution of cyclones damages of the current climate (we call it the benchmark growth path) and the same growth and tax scenario but with the cyclones damages modified by climate change (RCP4.5 or 8.5). This way, the economic conditions are the same under the benchmark and the climate change growth paths. We isolate the sole effect of the change in the cyclone distribution. The initial estimates of the tropical cyclone damages are the ones of Table 2.1.[4] We conduct 100 Monte Carlo runs for each climate change scenario, randomly drawing shocks in each period as in the previous section.

Table 2.3 reports the main results at year 2100. The first thing to note is the regional variation in the cyclone damage statistics. In the RCP4.5 scenario, the cy-

[4]We provide details on the new cyclone distribution under the two RCPs and in all our regions of study in Appendix A.1.6.

clone intensity in the North Atlantic basin (Caribbean Islands and the U.S. Atlantic coast) increases by 4.5%, whereas there is no significant change in cyclone frequency (Knutson et al., 2015). As a result, in our framework, the mean cyclone damage $\bar{\delta}_{TC}$ increases both for the U.S. and the Caribbean Islands. For the Northwestern Pacific Ocean basin (China, Japan, Philippines), on the other hand, the cyclone frequency falls by 34.5%, but the intensity increases by 5.5%. These counter-acting factors first increase the mean damage in the corresponding regions until the year 2060 before lowering it for the next decades up to 2100. Therefore, the results of the RCP4.5 scenario for the pacific regions should be interpreted with caution. They hide non-linearities over the whole period 2020-2100.

For the RCP8.5 scenario, the estimated change in cyclone intensity is based on a linear interpolation from Knutson et al. (2015) using relative radiative forcings as scaling terms. We use Emanuel (2013) for the changes in cyclone frequency. In RCP8.5, both the frequency and intensity of cyclones increase in all considered ocean basins, leading to large increases in the projected damages in our economic model. Table 2.3 shows particularly striking results in the North Pacific basin where this increase is the largest. China, which would suffer less from cyclones under RCP4.5 than under the current the climate, bears a change in consumption losses that is close to ten times larger than the U.S. under RCP8.5. In RCP8.5, just like in RCP4.5, Japan endures the largest decrease in its welfare due to climate change.

Table 2.3: Change of tropical cyclone impacts in 2100 under different climate scenarios compared to estimates under constant climate

Statistics (% change)	USA	CAR	JPN	CHN	PHL
	RCP4.5				
Mean damage, $\bar{\delta}_{TC}$	30.16	24.03	-9.73	-12.66	-13.47
Std. of damages, σ_{TC}	25.94	18.72	5.86	-1.22	-2.18
Consumption	-0.10	-1.18	-0.06	0.32	-0.31
Welfare	-0.05	-0.78	-1.87	0.28	-1.11
Capital stock	-0.85	-1.07	-1.87	0.56	0.58
GDP	-0.02	-0.16	-0.48	0.13	-3.07
	RCP8.5				
Mean damage, $\bar{\delta}_{TC}$	112.92	87.95	166.83	151.50	126.55
Std. of damages, σ_{TC}	93.11	66.39	115.51	103.22	81.92
Consumption	-0.19	-2.10	-7.10	-1.74	-5.90
Welfare	-0.11	-1.78	-4.12	-1.43	-3.64
Capital stock	-0.96	-5.95	-25.95	-6.42	-24.10
GDP	-0.08	-0.83	-3.11	-0.46	-1.76

Notes: Welfare impacts are measured in terms of Hicksian equivalent variation.

All in all, the comparison of results from both climate scenarios shows non-linearities in the climate system to the climate change process. The comparison emphasizes that different regions may have to adapt differently according to the future state of the climate.

2.4 Discussion

We have constructed a modeling framework that integrates probabilistic, region-specific cyclone damage functions in a dynamic economic growth model. That enables us to isolate how tropical cyclone strikes affect economic variables over time in general equilibrium. The chapter's main goal was to set up a globally consistent modeling framework. However, several possible extensions remain for studying additional cyclone impact channels or the role of public policies in disaster impact management.

First, we have excluded the role of adaptation. In our model, local adaptation measures could affect either the cyclone impact function (for instance, the construction of sea walls, mangrove restoration, or the implementation of new building codes) or the distribution of exposed assets (such as spatial planning in high-risk areas), and therefore have interesting broader impacts in the economy.

In our coupled system, tropical cyclones only enter the economy through damages on capital stock. In reality, cyclone impacts are much more complex. Disaster strikes might reduce the economy's total factor productivity via, say, electricity blackouts (Bakkensen and Barrage, 2018) or business interruptions (Gertz et al., 2019). Moreover, there are externalities that are not directly captured by the general equilibrium response. For instance, a drop in post-disaster quality of public services might make attracting workers more difficult, directly affecting the recovery period dynamics (Hallegatte and Vogt-Schilb, 2016).

Throughout, we have considered countries as the units of regional aggregation. With detailed enough economic accounts, it is possible use even higher regional detail. For instance, Carrera et al. (2015) use a sub-national model to study flood impacts in Italy, and Gertz et al. (2019) use a numerical general equilibrium model calibrated to a single city. This might better allow studying local questions such as labor reallocations or comparing adaptation alternatives.

Finally, we acknowledge some caveats. First, by design, our model economy is always in equilibrium. This might be unrealistic especially in the time periods directly after a disaster where bottlenecks and misallocations are likely to happen in all markets. That might make the early stages of the recovery path in our model overly optimistic, ignoring some of the real-world rigidities. We also assume that the regional distribution of exposed assets remains constant throughout the simulation periods. In reality, there might be a considerable shifts if people and firms leave the most exposed areas or with gradual urban expansion. We have also explicitly focused on tropical cyclone impacts, although the simultaneous effects from cyclones, storm surges, and on the long term even sea level rise, might give a more complete picture of the disaster impacts. The wind impact model parameterization in Eq. (2.2) also relies on data solely from the US, and might not be directly applicable to other regions.

2.5 Conclusion

We develop a methodology for estimating the long-run economic impacts of tropical cyclones. Our framework features a dynamic general equilibrium economic growth model and a probabilistic disaster impact model. Our coupled system allows us to consider region-specific damage functions and post-disaster recovery profiles. We focus on the effects of cyclone strikes that enter the economy through damages to capital stock.

We apply our framework to five regions: the US, Caribbean islands, Japan, China, and the Philippines. The general findings are similar for all regions. Cyclone shocks harm GDP, consumption, and welfare as they increase capital depreciation, thereby forcing higher investments for reconstruction. After 30 years of simulation, the aggregate capital stock in the U.S. is 0.5% smaller compared to a no-shock baseline path. In the Philippines, which is the most affected region, the difference is almost 13%. Consistent with previous literature, the recovery period after a cyclone shock towards the original steady-state growth path is long and can take up to decades. Our results also highlight the need to disentangle GDP and welfare impacts. The GDP effects often appear artificially small since they aggregate cyclones' many heterogeneous macroeconomic impacts with opposite signs.

Assumptions on the economic growth engine and future climate change affect the long-run numerical results but do not change the overall qualitative findings. When endogenous productivity gains from specialization drive growth, cyclone impacts are smaller but still unambiguously negative. Under the RCP4.5 climate change scenario, cyclone damages increase in the North Atlantic Ocean basin (the US, Caribbean islands) but fall slightly in the Northwestern Pacific basin (China, Japan, the Philippines). Under a high-emission scenario (RCP8.5), cyclone damages increase in all regions from the current climate conditions.

Chapter 3

The Elements of Global Adaptation to River Flood Risk[1]

Abstract

This work examines the macro drivers of adaptation to river flood risk worldwide. It is the first study to use the sub-national features of a publicly available database on disasters in combination with the output of a global hydrological model measuring river flooding. To identify adaptation, I estimate the elasticity of damages and fatalities to income, population density, and long-run average flood depth in the areas affected. I find evidence of adaptation as income and population density increase. Yet, GDP per capita is less critical for the adaptation to the fatality risk of flooding in high-income provinces, which may induce a convergence in vulnerability between high and low-income regions. At last, the results of this study show recurring signs of maladaptation to intense and less frequent river floods—the type of events that are very likely to intensify with climate change.

[1]This chapter is part of a project that has received funding from the European Union's Horizon 2020 research and innovation programme under the Marie Skłodowska-Curie grant agreement No. 870245.

3.1 Introduction

Every year since 1980, fluvial floods have caused, on average, more than 3,000 fatalities and more than $13 billion in direct economic damages globally, placing them among the most socially and economically devastating natural disasters (EM-DAT, 2020). In 2050, there could be additional 31–450 million people, 59 to 430 thousand km^2 of cropland, and between -9 and +376% of asset value exposed to river flood risk (Arnell and Gosling, 2016).[2] There is substantial variability in these results across regions and climate models. But the potential risk is such that we ought to examine further its drivers and the potential for adaptation.[3] What are the drivers of adaptation to river flood risk?

This chapter seeks to quantitatively answer this question from an empirical analysis of the damages and fatalities caused by individual river floods worldwide. I analyze adaptation at a sub-national level across three main dimensions: the population concentration, GDP per capita, and the flood experience of the affected locations. This way, I identify the macro drivers of adaptation to river floods across three sub-questions. First, do rich places suffer fewer fatalities and damages than poor ones? Wealthy areas may have better prevention and emergency plans to reduce fatalities. They may also have better building standards and river and sewage management to limit damages in proportion to their assets. Second, do dense versus sparse areas react differently to river floods? On the one hand, dense regions may have better access to hospitals. On the other hand, population concentration increases land cover and may worsen water evacuation. Third, does long-term exposure to floods help to better prepare for this risk? Locations regularly hit by a river flood may more easily invest in protection measures. But there is also the risk of warning fatigue and reliance on state or public insurance (Kydland and Prescott,

[2] Arnell and Gosling (2016) compute these changes in exposure across 21 climate models under the SRES A1b scenario. The Special Report on Emissions Scenarios (SRES) contains greenhouse gas emissions scenarios from the Intergovernmental Panel on Climate Change (IPCC). It was first published in 2000 and was the basis of the IPCC's fourth assessment report Solomon et al. (2007). The A1b scenario projects a temperature change of 2.8°C (at 2090-2099 relative to 1980-1999) as the best estimate (in the likely range of 1.7-4.4°C) with very rapid economic growth, global population that peaks in mid-century and declines after that, and the rapid introduction of new and more efficient technologies.

[3] These indicators do not incorporate the effects of future adaptation.

1977; Bakkensen and Mendelsohn, 2016).

The flood data used in this work come primarily from two sources. The long-run average flood exposure data is only available by reconstruction from reanalysis data processed by global hydrological models that estimate river flooding. The data provider is the Inter-Sectoral Impact Model Intercomparison Project (ISIMIP2a). Hence, I must select only this type of flood to assess each region's flood exposure over several decades and identify the proper risk and adaptation effects. Data combining the information on the flood type (coastal, flash, ice jam, or river flood) and fatalities and damages caused by each flood is only publicly available in the EM-DAT database. I combine EM-DAT data on deaths, damages, disaster intensity, and locations of the river floods with GDP and population data of 1,800 administrative regions around the world over the period 1980-2020. I borrow the framework from Bakkensen and Mendelsohn (2016), which allows me to identify the fatality and damage equations and test for the presence of adaptation.

I use each river flood as a separate observation and regress the observed damages and fatalities on river flood intensity, population density, GDP per capita, and the long-run average flood exposure in the affected areas. Following Bakkensen and Mendelsohn (2016), without adaptation, the damage function should have an income elasticity of one. In the absence of adaptation, if GDP per capita in the region increases by 1%, the damages should also increase by 1%. With the same logic, the fatality function should have an income elasticity of zero, population density should have an elasticity of one in both the income and fatalities functions, and both functions should have an elasticity of zero to the long-run average flood exposure. I empirically measure these elasticities for both the fatality and damage functions and test their values against the theoretical ones in case of no adaptation.

My estimates support that economies globally adapt to river flood risk as they become richer (Jongman et al., 2015; Tanoue et al., 2016; Sauer et al., 2021).[4] A 1% increase in GDP per capita may reduce fatalities by up to 0.35% while increasing damages less than proportionally (about 0.3%). I also find that population density helps lower vulnerability to fatality and damage risk (with vulnerability defined as

[4]The fact that people and governments reduce mortality and damage rates as they get wealthier is not specific to river flood risk (Kahn, 2005; Hsiang and Narita, 2012; Ferreira et al., 2013; Fankhauser and McDermott, 2014; Jongman et al., 2015; Bakkensen and Mendelsohn, 2016; Sauer et al., 2021).

the inverse of adaptation). This last result complements studies on vulnerability trends that could only conclude on no clear trend in fatalities although the exposed population kept increasing (Jongman et al., 2015).

This work emphasizes the important role of long-term flood exposure in adaptation capacities. While provinces adapt to fatality and damage risk as low-intensity floods regularly hit them, I find they have a maladaptation to rare and intense floods. A 1% increase in the average exposure to low-intensity floods in an area might reduce fatalities by 0.083%. In contrast, a 1% increase in the average exposure to high-intensity floods may increase fatalities by 0.112% and damages by 0.362% (with no impact of low-intensity flood experience on damages).

The maladaptation to high-intensity, low-frequency floods is present in both rich (GDP per capita greater than $20,000) and poor (GDP per capita low than $5,000) locations for the fatality risk. These results are at odds with previous research on adaptation to tropical cyclones (Hsiang and Narita, 2012; Bakkensen and Mendelsohn, 2016), which find economies adapt to intense and less frequent events but maladapt to smaller and more frequent storms. Moreover, GDP per capita is less critical for the adaptation to the fatality risk of flooding in high-income provinces. This may explain the convergence in vulnerability between high and low-income regions found in part of the literature (Jongman et al., 2015; Tanoue et al., 2016).

When I analyze adaptation in rural versus urban areas (with 200 people per km^2 as a threshold), I find that, on average, for a 1% increase in flood intensity, urban areas suffer about two times more fatalities and four times more damages. They are also more sensitive to intense floods but show signs of a better adaptation to low-intensity floods when I account for the region- and time-specific fixed effects.

Related literature

Ferreira et al. (2013) is one of the first attempts to examine the adaptation to flooding risk in the economics literature. Their analysis covers 92 countries between 1985 and 2008 and assesses whether higher income and better governance reduce fatalities during flood events. Their results show that countries adapt thanks to a higher income and improved governance. But this relationship does not hold when

unobserved country heterogeneity and within-country correlation of standard errors are considered. They may lack critical information on the countries' exposure to flood, with physical measures of floods, to complete their analysis.

This study builds upon the findings of Ferreira et al. (2013). It expands on them by examining the influence of development *and* flood experience on flood fatalities *and* damages using a unique combination of data. In terms of damage estimates, this study is the first, to the best of my knowledge, to fully utilize the sub-national features of the Emergency Events Database (EM-DAT, 2020) to investigate adaptation to floods.[5] Additionally, this study is one of the initial works in the economics literature on flood to employ physical measures of flooding to explain adaptation to the hazard (to damages and fatalities).[6]

Studies at the intersection between natural science and economics also use physical measures of floods. The ones that focus on the long-term vulnerability trend analyze the time evolution of the ratio of the reported flood fatalities or damage to the modeled flood exposure (population or assets respectively) using a global river and inundation model (Jongman et al., 2015; Tanoue et al., 2016; Sauer et al., 2021). The assumption behind these analyses is that in case of no adaptation, the ratio of reported fatalities (or damages) to the modeled exposed population (or assets) should be constant. If the ratio decreases, it is a sign of adaptation (i.e., a decrease in vulnerability). They can then proceed to correlation analysis between the obtained ratio and some macroeconomic variables like GDP per capita or population density. Although this method is handy, it cannot disentangle the different macroeconomic drivers of the vulnerability trend.

I see three main limitations to overcome. First, since they have to aggregate reported flood damages per year, these studies are subject to the well-documented under-reporting bias of catastrophes (Ferreira et al., 2013; Tanoue et al., 2016; Bakkensen and Mendelsohn, 2016; Jones et al., 2022). Second, a simple correlation analysis is subject to country-specific geographical, topographical, and institutional

[5]Bakkensen and Mendelsohn (2016), and Eberenz et al. (2021) also use the EM-DAT data sub-nationally although for cyclone risk and a limited amount of countries.

[6]Guiteras et al. (2015) is the first attempt in the economic literature on adaptation to floods to try building "objective long-run time series measures of floods" using satellite data. Yet, their study focuses on the flooding experience of the people in Bangladesh, omitting the role of income or population density.

bias and cannot provide information on the impact of income or population density on flood risk, all else being equal. Third, these studies don't consider the link between long-term flood experience and vulnerability.

The framework I use allows me to tame these limitations and increase the understanding of general patterns of adaptation the literature typically finds. Since I don't aggregate floods annually, this analysis is less subject to the data limitations on reporting (especially present before the 21^{st} century), and the damages are directly linked to the intensity of each reported flood. Carefully accounting for the intensity of each hazard, instead of grouping them by year, may avoid bias due to non-linear response to the intensity. The framework also guides me in estimating a functional form for vulnerability, damage, and fatality. I benefit from cross-sectional and panel techniques to identify the elasticities of income, population, and flood exposure for both the fatality and damage function. The relation between damages or fatalities to long-term flood exposure is precious in light of coming changes in flood dynamics due to climate change. The inadequate adaptation of economies to severe flooding incidents may pose an escalating threat to the insurability of assets and the population's welfare.

The remainder of the chapter is organized as follows. Section 3.2 defines the theoretical framework that guides us in analyzing the empirical results. Section 3.3 describes my empirical strategy, the damage and fatality functions I estimate, and the data I use. Section 3.4 displays the study results, first using the whole set of countries and then with a sub-sample analysis of income levels and groups of different population densities. I also provide some robustness checks to these results. Section 3.5 concludes.

3.2 Theory

It is common in the literature on natural catastrophes' to find the reported impacts (i.e., materialized risk) from a disaster defined as $Risk = Hazard \times Exposures \times Vulnerability$ (Jongman et al., 2015; Winsemius et al., 2016; Gettelman et al., 2018; Geiger et al., 2021; Kam et al., 2021). Yet, taking this definition of the risk may implicitly assume a unitary elasticity of risk to exposure ($\frac{\partial Risk/Risk}{\partial Exposure/Exposure} = 1$). Such an assumption is reasonable in the absence of adaptation. But in the presence of

adaptation, vulnerability (V) may be a function of the level of exposure (E) or the hazard (H) characteristics ($V \equiv f(E, H)$). The potential links between vulnerability and the other two risk components may change the sign of the risk elasticity to exposure. To better understand the dynamics of changes in vulnerability, I highlight these underlying links.

Let me define the exposure of a province by its population density Pop and income per capita Y, and the hazard as a combination of the hazard intensity I and probability M. The definition of risk in terms of materialized fatalities ($Risk_F$) becomes $Risk_F = I^{\psi_3^F} \times Pop \times V$ and the risk in terms of materialized economic damages ($Risk_D$) writes as $Risk_D = I^{\psi_3^D} \times Y \times Pop \times V$. I assume that $\{\psi_3^i\}_{i\in(F,D)}$ are positive, which means that an increase in the intensity of the flood increases the reported risks. Note that a decrease in vulnerability would be a sign of adaptation (i.e., a decrease in the risk) and reciprocally for an increase in vulnerability.

To model the link between vulnerability V and the other two components of the risk (E and H), I approximate vulnerability with the following constant elasticity functional form:

$$V \approx (1 - \gamma_0) Y^{-\gamma_1} Pop^{-\gamma_2} I^{-\gamma_3} M^{-\gamma_4}$$

such that if $\gamma_i = 0$ for $i \in 0, 1, 2, 3, 4$ there is no adaptation. The expression for risk becomes:

$$Risk_F = (1 - \gamma_0^F) Y^{-\gamma_1^F} Pop^{1-\gamma_2^F} I^{\psi_3^F - \gamma_3^F} M^{-\gamma_4^F}, \tag{3.1}$$

$$Risk_D = (1 - \gamma_0^D) Y^{1-\gamma_1^D} Pop^{1-\gamma_2^D} I^{\psi_3^D - \gamma_3^D} M^{-\gamma_4^D}. \tag{3.2}$$

It is now easier to identify adaptation based on the elasticity of the risk to the exposures (Pop and Y) or provinces' flood experience (M). Suppose provinces adapt to floods based on their experience. In that case, the elasticity of the risk to the floods' probability should be negative ($\frac{\partial Risk_F / Risk_F}{\partial M/M} < 0$ and similarly $\frac{\partial Risk_D / Risk_D}{\partial M/M} < 0$). If provinces adapt to floods as they become more densely populated, the elasticity of the risk to population density should be less than unitary ($\frac{\partial Risk_F / Risk_F}{\partial Pop/Pop} < 1$ and similarly $\frac{\partial Risk_D / Risk_D}{\partial Pop/Pop}$¡1). At last, if provinces adapt to floods as they prosper, the elasticity of fatality risk to income per capita should be negative ($\frac{\partial Risk_F / Risk_F}{\partial Y/Y} < 0$), and the elasticity of damage risk to income per capita should be less than unitary ($\frac{\partial Risk_D / Risk_D}{\partial Y/Y} < 1$).

In the subsequent analysis, I split the probability of experiencing floods (M) into two parts, M_l and M_h, corresponding to the likelihood of low- and high-intensity floods, respectively. I proxy these two measures with the long-run average exposure (from 1971-2010) of a province to floods of intensity below (for the low intensity) and above (for the high intensity) 100-year return period. The logic behind the risk elasticities stays the same as with a single probability of floods.

This study doesn't aim to understand the specific measures that may or may not lead to adaptation. I assume that governments, as well as private actors, make their own decisions regarding adaptation. These decisions may not be optimal, and it is not the object of this analysis to find the optimal adaptation level; I test whether adaptation increases as income per capita, population density, or flood experience increases. In other words, I examine the combined effect of private individuals, firms, and governments' behavior on their province's adaptation to riverine floods as their economy develops.

3.3 Empirical strategy

Guided by the theoretical framework above, I identify the presence of adaptation to riverine flood damages and fatalities. To do so, I rigorously follow the methodology of Bakkensen and Mendelsohn (2016). I first estimate damage and fatality functions using a log-log functional form through cross-sectional and panel techniques. The results of a log-log estimation can be interpreted as elasticities. I test to see if these elasticities are different from the values expected with no adaptation.

3.3.1 Model

I model fatalities for floods f at year t in province i as:

$$lnF_{fit} = \alpha_0 + \alpha_1 lnI_{fit} + \alpha_2 lnPop_{fit} + \alpha_3 lnY_{fit} + \alpha_4 M^h_{fi} + \alpha_5 M^l_{fi} + \alpha_i + \gamma_t + u_{fit} \quad (3.3)$$

and damages as:

$$lnD_{fit} = \beta_0 + \beta_1 lnI_{fit} + \beta_2 lnPop_{fit} + \beta_3 lnY_{fit} + \beta_4 M^h_{fi} + \beta_5 M^l_{fi} + \alpha_i + \gamma_t + u_{fit} \quad (3.4)$$

where F_{ift} is the number of fatalities and D_{ift} is direct economic damages. These impacts are explained by I_{ift}, the intensity of flood f; Pop_{it}, the population density; Y_{it}, the income per capita; M_i the long-run average of the maximum yearly flood depth in province i over the period 1971-2010.[7] In the error components model, I also include fixed effects for time (γ_t) and region (α_i). u_{ift} is a mean-zero error term. Like in Bakkensen and Mendelsohn (2016) and Ferreira et al. (2013), my observation unit is a single event—a single flood. I treat each observation independently if multiple floods occur in a province during the same year. As noted by Bakkensen and Mendelsohn (2016), this ensures that any missing floods or missing data on the hazard are not treated as zero. If the same flood spreads over multiple provinces, I group them into a single geographical entity. This entity inherits GDP per capita, population density, and long-term level of flood exposure from the average of each variable over the provinces.

I estimate both functions (3.3) and (3.4) using the ordinary least squares (OLS) estimator. I use a cross-sectional and an error components model to limit the risk of bias due to omitted variables in calculating the damage and fatality functions. I use year- and region- (defined as a group of countries) fixed effects. I cannot use province or country-fixed effects because some countries are hit only a couple of times during the whole 40 years of analysis, which prevented me from using provinces and year fixed-effects at the same time. For the main regressions, results for the country-only fixed effects are similar to the regional-only fixed effects. I detail the thirty different regions and results for the country-fixed effects regressions in Appendix A.2.2.

Ferreira et al. (2013) highlight the importance of using fixed-effect in such analysis. They point out that unobserved topographical or climatic characteristics are examples of time-invariant factors that could confound the estimation of the effects of development on natural disaster fatalities, as they could affect both economic growth and casualties. The variation captured in the error components model occurs in deviation from region and year averages. Yet, if adaptation changes very slowly over time, the within-country and within-year variation may not capture it. The cross-sectional is thus considered a valuable tool to shed light on long-run pat-

[7] I approximate a province's climatic experience of riverine floods, i.e., its probability to experience a flood, by its 40-year average of yearly maximum exposure to the hazard. I explain more about the flood depth data in Section 3.3.2

terns of adaptation (Mendelsohn et al., 1994; Bakkensen and Mendelsohn, 2016). Ferreira et al. (2013) also note the importance of country-clustered standard errors for cross-country disaster analyses. I follow their findings and cluster the standard errors at the country level in all specifications (unless stated otherwise), to account for any within-country correlation across error term observations.

3.3.2 Data

I take records of damages and fatalities caused by riverine floods from the EM-DAT database (EM-DAT, 2020). The literature on natural catastrophes widely uses the EM-DAT (Skidmore and Toya, 2002; Kahn, 2005; Toya and Skidmore, 2007; Crespo Cuaresma et al., 2008; Noy, 2009; Loayza et al., 2012; Bakkensen and Mendelsohn, 2016). Yet, to my knowledge, this study is one of the first to fully exploit the dataset's sub-national information. One explanation for why sub-national analyses don't use the EM-DAT dataset is that the information on the sub-national location of the hazards is hardly usable for extensive studies (over many countries, years, or on many disasters type). This information spreads over seven different variables (location, latitude, longitude, administrative level, Admin1 Code, Admin2 Code, and Geo Locations) that may complement or substitute each other, and where sometimes the name of a province or area is mentioned, sometimes the name of a city, a county, etc. Since this study focuses only on riverine floods since 1970, I can regroup the information from the different columns and assign it to the corresponding administrative province of level 1 (e.g., states in the United States of America). I also exploit another resource rarely explored in the EM-DAT database: the magnitude of the disasters. In the case of riverine floods, the magnitude is the km^2 of the flooded area. I use this statistic as a proxy for each disaster's intensity. Consequently, I omit an event when data on the flood's intensity is missing.

The EM-DAT database is, to my knowledge, the unique publicly available database that goes back to 1970 and contains information on damages and deaths caused by disasters. Studies on floods tend to use the Dartmouth Flood Observatory database instead. It contains more floods since they specialize in this specific type of disaster. But it does not distinguish floods by type (riverine, flash, or coastal), nor does it include damage estimates for each flood. Yet, I used the DFO database

to complement missing data in the EM-DAT riverine floods. I matched floods of the two databases by date (year, month, and day) and country to fill in missing information in the EM-DAT data on the number of deaths and the localization of the flood (latitude and longitude) with DFO data.

I focus on riverine floods because the long-run average flood exposure data is only available by reconstruction from reanalysis data processed by global hydrological models that estimate river flooding. These data are part of the so-called "ISIMIP2a" dataset. They reconstruct the flood depth of the maximum flood event each year for the period 1971-2010 at 30 arc-min (about 60km^2 at the equator) resolution under two scenarios of protection standards: '0', no protections, and '100', protection against all events smaller than 100 year return period. Thirteen Global Hydrological Models (GHM) and four climate reanalysis data sets have been used within the ISIMIP framework. I use the output from the CLM4.0 model with the Global Soil Wetness Project version 3 (GSWP3[8]) data. I visually represent these data in Figure 3.1. For more information and a technical description of the ISIMIP2a Simulation Data from Water (global) Sector, see Gosling et al. (2017). I aggregate these flood data into the different administrative provinces of level 1 for all world countries. I use the province and year average of the yearly maximum flood event as a proxy for the riverine flood climate of the respective provinces. I interpret the maximum flood event under the 100 protection standard as high-intensity floods and the difference between the 0 and the 100 protection standards as low-intensity floods.

My exposure data are twofold: local GDP and population. For the GDP data, I gather different sources. I use the ISIMIP2a GDP data from 1970 to 2005, available yearly and globally at 30 arc-min resolution[9]. For 2005 to 2015, I use data from Kummu et al. (2018) available yearly at the 5 arc-min ($\approx$ 10km^2 at the equator) resolution. Finally, I extend my data on gridded GDP to 2020 based on the United Nations (UN) dataset.[10] The UN's data are only available at the country level, but I computed the share of each province in the total GDP of its country in 2015 to estimate the GDP of each province in 2020. I then interpolate the provinces' GDP between 2015 and 2020 linearly. I adjust all GDP data to the UN's reference of

[8]Source: http://hydro.iis.u-tokyo.ac.jp/GSWP3.
[9]Source:https://data.isimip.org/files/21f0fd44-a51e-4100-a03b-787255066f0f/.
[10]Source: https://data.un.org/.

Figure 3.1: Maximum flood event in western Europe for the year 2000

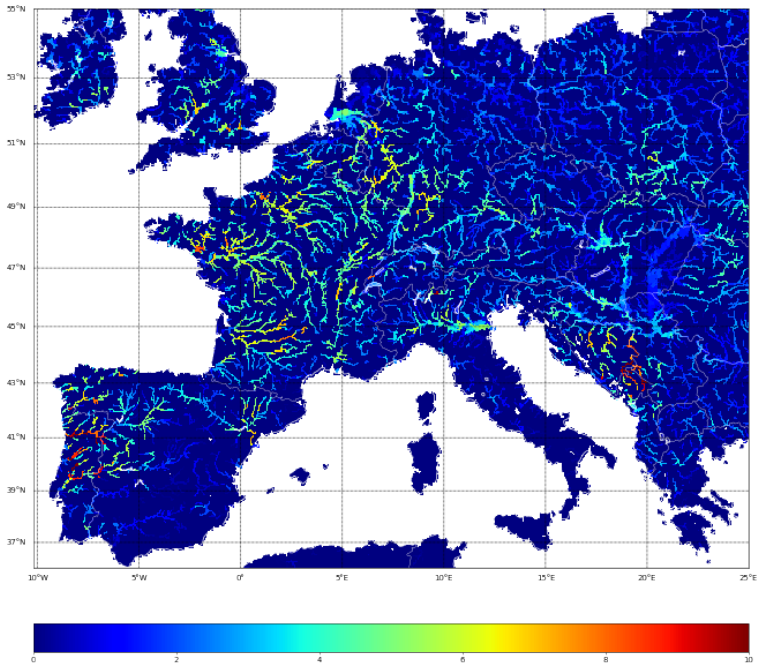

Notes: The legend represents the depth of the flood (in meters) under no protection standards.

constant 2015 prices in US Dollars.

The reported damages in EM-DAT are in $USD (in thousands) in the value of the year of occurrence. To keep damage data consistent with GDP data, I set prices from the reported damages of the EM-DAT database at constant 2015 $USD. I follow the same methodology as Eberenz et al. (2021) to do so. The reported damages normalized to 2015 $USD prices ($NRD$) for the event f are computed from the reported damages of the event (RD_f), the GDP at the year of occurrence (GDP_t), and the GDP of 2015 as follows:

$$NDR_f = \frac{GDP_t}{GDP_{2015}} \times RD_f. \tag{3.5}$$

The second part of my exposure data is the population. I collect sub-country data from the Gridded Population of the World (GPW), v4 dataset CIESIN (2016).

The data is at the 2.5 arc-min resolution and available for the years 2000, 2005, 2010, 2015, and 2020. To get gridded population data back to 1970, I take the UN's population estimates.[11] Just like the GDP data, the UN's population data are only available at the country level. Again, I compute the share of each province in the total population of its country in 2000 to estimate the population of each region in 1970. I then interpolate the missing years from 1970 to 2020 linearly.

At last, to gather all gridded data (the ones from ISIMIP, the GDP data, and the population data) into provincial data at the administrative level 1, I use shapefiles from the GADM database.[12] Each country's shapefile contains a set of polygons with their associated coordinates representing the country's different regions. I overlap these polygons with the gridded data (which are like weighted pixels on a map) and compute the sum of each pixel per polygon. As a result, I have the value of my gridded variable of interest per province.

Altogether, the final dataset has 127 different countries affected in 1861 different provinces over the period 1980-2020[13]. The affected areas have an average population density of 257 persons/km^2 (with a standard deviation of 965) and an average GDP per capita of \$8,341 (2015 \$USD, with a standard deviation of 14,950). Each flood causes, on average, 63 deaths and 1.1 billion dollars in damages (prices in 2015 \$USD). I provide further summary statistics in Appendix A.2.1.

3.4 Results

This section presents the main results using cross-sectional and fixed effects specifications. I first estimate the elasticity values across the whole sample of countries. I then refine these tests by estimating several regressions across different sub-samples. The first sub-sample is across provinces' income levels; the second is based on population density to simulate urban and rural samples. At last, I provide robustness checks.

[11] The United Nations' population data are available from their data portal at the following address: https://population.un.org/dataportal/home.

[12] Source: https://gadm.org/data.html.

[13] Although I have the data from 1970 to 2020, I have no riverine floods with complete data on the disaster magnitude or the provinces affected before 1980.

3.4.1 Fatalities

Table 3.1 shows the regression results for the fatality function using all countries. Column 1 shows results for the cross-sectional regression. Columns 2 and 3 display year- and region-fixed effects, respectively. Column 4 contains both year- and region-fixed effects. I use the t-statistic on observed coefficients to test if estimated elasticities are statistically different from zero.

The sign of the estimated elasticity for the intensity of the floods is positive, as expected. Fatalities rise with higher flood intensity. I find evidence of solid adaptation to fatalities through the income level for all specifications, with $-0.351 < \alpha_3 < -0.165$. I reject the null hypothesis that the income elasticity is equal to zero for all specifications and reject at the 95% confidence level the more conservative specification in column 4. I also find evidence of adaptation to fatalities with respect to population density $\alpha_2 < 1$. Even though the elasticity of population density is positive (fatalities increase when the flood hits densely populated areas), the fatalities per person fall. This may be due to the more significant deployment of flood protection measures in more urbanized provinces (Ferreira et al., 2013). Kellenberg and Mobarak (2008) also speculate that in metropolitan areas, disaster risk may be mitigated by larger numbers of people having access to more adequate economic and social institutions, well-designed infrastructure, and thoughtful urban planning not found in more rural areas. Using the F-test, I reject the hypothesis that the estimated elasticities of population density and GDP per capita are equal to 0 and 1, respectively, with 99% confidence. This is a strong sign of the presence of adaptation to flooding fatalities.

I find a divided result for the impact of average flood depth experience. The coefficient on the frequency of high-intensity floods is positive, $\alpha_6 > 0$, implying that people are not adapting to more frequent intense floods. Instead, I find the opposite result for the frequency of low-intensity floods. Although the link seems weak, the elasticity of fatalities to the frequency of low-intensity floods is negative in all specifications and significantly different from 0 with the region and region-year fixed effects. Jongman et al. (2015) find comparable results in the literature on floods. However, these results contradict the finding of Hsiang and Narita (2012) and Bakkensen and Mendelsohn (2016) for tropical cyclone frequency, who find an

adaptation to intense and less frequent events but a maladaptation to the smaller and more frequent storms. Although they don't thoroughly make the distinction between low- and high-intensity floods, Kocornik-Mina et al. (2020) find that cities fully recover from a major flood within a year, suggesting there is no significant adaptation, at least in the sense of relocation of economic activity away from the most vulnerable locations. The adaptive investments, improved warning signals, and evacuation strategy developed along the flooding experience seem to work well for low-intensity floods. Still, they are insufficient for high-intensity floods that may require a structural reorganization of the economic activity.

Table 3.1: Evidence of adaptation to fatalities

	Base	Year FE	Region FE	Year&Region FE
	(1)	(2)	(3)	(4)
Ln km^2 flooded	0.168^{***}	0.189^{***}	0.128^{***}	0.148^{***}
	(0.027)	(0.030)	(0.026)	(0.025)
Ln pop. density	0.370^{***}	0.371^{***}	0.211^{***}	0.211^{***}
	(0.046)	(0.048)	(0.054)	(0.050)
Ln GDP pc	-0.351^{***}	-0.317^{***}	-0.250^{***}	-0.165^{**}
	(0.047)	(0.047)	(0.078)	(0.073)
Ln low flood depth	-0.008	-0.014	-0.075^{*}	-0.083^{*}
	(0.051)	(0.052)	(0.043)	(0.043)
Ln high flood depth	0.144^{**}	0.131^{*}	0.130^{**}	0.112^{**}
	(0.066)	(0.068)	(0.056)	(0.056)
Constant	1.562^{***}	-2.459^{***}	2.954^{***}	-1.365^{***}
	(0.527)	(0.612)	(0.505)	(0.404)
Observations	1,411	1,411	1,411	1,411
R^2	0.247	0.293	0.334	0.382

Notes: Dependent variable: log fatalities. FE = fixed-effects. All specifications have robust standard errors clustered at the country level. $^{*}p<0.1$; $^{**}p<0.05$; $^{***}p<0.01$.

To parallel results by Ferreira et al. (2013), I find that controlling for unobserved region effects and clustering of standard errors impact results for the elasticity of fatalities during a flood event. Yet, I don't find the significance of the role of

population or income drops by adding these components to the analysis. Controlling for unobserved region fixed effects reduces the size of these coefficients, but they remain significant in my specification.

In Appendix A.2.3, I provide evidence of adaptation to fatality risk using a negative binomial model. Unlike Ferreira et al. (2013), who also use this modeling approach, I again find that GDP per capita and population density still have a significant effect on fatality risk. I see two possible explanations. First, we do not use the same data source. We don't look at the same types of floods. Although I focus on river floods, they have confounding effects from other types of floods (flash or coastal floods), which may cause results to differ. Second, they emphasize the role of governance quality in their study, whereas I take it as a by-product of GDP per capita and follow the theoretical structure of Section 3.2 for my empirical model.

3.4.2 Damages

Table 3.2 shows the results of the damage regressions using data from all countries. The column specifications are identical to Table 3.1.

Again and as expected, damages increase with the intensity of the flood ($\beta_1 > 0$). There is also evidence of adaptation in the income elasticity of damages. The income elasticities vary from 0.275 to 0.336 and are significantly less than one (β_3) in all specifications. These results reinforce the findings by Jongman et al. (2015) and Sauer et al. (2021). In their correlation analysis, both studies find that rising per-capita income coincides with a global decline in vulnerability to flooding risk between 1980 and 2010. The population elasticity varies between 0.437 and 0.518. These values are all significantly less than one ($\beta_2 < 1$). As population density increases, damages increase but less than proportionally. It is again a sign of adaptation. I perform an F-test and reject at the 99% confidence level that β_2 and β_3 are jointly equal to 1.

Similar to my results on fatalities, the coefficient on the frequency of high-intensity floods is positive. It even displays higher values of maladaptation ($0.362 < \beta_6 < 0.462$) from high flood depth experience. The coefficient on the frequency of low-intensity floods is negative, as for the fatalities, but this time I fail to reject

the null hypothesis of no adaptation ($\beta_5 \neq 0$). These results reinforce the findings by Jongman et al. (2015) and Sauer et al. (2021) on adaptation to flood risks and highlight the difference with the adaptation to cyclone risk again. As we noted before on fatality risk, this may be partly attributable to the non-reallocation of assets even after major events (Kocornik-Mina et al., 2020). Jongman et al. (2015) also attribute these effects to flood protection measures: large events may overrun existing protection measures and cause enormous damage, whereas the exposed elements may still benefit from partial protection during smaller events.

Table 3.2: Evidence of adaptation to damages

	Base	Year FE	Region FE	Year&Region FE
	(1)	(2)	(3)	(4)
Ln km^2 flooded	0.204***	0.255***	0.182**	0.235***
	(0.066)	(0.081)	(0.071)	(0.080)
Ln pop. density	0.485***	0.518***	0.437***	0.461***
	(0.087)	(0.097)	(0.128)	(0.128)
Ln GDP pc	0.275***	0.335***	0.291*	0.336*
	(0.098)	(0.098)	(0.164)	(0.200)
Ln low flood depth	−0.082	−0.088	−0.130	−0.101
	(0.109)	(0.116)	(0.113)	(0.105)
Ln high flood depth	0.410***	0.403***	0.462***	0.362**
	(0.148)	(0.155)	(0.156)	(0.144)
Constant	4.007***	2.208	4.073***	3.813*
	(1.354)	(1.757)	(1.497)	(2.077)
Observations	616	616	616	616
R^2	0.163	0.230	0.242	0.311

*Notes: Dependent variable: log damages. FE = fixed-effects. All specifications have robust standard errors clustered at the country level. *p<0.1; **p<0.05; ***p<0.01.*

These results on the elasticity of damages to intense climate experience may be particularly worring in light of the increasing trend in frequency and intensity of flood events due to climate change (Masson-Delmotte et al., 2021). Until now, trends in damages are dominated by increasing exposure and modulated by changes

in vulnerability (Jongman et al., 2015; Tanoue et al., 2016; Sauer et al., 2021). But Sauer et al. (2021) find, in specific areas, a statistically significant impact of climate change as a driver of flood-induced damages over the period 1980-2010. The maladaptation of economies to intense flooding events may increasingly threaten the insurability of assets and the population's well-being.

3.4.3 Adaptation across income levels

A higher GDP per capita allows for more investments in disaster risk reduction measures, better building quality, and better communication (Jongman et al., 2015). It is reasonable to think that adaptive capacity increases with income, and it is the results by Bakkensen and Mendelsohn (2016) for cyclone risks. In Tables 3.3 and 3.4, I examine whether the adaptation elasticities for fatalities and damages in low- ($<$ \$5000) versus high-income ($>$ \$20000) locations. The low-income areas come from the least developed countries and poor rural areas of emerging countries. The income per capita of the locations is the one in the year before the observed flood. Therefore provinces can move in and out of the income definitions through development, and the income loss due to the flood may not confound the measure of the province's income.

I find that GDP per capita is less critical for the adaptation to the fatality risk of flooding in high-income provinces. Although the elasticities of GDP per capita are negative in high-income provinces, they are not statistically different from zero. They are higher than the elasticities of GDP per capita in low-income provinces. A higher income helps to adapt to flood risk but only to a certain extent. High-income regions don't seem to keep adapting to fatality risk with their economic development. This result goes against the finding of Bakkensen and Mendelsohn (2016) for the case of cyclone risk but is consistent with the findings by Tanoue et al. (2016) on river flood risk. The latter find mortality rates in higher-income countries did not show significant changes in recent decades, while those in lower-income countries showed a negative trend. Jongman et al. (2015) find that over the years 1980-2010, the average mortality and loss rates in lower-income countries have declined relatively faster than in higher-income countries. The greater importance of GDP per capita for the adaptation to flooding risk in low-income locations may

be one of the factors driving this relative convergence of vulnerability between developing and developed countries.

There is, however, a better and more significant adaptation to the low-intensity floods in high-income versus the low-income locations ($\alpha_5 < 0$ for the high-income group). The low-income group shows no clear sign of adaptation to low-intensity flooding. On the adaptation to high-intensity flooding, both groups show signs of mild maladaptation like in the sample of all countries we analyze in Section 3.4.1. The flood-control measures that high-income locations implement may lower fatalities from frequent and low-intensity flooding. But they also increase the probability of catastrophic events (White, 1975; Ferreira et al., 2013).

Table 3.3: Evidence of adaptation to fatalities in across low- and high-income groups

	$>$ \$20000 Base	$>$ \$20000 Year&Region FE	$<$ \$5000 Base	$<$ \$5000 Year&Region FE
	(1)	(2)	(3)	(4)
Ln km^2 flooded	0.118***	0.110***	0.170***	0.172***
	(0.023)	(0.026)	(0.031)	(0.030)
Ln pop. density	0.255***	0.163***	0.331***	0.175***
	(0.065)	(0.062)	(0.051)	(0.060)
Ln GDP pc	−0.137	−0.122	−0.297***	−0.248***
	(0.273)	(0.269)	(0.108)	(0.107)
Ln low flood depth	−0.173**	−0.322***	0.041	−0.073
	(0.078)	(0.124)	(0.058)	(0.052)
Ln high flood depth	0.144	0.237**	0.163**	0.136*
	(0.107)	(0.104)	(0.077)	(0.076)
Constant	1.406	2.464	0.958	-1.099*
	(3.060)	(3.431)	(0.827)	(0.564)
Observations	183	183	968	968
R^2	0.189	0.475	0.187	0.361

*Notes: Dependent variable: log fatalities. FE = fixed-effects. All specifications have robust standard errors clustered at the country level. *p<0.1; **p<0.05; ***p<0.01.*

In Table 3.4 like in Table 3.3, the elasticity of risks to population density are in

the order of magnitude between high- in low-income groups. The income elasticity of damage for high- and low-income locations is statistically below one (99% confidence level). Both income groups show signs of adaptation through their income level. The coefficients tend to be even lower for high-income provinces, but the estimates' variance is too high to tell. To test for the potential difference between the income elasticities across income groups, I run a new model, similar to the model 3.4 but with the interaction between income groups and GDP per capita instead of running the two regressions separately. I cannot reject the null hypothesis of the coefficients being the same between the two groups (i.e., the interaction coefficient is null). The elasticity coefficients on climate adaptation are also not statistically different from zero. All included, I fail to accept the hypothesis that locations show increasing signs of adaptation to economic damages with income.

Table 3.4: Evidence of adaptation to damages across low- and high-income groups

	$>$ \$20000 Base	$>$ \$20000 Year&Region FE	$<$ \$5000 Base	$<$ \$5000 Year&Region FE
	(1)	(2)	(3)	(4)
Ln km^2 flooded	0.281***	0.409***	0.235***	0.245**
	(0.088)	(0.134)	(0.079)	(0.110)
Ln pop. density	0.496***	0.445***	0.402***	0.393*
	(0.128)	(0.130)	(0.132)	(0.207)
Ln GDP pc	−0.344	−0.666	0.077	0.462*
	(0.493)	(0.698)	(0.184)	(0.271)
Ln low flood depth	−0.191	−0.035	0.093	0.119
	(0.229)	(0.265)	(0.181)	(0.203)
Ln high flood depth	0.394	0.181	0.324	0.185
	(0.307)	(0.299)	(0.201)	(0.225)
Constant	10.606**	9.971	4.498*	4.476
	(5.200)	(6.555)	(2.312)	(2.975)
Observations	112	112	387	387
R^2	0.130	0.513	0.180	0.360

*Notes: Dependent variable: log damages. FE = fixed-effects. All specifications have robust standard errors clustered at the country level. *p<0.1; **p<0.05; ***p<0.01.*

3.4.4 Adaptation across urban versus rural areas

In this section, I analyze the adaptation to flooding risk across groups of different population densities, the second dimension of the exposures. I follow Bakkensen and Mendelsohn (2016) and define urban locations as the ones with a population density of more than 200 people per km^2. The rural areas have a population density below this 200 people per kilometer squared threshold. Tables 3.5 and 3.6 present the results for the adaptation to fatality and damage risk, respectively.

Table 3.5: Evidence of adaptation to fatalities in rural and urban locations

	Rural Base	Rural Year&Region FE	Urban Base	Urban Year&Region FE
	(1)	(2)	(3)	(4)
Ln km^2 flooded	0.137***	0.121***	0.225***	0.254***
	(0.022)	(0.019)	(0.065)	(0.062)
Ln pop. density	0.366***	0.325***	0.076	−0.119
	(0.058)	(0.055)	(0.151)	(0.168)
Ln GDP pc	−0.300***	−0.208***	−0.367***	0.028
	(0.050)	(0.084)	(0.107)	(0.100)
Ln low flood depth	−0.094*	−0.107*	0.162	−0.273**
	(0.049)	(0.044)	(0.108)	(0.132)
Ln high flood depth	0.188***	0.168***	0.0002	0.153
	(0.072)	(0.061)	(0.140)	(0.152)
Constant	1.885***	2.750***	2.256	−0.166
	(0.515)	(0.747)	(1.594)	(1.669)
Observations	1,020	1,020	391	391
R^2	0.174	0.303	0.394	0.516

*Notes: Dependent variable: log fatalities. FE = fixed-effects. All specifications have robust standard errors clustered at the country level. *p<0.1; **p<0.05; ***p<0.01.*

I find that the population density of urban areas doesn't affect fatalities. Not only the elasticity of deaths to population density is below one, but it also is not significantly different from having no effect. Kellenberg and Mobarak (2008) and Ferreira et al. (2013) find similar patterns concerning the impact of urban population

on a country's mortality rate after a flood. Rural areas also show signs of adaptation to the risk with increasing population density, although less pronounced ($0.325 ¡ \alpha_2 < 0.366$ for rural areas). Less densely populated areas seem more vulnerable to the risk of intense flooding (which is not the case for urban locations) but adapt better to increasing GDP per capita than densely populated areas. Since both sub-samples combined constitute the whole dataset, I conclude that rural areas are the primary driver of maladaptation to fatalities risk in case of extreme flood events.

Table 3.6: Evidence of adaptation to damages in rural and urban locations

	Rural Base	Rural Year&Region FE	Urban Base	Urban Year&Region FE
	(1)	(2)	(3)	(4)
Ln km^2 flooded	0.109*	0.083	0.441***	0.604***
	(0.059)	(0.068)	(0.109)	(0.154)
Ln pop. density	0.231*	0.317**	0.464*	0.895**
	(0.118)	(0.149)	(0.239)	(0.372)
Ln GDP pc	0.371***	0.425**	0.296**	−0.098
	(0.104)	(0.197)	(0.137)	(0.573)
Ln low flood depth	−0.014	0.010	−0.213	−0.669***
	(0.111)	(0.120)	(0.211)	(0.190)
Ln high flood depth	0.154	0.255	0.705***	0.693***
	(0.153)	(0.179)	(0.212)	(0.220)
Constant	5.458***	4.827*	1.677	3.185
	(1.399)	(2.822)	(3.083)	(4.069)
Observations	427	427	189	189
R^2	0.092	0.293	0.288	0.529

*Notes: Dependent variable: log damages. FE = fixed-effects. All specifications have robust standard errors clustered at the country level. *p<0.1; **p<0.05; ***p<0.01.*

Although rural areas don't adapt to extreme flood events, they seem less vulnerable to the flood's intensity. The elasticity coefficient of fatalities to km^2 flooded is two times bigger in urban areas than rural ones. Bakkensen and Mendelsohn (2016) also find urban locations are more vulnerable to more intense storms with a similar

order of magnitude. This difference in vulnerability to flooding intensity is even more pronounced for damage risk. Table 3.6 shows estimates of vulnerability to floods' intensity that are four to six times larger in urban compared to rural areas. It again goes in the same direction as the results by Bakkensen and Mendelsohn (2016) for cyclone risks, although I find a greater difference in the case of flood risk.

I also find that urban locations are the main drivers of the overall maladaptation to intense flood experiences in the case of damage risk. Yet, with year- and region-fixed effects, urban locations also seem to adapt better than rural areas to damage risk from less intense floods probability. From a policy perspective, the improved forecasting, warning, and evacuation methods, along with urban planning, developed to reduce the risk of high-probability low-intensity floods, may have created a false sense of security toward less frequent but more intense events.

3.4.5 Robustness

In this section, I provide details on the robustness of the results. My dataset of river floods contains only 1,411 events that I can exploit. The relatively low number of observations is a typical limitation in the literature on natural catastrophes (Kahn, 2005; Nordhaus, 2010; Hsiang and Narita, 2012; Ferreira et al., 2013; Jongman et al., 2015; Bakkensen and Mendelsohn, 2016). This gives little room for sub-sampling analysis. However, the alternative estimations I propose in this section (and further details in the Appendices) indicate my main results are consistent and robust across the different methods. At last, I deepen the analysis for the particular case of the United-States.

Alternative estimations

I test and find that the logarithm of damages follows a normal distribution: the Kolmogorov-Smirnov test has a $p-$value of 0.27, indicating the data is not significantly different from a normal distribution at a typical significance level of 0.01. The OLS regression on the log of damages I use in the main analysis is appropriate.

I test an alternative estimator for the fatalities in Appendix A.2.3. Since the number of deaths is a count variable, not normally distributed, I estimate semi-log regressions with a negative binomial estimator. Like Bakkensen and Mendelsohn

(2016), I test for and find evidence of over-dispersion in the data, implying that one prefers the negative binomial estimator to the Poisson. Some of the fixed effects negative binomial results can be more easily compared to results by Ferreira et al. (2013) as they use this same model specification. Overall, results from this alternative model specification don't change the main conclusions from Section 3.4.1. But one should interpret fixed effects negative binomial results with caution; there is still some debate in the literature about the proper implementation of fixed effects in these models (Greene, 2007).

Additionally, I provide elasticities of fatalities and damages by income into five different income bins in Appendix A.2.4. Overall, these additional results confirm the ones of Section 3.4.3. Results for fatalities also show some additional dynamics concerning the adaptation to fatality risk in the middle-income range. The distribution of elasticity coefficients follows a U-shaped curve where adaptation increases (i.e., the coefficient is lower) for the 5,000-10,000 2015 $USD income per capita bin before decreasing back (i.e., the coefficient increases). These dynamics go opposite to the findings by Ferreira et al. (2013), who find an inverse U-shape relationship between income and fatalities.

The damage function in the United States

Previous studies on damage functions from cyclones have noted the damage in the United States (U.S.) appears to be an outlier compared to the rest of the world (Hsiang and Narita, 2012; Bakkensen and Mendelsohn, 2016). Bakkensen and Mendelsohn (2016) find the damage function of the USA is significantly different than the rest of the world, but the fatality function is not. They find that damage per storm would fall from $2 billion to $166 million if the U.S. damage function had the same damage coefficients as other OECD countries.

Consequently, I first test whether the damage function of the U.S. differs from that of the rest of the world. I conduct a Chow test for the equality of regression functions across two groups: the U.S. and the rest of the world, for both the damage and fatalities functions. I fail to reject the null hypothesis of equality of damage and fatality functions across the two groups with a $p-$value of 0.437 and 0.676, respectively.

I then follow Bakkensen and Mendelsohn (2016) and compare the U.S. with the other OECD countries. This analysis is more careful because it compares countries with similar levels of development. I again fail to reject the null hypothesis of equality of damage and fatality functions between the U.S. and other OECD countries. From a policy perspective, adaptation policies in the U.S. seem more effective in the case of river floods than in the case of cyclones.

3.5 Conclusion

This study uses a holistic framework to test adaptation to damage and death caused by river flooding. The theoretical underpinnings of this work come from the risk equation regularly used in the natural disaster literature. To analyze risk, I must highlight the links between vulnerability and the other two components of the risk equation: hazard and exposure. This foundation allows us to use the framework developed by Bakkensen and Mendelsohn (2016) to test for the presence of adaptation.

I perform an empirical analysis by combining EM-DAT data on fatalities, damages, disaster intensity, and river flood locations with GDP and population data from 1,800 administrative regions worldwide from 1980 to 2020. This study is one of the first to use EM-DAT data at the sub-national level. I use each river flood as a separate observation and regress the damage and fatalities on river flood intensity, population density, GDP per capita, and the long-term average flood depth in the affected areas. Sitting on the shoulders of Bakkensen and Mendelsohn (2016), I identify adaptation by comparing the empirical parameters of the damage and death regressions to the hypothetical values of the parameters that would be expected in the absence of adaptation.

I find that economies decrease their vulnerability to river flood risk in terms of deaths and damages as they become richer, which confirms the current literature. This work adds to previous studies that overlooked a potentially important role of flood exposure. While provinces adapt to the risk of death and damage when regularly affected by low-intensity floods, they adapt poorly to rare and intense floods.

I then conduct a similar analysis by dividing my data into sub-samples by income

and population density. Deficient adaptation to the risk of death to low-frequency, high-intensity floods is present in rich and poor regions. On average, urban areas are more sensitive to flooding intensity than rural areas.

Although the study clarifies the various factors that drive adaptation to river flood risk, it lacks crucial information regarding the specifics of the adaptation measures. Future work may focus on the causal relations between adaptation measures and vulnerability reduction. Does a specific land-use policy reduce vulnerability to river flood risk? Does a higher insurance premium raise private adaptation? If a city implements river flood protections, does it also increase the neighboring cities' protection? If so, is there a free-riding risk in adaptation?

Chapter 4

Misfortunes Never Come Singly: Managing the Risk of Chain Disasters[1]

Abstract

The recent COVID-19 pandemic has confirmed two facts: First, a large initial disaster, the pandemic, can trigger a whole chain of secondary economy-wide disasters, like a domino effect. Second, governments worldwide implemented disaster-mitigation efforts only after the gravity of the pandemic became evident instead of taking preventive measures ahead of time. In this chapter, we question the optimality of such a "reactive" approach to disaster management by studying disaster-prevention and growth policies in an environment where a primary shock to the economy may provoke future calamities through contagion effects. We develop a novel dynamic stochastic framework where disasters follow a Hawkes process. We derive analytical solutions and show that the optimal policy devotes a stochastic fraction of the output to disaster mitigation. The mitigation propensity is an increasing function of the Hawkes intensity and essentially tracks disaster arrivals. The latter implies that the policy is indeed reactive. This result contrasts with the existing literature, which does not consider the possibility of contagion and therefore finds a constant mitigation propensity optimal.

[1]This chapter is joint work with Alexandra Brausmann, Lucas Bretschger, and Aleksey Minabutdinov.

4.1 Introduction

The COVID-19 pandemic has confirmed the old saying: misfortunes never come singly. A cascade of economic and social disruptions caused by the disease outbreak aggravated the loss of human lives due to the virus. While the COVID-19 pandemic is a vivid example of how one initial disaster, the pandemic, can trigger further calamities with hefty economic losses, it is by far not unique. There are plenty of other examples where one catastrophe, be it a war, a financial crisis, or a natural disaster, triggers a chain of interlinked shocks to economic activity, ecosystems, and humans. For example, an initial earthquake might cause secondary disasters such as a tsunami, a landslide, a fire, or a loss of infrastructure and human lives. Financial distress in one economy may cause a contagion effect through interlinked markets and even result in a global financial crisis.[2] A key policy question is how a government should deal with the possibility of disasters capable of causing cascades of shocks to economic activities, substantial financial losses, and impediments to growth and development. In other words, what are the optimal disaster-mitigation policies in the presence of contagion effects? In this work, we answer these and related questions using a novel methodology that allows us to explicitly introduce contagion effects in a stochastic and dynamic macroeconomic framework.

Several empirical observations concerning the critical features of rare disasters, especially those that arise following some initial trigger shock, motivate our theoretical model. A notable trait of these secondary perils is that they do not arrive at regular intervals but tend to cluster in time as a cascade of events after the initial trigger. For instance, only six days after the onset of hurricane Katrina, New Orleans experienced levee failure, followed immediately by an electrical chain blackout, cell phone station malfunction, business collapse, medical care scarcity, security problems, and violence. Likewise, in a matter of weeks, the COVID-19 pandemic put enormous strain on national healthcare systems resulting in partial breakdowns because intensive care units were in insufficient supply. Travel restrictions and disruption of supply chains followed shortly, resulting in rising unemployment and

[2]Examples include the Asian crisis of 1997, which started in Thailand and spread to practically every Asian economy; the Russian crisis of 1998, which affected many Eastern-European economies; and, of course, the global financial crisis of 2008.

overall economic draw-down. Other examples include the Chernobyl 1986 nuclear plant catastrophe, which caused a nuclear cloud over Europe, an agriculture crisis, and radiation-related diseases. The 2011 Tohoku earthquake resulted in Fukushima nuclear accident and associated perils.

To illustrate the contagion and clustering effects during the COVID-19 pandemic, we plot in Figure 1 the weekly COVID cases and deaths count[3] (left panel) and the weekly GDP index (right panel) in the Euro area from 2020 till the second quarter of 2022.[4] The three shaded areas in panel (b) indicate the drops in GDP following the respective waves of spiking COVID-19 cases visible in panel (a). The figure also shows that declines in GDP during the later periods were less pronounced than the first drop, despite a large number of cases during that period, potentially due to the effects of policies and the weakening of the virus.

Figure 4.1: Illustration of contagion effect during the COVID-19 pandemic

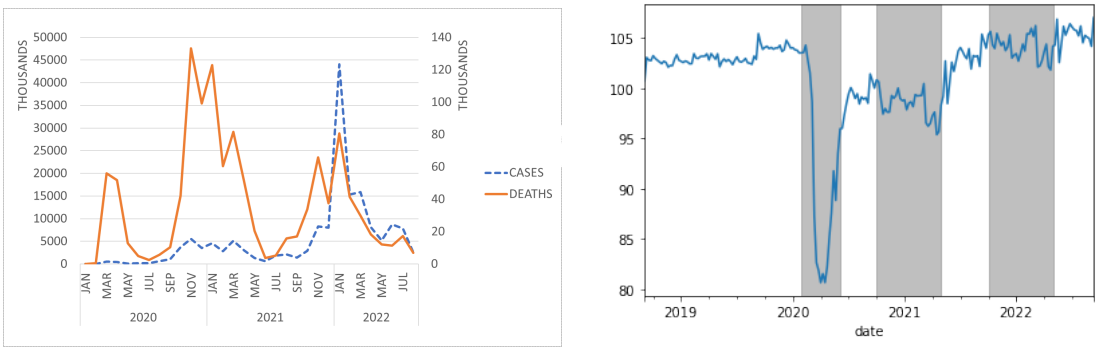

(a) COVID cases and deaths in Europe **(b)** Weekly GDP index of the Euro area

Another notable feature associated with large-scale interlinked disasters, which the literature has yet to uncover, is that measures aimed at mitigating their effects tend, in practice, to have a reactional, as opposed to precautionary, character. An excellent example to illustrate this point is again the recent COVID-19 pandemic. Even though many countries had provisions in their legislation requiring a sufficient

[3]We aggregate the data from:
https://opendata.ecdc.europa.eu/covid19/nationalcasedeath/csv/data.csv.

[4]Source: author's calculation using weekly GDP data for European countries from Year-On-Year OECD tracker. Available at https://www.oecd.org/economy/weekly-tracker-of-gdp-growth/. We show the GDP data starting at the end of 2018, and the fluctuations related to the virus begin from January 2020.

amount of medical supplies to be available in stock for the case of an emergency (like a pandemic), when the pandemic did occur, it turned out that supplies of even the most basic equipment, such as surgical masks and protective suits, not to mention hospital beds, were lacking. This outcome questions whether incurring sunk costs associated with keeping equipment stocks and maintaining extra intensive care units as a precaution was deemed unjustified, given the very low historical probability of a pandemic. Yet, once a pandemic did occur, governments had to take (sometimes) draconian measures to contain the spread of the virus. Travel restrictions and multiple lockdowns, resulting in school closure and business failure, forced governments worldwide to deploy substantial aid packages to support at least parts of the population financially. In Wuhan, China (the province considered to be the origin of the pandemic), the authorities built an entire hospital for up to 1,000 patients from scratch in just ten days. Mask production in China alone has been ramped up by a whopping 450% from 2019 to 2020. Around the world, the production of quick antigen tests has gone up multiple-fold as well. Several vaccines have been developed in a record-breaking time of approximately one year (for comparison, the fastest vaccine ever developed before took four years). Given such a last-minute increase in government spending to contain the spread of the virus, as opposed to taking precautionary measures ahead of time,[5] raises the question of whether such a response is indeed justified in the context of rare calamities which may trigger a chain of further *highly damaging* shocks to the economy.[6] How should the government optimally choose its disaster mitigation or prevention policies? Is there a rational justification for the reactional approach, or will society fare better if it takes timely precautionary measures?

To answer the above questions and to highlight the dynamic and long-term nature of the problem at hand, we develop a general equilibrium growth model

[5]Already more than a decade ago, some economists and ecologists called for paying more attention to incorporate the possibility of a pandemic in economic analysis (e.g., Ehrlich (2008)). Other scientists even explicitly referred to a chance of a significant coronavirus outbreak several years before the onset of COVID-19 (e.g., Cheng et al. (2007)).

[6]In the case of earthquakes, Daniell et al. (2017) find that 40 percent of economic losses and deaths result from secondary effects rather than the shaking itself. According to the Swiss Re Institute's annual review of natural catastrophes and man-made disasters, more than 60 percent of the USD 76 billion of insured natural catastrophe losses in 2018 were due to "secondary peril" events.

with multiple interrelated risks. The economy accumulates a productive input, e.g., a capital stock, through endogenous investment decisions. The capital stock is subject to damages from randomly arriving disasters. In addition, one disaster may trigger a whole chain of interlinked disasters, producing a contagion effect. We can introduce and analyze contagion effects by modeling disaster arrivals via Hawkes processes, which possess a self-excitation mechanism. Economic activity generates a negative externality (e.g., carbon emissions, intensive food production, or simply opportunistic behavior) which increases the size of the damage when a disaster strikes. Society can reduce losses by spending part of the output on mitigation measures. In the case of climatic disasters, for example, the policy would be emissions abatement; in the health sector, it can promote vaccination and a healthy lifestyle; in the financial industry, it would set the correct incentives to reduce opportunistic behavior or regulation of reserve requirements. Our main finding is that the presence of contagion among disasters warrants a particular type of disaster-management policy. Contrary to the existing literature, which looks at multiple but independent shocks, we find that the optimal mitigation propensity is not constant but stochastic. It tracks the disaster arrivals, which is consistent with the reactional policies we have observed during pandemics and some major disaster-relief programs.

Related literature

There is abundant literature studying optimal policies under uncertainty and society's willingness to pay to avoid it. In their seminal contribution, Brock and Mirman (1972) developed the first optimizing growth model with unpredictable shocks. It has been widely used in the macroeconomics literature to derive the dynamic effects of shocks on output. However, a limiting fundamental assumption of the model is that capital fully depreciates within a period. Considering capital as a stock variable, Wälde (2011) and Sennewald and Wälde (2006) derive optimal economic growth and precautionary savings under Poisson uncertainty associated with capital returns. Based on a representative-consumer model including rare disasters, Barro (2009) finds that the welfare cost from small-scale economic fluctuations is about 1.5 percent yearly. In comparison, society would willingly reduce GDP by

around 20 percent yearly to eliminate all rare disasters.[7] However, the macroeconomic literature has yet to address the broad topic of interrelated shocks, and the present work aims to fill this gap.

A large environmental economics literature also studies mitigation and abatement policies aimed at limiting environmental and climate change risks. According to the IPCC reports, climate change is causing an intensification of natural disasters and their more frequent occurrences (Masson-Delmotte et al., 2021). For instance, the frequency of hurricanes in the United States has risen from 1.6 per year in the 1970s and the 1980s to 3.1 - 3.8 per year in the 2000s and 2010s.[8] At the same time, the severity of major natural disasters in the U.S., in terms of average yearly economic damages, has gone up from $20.2 billion in the decade 1980-1989 to $152.6 billion in 2021.[9] Therefore, reducing emissions of greenhouse gases is necessary not only to limit Earth warming *per se* but also to prevent future economic losses from climate-driven disasters, including tipping points.[10] The environmental economics literature featuring stochastic climate shocks has been shaped by the pioneering contributions of Tsur and Zemel (1996, 1998). It proposed optimal policies to deal with climate risks, numerous approaches to estimate the social cost of carbon, and also provided quantitative results.[11] Tsur and Zemel (1996, 1998) introduce the notion of an uncertain pollution threshold beyond which the economy collapses (or switches to a new regime that yields very low welfare) and show that the optimal abatement policy is strongly precautionary, in the sense that it is geared to avoiding the threshold. That optimal emission taxes reduce environmental risks but do not eliminate them as explained in Tsur and Zemel (2008). Tsur and Zemel (2009) find that disaster hazard rates affect discounting of households and thus optimal

[7]Bloom (2009) offers a structural framework to analyze the impact of large shocks on subsequent uncertainty at the firm level but does not explain why this secondary uncertainty should arise.

[8]Source: https://www.statista.com/chart/11009/hurricanes-over-the-atlantic-basin/.

[9]The major disasters are the so-called Billion-Dollar disasters, which include those that caused at least $1 billion in damages. Source: https://www.ncei.noaa.gov/access/billions/summary-stats

[10]The issue of tipping points has been investigated by Dietz et al. (2021) and Lemoine and Traeger (2014).

[11]Early contributions to the topic of catastrophic events include Van Long (1975); Cropper (1976); Reed (1984); Reed and Heras (1992); Clarke and Reed (1994). Applications to climate policy are provided in De Zeeuw and Zemel (2012) and van der Ploeg and de Zeeuw (2018), where different hazard functions and types of uncertainties are used.

environmental policy in an intertemporal framework with exogenous growth.[12] Yet, this strand of literature often assumes that the shock (or crossing of an uncertain threshold) leads to an irreversible change of the system dynamics or even a total economic collapse. While certain special situations call for such a framework, it appears to be limiting for answering our questions. Importantly, recurring and interlinked shocks represent a more relevant description of reality. Disasters may be large but must not be fully destructive or irreversible.[13]

Multiple large, yet independent, shocks to the economy are considered in Martin and Pindyck (2015) where cost-benefit analysis is applied to derive society's willingness to pay for avoiding them. The authors find that it may be optimal to mitigate only a subset of shocks and do nothing about the rest. Multiple threats with endogenous hazards are studied in Tsur and Zemel (2017) in an intertemporal approach. They, too, derive the willingness to pay for mitigation policies assuming an exogenous income stream for consumption and abstracting from linkages between disasters. The more recent literature incorporating endogenous growth has shown that the optimal policy in the presence of recurring (but independent) environmental shocks and tipping points consists of spending a constant fraction of output on mitigation, with more severe shocks requiring a larger mitigation propensity (Bretschger and Vinogradova (2019), Bretschger and Vinogradova (2018), Douenne (2020)).[14] Although the latter strand of literature acknowledges the importance of multiple disasters, it treats each one as a separate event and models disaster arrivals via independent jump processes (e.g., Poisson process) or jump-diffusions, which precludes the analysis of contagion effects.

The present chapter complements the existing literature because we also study multiple and recurring disasters. A significant difference is that we relax the assump-

[12] A recent multi-region model by Brock and Xepapadeas (2021) analyzes the climate policy under deep uncertainty, which includes ambiguity about alternative models, on the one hand, and model misspecification, on the other hand.

[13] The contribution of Bretschger and Vinogradova (2019) derives optimal policies in the presence of pollution-induced health shocks in a growing economy that harm individual welfare. There is also a growing literature attempting to incorporate pandemics into economic analysis and to derive implications for pandemic-management policies using SIRD type of models (e.g., Acemoglu, D., and V. Chernozhukov and I. Werning and M. Whinston (2021) and Ferraro and Peretto (2020)). Brock and Xepapadeas (2020) offer a general framework where a risk of epidemic coexists with environmental change.

[14] See also Golosov et al. (2014).

tion of shock independence and model an initial shock as a trigger for future arrivals. This novel approach has the advantage of being rather general; it can be applied to study optimal disaster management in various fields, including macroeconomics, health economics, and environmental economics. While this approach is relatively new in the economics literature, it has been widely used in other disciplines, such as, for instance, financial mathematics and portfolio theory in finance. For example, Aït-Sahalia and Hurd (2015) show that introducing a contagion effect among asset prices in a standard partial equilibrium CAPM model leads to stochastic portfolio shares being optimal. Yet, one drawback of the financial models is that they are partial equilibrium and, therefore, unsuitable for policy analysis. This chapter focuses on policy implications and will adopt a general-equilibrium perspective.

The remainder of the chapter is as follows. Section 4.2 describes our general setting. In Section 4.3, we add more structure to the model by assuming specific functional forms and then proceed to the analytical solution. In Section 4.4, we analyze the optimal policy under alternative scenarios concerning the prevalence of one or another type of shock. Section 4.5 discusses the results. Section 4.6 concludes.

4.2 The Model

In this Section, we describe the general setup of our model. In subsection 4.2.1, we introduce the notion of interlinked disasters and explain how we model these linkages with the help of the Hawkes process. In subsection 4.2.2, we describe the planner's optimization problem, derive the optimality conditions, and show that the solution of the maximization problem is fundamentally different from the outcomes obtained when disregarding the contagion effect among disasters.

4.2.1 The Economy and Chain Disasters: A General Specification

Time is continuous and denoted by t. At each moment t, the economy produces output $Y(K_t)$ and consumes C_t. We impose a standard set of assumptions on Y such that $Y'(K_t) > 0$ and $Y''(K_t) \leq 0$. One may think of K_t as a broadly defined

productive input such as human or man-made capital, ecosystems, and other tangibles that can be used to produce goods and services. In what follows, we shall refer to K_t as capital. The production process generates a negative externality, E_t, which harms the productive input. We assume that K_t is subject to shocks (or disasters) that arrive at random time intervals and are governed by the stochastic counting process N_t, defined below. When one such shock occurs, it destroys a fraction $\zeta_t(E_t)$ of capital, with $\zeta'(E_t) > 0$, such that the larger the externality, the larger the damages.[15] We interpret these shocks widely, including natural disasters, pandemics, wars, and other possible calamities or a sudden deterioration in socioeconomic conditions. For simplicity, we shall refer to them as "disasters" in the rest of the chapter. We also allow for continuous (smaller-scale) random fluctuations in K_t of size $\varepsilon_t(E_t)$ and mean zero, which are governed by the Brownian motion process W_t. Both stochastic processes N_t and W_t are defined on the filtered probability space $(\Omega, \mathcal{F}, \mathbb{P})$, where $\mathcal{F}$ is the filtration generated by the Brownian motion and the counting process. By spending a fraction $\theta_t \in [0, \theta_{max}]$ of output on mitigation measures, the economy can reduce the size of the externality so that $E'(\theta_t) < 0$.[16] We can therefore express the damage function as $\zeta_t = \zeta(\theta_t)$ with $\zeta'(.) < 0$ and likewise $\varepsilon = \varepsilon(\theta_t)$ with $\varepsilon'(.) < 0$.

Under the assumptions above, the law of motion of capital follows:

$$\mathrm{d}K_t = [(1-\theta_t)Y_{t-} - C_t]\mathrm{d}t - \zeta_{t-}(\theta_t)\mathrm{d}N_t + \varepsilon_{t-}(\theta_t)\mathrm{d}W_t. \tag{4.1}$$

We depart from the common assumption in the literature that disasters follow a jump process, such as the standard Poisson process with a constant intensity, and posit instead that the counting process N has an intensity given by

$$\lambda_t = \lim_{h \downarrow 0} \frac{\mathbb{E}[N_{t+h}|\mathcal{F}_t] - N_t}{h} = \bar{\lambda} + \sum_{t_j < t} \kappa(t - t_j), \tag{4.2}$$

with $\kappa(t) = \alpha e^{-\beta t}$. Here, t_j-s stand for the moments of the catastrophes, $\bar{\lambda} > 0$

[15] One may also consider a random component in the damage function, say Z with the underlying distribution f_Z. In what follows, we abstract from such random damage components to keep the exposition as simple as possible. We shall consider the role of Z in Section 4.4.4 below.

[16] The parameter θ_{max} stands for the maximal output fraction that can be spent on mitigation and is assumed to be less than 1. See also section 4.2.2.

stands for the baseline (or Poisson) intensity level, the parameter $\beta > 0$ is an exponential decay rate driving the jump intensity back to the long-run average, and $\alpha \in [0, 1)$ captures the scale impact of the jumps on the intensity dynamics.

The expression (4.2) indicates that the intensity λ_t is a sum of a weighted combination of the past jumps with weights defined by the exponential kernel (also called excitation function) and a baseline value. If $\alpha = 0$, then the counting process is a simple Poisson process with a constant intensity $\bar{\lambda}$. If $\alpha > 0$, then events are (positively) *self-exciting*. The condition $\alpha < \beta$ known as "no-explosion-condition"[17] is assumed everywhere below.

A counting process N with the intensity that solves the integral (4.2) is *a Hawkes process*.[18] In what follows, it is convenient to use (see Appendix A.3.1 for the formal derivation) the following stochastic differential equation:

$$\mathrm{d}\lambda_t = \beta[\bar{\lambda} - \lambda_t]\mathrm{d}t + \alpha \mathrm{d}N_t. \tag{4.3}$$

Neither the Hawkes process N_t, nor its intensity process λ_t is Markovian, but the process (N_t, λ_t) is. The latter property is going to be important for the model solution since it lets us use the standard Markov decision processes approach.

We provide a graphical representation of Hawkes processes in Figure 4.2. We classify events (shocks/catastrophes) either as zero-order events or first-, second-, and higher-order events. The occurrence of a zero-order event can trigger one or more first-order events, which in turn can trigger second-order events, and so on, over many generations. This process of event generation is self-exciting, meaning that the occurrence of an event increases the likelihood of future events.

One can introduce the concept of "branching ratio" in this context to describe the probability that a given event was generated endogenously (descendants to the x-order) versus exogenously (as a zero-order event).[19] More formally, we denote

[17] The term "explosion" refers to the occurrence of an infinitely large number of events in a finite amount of time. This explosion can happen with a positive probability if the rate at which events occur grows faster than the rate at which the process can dissipate the influence of past events, i.e., $\alpha \geq \beta$.

[18] The definition of a Hawkes process can be generalized to a larger class of kernels under the integral, c.f. Zhou et al. (2013).

[19] In the financial context, branching ratio was suggested to use as a measure of the level of "endogeneity of markets" by Filimonov and Sornette (2012).

Figure 4.2: The events' family representation

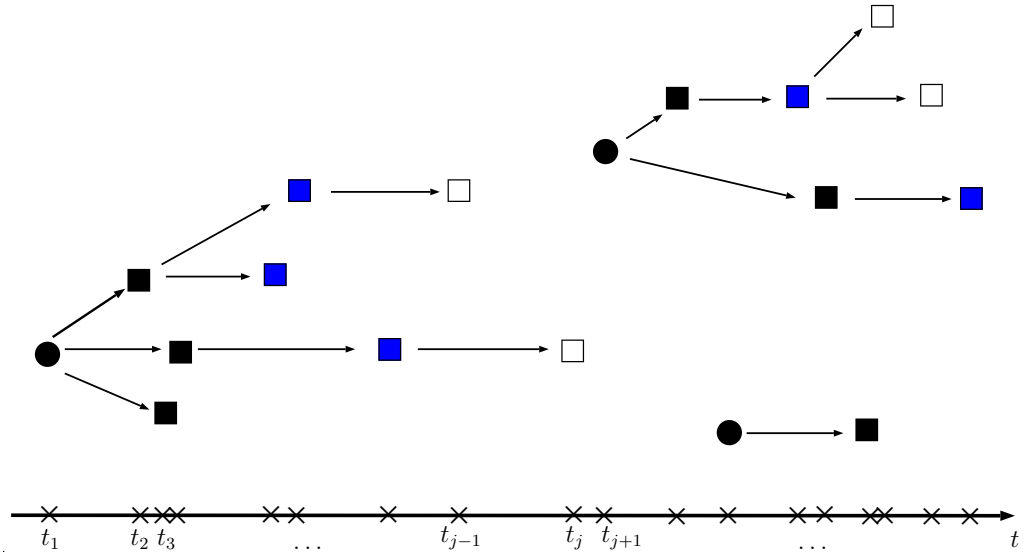

Notes: Circles denote zero-order events, while squares of different colors denote descendant events.

the branching ratio by n and define it as $n \equiv \int_0^\infty \alpha e^{-\beta s} \mathrm{d}s = \frac{\alpha}{\beta}$. One can show that when n is between 0 and 1, it equals the ratio of the number of descendants for one zero-order event to the size of their entire family (all descendants plus the original event).

4.2.2 The Planning Problem

Instantaneous utility $u(C_t, \lambda_t)$ is a three-times continuously differentiable function of the current consumption and at least once continuously differentiable function of the disaster frequency. We assume that $u_c > 0$, $u_{cc} < 0$ and $u_\lambda < 0$, with subscripts denoting partial derivatives. The latter expression reflects the fact that living in a risky environment (e.g., facing a risk of a natural disaster or a war) yields a lower utility.[20]

The Planner's problem is to maximize the expected present value of utility over an infinite planning horizon by choosing a consumption path C_t and a disaster-

[20]This assumption may also reflect a higher vulnerability or exposure to disasters being a dis-amenity.

mitigation policy θ_t given the law of motion for the capital stock and disaster arrival rate:

$$\max_{(C_t,\theta_t)} \quad \mathbb{E}\int_0^{+\infty} u(C_t,\lambda_t)e^{-\rho t}\mathrm{d}t \tag{4.4}$$

subject to equations (4.1) and (4.3).

Definition. Controls $(C_t,\theta_t)_t$ are assumed to be progressively measurable random variables. They are called *admissible* if capital stock does not vanish and $\theta_t \in [0,\theta_{max}]$.

The dynamic stochastic program leads at time t to the discounted expected utility of consumption in the form $V(K_t,\lambda_t,t)$ defined by

$$V(K_t,\lambda_t,t) = \max_{\{C_t,\theta_t;\, t\le s<\infty\}} \mathbb{E}_t \int_t^{+\infty} u(C_s,\lambda_s)e^{-\rho s}\mathrm{d}s,$$

where the capital stock and the intensity satisfy equations (4.1) and (4.3) over $[t,\infty)$ with initial conditions $K_t = k, \lambda_t = \lambda$. We assume that capital process (4.1) is a semimartingale and V is sufficiently differentiable.[21] The standard time-homogeneity argument for recursive infinite horizon models (see, e.g., Ljungqvist and Sargent (2018)) implies that $V(k,\lambda,t) = e^{-\beta t}V(k,\lambda,0)$. Simplifying the notation we denote $V(k,\lambda,0)$ again by $V(k,\lambda)$.

The Hamilton-Jacobi-Bellman equation (HJB) associated with the maximization problem in (4.4) subject to dynamics driven by equations (4.1) and (4.3) can be written as:

$$\rho V(K_t,\lambda_t) = \max_{C_t,\theta_t} \{u(C_t,\lambda_t) + \frac{1}{\mathrm{d}t}\mathbb{E}_t \mathrm{d}V(K_t,\lambda_t)\}, \tag{4.5}$$

with the transversality condition $\lim_{t\to\infty} e^{-\beta t}\mathbb{E}[V(K_t,\lambda_t)] = 0$.

Using Ito's formula for semi-martingales (e.g. Jacod and Protter (2004)) we can

[21] These properties are to be verified below under some additional assumptions.

write $\mathrm{d}V$ (we skip the time index t for simplicity) as:

$$\mathrm{d}V(K,\lambda) = \Big(V_K[(1-\theta)Y - C] + \frac{1}{2}V_{KK}\varepsilon^2 - \beta(\lambda - \bar{\lambda})V_\lambda\Big)\mathrm{d}t + [V(\tilde{K},\tilde{\lambda}) - V(K,\lambda)]\mathrm{d}N + \varepsilon V_K \mathrm{d}W,$$

where $\tilde{K} = K_t - \zeta_t$ is the capital stock that remains after a disaster and $\tilde{\lambda} = \lambda + \alpha$ is the new value of the arrival rate of disasters once the first shock has occurred. Note that we have omitted the time subscripts and used subscripts to denote partial derivatives. The last term in parenthesis on the right-hand side, $-\beta(\lambda - \bar{\lambda})V_\lambda$, is the additional term that arises in the differential of V as compared to the $\mathrm{d}V$ expression when the standard jump-diffusion-driven dynamics are employed. This term reflects the change in the value function due to the change in the arrival rate following the initial jump. The expression for the conditional expectation in the right-hand side of (4.5) is then given by:

$$\frac{1}{\mathrm{d}t}\mathbb{E}_t\mathrm{d}V(K,\lambda) = V_K[(1-\theta)Y - C] - \beta(\lambda - \bar{\lambda})V_\lambda + \frac{1}{2}V_{KK}\varepsilon^2 + \lambda[V(\tilde{K},\tilde{\lambda}) - V(K,\lambda)]. \tag{4.6}$$

resulting in the following set of first-order conditions with respect to the controls[22] for problem (4.5):

$$u_C = V_K, \tag{4.7}$$

$$V_K Y = \frac{1}{2}V_{KK}\varepsilon\varepsilon_\theta + \lambda V_{\tilde{K}}\tilde{K}_\theta, \tag{4.8}$$

Equations (4.7) and (4.8) implicitly define the optimal consumption level and the optimal mitigation propensity of the economy, respectively. The latter is chosen such that the marginal cost of one unit of mitigation expenditure, in terms of marginal utility, i.e., the left-hand side of (4.8), is equal to the marginal benefit, which is given by a unit of capital saved in the event of a disaster thanks to the mitigation, i.e., the right-hand side of (4.8). Note that since the optimal mitigation propensity is a function of λ, it is a stochastic process. This result contrasts the

[22]Here we assume that the optimization problem (A.3.12) is a convex problem and time-t optimal controls can be chosen interior, i.e., $C_t^* \in (0, Y_t), \theta_t^* \in (0, \theta_{max})$.

previous findings, which argued for a constant optimal share of GDP spent on mitigation. Equation (4.7) gives the optimal consumption level C^* as an implicit function of the stock value K_t and, possibly, of the Hawkes intensity λ_t, depending on whether the value function is separable in K and λ or not. We can thus write the optimal consumption in general form as $C^*(k,\lambda) = U_C^{-1}\Big(V_K(k,\lambda)\Big)$. Combining the latter equation with the expression for $\mathrm{d}V_K$, we can derive the optimal consumption growth rate. We relegate the detailed derivations to the appendix while show here the final result:

$$\begin{aligned}\frac{\mathrm{d}C}{C} = \frac{1}{\mathcal{R}(C)}\Bigg((1-\theta_t)Y_K - \rho + \frac{\varepsilon_K}{\varepsilon_\theta}Y + \lambda_t\Big[\frac{U_C(\tilde{C})}{U_C(C)}\Big(\tilde{K}_K - \frac{\varepsilon_K}{\varepsilon_\theta}\tilde{K}_\theta\Big) - 1\Big]\Bigg)\mathrm{d}t \\ + \Big[\frac{\tilde{C}}{C} - 1\Big]\mathrm{d}N + \varepsilon \mathrm{d}W,\end{aligned} \tag{4.9}$$

where $\mathcal{R}(C) \equiv -\frac{CU_{CC}}{U_C}$ is the Arrow-Pratt measure of relative risk aversion. The first term in parenthesis on the right-hand side is the so-called trend growth rate, which prevails in-between disasters. Compared to the standard Poisson case (when $\alpha = 0$), the trend term is non-constant and stochastic. This stochasticity is in contrast to the previous findings in the literature, which showed that the optimal trend consumption growth is constant when contagion effects among disasters are not taken into account. To highlight this property, we have restored the subscript t on λ_t and θ_t. We, therefore, find that the presence of a contagion effect among shocks has two implications. The growth rate of consumption is affected by shocks both directly and indirectly. The last two terms represent the direct effects in eq. (4.9), while the indirect effect operates through the trend component, the first term. This effect is absent from the expression for the trend component in the standard case without contagion. Further, the indirect effect may be positive or negative. To illustrate the working of these effects in more detail and to derive closed-form solutions, we need to impose additional structure on the model and introduce functional forms.

4.3 Additional Structure

Assumption 1 (Preferences): The instantaneous utility of consumption is logarithmic:

$$u(C_t, \lambda_t) = \ln(C_t) \tag{4.10}$$

The logarithmic utility is commonly used in the growth literature (Golosov et al., 2014) or in the literature on disasters and economic growth to exemplify general results with closed-form solutions (Müller-Fürstenberger and Schumacher, 2015). As Golosov et al. (2014) put it, the risk aversion and intertemporal elasticity of substitution implied by logarithmic curvature are probably not unreasonable at long time horizons.

Assumption 2 (Mitigation): Following Bretschger and Vinogradova (2019), we posit that the mitigation function, M_t, exhibits constant returns to scale. The coefficient $\upsilon \in (0, 1)$ measures the efficiency of the mitigation technology:

$$M_t = \upsilon \theta_t Y_t$$

Assumption 3 (Externality): The size of the externality is proportional to economic activity with a fixed proportionality factor φ and can be reduced by mitigation efforts:

$$E_t = \varphi Y_t - M_t(\theta_t Y_t) = (\varphi - \upsilon \theta_t) Y_t. \tag{4.11}$$

Assumption 4 (Production): Output Y_t is produced with an AK technology, with $0 < A < 1$ being the productivity measure of the economy:

$$Y_t = AK_t.$$

This assumption is frequently adopted in the economics literature on (natural) catastrophes (see Bretschger and Vinogradova (2019, 2018); Akao and Sakamoto (2018); Bakkensen and Barrage (2018) among others).

Assumption 5 (Damages): The size of the damage from j-th disaster occurring in period t_j is proportional to the size of the externality in that period but also has

a random component that the planner cannot control. The latter is represented by i.i.d. positive bounded random variables $\{Z_{t_j}\}_{j=1}^{\infty}$ independent of the Hawkes process and of the Brownian motion. The proportionality factor is denoted by $\gamma \in (0,1)$. For $t = t_j$ we therefore obtain

$$\zeta_t = \gamma Z_t E_t = \gamma Z_t(\varphi - \upsilon\theta_t)Y_{t-}. \tag{4.12}$$

Similarly, the size of the continuous Brownian fluctuations is proportional to E_t with the proportionality factor $\delta \in (0,1)$.[23]

$$\varepsilon_t = \delta E_t = \delta(\varphi - \upsilon\theta_t)Y_{t-} \tag{4.13}$$

It is reasonable to assume that $\delta < \gamma$, although we do not need this assumption to derive our results.

4.4 Closed-Form Solution and Analysis

With our Assumptions 4 and 5, we can write the size of the damage as the fraction $\omega_t \equiv \gamma(\varphi - \upsilon\theta_t)A = \gamma\Gamma_t$ of the pre-shock capital stock.[24] The post-disaster level of capital becomes:

$$\tilde{K}_t = K_{t-} - \zeta_t = (1 - \omega_t)K_{t-} \tag{4.14}$$

and the law of motion for the capital stock now reads:[25]

$$\mathrm{d}K_t = [(1-\theta_t)Y_{t-} - C_t]\mathrm{d}t - \gamma\Gamma_t Z_t K_{t-}\mathrm{d}N_t + \delta\Gamma_t K_{t-}\mathrm{d}W_t. \tag{4.15}$$

Under Assumption 1, it is reasonable to consider a candidate solution of the

[23]Both γ and δ could be functions of the disasters' frequency λ_t, so our model can be easily extended to include a stochastic volatility case. The functions $\gamma(\cdot)$ and $\delta(\cdot) \in C^2([0,\infty))$ are assumed to be positive and to satisfy quadratic growth constraint: $|\gamma(\lambda)| \leq m(1+|\lambda|^2)$ and $|\delta(\lambda)| \leq m(1+|\lambda|^2)$ for some constant m.

[24]If one thinks about E as a pollution externality then Γ can be interpreted as the net pollution intensity (NPI) of capital.

[25]To be more precise, the integral $\int_0^t Z_t dN_t$ is defined as $\sum_{1 \leq j \leq N_t} z_j$, where $\{z_j\}_{j=1}^{\infty}$ are i.i.d. random variables that are independent of the jump process and the Brownian motion and t_j stand for the moments of the jumps.

HJB equation (4.5) in the form:

$$V(K,\lambda) = X_1 \ln(K) + g(\lambda) \tag{4.16}$$

for some function g and constant $X_1 > 0$. Then,

$$V_K = X_1 K^{-1}, \quad V_\lambda = g_\lambda, \quad V_{KK} = -X_1 K^{-2}.$$

The optimality condition (4.7) then implies that $C_t^* = \rho K_t$, and the optimal mitigation policy is $\theta_t^* = \theta^*(\lambda_t)$ such that

$$\theta^*(\lambda) = \text{argmax}_{\theta\in[0,\theta_{max}]} R(\theta,\lambda) \tag{4.17}$$

$$R(\theta,\lambda) \equiv (1-\theta)A - \frac{1}{2}\delta^2\Gamma^2 + \lambda \int \ln\left(z(1-\omega)\right)\mathrm{d}\nu(z),$$

where $\Gamma(\theta) = (\varphi - \upsilon\theta)A$, $\omega = \gamma\Gamma$, ν stands for the distribution of Z, and integral should be understood in Lebesgue sense. In Appendix A.3.4, we prove that (4.17) defines optimal mitigation; we (implicitly) derive the value function and prove the verification theorem, which guarantees the problem has a unique classical solution.

In what follows, we derive closed-form solutions to our model in three special cases: *i)* Hawkes-only uncertainty, *ii)* mixed Hawkes-Brownian uncertainty, and *iii)* Hawkes uncertainty with random catastrophe magnitude. The first case is key to our understanding of the role of contagion effects in shaping the optimal policy response. It is the scenario we chose to present in detail. The second case illustrates the changes in the optimal policy when smaller-scale continuous fluctuations also accompany disasters. The last case adds another layer of riskiness to the baseline case (i).

4.4.1 Baseline: Hawkes Uncertainty

We assume there is no random component in the damage function by setting $Z \equiv 1$. Likewise, we abstract from the Brownian fluctuations (so that in (4.13), $\delta \to 0$) . Omitting time indexes, the dynamics of the capital stock are then described by:

$$\mathrm{d}K = [(1-\theta)AK - C]\mathrm{d}t - \omega K \mathrm{d}N.$$

Optimal Policy and Trend Growth

The optimization problem (4.17) can be solved explicitly (see Appendix A.3.5). Let $\lambda^{min} = \frac{1}{\upsilon\gamma} - \frac{A\varphi}{\upsilon}$ and $\lambda^{max} = \lambda^{min} + A\theta^{max}$. We define truncated process $\lambda_t^{\#} = \min\{\lambda_t, \lambda^{max}\}$. Under the assumption that $\lambda^{min} \geq \bar{\lambda}$ the optimal mitigation is given by: [26]

$$\theta_t^* = \frac{\varphi}{\upsilon} - \frac{1 - \lambda_t^{\#}\upsilon\gamma}{A\upsilon\gamma}. \tag{4.18}$$

The solution in (4.18) looks very similar to the expression for the optimal abatement found in the earlier literature (e.g. Bretschger and Vinogradova (2019)). There is, however, one key difference. In our setting, the optimal mitigation propensity is a stochastic process because it is a function of the Hawkes intensity λ_t, which is stochastic.

Similarly to the previous findings, higher values of λ_t imply a higher mitigation propensity. Yet, different from the current studies, we find that this propensity is not constant but reactional. The intuition behind this is that the planner correctly anticipates the contagion effect (i.e. more forthcoming shocks due to the clustering effect) and essentially "tracks" the arrivals with the corresponding policy θ_t^*.This is illustrated in Figure 4.3.

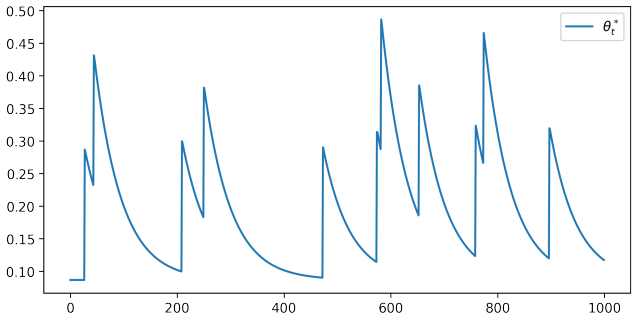

Figure 4.3: Stochastic mitigation policy.

The next important aspect to consider is how the economy's growth rate is affected by the contagion between disasters. The growth rate of consumption can be obtained from (4.7) and the differential of the value function, dV. It is a sum of two components: the trend growth rate g_t^{tr}, which takes place in periods between

[26] This assumption simply excludes zero corner solution (see (A.3.21)).

two consecutive shocks, and a jump counterpart. The former is represented by the dt- term in expression (4.9) while the latter is given by the dN-term, which is equal to the share of lost capital ω_t. Under our assumptions, the trend component can be written as follows:

$$g_t^{tr} = (1 - \theta_t^*)A - \rho = A\left(1 - \frac{\varphi}{\upsilon}\right) + \frac{1}{\upsilon\gamma} - \lambda_t^{\#} - \rho. \tag{4.19}$$

Two points concerning the expression in (4.19) are worth noting. First, it is the same as in the case of pure Poisson shocks (see Bretschger and Vinogradova (2019)), except that now the jump intensity is not constant but time-varying and stochastic. The policy stochasticity implies that the trend growth rate is also stochastic. Second, in the pure Poisson case with intensity $\bar{\lambda}$, we have $\bar{\lambda} < \lambda_t^{\#}$ and, therefore, the trend growth rate without the contagion effects is higher than with contagion, assuming the same baseline intensity. The intuition behind this result is that contagion effectively reduces the real interest rate of the economy, given by the term $(1-\theta_t^*)A$ in (4.19). The real interest rate depends negatively on the optimal mitigation, while the latter is necessarily higher when the contagion effect is present (see (A.3.21)), the interest rate is therefore lower. Another way to see why the optimal growth rate is smaller with contagion is to realize that capital stock growth implies a larger externality from economic activity and, consequently, larger damages. By choosing a lower growth rate, the economy can mitigate the disasters' impact in addition to direct abatement through θ^*. A similar intuition applies in the earlier models with Poisson-driven shocks, except that the effect is reinforced in our setting due to contagion. Now that we understand the effect of interlinked shocks on consumption growth, we can question the long-term cost of contagion in terms of growth losses and overall welfare.

Long-Term Expected Growth

Let us consider the growth rate that is *expected* to prevail in the future starting from some moment τ_0. It is defined by the identity $g_{\tau_0}^e = \mathbb{E}\left[\frac{dC_t/dt}{C_t} | \mathcal{F}_{\tau_0}\right]$. For simplicity, let us say that $\tau_0 = 0$ and denote the corresponding growth rate by g^e. Such a growth rate would correspond to the case of perfect consumption smoothing since all the jumps would be smoothed out due to the expectation operator. In Appendix

A.3.6 we show that

$$g_0^e = \mathbb{E}_0\Big[\frac{\mathrm{d}C_t/\mathrm{d}t}{C_t}\Big] = A\Big(1-\frac{\varphi}{\sigma}\Big) + \frac{1}{\sigma\gamma} - \rho - \mathbb{E}\lambda_t^{\#} - \mathbb{E}\lambda_t + \sigma\gamma\mathbb{E}[\lambda_t^{\#}\lambda_t]. \qquad (4.20)$$

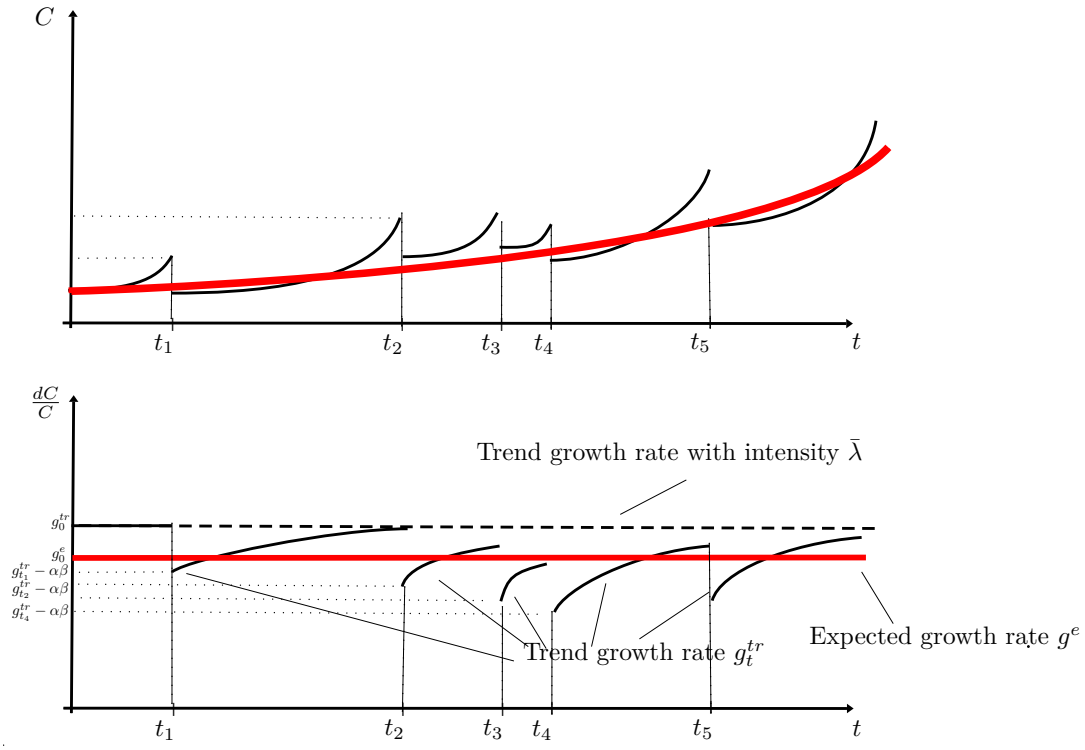

Figure 4.4: Trend and expected consumption growth rates and levels

We illustrate the stochastic time profile of consumption and the corresponding growth rate in Figure 4.4. In the top panel, the solid lines show the consumption behavior over time between disaster occurrences at times $t_1, t_2, etc.$ When a disaster arrives, consumption C_t drops discontinuously to its new level $\tilde{C}_t$ and then continues to grow at the rate g_t^{tr} until the next disaster. The thin solid continuous line shows the expected consumption path.

In the bottom panel, the solid lines show the *growth rate* of consumption. Unlike in the no-contagion case, the trend growth is not constant but increasing over time due to the decaying impact of the arrival rate. At each disaster arrival, including those due to contagion, the growth rate jumps downward, e.g., at times $t_1, t_2, etc.$ The thin solid line shows the expected growth rate and lies below the dashed line

labeled g_P^{tr}, the trend growth rate in the pure Poisson case. Note that g_t^{tr} always lies below g_P^{tr} and converges to this value over time in the absence of disasters.

4.4.2 Costs of a Myopic Policy

In this subsection, we are interested in the following question: How high is the welfare cost of implementing a "wrong" disaster-mitigation policy? Suppose the planner is "myopic" and believes the arrival rate of disasters is constant instead of stochastic. Specifically, if the planner believes the disaster arrivals follow a Poisson process with a constant intensity λ^m, whereas the true arrivals follow the Hawkes process with intensity λ_t. It is natural to assume that λ^m is equal to $\mathbb{E}\lambda_t = \frac{\bar{\lambda}}{1-\alpha}$, which corresponds to the case when the central planner approximates the true Hawkes process by a Poisson process in the mean-square sense.

First, it is not difficult to show that already in the short-run, on average, the difference between trend growth rates of the optimal and the myopic planner is non-negative (i.e., $g^{tr} - g^{tr,m} \geq 0$).[27] In the long run, for the expected growth and welfare costs, we can prove the following proposition:

Proposition 1. *Let $V^m(K,\lambda)$ denote the lifetime utility of the myopic (Poisson) planner, and set $\lambda^m = \mathbb{E}\lambda_t$. Then assuming $\lambda^{max} \to +\infty$ the welfare loss $V - V^m$ resulting from the myopic policy $C^m = \rho K$, $\theta^m = \frac{\varphi}{\upsilon} - \frac{1-\lambda^m \upsilon\gamma}{A\upsilon\gamma}$ equals $\frac{1}{\rho}\mathbb{E}\,\lambda \ln\left(\frac{\lambda^m}{\lambda}\right)$, and the expected growth rate loss $g^e - g^{e,m}$ equals $\sigma\gamma\mathbf{Var}\,\lambda$.*

Proof. We start with the growth rates. From (4.19)[28] for the trend growth rates we have $g^{tr} - g^{tr,m} = \lambda^m - \lambda_t$ and for the expected growth rates:

$$\lim_{\lambda^{max}\to+\infty} g^e - g^{e,m} = \lim_{\lambda^{max}\to+\infty} \sigma\gamma\frac{\alpha^2\beta}{2(1-\alpha)^2}\bar{\lambda} = \lim_{\lambda^{max}\to+\infty} \sigma\gamma\mathbf{Var}\lambda.$$

For the value function under the myopic policy (C^m, θ^m), the dynamic programming principle yields

[27] From (4.19) we have $\mathbb{E}[g_t^{tr} - g_t^{tr,m}] = \mathbb{E}[\lambda^m - \tilde{\lambda}_t] \geq 0$, in the limit as $\lambda_{max} \to +\infty$ the difference is zero.

[28] In the same way, the reader can obtain results under alternative choices of the myopic intensity $\lambda^m \neq \mathbb{E}\lambda$.

$$V^m(k,\lambda) = u(C^m) + \frac{\mathrm{d}}{\mathrm{d}t}\mathbb{E}V^m(k,\lambda).$$

The (myopic) value function V^m can be guessed again in the form

$$V^m = \rho^{-1}\ln(C) + g^m(\lambda),$$

with $g^m(\lambda) = \mathbb{E}\int_0^\infty e^{-\rho s}G(\lambda_t)dt$, where $G(\lambda) = -\log(\rho) - R(\theta^m(\lambda),\lambda)$, resulting

$$V - V^m = g - g^m = \mathbb{E}\int_0^\infty e^{-\rho s}[R(\theta^m,\lambda) - R(\theta^*,\lambda)]\mathrm{d}s$$

the latter can be rewritten as

$$\mathbb{E}\int_0^\infty e^{-\rho s}[A(\theta^* - \theta^m) + \lambda\ln\Big(\frac{1-\omega^m}{1-\omega}\Big)]\mathrm{d}s$$

and using that $1-\omega^* = \lambda^{\#}\upsilon\gamma$,$1-\omega^m = \lambda^m\upsilon\gamma$ and $\theta^* - \theta^m = \frac{\lambda^{\#}}{A} - \frac{\lambda^m}{A}$ this simplifies to

$$\mathbb{E}\int_0^\infty e^{-\rho s}[(\lambda - \lambda^m) + \lambda\ln\Big(\frac{\lambda^m}{\lambda^{\#}}\Big)]\mathrm{d}s.$$

Finally, setting $\lambda^m = \mathbb{E}\lambda$ and changing the order of summation and going to the limit $\lambda^{max} \to +\infty$ we get the desired expression

$$\frac{1}{\rho}\mathbb{E}[\lambda\ln\Big(\frac{\lambda^m}{\lambda}\Big)] = \frac{1}{\rho}\Big(\lambda^m\ln(\lambda^m) - \mathbb{E}\lambda\ln(\lambda)\Big).$$

Due to Jensen's inequality, the latter expression is nonnegative. □

4.4.3 Mixed Hawkes-Brownian Uncertainty

Let us now reintroduce the Wiener uncertainty in addition to the Hawkes-driven disasters. The capital dynamics follows:

$$\mathrm{d}K = [(1-\theta)AK - C]\mathrm{d}t - \gamma\Gamma K\mathrm{d}N + \delta\Gamma K\mathrm{d}W.$$

The optimal policy is the solution of the following quadratic equation:

$$-A + \delta^2 \upsilon A\Gamma + \frac{\lambda\gamma A\upsilon}{1-\gamma\Gamma} = 0.$$

Solving this quadratic equation in $\Gamma = (\varphi - \theta\upsilon)A$ we obtain:

$$\Gamma^* = \frac{1}{2}\frac{A\delta^2\upsilon + \gamma - \sqrt{4\lambda_t A\delta^2\gamma^2\upsilon^2 + (\delta^2\upsilon A - \gamma)^2}}{\gamma\delta^2\upsilon}.$$

Then the resulting interior optimal abatement is:

$$\theta^* = \frac{\varphi A - \Gamma^*}{A\upsilon} = \frac{\varphi}{\upsilon} - \frac{\Gamma^*}{A\upsilon}.$$

Further, we work out asymptotic linear representations for the following two special cases. First, we consider the case where the Hawkes uncertainty dominates, i.e., $\delta \to 0$. Then,

$$\theta = \theta^H + \upsilon\lambda\Gamma^H\delta^2 + o(\delta^2),$$

where $\Gamma^H = \Gamma^H_t = (1 - \lambda_t\gamma\upsilon)/\gamma$ and $\theta^H = \theta^H_t = \frac{\varphi}{\upsilon} - \frac{1-\lambda_t\upsilon\gamma}{A\upsilon\gamma}$ are the random processes for the optimal Γ and θ in the case of pure Hawkes uncertainty obtained in the previous section.
Second, if the Wiener uncertainty dominates, i.e., $\gamma \to 0$. Then:

$$\theta = \theta^W + \frac{\lambda}{\delta^2 A^2\upsilon}\gamma + o(\gamma),$$

where $\theta^W = \frac{\varphi}{\upsilon} - \frac{1}{(A\upsilon\delta)^2}$ is the value of abatement in the pure Wiener uncertainty case.

4.4.4 Hawkes Uncertainty and Random Catastrophe Magnitude

In this subsection, we abstract from the Brownian fluctuations and focus again only on the Hawkes uncertainty but with a random component of the damages.

The dynamics of the capital stock are driven by the following:

$$\mathrm{d}K = [(1-\theta)AK - C]\mathrm{d}t - Z\omega K\mathrm{d}N,$$

where Z is a positive bounded random variable independent of the Hawkes process. Let Z have a Bernoulli distribution with outcomes b and s representing big and small relative loss ($b > s > 0$) taking place with probabilities $(p, 1-p)$, respectively. One may also think of the "small" damage as $s = 1$ in order to make this model comparable with the baseline.

The solution to the following quadratic equation gives the optimal mitigation propensity:

$$\lambda_t \gamma \upsilon \Big[\frac{b}{1-b\omega}p + \frac{s}{1-s\omega}(1-p)\Big] - 1 = 0.$$

If we assume that the probability p of a big disaster is small, we can derive the following asymptotic expansion:

$$\theta = \theta^H + \Delta_1 p + o(p),$$

where $\theta^H = \frac{\varphi}{\upsilon} - \frac{1-\lambda_t \upsilon\gamma s}{A\upsilon\gamma s}$ and $\Delta_1 = \frac{\lambda(b-s)}{|A(s-b(1-\lambda\upsilon\gamma s))|}$. Note that with $s = 1$, $\theta^H = \theta^*$.

4.5 Discussion

The economics literature on catastrophes mostly finds abatement to be a constant fraction of output because of the independence of the shocks. If we assume shocks are linked to one another, the optimal investment in abatement becomes a stochastic fraction of output.

Practical examples show that abatement policies increase right after a major shock. A first and recent example is the reaction of governments to the COVID-19 crisis. Before the pandemic, governments had some budget dedicated to preventing a potential pandemic. But in response to the outbreak, governments set substantial mitigation policies to limit the spread of the disease and the risk of economic and financial breakdowns due to the pandemic. A second example is a drastic reduction in the use of nuclear power by some governments worldwide following the 2011 Fukushima explosion. Germany and Japan, for instance, drastically reduced their

number of active reactors shortly after the catastrophe. This partial phase-out of nuclear power immediately raised investments in renewable energies in these countries. At last, it is also common to notice (non-)governmental help following some major flood or cyclone event. The authorities intervened to increase the number of shelters available, and some financial aid was provided to rebuild and overcome the economic downturn following the disaster as quickly as possible. It is also expected that prevention plans will arise following big natural disasters.

We plan on further extensions of this work. First, we want to estimate (or at least calibrate) the model. Several approaches to estimating and calibrating multi-dimensional Hawkes kernels were introduced and studied recently. Apart from the max-likelihood method, Kirchner (2017) and Kirchner and Bercher (2018) developed a multi-step procedure based on Embrechts and Kirchner (2018) and earlier works. We would take our model's baseline Hawkes uncertainty version and use data on the COVID-19 waves in Europe (that we show in the introduction) as our main shocks. The rest of the model's calibration would be standard to the economics literature.

Once we have numerical estimates of the optimal policy, we could provide a numerical estimate of the cost of a myopic policy in Section 4.4.2 and estimate how the optimal mitigation policy compares under the different assumptions on the shock dynamics that we present in Sections 4.4.1-4.4.4 (only Hawkes uncertainty, Hawkes and Brownian, or Hawkes with random catastrophe magnitude).

With a numerical approach, we could also broaden our welfare analysis. We could revisit some of the results concerning the cost of consumption fluctuations or the welfare costs of uncertainty initiated by Lucas and Lucas (1987). The latter argues that the costs of consumption fluctuations are relatively low. At the same time, Barro (2006) suggests that these costs can go up to 20% of GDP if large economic disasters are adequately accounted for. Yet, the literature has failed to address the welfare cost of contagion between disasters and thus may have underestimated the actual welfare costs of fluctuations. Another important issue we would like to highlight is that the economy responds *endogenously* to the possibility of a disaster (risk) in two ways: by choosing a mitigation propensity and adjusting the growth rate. The second effect is often neglected in the literature on the welfare costs of economic shocks or is absent due to an exogenous growth rate assumption. Thus,

we have two potentially counteracting forces. On the one hand, interdependent shocks are likely to lead to larger welfare losses, due to the contagion effect, than the standard Poisson or Wiener-type shocks used in the literature. On the other hand, consumption growth slows down endogenously in the presence of random disasters and even more so in the presence of interlinked disasters, which attenuates the fluctuations.

Following Barro (2006), Martin (2008), and (Martin and Pindyck, 2015), we are interested in society's willingness to pay (WTP) to avoid consumption fluctuations. However, we would take a different approach. Instead of looking at the WTP to avoid *all* fluctuations, we would compute only the WTP to avoid extra fluctuations arising from contagion. We, therefore, need to consider two scenarios. The first scenario is purely stochastic, like in our model of Section 4.2. The second scenario assumes that there is no contagion so that a standard Poisson process (with a constant intensity) drives disaster arrivals $\lambda^p = \bar{\lambda}$.

Yet, the need to find a closed-form solution limits the spectrum of our conclusions. The model developed in Section 3 has certain limitations compared to a more general setup exposed in Section 2. It would be interesting to obtain results beyond the logarithmic-utility.[29] A second potential direction is the study of different policies. We could change how the policy interacts with the shocks. So far, the policy merely translates into a reduction of economic activity to decelerate capital accumulation subject to shocks and smooth consumption in time. Another possibility would be to endogenize the arrival rate of the disasters to the economic policy. That way, the mitigation policy would aim to slow down the contagion effect of the shocks. In our COVID-19 example, that would resemble a vaccination policy.

At last, it is possible to derive a multidimensional analog of our model shocks, where processes of different natures would be mutually exciting. The latter could be further generalized to a spatiotemporal model to study multi-country setups. All in all, our general framework can bring many more exciting results but also need the development of specific numerical methods.

[29]For instance, it zeroes precautionary savings term $\lambda\left[\frac{U_C(\tilde{C})}{U_C(C)}\tilde{K}_K - 1\right]$ in (4.9)

4.6 Conclusion

We use a general-equilibrium endogenous growth model with stochastic shocks. We derive closed-form solutions for the economic growth rate and the optimal spending on disaster prevention (abatement). The economy needs to invest more in abatement compared to previous studies without interlinked shocks because preventing the first shock also has the benefit of preventing future shocks and reducing the arrival rate of secondary perils. This extra investment in abatement is also stochastic, while the existing literature, which ignores the contagion effect, finds that a constant mitigation propensity is optimal. The stochastic nature of the optimal policy is a new result in the literature. At last, we find that, compared to the well-studied case where shocks arise with a constant arrival rate (the Poisson case, for instance), the growth trend is likely to decrease due to interlinked shocks. That is because, in the case of Hawkes shocks, the economy faces a higher occurrence rate of shocks.

Chapter 5

Economic Growth and Equity in Anticipation of Climate Policy[1]

Abstract

We study the role of the anticipation of climate policies on equity and economic growth in a numerical model of general equilibrium. The presence of an anticipation period allows the agents to adjust their choices before policy implementation. This period might change the equilibrium dynamics and impact the redistribution of wealth in the economy. We choose the Swiss economy to exemplify and analyze these effects. The economy's supply side adjusts by redirecting the investments to "cleaner" sectors with a lower tax burden and higher profitability. On the demand side, welfare impacts by households vary according to their principal source of income. Households with a high share of their income from capital rents benefit more from the policy's announcement than others. We find that, for the most stringent climate policies, the effect of anticipation is strongly positive but also regressive.

[1]This chapter is joint work with Alena Miftakhova. This chapter is reprinted with minor edits from Miftakhova and Renoir (2021).

5.1 Introduction

As global CO_2 emissions keep rising, economic instruments that aim at reducing fossil fuel use may have to reach high stringency levels (Allen et al., 2018). Typically, such instruments are not introduced unexpectedly but rather devised, debated, and announced beforehand (Gupta, 2010). The more demanding the policies are, the more impactful their credible announcements may become. The information about upcoming climate policies can help agents reallocate their resources optimally by the time the policy is enacted (Di Maria et al., 2012). The ability to take advantage of an announcement is heterogeneous across the population. Even though individuals might be given equal time and opportunity to adjust, their ability to do so depends on the number of resources they own. Policy announcements may thereby induce a strong distributional impact and aggravate social inequality even before the actual implementation.

We study the repercussions of anticipating the carbon tax of various stringency levels for the economy. First, we run the usual anticipation scenario where the policymaker announces the carbon tax before its implementation.[2] Second, we simulate an unanticipation world where agents in the economy cannot adjust to the upcoming carbon tax—as if there were no prior announcements. The policy target (the carbon emissions limit) is the same in both the anticipated and the unanticipated cases. We then compare the results from the two scenarios and attribute the differences to the role of anticipation.

We aggregate data from the Swiss input-output table (IOT) into 11 economic sectors and five household groups distinguished by income and activity status. Data on the households come from the Household Budget Survey data (HABE) of the year 2014.

Our study is the first to analyze the effects of policy anticipation on economic growth and the welfare of heterogeneous households. It is critical to do so through the prism of endogenous growth. Recent studies emphasize the role of induced technological change in the effectiveness of climate policy (Bretschger et al., 2011; Acemoglu et al., 2012). In this case, advanced investment decisions redirect invest-

[2]We always treat a policy announcement as credible and do not consider the uncertainty of political decision-making.

ments to innovation in low-carbon technologies (Bosetti et al., 2009). Technological progress and learning can thus counterbalance the adverse effects of policy anticipation (Di Maria and van der Werf, 2008; Nachtigall and Rübbelke, 2016). Our results suggest that the anticipation period alters the investment decisions, and the anticipation of carbon tax induces early divestment from fossil fuels. These decisions, in turn, impact the sectoral and aggregate growth, households' choices for labor supply, and consumption growth rates.

We find that policy announcement allows economic agents to align their investment decisions accordingly and lower the future costs of compliance with the policy. Yet, the extent to which individuals can benefit from early capital reallocation is not homogeneous and depends on their participation in the capital market. Individuals that own most of the capital in the economy and enjoy a high share of capital rents in their income (we call them *capitalists*) benefit from the investment reallocation the most. Other individuals relying primarily on labor income and government transfers must face the new market conditions and adjust their consumption and labor decisions. Therefore, the presence of an anticipation period has a regressive effect—regardless of the stringency of the policy target. The regressive effect of the anticipation deepens as the policy's stringency increases.

This chapter also explores the impacts of stringent climate policies on the economy's path to decarbonization. We simulate carbon emissions policies that target CO_2 up to 95% reductions from its current level by 2050. We find that the policy's stringency has a non-linear effect and impacts the anticipation dynamics quantitatively and qualitatively. For a low enough carbon reduction target, households' consumption-smoothing dominates their consumption-investment decisions. When the policy's stringency goes beyond a certain point (around 50% of CO_2 emission reduction), capital reallocation dynamics come into play. Since the capital owners foresee the increase in the profitability of the "clean" technologies at the time of the policy's announcement, the anticipation allows them to adapt to the strict carbon targets. Under carbon reduction targets of around 95%, anticipation positively impacts the welfare of all households. Because of the intrinsic inequality of the anticipation effect, capitalists benefit more from the adaptation opportunity than poorer households.

For low and mild carbon taxes, the anticipation decreases the welfare of all active

households by about 0.2% over the 30 years of study. The same policies are neutral or even positively affect the welfare of retired households. The welfare of the most wealthy (named "retired high") may increase to 0.25% for an 80% carbon reduction policy. For the most stringent policy (95% of carbon reduction), the welfare increase of the "retired high" households is about 0.5% point higher than the "active low" (the least wealthy households of the working group) type of households.

At last, we look at a scenario where the redistribution to the households is inverse-proportional to their income level. This redistribution scheme is standard in the carbon tax literature (see, for example, Beck et al., 2015) and aims to foster a progressive tax effect. We find that the anticipation of this policy undermines its purpose. Wealthier households anticipate lower tax revenues compared to a homogeneous lump-sum redistribution scheme. To counter-balance this loss, they reallocate even more of their capital, amplifying the adverse effects on the working group of households.

Related literature

A long series of macroeconomic studies underline the role of a policy's announcement on its total effect. Recent empirical analyses by Mertens and Ravn (2012) and Favero and Giavazzi (2012) provide evidence that anticipation effects contribute largely to business cycles in the U.S. They find pre-announced tax cuts give rise to contractions in output, investment, and hours worked before their implementation, whereas real wages increase. van der Wielen (2020) find similar results for the European Union. Mertens and Ravn (2011) confirm these empirical findings in a DSGE model. Our work differs from these ex-post analyses in that we perform an ex-ante analysis of an environmental policy.

A large part of environmental economics considers the effect of the policy announcement through the prism of the green paradox (Sinn, 2008). The concept of the green paradox applies when climate regulations have an effect that contradicts the intended one. Under resource scarcity, the regulation's announcement may induce more intensive extraction of fossil fuels instead of their conservation. Resource owners are incentivized to accelerate the extraction before the policy makes it costlier (Di Maria et al., 2012; Riekhof and Bröcker, 2017; Di Maria et al., 2017).

Jensen et al. (2015) find that such adverse effects are even more likely when the policy's stringency increases steeply in time.

The presence and strength of the green paradox effect depend on many factors, such as the extraction and adjustment costs for fossil energy and the availability of clean substitutes (van der Ploeg and Withagen, 2015). Smulders et al. (2012) show that the green paradox may arise even without resource scarcity. The anticipation of a carbon tax might lead to an early increase in investments and capital accumulation accompanied by more intensive fossil energy use. In this case, the green paradox arises from the adjustments in consumption-investment decisions. Baldwin et al. (2020) show that agents might choose to divest from carbon-intensive sectors early, thereby preventing asset strands under the policy.[3] As Bauer et al. (2018) and Okullo et al. (2020) suggest, the benefits from earlier and higher investments in clean energy technology might outweigh the incentives to turn to fossil fuels before the policy is enacted.

Our analysis departs from the green paradox-divestment dilemma and explores the changes in welfare distribution and key macroeconomic variables driven by a policy announcement.[4]. Incorporating heterogeneous groups of households is a critical step towards a better understanding of the distributional effects of climate policies (Rao et al., 2017; Keppo et al., 2021). According to the early review by Wang et al. (2016), studies generally tend to suggest regressive effects, though the conclusions depend on the design of a policy. To investigate the equity effects, Rausch et al. (2011) thoroughly incorporate households' heterogeneity and find that revenue recycling scheme impacts both the efficiency and equity of a carbon policy. They suggest that the trade-off between the progressivity on the income side and the regressivity on the consumption side defines the outcome. Fremstad and Paul (2019) support this finding and suggest that lump-sum redistribution makes the tax pro-

[3]In support of this claim, the literature suggests that investors timely adjust their expectations to future policies and consider stranded assets risks (Vikash Ramiah et al., 2013; Sen and von Schickfus, 2020).

[4]The more general literature that juxtaposes "history" with expectations finds that it is not only the current state of the economy that determines its equilibrium path. Expectations about the future economy's state can also play an important role in determining an equilibrium (Krugman, 1991). Applications to environmental policy suggest that a policy may raise self-fulfilling "green" expectations and might even have to do so to shift the economy's trajectory towards energy transition (Bretschger and Schaefer, 2017; van der Meijden and Smulders, 2017; Schäfer and Stünzi, 2019)

gressive. Karydas and Zhang (2019) show that the progressivity is unlikely to hold under stringent policies. The recent meta-analysis in Ohlendorf et al. (2021) shows that studies are more likely to find regressive effects in developed countries and proportional or progressive effects in low-income countries. Including general equilibrium effects also plays an essential role in the results. Our chapter offers insight into the distributional effects of anticipation, as opposed to the implementation of a climate policy.

The rest of the chapter is structured as follows. Section 5.2 presents the CITE model, its calibration, and major assumptions. Section 5.3 describes the policies and scenarios designed to isolate the anticipation effect. Section 5.4 presents results for the total and disaggregated effects of policy anticipation for welfare and economic growth. Section 5.5 discusses the policy implications in a broader context. Section 5.6 concludes.

5.2 Model and Methods

In this section, we outline the main features of our economic model. We describe the data used for calibration, the key modeling assumptions, and the computational strategy to solve the model.

5.2.1 Economic model

We use the CITE economic model of general equilibrium with endogenous growth developed by Bretschger et al. (2011). The growth mechanism in CITE is an extension of the increasing-variety model of Romer (1990) and includes energy use in the production of the intermediate good. This extension makes it possible to examine how the substitutability between labor and energy might affect economic growth when their relative prices change under various policies or other changes in economic conditions. CITE models a small open economy that consists of different regular, non-energy sectors of an economy and four energy-specific sectors—oil, gas, heat, and electricity. All sectors have similar structures of production that feature three levels: the production of the intermediate goods, the production of sector-specific intermediate composite, and that of the final good. We assume that knowledge

is sector-specific, and we do not consider international knowledge spillovers.[5] Below, we outline the main features of the model. Appendix A.4.1 offers its rigorous presentation.

Production

For each sector i, the markets for final good (Y_i), intermediate composite good (Q_i), and labor in manufacturing and R&D (L_{X_i} and L_{J_i}) are perfectly competitive. Firms, however, can invest in physical (I_{P_i}) and non-physical (I_{N_i}) capital to invent new varieties of goods and enjoy profits from their monopolistic position. These new varieties constitute the capital (J_i) of the sector. The nesting of the model is such that the fossil fuels are combined with electricity first to produce the energy aggregate. This aggregate is nested with labor to produce intermediate goods, which then combine with capital to produce the intermediate composite. Our nesting of capital (K), labor (L) and energy (E) follows a $K - LE$ form.[6] The amount of accumulated capital (J_i) determines the number of varieties that comprise the intermediate composite Q_i. Figure 5.1 provides an overview of the production structure for each sector of the economy.

At any time t, the labor employed in research, L_{J_i}, and labor employed in the production of the intermediate goods, L_{X_i}, face the same wage w_t determined on the competitive market.

Consumption and welfare

Following the procedure in Karydas and Zhang (2019), we define five categories of households based on their income levels and activity status. All households maximize their utility from consumption and leisure. We proxy leisure with the complement of the labor force participation rate, taking the calibration from Karydas and Zhang (2019).[7] Figure 5.2 sketches consumption and welfare choices in

[5]For a use of CITE with international knowledge diffusion, see Bretschger et al. (2017).

[6]Models with exogenous growth are commonly specified in $KL - E$ form (Manne et al., 1995; Paltsev et al., 2005b; Bosetti et al., 2006). In our endogenous growth framework, capital accumulation enhances the productivity of all other input factors, hence the $K - LE$ formulation. See Appendix A.4.1 for more details.

[7]Karydas and Zhang (2019) use data on income and labor force participation rates provided by the Swiss Federal Office of Statistics. They map the time endowment of the households be-

Figure 5.1: Sectoral production structure of the economy

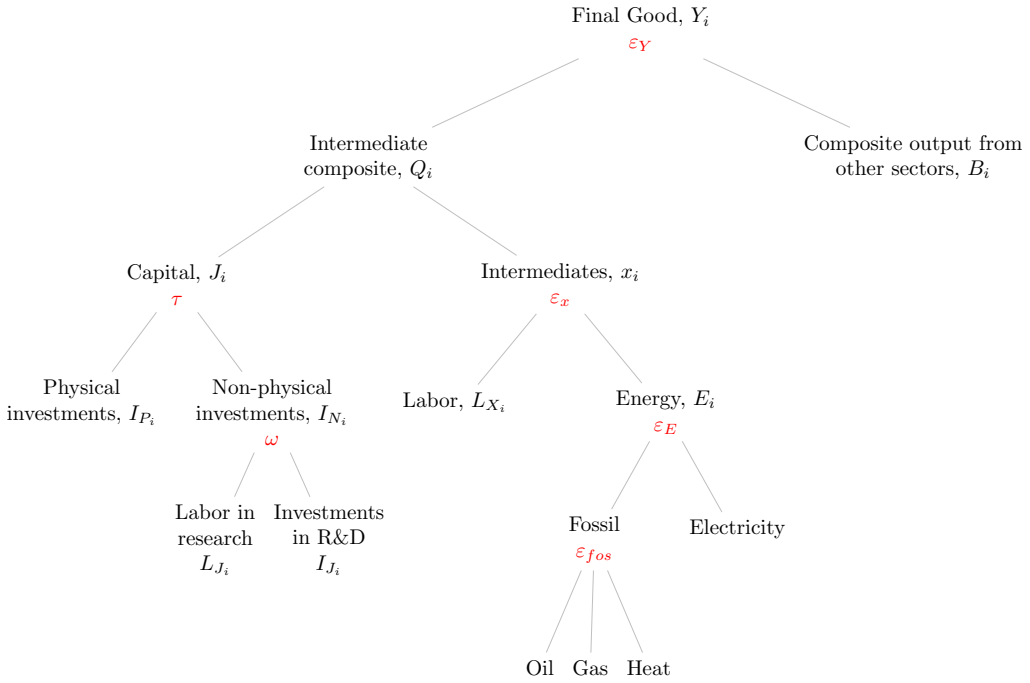

the economy. The agents have perfect foresight and allocate their income between consumption and investment.

International trade

As CITE models a small open economy, international trade matters in production. We follow the Armington approach (Armington, 1969) to model international trade. In the production process, we assume that domestically produced and imported goods are imperfect substitutes in each sector. At the final good production level, the goods from international trade are represented by the composite input B_i—which is an aggregate of Armington goods from all sectors. Once the final good is produced, it is divided between export and domestic consumption according to the exogenous foreign prices and under the constraint that trade is balanced in every period. The exported goods and the output produced for the home market

tween age groups and income groups for the following household categories (with their labor force participation rates given in brackets): Active low (0.15), Active mid (0.1), Active high (0.25), Retired low (0.9), Retired high (0.9).

Figure 5.2: Welfare and demand structure of the economy

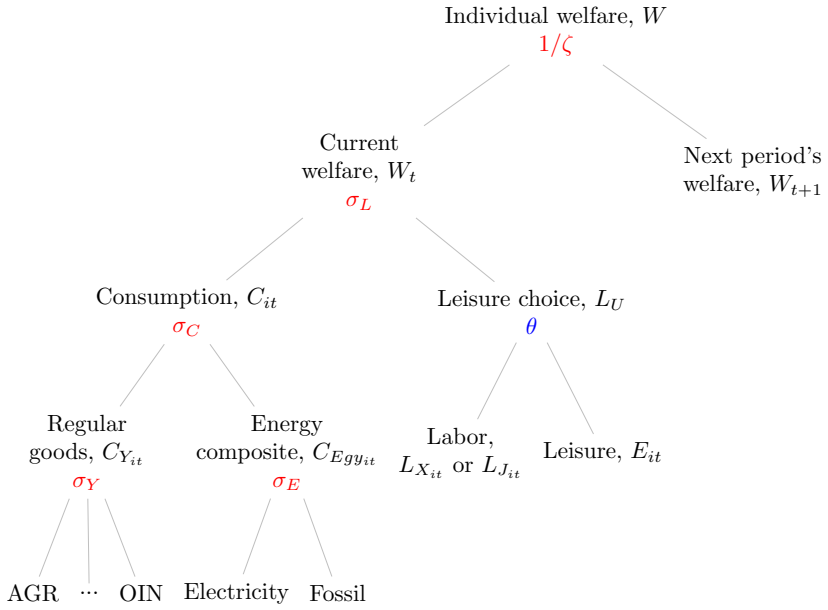

are also imperfect substitutes. Consumers, who purchase the final output, consume Armington aggregates—that is, combinations of domestic and foreign production.

Government

The model also includes a government whose role is to collect and redistribute the pre-existing taxes (capital and labor taxes, subsidies, and tariffs), the new carbon tax, and transfers. The governmental budget is initially balanced and stays such throughout the analysis. In our main scenario, the government redistributes the revenues from the carbon tax in a lump-sum fashion.

5.2.2 Solving the model

We first calibrate CITE to the balanced growth path (BGP) to solve the model for the different policy scenarios. In this section, we describe the data and expose our main assumptions for the calibration to the BGP and our computational strategy to isolate the effect of anticipation.

Table 5.1: Description of the data on the 9,367 Swiss households

Category	Source
Income	Labor, Capital, Transfers
Spending	Consumption, Investments
Taxes	Income, Labor, Subsidies, Tariffs
Activity status	Active or Retired
Size	Number of people living in each household

Households and sectors data

We use the Swiss Input-Output Table (IOT), Energy Input-Output Table (EIOT), and the Household Budget Survey data (HABE) of the year 2014 (they are the latest data available) to construct the Social Accounting Matrix (SAM) for Switzerland.[8] We aggregate the 77 economic sectors of the IOT into the 11 sectors used in the study (see Table A.4.1 in Appendix A.4.2). The energy sector is further disaggregated into fossil (oil, gas, heat) and electricity sources following Bretschger et al. (2011). Because the electricity sector in Switzerland emits hardly any CO_2, we consider it a clean energy technology and an alternative to fossil fuels.

The HABE data contains information on 9,367 Swiss households summarized in Table 5.1. We aggregate these households into five categories based on their working status (active or retired) and level of net income (low, medium, or high for active households and low or high for retired households). After aggregating the households and considering the number of people living in each household, we find that about 80% of the population is active, among which 44% is in the active-low group. The active-high and the retired income groups own most of the economy's capital (62%). But the active-high receives about two times as much income from labor than from capital, whereas the two retired income groups rely to a large extent on their capital earnings. The numbers are comparable to those in Karydas and Zhang (2019). The model's calibration considers the pre-existing taxes and subsidies of the Swiss economy.

[8]The Federal Statistical Office of Switzerland provides the data. Nathani et al. (2019) document the EIOT.

Key assumptions and the benchmark scenario

The economy is calibrated to follow the BGP with growth rates that match the Swiss economy. We set the economy's growth rate, g, to 1% per year—which follows from the average growth rate of GDP per capita in Switzerland in the last two decades.[9] On the balanced growth path, all sectors grow at the same rate as the entire economy.

However, the growth rate for capital, g_K, is different and derives from the expansion in variety mechanism of endogenous growth. It relates to the economy's growth rate as $g_K = g^\kappa$, where κ is the share of non-capital goods in production across all sectors. Based on the IOT data, we set the value for κ to 0.7, implying the capital growth rate equals 0.7%. The annual rate of return on capital, r, takes the average value of the interest rate set by the Swiss National Bank. The average value for this interest rate over the last 20 years is 0.6%.[10]

Once the economy's growth rate and the interest rate are chosen, the discount rate is determined endogenously by the Keynes-Ramsey rule,

$$g = \left(\frac{1+r}{1+\rho} \frac{P_{C,t}}{P_{C,t+1}} \right)^{\frac{1}{\zeta}}, \tag{5.1}$$

where $P_{C,t}$ is the price of consumption in period t and on the BGP it must hold that $\frac{P_{C,t}}{P_{C,t+1}} = 1 + r$. The discount rate can thus be calculated from

$$\rho = \frac{(1+r)^2}{g_C^\zeta} - 1. \tag{5.2}$$

We assume the intertemporal elasticity of substitution, $1/\zeta$, is equal to 0.85, which yields a rather conservative discount rate of 0.03%. The values for the remaining parameters used in calibration are listed in Table A.4.2 of Appendix A.4.3.

Finally, using a finite number of periods, the numerical solution approximates

[9] According to the World Bank Open Data, the 10- and 20-year average growth rates for GDP per capita in Switzerland are 1% and 1.03% correspondingly. The data can be retrieved from https://data.worldbank.org/indicator/NY.GDP.PCAP.KD.ZG?locations=CH.

[10] The current interest rate policy is published on the website of the Swiss National Bank at https://www.snb.ch/en/iabout/stat/statrep/id/current_interest_exchange_rates; the historical data can be retrieved from the Bank for International Settlements at https://www.bis.org/statistics/cbpol.htm.

the theoretical model described in Appendix A.4.1. We employ the method from Lau et al. (2002a) to solve for the infinite horizon equilibrium by imposing additional constraints for capital accumulation in the terminal period T. We fix the growth rate of investments in the terminal period to be equal to the output growth rate,

$$\frac{I_T}{I_{T-1}} = \frac{Y_T}{Y_{T-1}}. \tag{5.3}$$

That is, we impose a constraint on the growth rate of investments only. The actual growth rate of the economy and the terminal level of capital stock are free variables.

Computational strategy

Given our initial SAM and calibration to the balanced growth path, the model's competitive equilibrium follows from a vector of prices and quantities such that firms maximize their profits, consumers maximize their intertemporal utility according to their budget constraints, and the adjustment of the price mechanism clears all markets. We use the General Algebraic Modeling System (GAMS) software and the GAMS/MPSGE higher-level language (Rutherford, 1999a) together with the PATH solver (Dirkse and Ferris, 1995) to solve the model as a mixed-complementarity problem.

5.3 Scenarios and analysis

In this section, we provide the details on the policy scenarios and the way we measure the effect of anticipation.

5.3.1 Policy scenarios

We implement policies linearly over the three decades from 2020 to 2050. For all policies, we set a target reduction in CO_2 emissions in proportion to their benchmark value in the first year of the business-as-usual (BAU) scenario. For example, a target of 90% reduction corresponds to a policy that aims at 90% less CO_2 emissions by 2050 compared to their level in 2020. We study policies with CO_2 emissions reduction targets from 1% to 95% from their benchmark level. The key object of

our interest is the effect caused by the anticipation of these policies on the dynamics of the macroeconomic variables.

We focus on a carbon tax as the main policy instrument. The economic sectors and final consumers pay the tax according to the carbon intensity of their consumed energy. The government collects the tax and redistributes it in lump-sum to households. The results of this redistribution are later compared to two alternative ways to recycle the tax income. First, the revenue is used in an attempt to alleviate income inequality across the different income groups of households. In this case, the redistribution is inversely proportional to the household income. Second, the revenue from the carbon tax is directed to stimulate research in all sectors and facilitate overall economic growth.

5.3.2 Design of the anticipation effect

We study the effect of anticipation by comparing two different cases of policy implementation. In the first case, in anticipation, the policy is announced in 2020 and scheduled for implementation in 2030. In the second case, in unanticipation, the policy is not announced until its implementation in 2030, and thus no adjustments from economic agents are possible beforehand. The differences in macroeconomic dynamics between the two cases represent the effect of anticipating the policy.[11]

More formally, to obtain the effect of anticipation on a given economic variable X (for example, X can represent welfare, GDP, or wages), we compute the difference between the values that X takes under the two implementation schemes. Under the anticipation scheme, at time t_0, the policymaker announces a climate policy to be implemented at time t_1. Agents can thus adjust their optimal choices before the implementation. We call the optimal path of X under anticipation X_A. Under the unanticipation scheme, the policymaker does not announce the coming climate policy at t_0 but implements it immediately at time t_1. Since the agents do not know about the policy in advance, they cannot prepare for the coming regulation at time t_0 and adjust their behavior only at t_1. We call the optimal path of X

[11] What we call the anticipation period is sometimes called a "phase-in" in the literature (Williams III, 2011). We choose not to use this term in order not to confuse the reader. Most studies use it to refer to a policy already implemented but set to become more stringent gradually. In our case, the policy is enacted later than it is announced.

under unanticipation X_U. The effect of anticipation, Δ_X^A, is the difference between the two optimal paths of X under the two schemes:

$$\Delta_X^A = X_A - X_U. \tag{5.4}$$

In practice, to obtain the unanticipated path X_U, the agents' choices at time t_0 are fixed to their benchmark values (as these values are optimal in the absence of policy). Only from time t_1 onward can the optimal allocations deviate from the BAU to comply with the policy.[12]

5.4 Results

This section presents the main results of our analysis. First, we state the general effects of policies of different stringency levels. Second, we highlight the anticipation effect of these policies on welfare distribution and economic growth. The objective is not to propose optimal policies but rather to show the impact of the policy announcement on the production side and the consumption side of the economy.

5.4.1 General effects on aggregate economic variables

Carbon policies of any stringency slow down economic growth—at least in the first two decades. Figure 5.3 shows the decadal growth of the aggregate output under the implemented policies and agents' full anticipation.[13] In most cases, the growth rates lie below the benchmark level of 1%. At the same time, they hardly ever fall below 0.9%, which indicates slightly slower yet persistent growth. For mild policies (that is, policies that aim at 20% to 50% reduction in CO_2 emissions), higher emission reduction targets directly correspond to a gradual deceleration of economic growth. Under more stringent policies, the economy mobilizes more of its resources to stimulate the production of final goods. Therefore, even with a

[12]Note that the values of a variable in the two implementation schemes can also differ in the later periods $t_i, i > 1$. The anticipation effect refers to the deviations in the optimal paths before and under the policy compared to the unanticipation path.

[13]For both the supply and demand sides of the economy, we first present the overall impact of the policies. The anticipation effect is isolated in subsequent figures.

Figure 5.3: The effect of carbon policies on the aggregate output growth

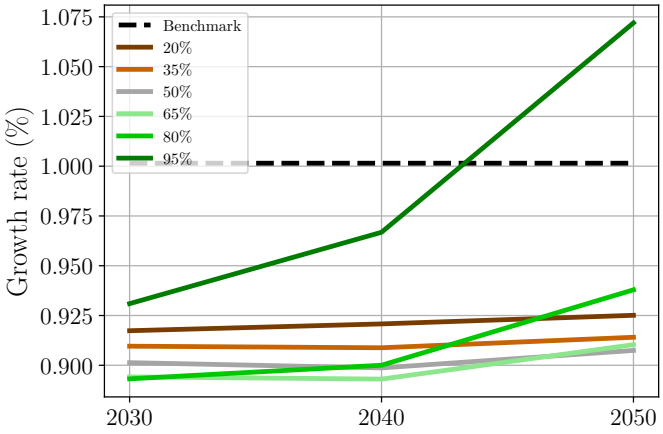

Notes: The figure shows the results for various policy targets under full anticipation of future policies. For example, a 65% policy implies a 65% reduction in CO_2 emissions in comparison to the benchmark year.

low start, the growth rate tends to have an increasing profile and, under the 95%-reduction policy, reaches 1.075% in 2050.

This overall effect on output growth derives from consumption and investment dynamics. All implemented carbon reductions hamper consumption growth —in the most extreme case, the growth rate falls below 0.8%.[14] Under moderate emissions reductions, the aggregate investment grows slightly slower too. When the economy has to cut emissions drastically, aggregate economic growth requires higher levels and steeper profiles of investments. Their growth rate eventually surpasses the benchmark level—drawing even more resources away from consumption.

Like the general effect of policy implementation, the anticipation effect on the total output is more pronounced the stricter the policy. As shown in Figure 5.4, the output is higher in the first period if the agents know that carbon regulation is coming in the next period. In the case of less stringent policies, the anticipation shifts the production profile towards the earlier periods—the output volumes are higher in the first decade and notably lower in the later decades. Under the most ambitious policy, knowledge about the upcoming regulation ensures higher levels of final production in the first three decades of the modeled period, with a maximal

[14]See the Figure A.4.1 in the Appendix.

Figure 5.4: The effect of anticipation on the aggregate output

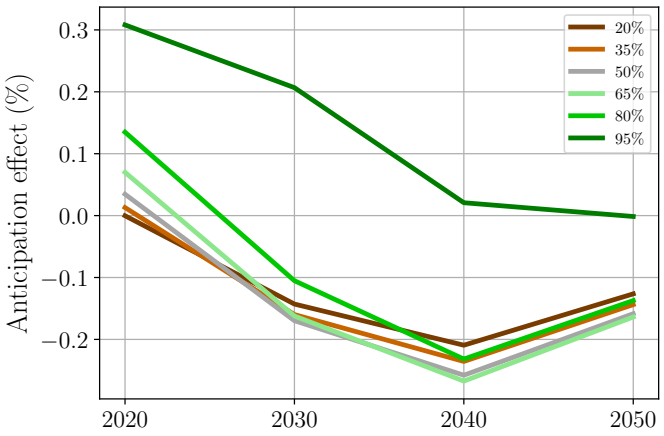

Notes: The figure shows the effect of anticipation for various policy targets. A 65% policy implies a 65% reduction in CO_2 emissions in comparison to the benchmark year. The anticipation effect represents the difference in aggregate output between a scenario where agents can anticipate in 2020 a policy to be implemented in 2030 and a scenario where they can observe the policy only in 2030. A positive effect means that the aggregate output is higher in the anticipation case.

difference of 0.3% in 2020.

Figure 5.5 sheds more light on these dynamics by displaying the effects of anticipation on the aggregate levels of consumption (left panel) and investment (right panel). Informed about an upcoming mild policy, the agents shift their consumption in time such that more goods can be consumed beforehand—at the expense of the later consumption subject to carbon taxation.[15] As a result, fewer resources are invested in sectoral growth. Under stringent policies, however, the opposite effect dominates as households tend to reduce their consumption in the first period in favor of increasing investments in the economy. These additional investments ensure that the economy's capital distribution can start adjusting to a new optimum beforehand. Under the most stringent policy, the initial forgone consumption of over 1% of the total consumption allows the households to consume more in the later periods.

[15]Note that if higher consumption implied proportionally higher dirty energy use, the green paradox could occur here. But, thanks to advanced substitution towards clean energy, the amount of dirty inputs does not increase with higher consumption.

Figure 5.5: The effect of anticipation on the aggregate consumption and investment

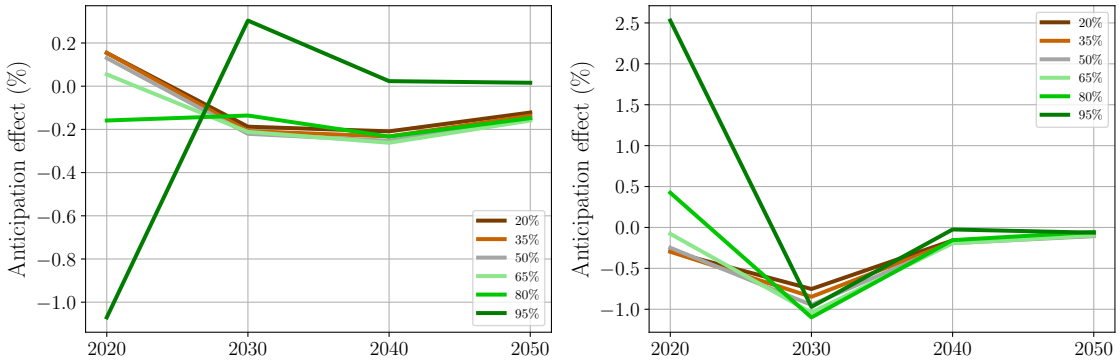

(a) Consumption **(b)** Investment

Notes: The figure shows the effect of anticipation for various policy targets. A 65% policy implies a 65% reduction in CO_2 emissions in comparison to the benchmark year.

Sectoral impacts

The impacts of carbon taxation are highly asymmetric across the economic sectors. The policies generally favor sectors with lower carbon intensity and higher substitution possibilities. On the other hand, the sectors that strongly rely on fossil energy are left at a disadvantage. Even before the actual policy implementation, the consumption of fossil fuels falls (see Figure A.4.2 in the Appendix).

Figure 5.6 shows these diverse sectoral effects on the example of the most stringent policy that aims at 95% emissions reduction under full anticipation. The sector with the highest energy intensity —transport—is hit by this policy the strongest and loses over a quarter of its benchmark level of output by 2050. Less carbon-intensive sectors—such as the agriculture and the chemical sector—end up benefiting from the policy. Their corresponding levels of output rise by 32% and 24% by the end of the modeled period. The industries classified as "other" increase their output level by almost 70% by the time the policy target is reached.

The isolation of the effect of the anticipation period reveals more sophisticated dynamics. Figure 5.7 provides three demonstrative examples of the effects of anticipation on sectoral investments and capital accumulation under the policies with increasing targets. One intuitive example of such effects is provided by the bank-

Figure 5.6: The effect of 95%-reduction policy on the sectoral output

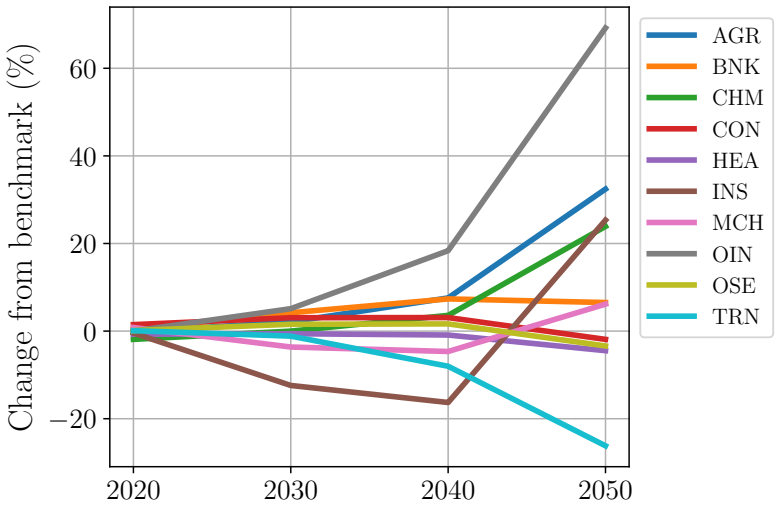

Notes: The figure shows the results under the anticipation of the policy.

ing sector (panel **(a)** of Figure 5.7). Knowing about the upcoming policy and its positive impact on the banking sector, investors choose to reallocate some of their resources to this sector in advance—hence the positive anticipation effect on the investment in 2020. Consequently, much less of such reallocation takes place in the second period—hence the negative anticipation effect on the investment in 2030. By this time, in the case of anticipation, the additional early investment is already transformed into a higher level of capital—hence the positive anticipation effect on capital in 2030.

The fact that the transport sector has a similar effect of anticipation (panel **(b)** of Figure 5.7) at first seems less intuitive. This sector is energy-intensive and heavily burdened by carbon taxation. Yet, in anticipation of such a policy, the investors also decide to stimulate this sector with additional investments. The reason for such a reaction becomes clear when we take into consideration the cross-sectoral structure of the demand in the economy. The transport sector enjoys relatively high demand from all other sectors, especially those that grow faster under the policy. To maintain the production level such that it meets the demand, the investment made in advance of the policy promotes the substitution of capital for energy in this sector. Advance anticipation, therefore, to a certain extent, alleviates the negative

Figure 5.7: The effect of anticipation on the investment and capital accumulation in the banking sector, the transport sector, and the insurance sector

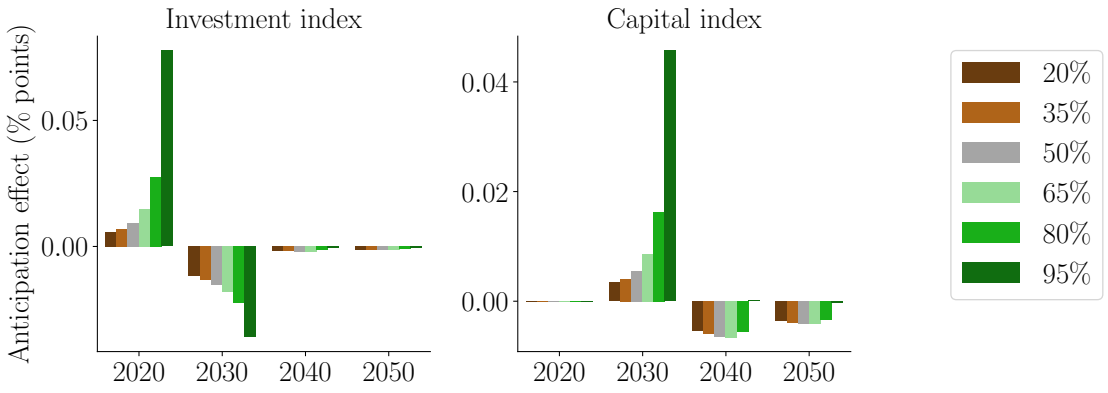

(a) Banking sector

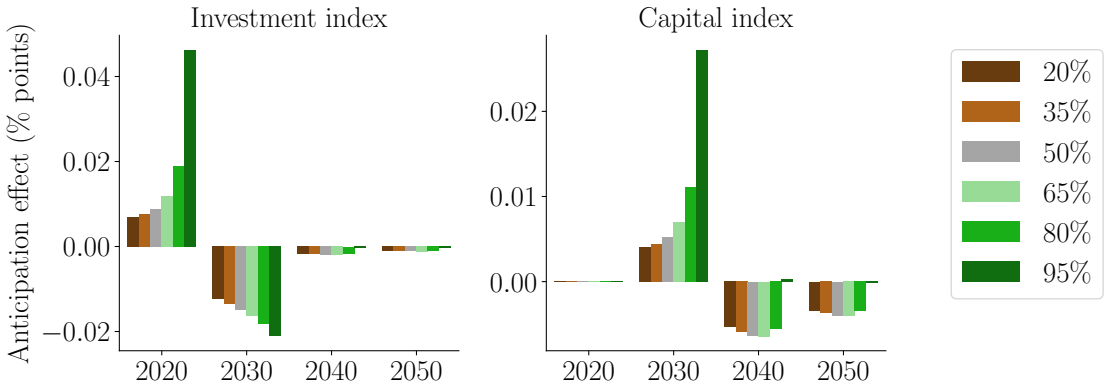

(b) Transport sector

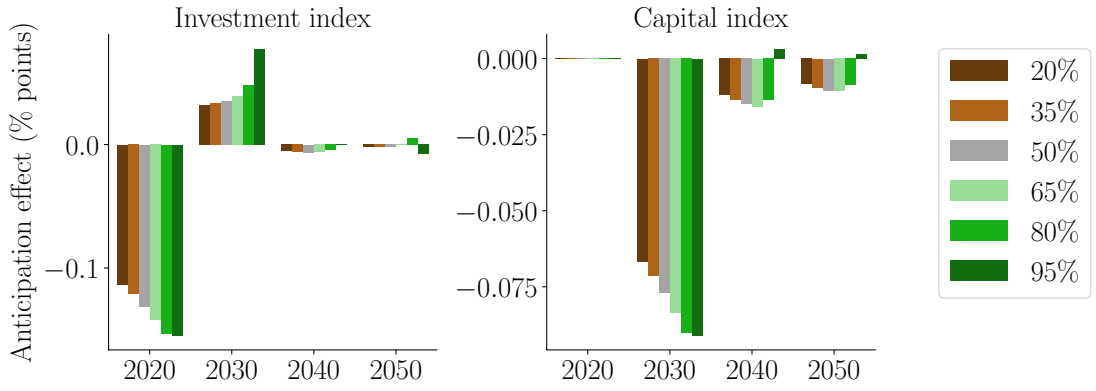

(c) Insurance sector

effect of a carbon tax on this sector.

The insurance sector is an example of a completely opposite effect of anticipation (panel **(c)** of Figure 5.7). Under the stringent carbon policies, the growth of this sector slows down initially and accelerates only in the last modeled decade. The demand from the other sectors for its products is also relatively low—both in the benchmark scenario and under the policies. The sector thus witnesses a divestment already in the first period if the investors anticipate a carbon tax—hence the negative anticipation effect on the investment in 2020, which transfers into a lower capital level in 2030. Without such anticipation, this reaction is triggered directly by implementing the policy in the second period.

5.4.2 Welfare effects

The aggregate welfare reflects the utility the households enjoy from their consumption and leisure. Carbon taxation of any stringency lowers this welfare by imposing an additional tax distortion on the economy. Figure 5.8 shows the highly nonlinear magnitude of such losses with respect to the policies' stringency. For example, a policy that aims at a 50% reduction in CO_2 emissions is associated with a welfare loss of around 0.5%, whereas further reductions to 80% and 95% correspond to roughly two- and a five-fold increase in this cost. These results are consistent with earlier studies (Karydas and Zhang, 2019; Landis et al., 2019) and include policy targets up to almost full decarbonization.

The effect of anticipation on welfare can be positive or negative, as shown in Figure 5.9. With policy targets becoming more stringent, the anticipation effect changes from clearly negative to strongly positive, starting from a 90% reduction in CO_2 emissions. The anticipation effect on aggregate welfare spans from -0.08% to over 0.11%. At first, anticipating the coming carbon tax improves aggregate welfare under stringent policies and harms it otherwise. To better understand the forces that drive such a difference, the dynamics of the anticipation effect have to be explored in more detail.

First, a closer look at the distributional effect of anticipation in Figure 5.10 reveals that the negative impact entirely relates to the working groups of households (named *Active low*, *Active mid*, and *Active high* in the figure). For these households,

Figure 5.8: The effect of carbon taxation on the aggregate welfare

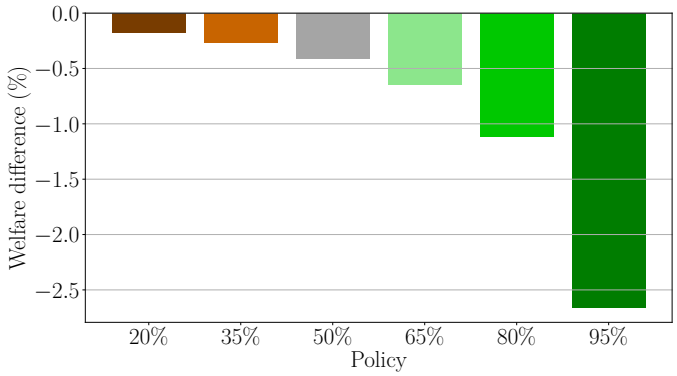

Notes: The figure shows the effect of the carbon tax on aggregate welfare for various policy targets. The y-axis represents the welfare difference between the business-as-usual scenario and the policy scenario under full anticipation. A 65% policy implies a 65% reduction in CO_2 emissions in comparison to the benchmark year.

Figure 5.9: The effect of anticipation on the aggregate welfare

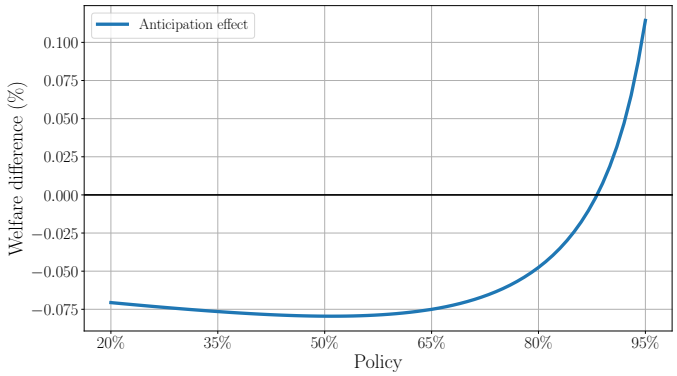

Notes: As the graph reads, the welfare difference between the anticipation and the unanticipation scenario is about -0.05% of the benchmark welfare level for a 80% carbon reduction policy. This difference is due to the effect of anticipating the policy. A 80% policy implies a 80% reduction in CO_2 emissions in comparison to the benchmark year.

Figure 5.10: The effect of anticipation on welfare across the five groups of households

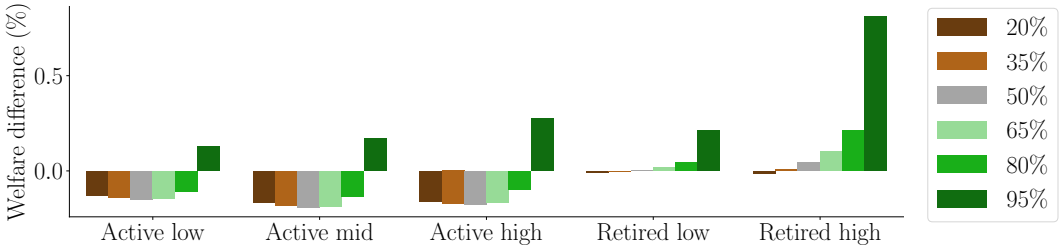

Notes: We show the results for scenarios that go from 20% to 95% reduction of carbon emissions. As the graph reads, the welfare difference for the "Retired high" household group between the anticipation and the unanticipation scenario is about 0.8% of the benchmark welfare level for a 95% carbon reduction policy. This difference is due to the anticipation of the policy.

labor is the major source of income. In anticipation of a carbon tax, households expect the prices for energy and energy-intensive goods to rise. That is, they anticipate a loss of consumption. Thus, in line with consumption smoothing, they decrease their consumption before the actual imposition of the tax burden.[16] On the supply side, the anticipation of the policy implies a shift toward labor-intensive goods.[17] For working households, that shift corresponds to higher levels of labor supply and less leisure. This higher labor supply ensures higher output levels in the first period, as the additional labor mostly flows to production, not research. The lower leisure levels, together with the lower levels of consumption, lead to a negative aggregate welfare effect.

The households' budget constraint allows us to understand the mechanisms at stake better. At any time, households face the following constraint from equation (A.4.3) in the model description (Appendix A.4.1):

$$\sum_i p^J_{i,t+1} J_{i,t+1} = w_t(L_{X_t} + L_{J_t}) + \sum_i (1 + r_t) p^J_{i,t} J_{i,t} - p^C_t C_t - T_t. \tag{5.5}$$

The left-hand side of the equation represents the value of the households' asset in

[16] Appendix A.4.6 provides the figures for the decomposition of consumption and labor supply across the households' groups.

[17] The literature documents this effect well (Williams III, 2016).

sector i at time $t+1$. In equilibrium, it is equal to the households' income from their work (w_t), either in research (L_J) or in the production of the final good (L_X), plus rents from their assets at time t, minus their consumption C_t at price p_t^C, and the net transfers T. When the households learn about the upcoming policies, they immediately adjust the future value of their assets $\sum_i p_{i,t+1}^J J_{i,t+1}$. The value of the "green" capital increases, and the value of the "dirty" capital decreases. Since, in the economy, most of the sectors are in the "grey" area (that is, they require both clean and dirty energy as inputs), mild policies are not enough to incentivize a large reallocation of capital to clean technologies. The investors can anticipate the value of their assets to decrease. They compensate the excess capital subject to future tax by investing less than they would have without policy announcement (see Figure 5.5). Because, in this economy, production and research activities compete for resources, lower investments translate into higher output in the same period. Sectors already start to rely more on labor for their production. The rents households receive from their assets at time $t = 0$ and the net taxes they pay are given and cannot adjust.

The extra labor supply in $t = 0$ goes hand in hand with a decrease in leisure. The welfare impact of the loss of leisure, on the one hand, and the decrease in consumption, on the other hand, is negative. Retired households suffer less from these mechanisms since, by definition, they work much less. In the anticipation scenario, they also enjoy the possibility of reallocating their investments earlier. Since their investment also decreases, they have spare resources. The retired households are the only ones to enjoy increased consumption in the first period.

In the anticipation scenario, the lower level of investment at the time of the announcement induces a lower level of capital at time $t = 1$. Households have fewer resources to allocate to produce the final good or reinvestment. Because capital owners pay lower carbon taxes if they can anticipate a policy, the overall level of taxes to redistribute is lower. In this case, households that do not own much capital consume less and receive fewer lump-sum transfers from the redistribution. The regressive effect of the anticipation of the policy is clear.

As the policies become more stringent, investment reallocations become more and more important. High carbon taxes lower the expected returns on dirty capital enough to trigger a large redistribution of the investments—and subsequently

capital—from carbon-intensive sectors to "cleaner" sectors with lower tax burden and higher profitability. This redistribution adjusts the production side of the economy to the upcoming carbon tax. For the working group of households, the mechanisms already in place for mild policies do not change; they even amplify. These households must supply more labor and forgo more consumption during the anticipation period. Capitalists, however, can earn notably higher returns on investment if they anticipate a stringent carbon tax. The anticipation effect is highly regressive since capital returns comprise a large share of income for richer and retired households.

Overall, the economy has a higher capital stock than it would have in the unanticipated scenario, and all households can earn more capital rents. Also, the redistributed tax revenues are higher than in the mild-policy scenarios. This welfare benefit for poorer households can partly offset their initial consumption loss. Even though the anticipation of strict carbon policies has regressive effects, it increases the welfare of all household groups.

5.4.3 Redistribution inverse-proportional to income

As we show in Section 5.4.2, stringent policies might disadvantage less affluent households. We explore this result for an alternative revenue recycling scheme that distributes tax revenues in inverse proportion to the households' income level. In its naïve interpretation, such a scheme should utilize the tax revenues to reduce income inequality across households.

Figure 5.11 shows that the anticipation effect for policies with the inverse-proportional redistribution scheme is comparable to that of the lump-sum redistribution for mild policies (around 0.1–0.3% of welfare loss for the working groups of households in mild policies). Yet, in anticipation of a stringent policy, capital owners adapt their investment decisions even more intensely. They reallocate more capital to cleaner sectors, thereby securing higher consumption levels despite their lower income from tax redistribution. The overall anticipation effect of the strict policies, therefore, stays regressive.

These dynamics become even more evident when we consider the absolute effects

Figure 5.11: The effect of anticipation on welfare across the five groups of households under inverse-proportional redistribution scheme

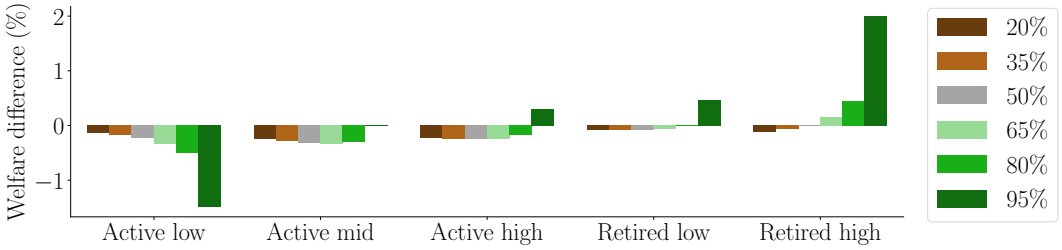

Notes: We show the results for scenarios that go from 20% to 95% reduction of carbon emissions.

of carbon taxation.[18] Wealthy households end up with higher welfare under all policy targets. For a 95% carbon reduction policy, the welfare of the "Retired high" household group increases by about 7.5% when the tax revenues are redistributed inversely proportional to total income compared to the lump-sum redistribution scheme. The inverse-proportional reallocation scheme can thus benefit the richer groups of households and leave the poorer groups at a disadvantage.

5.5 Discussion

We find that under lump-sum redistribution of the tax revenues, the prior announcement of the carbon tax has regressive effects. We also show that this regressive effect of the anticipation period is even more pronounced under policy schemes that try to alleviate the tax's regressivity. These alternative redistribution schemes might successfully turn a carbon tax to be progressive.[19] But our results highlight the welfare effect of the anticipation period and not the overall effect of the tax after its implementation. The anticipation period has regressive effects because of the *ex-ante* economic adjustments (e.g., capital re-allocation), although the tax and the redistribution of its revenues are not yet in place.

The regressive anticipation effect that we find is an issue to be addressed. Yet, we

[18] Figure A.4.5 in Appendix A.4.7 shows the difference in absolute welfare impacts between the policies with inverse-proportional and lump-sum redistribution schemes.

[19] See for example Beck et al. (2015) for the case of British Columbia's revenue-neutral carbon tax.

do not advocate hiding or hindering the political process that leads to the adoption of the tax. The textbook's unanticipated implementation of a carbon tax is practically impossible. More likely, some scarce and asymmetric information about the upcoming "surprise" policy could influence the agents' expectations and strengthen economic inequality. A less transparent political decision-making mechanism would favor those who are better informed about the upcoming policies. The policymaker ought to keep the democratic process and the political decisions that result from it transparent. With this transparency, agents might have more trust in the government. The lack of transparency can increase uncertainty and slow economic growth (Bosetti and Victor, 2011; Koch et al., 2016; Nemet et al., 2017). Besides, the results suggest that a carbon tax's overall anticipation effect might benefit the economy—provided that these benefits are distributed evenly across society.

The policymaker might consider several tools to tackle the effects of the anticipation period. We show that the carbon tax is regressive partly because of the profit increase that benefits the capital owners. First, the state could choose to increase capital taxation. The increase could be either permanent or temporary during the anticipation period and until the redistribution of the carbon tax revenues kicks in. Second, the state could change the allocation of the capital share of a company between the workers and the owners. As Piketty (2020) suggests, the workers should be entitled to take part in the company's decision process. Workers would also receive a minimum share of the company's dividend. This way, the reallocation of capital and increased profits in the "clean" sectors would also benefit the workers. Third, when they announce the tax implementation, policymakers may consider organizing training programs. Such programs aim to provide workers with the new competencies they need to better adjust to the capital reallocation in the economy.

One known limitation of the analysis of stringent climate policies is the models' limited ability to reflect the economy's transition to deep decarbonization targets (Pye et al., 2021). Studying the policies that almost eliminate CO_2 emissions by the mid-century comes at a price of making strong assumptions on the future technological frontiers. To address this concern, modelers ensure their calibrations match the latest data and adequately include substitution possibilities. The results also depend on mechanisms for energy transition and efficiency improvement.

In our analysis, we assume no mechanisms of energy efficiency improvement in

the business-as-usual scenario. The economy is initially calibrated to follow a balanced growth path. The producers have no incentives to improve energy efficiency unless a policy pushes the production away from dirty energy. This calibration makes our results immune to the rightful critique on the uncertainty of the extent of technological progress in the business-as-usual scenario. We also do not assume any carbon capture and storage (CCS) or negative emissions technology (NET), neither in BAU nor under the policies. Even though NET can arguably be a viable solution for eliminating residual emissions, we depart from this concept and focus on absolute emissions reductions.

Under these rather conservative assumptions, we interpret the results of our scenarios as the upper bounds of the impact of a CO_2 policy on welfare. Besides, we use an updated estimate of the elasticity of substitution between clean and dirty energy (set to 2) based on the recent results from the empirical literature (Papageorgiou et al., 2017; Jo, 2020). This estimate reflects the latest technological advances that make dirty and clean energy better substitutes. Good substitutability between clean and dirty technologies alleviates the negative effect that CO_2-reduction policies have on welfare. It also allows the economy to reach ambitious policy targets, almost eliminating CO_2 emissions.

5.6 Conclusion

We study the role of the anticipation period of climate policies in a numerical model of general equilibrium with endogenous growth, heterogeneous households with a labor-leisure choice, and multiple economic sectors. The anticipation period is the time the policymaker gives to the agents in the economy to adjust their decisions before implementing a policy.

On an example of the Swiss economy, we analyze the implications of such an anticipation period for welfare and economic growth at various stringency carbon tax levels. We find that the magnitude and sign of the effect of policy anticipation may vary depending on the strength of the underlying economic incentives. Under moderate policy targets, the incentive to increase immediate consumption dominates and negatively affects aggregate long-term welfare. In anticipation of more stringent carbon policies, the agents more actively redistribute their invest-

ments beforehand and achieve a more profitable allocation under the upcoming policies. Thus, the given opportunity to adjust in advance turns out beneficial on the aggregate level.

An equally important result is that the knowledge about future policies can have an unequal effect on different groups of households and can amplify the existing income inequality. The households' sources of income determine their ability to prepare and adapt to the upcoming taxation. The dynamics of the economy in anticipation of a carbon tax might change the economic environment against the working and poorer households, who might find themselves working more in an attempt to maintain their consumption level. For the richer and retired groups, on the contrary, additional capital earnings due to advanced adjustments of their investment strategies partially offset the tax burden. Redistributing the tax revenues directly to the consumers does not alleviate these disparities. Even distributing higher shares of tax revenues to less affluent households does not change these dynamics—instead, it reinforces the advance adjustments to the policies.

Appendices

A.1 Appendices to Chapter 2

A.1.1 Economic growth model

We employ a dynamic, multi-regional, and multi-sectoral numerical general equilibrium model following Bretschger et al. (2011) and Bretschger et al. (2017).

Production

In each region, we model the economy's production structure as the interaction between three agents: *i*) final good producers, *ii*) producers of intermediate goods, and *iii*) producers of intermediate composites. The markets for the final goods and intermediate composites are perfectly competitive, whereas the market for intermediate goods can also be monopolistic. Figure A.1.1 provides an overview of the nested production structure.

Final good production

The final good producers in sector i, region r, and time t produce output $Y_{i,r,t}$ according to the following constant elasticity of substitution (CES) production function:

$$Y_{i,r,t} = \left[\alpha_{i,r} Q_{i,r,t}^{\frac{\sigma_{i,r}-1}{\sigma_{i,r}}} + (1-\alpha_{i,r}) B_{i,r,t}^{\frac{\sigma_{i,r}-1}{\sigma_{i,r}}} \right]^{\frac{\sigma_{i,r}}{\sigma_{i,r}-1}}. \tag{A.1.1}$$

Figure A.1.1: Production structure of the economy

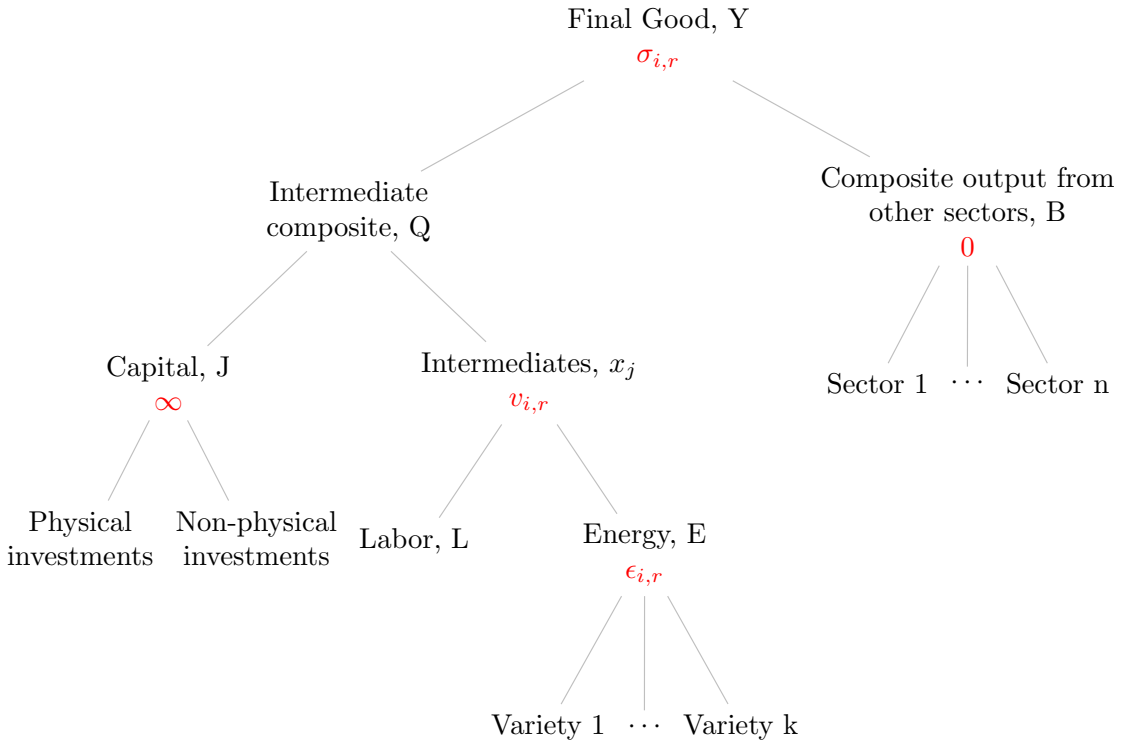

Notes: Substitution elasticity within a sub-nest is highlighted in red.

Above, $Q_{i,r,t}$ is the sector-specific composite intermediate good. $B_{i,r,t}$ denotes the composite final good from all other sectors needed for producing i, capturing how different sectors (and regions) link through a complex network of value chains. Outputs from different sectors are assembled to $B_{i,r,t}$ according to a Leontief-type production function, that is, in fixed proportions. Share parameters $\alpha_{i,r}$ determine the value shares between $Q_{i,r,t}$ and $B_{i,r,t}$ in the production function. The elasticity of substitution between the two types of inputs is $\sigma_{i,r}$. All elasticity and share parameters are sector- and region-specific.

In each sector, the final good producer maximizes profits in a perfectly competitive market according to:

$$\max_{Q_{i,r,t},B_{i,r,t}} p^Y_{i,r,t}Y_{i,r,t} - p^Q_{i,r,t}Q_{i,r,t} - p^B_{i,r,t}B_{i,r,t}, \text{ w.r.t A.1.1,} \tag{A.1.2}$$

where $p^Y_{i,r,t}$, $p^Q_{i,r,t}$ and $p^B_{i,r,t}$ denote the prices of final goods, intermediate composite, and other inputs, respectively. Solving Eq. (A.1.2) and combining the resulting optimal demand functions for $Q_{i,r,t}$ and $B_{i,r,t}$ yields the following condition for the optimal input use:

$$\frac{Q_{i,r,t}}{B_{i,r,t}} = \left(\frac{\alpha_{i,r}}{1-\alpha_{i,r}}\right)^{\sigma_{i,r}} \left(\frac{p^B_{i,r,t}}{p^Q_{i,r,t}}\right)^{\sigma_{i,r}} . \tag{A.1.3}$$

According to Eq. (A.1.3), an increase in the price of one input type will increase the share of the other input in the optimal bundle. For most of the goods, we assume that the substitution elasticity $\sigma_{i,r}$ is below unity, which implies imperfect substitutability between different input types.

Intermediate composite production

In the second step of the production nest, producers of a sector-specific intermediate composite assemble their output $Q_{i,r,t}$ by combining different varieties of individual intermediate goods according to a standard Dixit-Stiglitz CES production function:

$$Q_{i,r,t} = \left[\int_{j=0}^{J_{i,r,t}} x^{\kappa}_{j,i,r,t} dj\right]^{\frac{1}{\kappa}} , \tag{A.1.4}$$

where $x_{j,i,r,t}$ denotes the j^{th} type of intermediate good variety that is available in sector i. $J_{i,r,t}$ denotes the sector-specific capital stock. We treat new innovations (that is, new varieties of $x_{j,i,r,t}$) as new varieties of capital, so new types of $x_{j,i,r,t}$ also imply an expansion in the capital stock. This specification gives us two channels through which the intermediate sector can induce growth in the overall economy. One is to produce a larger amount of any single variety $x_{j,i,r,t}$ by employing more labor and energy. The other is to expand the number of available varieties through investments in the sector-specific capital stock. The parameter κ measures the substitutability between different varieties, or equivalently, the gains from specialization. Setting $0 < \kappa < 1$ allows the increasing number of varieties to enhance final sector productivity in an endogenous manner (Romer, 1990), whereas $\kappa = 1$ switches off these productivity gains.

The producer of the intermediate good composite $Q_{i,r,t}$ maximizes profits on a competitive market, taking all prices as given, and solving:

$$\max_{x_{j,i,r,t}} p^{Q}_{i,r,t} Q_{i,r,t} - \int_{j=0}^{J_{i,r,t}} p^{x}_{j,i,r,t}\, x_{j,i,r,t}\, dj, \text{ w.r.t A.1.4,} \tag{A.1.5}$$

where $p^{x}_{j,i,r,t}$ is the price of intermediate varieties. Solving the optimization problem in Eq. (A.1.5) determines the optimal demand for $x_{j,i,r,t}$ as:

$$x_{j,i,r,t} = \left(\frac{p^{Q}_{i,r,t}}{p^{x}_{j,i,r,t}} \right)^{\frac{1}{1-\kappa}} Q_{i,r,t}. \tag{A.1.6}$$

From here onwards, we assume that all varieties of the sector-specific intermediate good are perfectly symmetrical, i.e. $x_{j,i,r,t} = x_{i,r,t}$.

Intermediate good production

As described in Eq. (A.1.4), the amount, variety, and substitutability between different intermediate goods determine the expansion of each production sector i. We assume that each intermediate variety $x_{i,r,t}$ is first invented, and then produced, by a single firm that receives a perpetual patent at the moment of invention. Therefore, the growth rate of the overall economy depends on the decisions of profit-seeking intermediate firms. To describe these intermediate firms in full, we need to describe both their optimal output decision for the already invented varieties, as well as their incentives to innovate new varieties.

i) Optimal output of existing varieties

To produce one unit of output, the intermediate good producer combines two types of inputs, labor $L_{i,r,t}$ and energy $E_{i,r,t}$, according to the following CES technology:

$$x_{i,r,t} = J_{i,r,t} \left[\lambda_{i,r} L_{i,r,t}^{\frac{v_{i,r}-1}{v_{i,r}}} + (1-\lambda_{i,r}) E_{i,r,t}^{\frac{v_{i,r}-1}{v_{i,r}}} \right]^{\frac{v_{i,r}}{v_{i,r}-1}}, \tag{A.1.7}$$

where $\lambda_{i,r}$ denote the value share parameters and $v_{i,r}$ the substitution elasticities.

From Eq. (A.1.7), there are within-sector spillover effects from the expanding capital stock $J_{i,r,t}$. We assume the supply of labor to be inelastic throughout the modeling horizon, mobile between sectors within a country, but immobile between countries. The energy aggregate $E_{i,r,t}$, on the other hand, is combined from a variety of K available energy sources according to:

$$E_{i,r,t} = \left[\sum_{k \in K} \phi_{k,i,r} (Z_{k,i,r,t})^{\frac{\epsilon_{i,r}-1}{\epsilon_{i,r}}} \right]^{\frac{\epsilon_{i,r}}{\epsilon_{i,r}-1}}. \tag{A.1.8}$$

We denote the amount of every energy input $k \in K$ by $Z_{k,i,r,t}$, and the respective price by $p^Z_{k,r,t}$. The output decision of the intermediate monopoly can be derived from two parts. First, it chooses an optimal bundle of labor and energy inputs under profit-maximizing conditions of a perfectly competitive market:

$$\max_{L_{i,r,t}, Z_{k,i,r,t}} \psi^x_{i,r,t} x_{i,r,t} - w_{r,t} L_{i,r,t} - \sum_k p^Z_{k,r,t} Z_{k,i,r,t}, \tag{A.1.9}$$

where $\psi^x_{i,r,t}$ is the price that would prevail under a perfectly competitive market. The firm, however, exploits its monopoly power in the output market and sets the optimal output price under:

$$\max_{p^x_{i,r,t}} p^x_{i,r,t} x_{i,r,t} - \psi^x_{i,r,t} x_{i,r,t}, \tag{A.1.10}$$

taking the demand for $x_{i,r,t}$ in Eq. (A.1.6) as given. Thus, it sets prices according to:

$$p^x_{i,r,t} = \frac{1}{\kappa} \psi^x_{i,r,t}, \tag{A.1.11}$$

making profits of:

$$\pi_{i,r,t} = (1-\kappa)p^x_{i,r,t}x_{i,r,t}. \tag{A.1.12}$$

This brings us to an alternative definition of the substitutability term κ: as the individual intermediate goods $x_{i,r,t}$ are imperfect substitutes, and the intermediate good producers compete in a monopolistic market with an output price $p^x_{i,r,t}$ and mark-up $\frac{1}{\kappa}$, we can consider $(1-\kappa)$ as the profit fraction of revenues from the intermediate composite sector going to the households that own the firms.

ii) Investments to new varieties

The model makes a distinction between physical and non-physical capital, which together make up the sector-specific capital composite $J_{i,r,t}$. Firms conduct innovation by investing an amount $I_{i,r,t}$ to this composite capital good. Access to the investment market is unrestricted. This implies that new innovations occur until the marginal cost of investments to the composite capital is equal to the firm's value so that no real profits remain. We follow the approach of Romer (1990) where the knowledge capital from the innovation process is non-rival but partially excludable with the use of patents. The equation of motion of the capital stock is:

$$J_{i,r,t+1} = I_{i,r,t} + (1-\delta_{i,r,t})J_{i,r,t}, \tag{A.1.13}$$

with $\delta_{i,r,t}$ denoting the capital depreciation rate. The depreciation parameter has a particular role for our work as it depends both on the baseline depreciation rate and the exposure to cyclones that varies by year and region.

Finally, the capital accumulation process requires introducing a no-arbitrage condition. New firms (capital varieties) emerge as a result of the household investment. In equilibrium, households must be indifferent between investing in a new firm and to a riskless loan with return $r_{i,r,t}$. As in standard endogenous growth models based on expanding input varieties, the value of the monopolist firm, that is, the value of owning a technology blueprint, is equal to the discounted value of all future profits. In our setting, this is also equal to the cost of investing to a new firm. We can write the relationship between the new firm value $V_{i,r,t}$, instantaneous

profits $\pi_{i,r,t,}$ and the interest rate as $r_{i,r,t}$ with the following asset value equation: [20]

$$\pi_{i,r,t} + \Delta V_{i,r,t} = r_{i,r,t} V_{i,r,t}, \tag{A.1.14}$$

where $\Delta V_{i,r,t}$ denotes the change in firm value. We can then extend Eq. (A.1.14) by writing:

$$\underbrace{\pi_{i,r,t}}_{\text{Direct return}} + \underbrace{\frac{p^J_{i,r,t+1}}{1+r_{i,r,t}} - p^J_{i,r,t}}_{\text{Time } t \text{ present value of the capital gain}} - \underbrace{\delta_{i,r,t} p^J_{i,r,t}}_{\text{Value lost to depreciation}} = \underbrace{r_{i,r,t}}_{\text{Interest rate of a riskless loan}} \times \underbrace{V_{i,r,t}}_{\text{Firm value = investment cost}}, \tag{A.1.15}$$

where p^J_t is the price of capital. The intermediate good producer borrows from households to pay the innovation activities in advance. We can also re-write the sectoral profits from Eq. (A.1.12) as:

$$\pi_{i,r,t} = \underbrace{(1-\kappa)}_{\text{Monopoly profit share}} \underbrace{p^Q_{i,r,t} Q_{i,r,t}/}_{\text{Sectoral revenue}} \underbrace{J_{i,r,t}}_{\text{Number of varieties}}. \tag{A.1.16}$$

Inserting Eq. (A.1.16) into Eq. (A.1.15) then yields the expression for equilibrium interest rates, and thus completes the no-arbitrage condition.

International trade

Our baseline dataset contains economic accounts of 129 regions, covering most of the global economy. Representing how different countries interact through international trade is, therefore, a central feature of our underlying general equilibrium model, and an important determinant of how countries can adapt to economic shocks.

All final sectors in the economy are open to international trade. That is, all producers can employ both domestically produced and imported inputs, and consumers can purchase both domestic and imported consumption goods. To give more structure to the representation of international trade, we follow the Armington approach (Armington, 1969), which is a standard assumption in the numerical general equilibrium literature. With this approach, the suppliers of the final good

[20] For details on deriving the relationship, see e.g. Acemoglu (2009) Ch. 13.

use both domestically produced goods and imported goods, and use them as inputs in creating an Armington aggregate good, which is the final good demanded in the economy. The domestic and imported inputs are combined with an elasticity of substitution less than one so that they function as imperfect substitutes. Intuitively, this means that consumers in any country can prefer domestically produced goods over imports varieties. More importantly, this allows for a realistic description of international trade, where any production sector in any region can simultaneously be an exporter and an importer of the same good, which is what we also observe in the real economies.

More formally, denoting domestic sectoral production in region r by $D_{i,r,t}$ and imports from region s to r by $M_{i,s,r,t}$, the Armington aggregate is given by:

$$A_{i,r,t} = \left(\zeta_{i,r} D_{i,r,t}^{\frac{\eta_{i,r}-1}{\eta_{i,r}}} + (1-\zeta_{i,r}) \left(\left[\sum_{s \neq r} m_{i,s,r} M_{i,s,r,t}^{\frac{\phi_{i,r}-1}{\phi_{i,r}}} \right]^{\frac{\phi_{i,r}}{\phi_{i,r}-1}} \right)^{\frac{\eta_{i,r}-1}{\eta_{i,r}}} \right)^{\frac{\eta_{i,r}}{\eta_{i,r}-1}}, \tag{A.1.17}$$

where we denote by $\zeta_{i,r}$ the share of domestic goods, and by $m_{i,s,r}$ the share parameters of different regions in the basket of imports. Parameters $\eta_{i,r}$ and $\phi_{i,r}$ are the respective substitution elasticities. With $p^A_{i,r,t}$ being the price of the Armington composite, and $p^Y_{i,r,t}$ the price of the domestic output, the profit maximization the final suppliers face is then:

$$\max_{D_{i,r,t}, M_{i,s,r,t}} p^A_{i,r,t} A_{i,r,t} - p^Y_{i,r,t} D_{i,r,t} - \sum_{s \neq r} p^A_{i,s,t} M_{i,s,r,t}. \tag{A.1.18}$$

We allow countries to run either trade surpluses or deficits, as also observed in the baseline dataset.

Preferences

For each region, we assume an infinitely lived, forward-looking representative household. The representative household derives utility from consumption according to

a standard constant intertemporal elasticity of substitution function:

$$U = \sum_{t=0}^{\infty} \left[\frac{1}{1+\rho}\right]^t \frac{C_{r,t}^{1-\theta} - 1}{1-\theta}, \tag{A.1.19}$$

where ρ denotes the time discounting parameter and θ the inverse of the intertemporal elasticity of substitution. As the economy consists of multiple production sectors, $C_{r,t}$ is a CES aggregate of the sector-specific consumption goods. Figure A.1.2 illustrates the nested consumption structure.

Figure A.1.2: Nested consumption structure

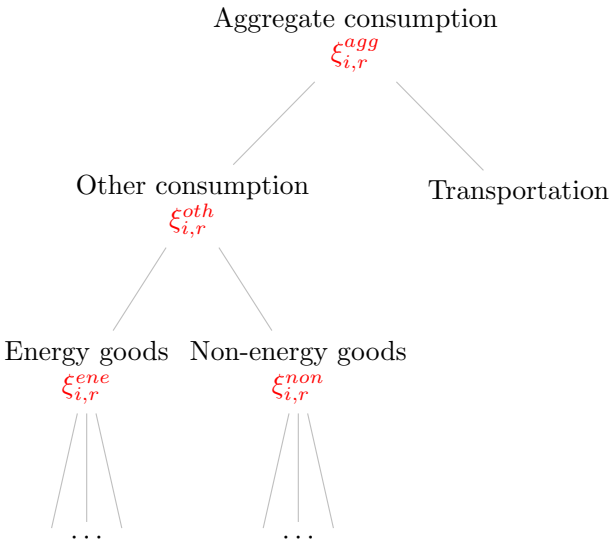

Notes: Substitution elasticity within a sub-nest is highlighted in red.

The household also owns all firms in the economy, so its budget reads:

$$p_{r,t}^C C_{r,t} = w_{r,t} L_{r,t} - T_{r,t} - \sum_i p_{i,r,t+1}^J J_{i,r,t+1} + \sum_i (1 + r_{i,r,t}) p_{i,r,t}^J J_{i,r,t}, \tag{A.1.20}$$

where $w_{r,t}$ denotes the wage rate, $T_{r,t}$ a lump-sum tax which ensures the public budget to remain balanced, and $p_{r,t}^C$ is the price for the consumption aggregate.

Calibration details

Our model calibration follows closely the steps outlined in Lau et al. (2002b) and Paltsev (2004). The key goal of the calibration process is to use the GTAP dataset as a static snapshot of the economy, and extrapolate—using a set of exogenous parameter assumptions—a balanced growth path on which all sectors, and therefore also all regional economies, grow at the same rate.

The household's problem involves maximizing the stream of utility over time in Eq. (A.1.19). The optimization is subject to the the economy's production function $F(K_t, L_t)$, a resource constraint $F(K_t, L_t) = I_t + C_t$ dividing the output between consumption and investment, and the capital stock law of motion from Eq. (A.1.13). Assuming constant returns to scale and perfectly competitive markets, we can derive the following price relationships from the first-order optimality conditions (Paltsev, 2004):

$$p_t = \Big[\frac{1}{1+\rho}\Big]^t \frac{\partial U(C_t)}{\partial C_t}, \tag{A.1.21}$$

$$p_t^K = p_t \frac{\partial F(K_t, L_t)}{\partial K_t} + (1-\delta) p_{t+1}^K, \tag{A.1.22}$$

$$p_t = p_{t+1}^K. \tag{A.1.23}$$

We can interpret these values as p_t being the price of output, $p_t \frac{\partial F(K_t, L_t)}{\partial K_t} \coloneqq R_t$ the rental rate of capital, that is, the value of the marginal product, and p_t^K the price of buying one new unit of capital. This distinction between capital stocks and capital services is central to the modeling approach: households own the stock, invest by buying new units of capital, and rent the capital to firms at the rate R_t.

Assuming a baseline interest rate $\bar{r}$, the calibration makes use of a declining reference price trajectory $p_t^{\text{ref}} = (1/(1+\bar{r}))^t$. Then, for all prices in the model, and for any arbitrary time instance τ, we have that:

$$p_{\tau+1} = \frac{p_\tau}{1+\bar{r}}. \tag{A.1.24}$$

We can use the reference price path to further highlight the distinction between the capital rental and purchase prices. Combining Eq. (A.1.24) and (A.1.22) gives:

$$R_t = p_t^K \Big(1 - \frac{1-\delta}{1+\bar{r}}\Big), \tag{A.1.25}$$

which states that the capital rental price R_t is equal to the price of buying a new capital unit, subtracting the discounted value of the depreciated stock in the subsequent time period. Further normalizing $p_0 = 1$ allows us to write the first-period rental rate as $R_0 = \delta + \bar{r}$.

The benchmark GTAP data does not provide the capital stock values directly but only the base year capital earnings, denoted with V_0^K. Using $V_t^K := R_t K_t$ and the base year rental rate from above, we can derive the initial capital stock as $K_0 = V_0^K/(\delta + \bar{r})$. The next task is to calibrate the initial investments on balanced growth path. Assuming a constant capital stock growth rate γ_K, we can write the next period capital stock either as in Eq. (A.1.13) or with $K_{t+1} = (1 + \gamma_K)K_t$. Combining the two equations gives $I_t = (\gamma_K + \delta)K_t$, such that on a balanced growth path the annual investment level must cover both the capital growth rate and depreciation. Plugging in the definition of K_0 from before gives:

$$I_0 = (\gamma_K + \delta)K_0. \tag{A.1.26}$$

The calibration process so far follows the standard conventions of numerical general equilibrium modeling. In our setting, however, the possibility to consider productivity gains from specialization requires some additional steps. When the gains from specialization are active, we assume that the size of the capital stock directly corresponds to the number of capital varieties. Moreover, the different varieties are imperfect substitutes, determined by the substitution elasticity parameter κ. The imperfect substitutability then creates monopoly rents and additional incentives for investing. The growth rate of output γ_Y then depends on two factors: an exogenously specified capital growth rate γ_K and an endogenous growth part determined by κ. The relationship between these parameters satisfies:

$$1 + \gamma_Y = (1 + \gamma_K)^{\frac{1}{\kappa}}. \tag{A.1.27}$$

Whenever $0 < \kappa < 1$, the output growth rate γ_Y exceeds the capital growth rate

γ_K. To make this difference in growth rates compatible with the balanced growth path, and to avoid situations where investments grow faster than the actual stock of capital, we also make the base depreciation rate time-dependent. This assumption is necessary for the balanced growth path to exist, but there is also an appealing intuition behind the adjustment. Namely, as the economies develop further, their capital stock grows more specialized and more susceptible to depreciation. The base depreciation rate is:

$$\delta_{r,t} = \left(\frac{1+\gamma_Y}{1+\gamma_K}\right)^t \delta_{r,0} + \gamma_K \left(\left(\frac{1+\gamma_Y}{1+\gamma_K}\right)^t - 1\right), \tag{A.1.28}$$

which collapses to a constant value when $\kappa = 1$ and the gains from specialization are switched off.

Finally, to obtain the baseline consumption growth rate $g_r = \frac{C_{r,t+1}}{C_{r,t}}$ on the balanced growth path calibration, we can maximize Eq. (A.1.19) with respect to Eq. (A.1.20) to obtain the standard Keynes-Ramsey rule:

$$g_r \equiv \left[\frac{1+\bar{r}}{1+\rho}\right]^{\frac{1}{\theta}}. \tag{A.1.29}$$

According to Eq. (A.1.29), a higher interest rate $\bar{r}$ boosts growth by inducing more saving, whereas a higher discount rate ρ gives incentives to present consumption, therefore reducing the rate of growth. A higher intertemporal substitution elasticity $1/\theta$ also increases growth rates, as the households become more willing to tolerate consumption variability in response to interest rate changes. In our setting, Eq. (A.1.29) also implicitly pins down the temporal discount rate ρ.

Numerical implementation

We follow Mathiesen (1985) and formulate the general equilibrium economy as a mixed complementary problem (MCP). The formulation includes three types of inequality constraints: market-clearing conditions, zero profit conditions, and income balance conditions. Each equilibrium condition f has a complementary variable z, such that the following conditions always hold: $f(z) \geq 0, z \geq 0, z^T f(z) = 0$. For

instance, we can write the market-clearing condition as $f(p) = S(p) - D(p)$, where we use the price level p as the complementary variable, and supply and demand functions S and D, respectively. When the market clears, $f(p) = 0$ and the equilibrium prices are positive. If supply exceeds demand, however, the complementary variable (prices) become zero. Similarly for the zero-profit conditions, the complementary variable is the output level. As long as sectoral profits are non-negative, the output level is positive. With negative profits, however, firms exit the market and the output becomes zero.

Although the theoretical model considers an infinite time horizon, the numerical implementation requires using a finite approximation. This introduces the risk of horizon-effects affecting the equilibrium outcome as we approach the terminal period. To remedy the risk around the terminal period, we employ the method from Lau et al. (2002b). This method imposes an additional constraint on capital accumulation at the terminal period T to approximate the infinite horizon equilibrium. We introduce the post-terminal capital stock as an additional variable and require that the growth rate of investments in the terminal period mirror the output growth rate:

$$\frac{I_T}{I_{T-1}} = \frac{Y_T}{Y_{T-1}}. \tag{A.1.30}$$

That is, we only fix the growth rate of investments, and do not have to fix the actual growth rate, nor the terminal level, of capital stock. To further reduce terminal effects, we discard the last two decades of simulation from the results.

We use the programming language GAMS (General Algebraic Modeling System) as well as the MPSGE (Mathematical Programming System for General Equilibrium, Rutherford (1999b)) sub-system to implement the economic model. To solve the model, use the PATH numerical solver Ferris and Munson (2000).

A.1.2 GTAP data aggregation

Table A.1.1: Aggregation of countries and regions

Aggregate region	GTAP region
USA	United States of America
Japan	Japan
Philippines	Philippines
Caribbean	Rest of Caribbean [1]
China	China, Hong Kong
Rest of the World	Australia, New Zealand, Rest of Oceania, Republic of Korea, Mongolia, Taiwan, Rest of East Asia, Cambodia, Indonesia, Lao PDR, Malaysia, Singapore, Thailand, Viet Nam, Rest of Southeast Asia, Bangladesh, India, Nepal, Pakistan, Sri Lanka, Rest of South Asia, Canada, Mexico, Rest of North America, Argentina, Bolivia, Brazil, Chile, Colombia, Ecuador, Paraguay, Peru, Uruguay, Venezuela, Rest of South America, Costa Rica, Guatemala, Honduras, Nicaragua, Panama, El Salvador, Rest of Central America, Austria, Belgium, Cyprus, Czech Republic, Denmark, Estonia, Finland, France, Germany, Greece, Hungary, Ireland, Italy, Latvia, Lithuania, Luxembourg, Malta, Netherlands, Poland, Portugal, Slovakia, Slovenia, Spain, Sweden, United Kingdom, Switzerland, Norway, Rest of European Free Trade Association, Albania, Bulgaria, Belarus, Croatia, Romania, Russian Federation, Ukraine, Rest of Eastern Europe, Rest of Europe, Kazakhstan, Kyrgyzstan, Rest of Former Soviet Union, Armenia, Azerbaijan, Georgia, Bahrain, Iran, Israel, Kuwait, Oman, Qatar, Saudi Arabia, Turkey, United Arab Emirates, Rest of Western Asia, Egypt, Morocco, Tunisia, Rest of North Africa, Cameroon, Côte d'Ivoire, Ghana, Nigeria, Senegal, Rest of Western Africa, Rest of Central Africa, South Central Africa, Ethiopia, Kenya, Madagascar, Malawi, Mauritius, Mozambique, Tanzania, Uganda, Zambia, Zimbabwe, Rest of Eastern Africa, Botswana, Namibia, South Africa, Rest of South African Customs Union, Rest of the World

[1] Includes: Anguilla, Antigua and Barbuda, Aruba, Bahamas, Barbados, British Virgin Islands, Cayman Islands, Cuba, Dominica, Dominican Republic, Grenada, Haiti, Jamaica, Montserrat, Netherlands Antilles, Puerto Rico, Saint Kitts and Nevis, Saint Lucia, Saint Vincent and Grenadines, Trinidad and Tobago, Turks and Caicos Islands, Virgin Islands.

Table A.1.2: Aggregation of sectors and production factors

Aggregate variable	GTAP variable
Goods and sectors	
Manufacturing	Textiles, Wearing apparel, Leather products, Wood products, Motor vehicles, Other transport equipment, Water, Construction, Paper products, publishing, Chemical, rubber, plastic products, Minerals, Ferrous metals, Other metals, Metal products, Electronic equipment, Other machinery and equipment, Other manufactures
Services	Trade, Communication, Financial services, Insurance, Business services, Recreation, Dwellings, Public Administration, Defense, Education, Health
Transport	Water transport, Air transport, Other transport
Agriculture	Paddy rice, Wheat, Cereal grains, Vegetables, fruits, nuts, Oil seeds, Sugar cane, sugar beet, Plant-based fibers, Other crops, Bovine cattle, Other animal products, Raw milk, Wool, Forestry, Fishing, Bovine meat products, Other meat products, Vegetable oils and fats, Dairy products, Processed rice, Sugar, Other food products, Beverages and tobacco
Electricity	Electricity
Coal	Coal
Natural gas	Gas, Gas manufacture, distribution
Crude oil	Oil
Refined oil	Petroleum, coal products
Factors of production	
Resources	Land, Natural resources
labor	Skilled labor, Unskilled labor
Capital	Capital

A.1.3 Main parameter values

Table A.1.3: Default parameter values used in numerical simulations

Parameter	Description	Value
Elasticities of substitution for production activities		
$\sigma_{i,r}$	Intermediate composite Q and inputs B from other sectors	0.5
$v_{i,r}$	Labor L and energy E in intermediate good production	1.0
$\epsilon_{i,r}$	Energy type Z in the energy aggregate	0.5
$\eta_{i,r}$	Imports and domestic goods	$\in [1.9, 6.0]$
$\phi_{i,r}$	Import regions	$\in [3.8, 12]$
κ	Intermediate varietes	$\in \{1.0, 0.86\}$
Elasticities of substitution for private consumption		
$\xi_{i,r}^{agg}$	Transportation and other consumption goods	1.0
$\xi_{i,r}^{oth}$	Energy and non-energy consumption goods	0.25
$\xi_{i,r}^{ene}$	Energy varieties	0.4
$\xi_{i,r}^{non}$	Non-energy consumption goods	0.25
Other parameters		
$1/\theta$	Intertemporal elasticity of substitution	0.5
$\delta_{i,r,t}$	Baseline capital depreciation	0.07
$\bar{r}$	Baseline nominal interest rate	0.05
γ_K	Capital growth rate	0.02

Notes: The calibration is based on Bretschger et al. (2017); Narayanan et al. (2012); Paltsev et al. (2005a); Hasanov (2007).

A.1.4 Additional results

For all graphs, we compare the levels under years of cyclone activity to a benchmark scenario where the economy would grow on a balanced growth path, without any cyclones. The bold lines represent the means of the 500 Monte Carlo simulations.

Figure A.1.3: Aggregate investment levels by country over 30 years of tropical cyclone activity

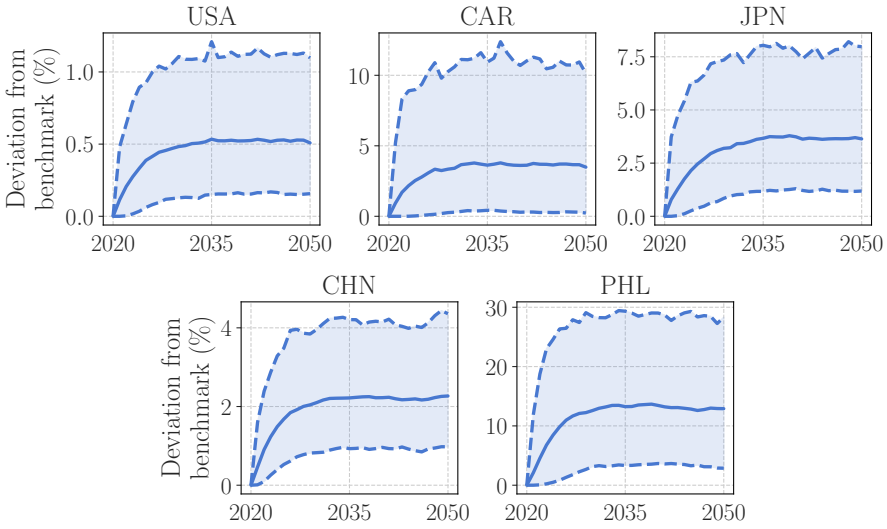

Figure A.1.4: GDP levels by country over 30 years of tropical cyclone activity

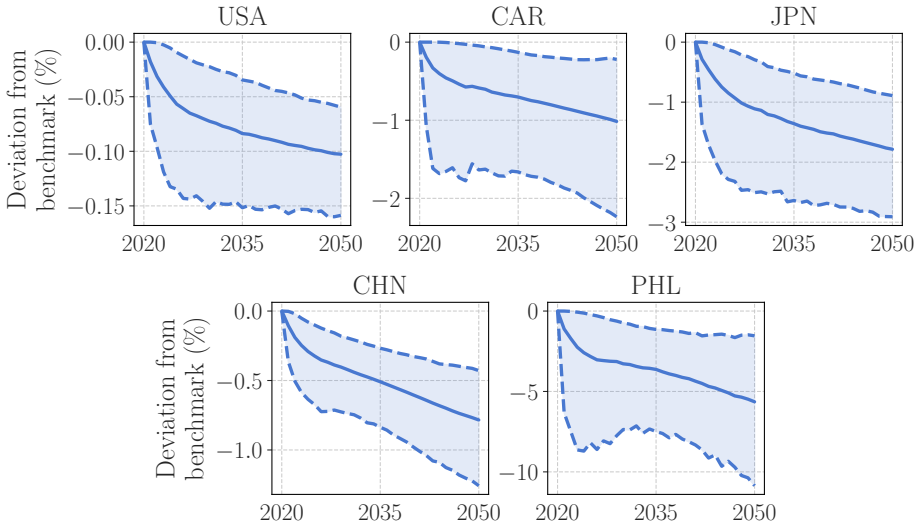

Figure A.1.5: Aggregate industry output levels levels by country over 30 years of tropical cyclone activity

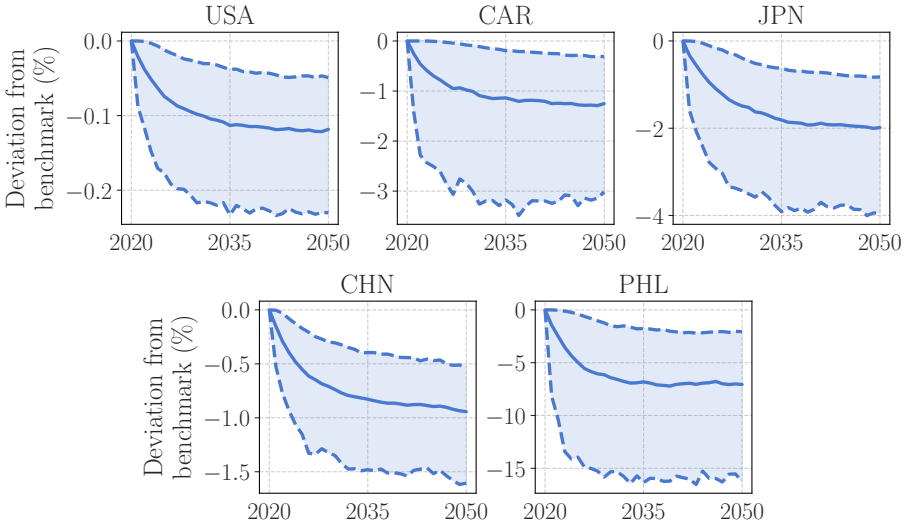

Figure A.1.6: Aggregate capital intensity by country over 30 years of tropical cyclone activity

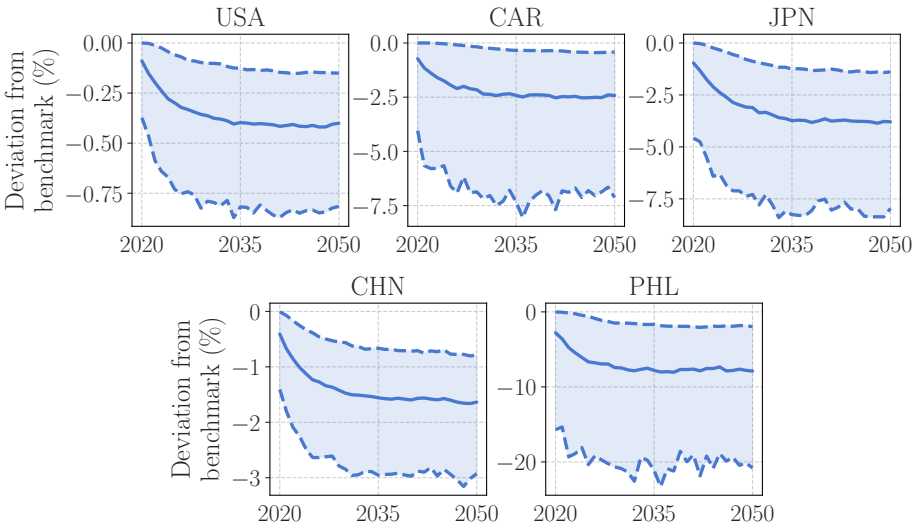

Figure A.1.7: Aggregate capital stock level by country over 30 years of tropical cyclone activity

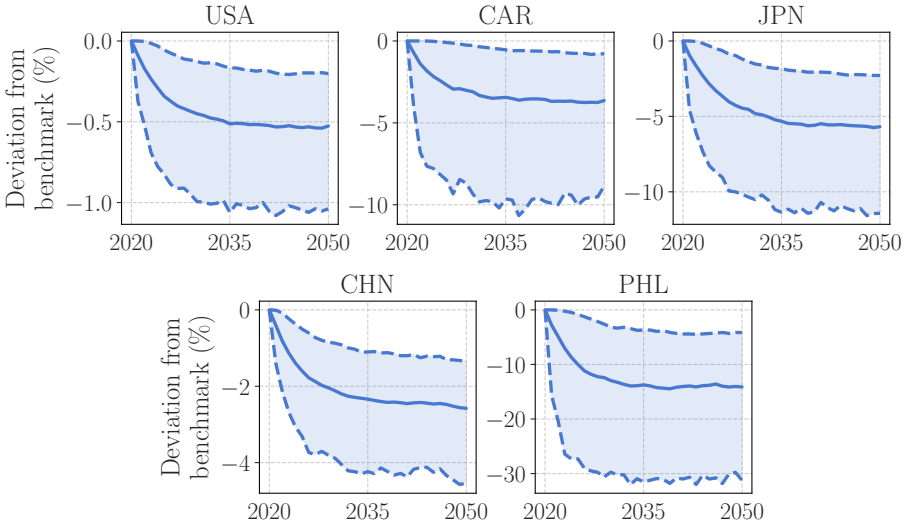

A.1.5 Cyclone simulation

Figure A.1.8 shows the fit between the new synthetic years and the historical ones. We use the methodology of section 2.2.1 to compute the damage caused by tropical cyclones. The synthetic years and the historical ones have a quite similar empirical cumulative distribution function. Table 2.1 of section 2.2.1 shows that the mean and the standard deviation of damages from the historical years stay close to the ones of the synthetic years. Figure A.1.8 reflects how yearly cyclone activity may differ from the 70 years we have on records so far.

Figure A.1.8: Probability estimates of tropical cyclone damages from the historical years versus the synthetic years under constant climate conditions

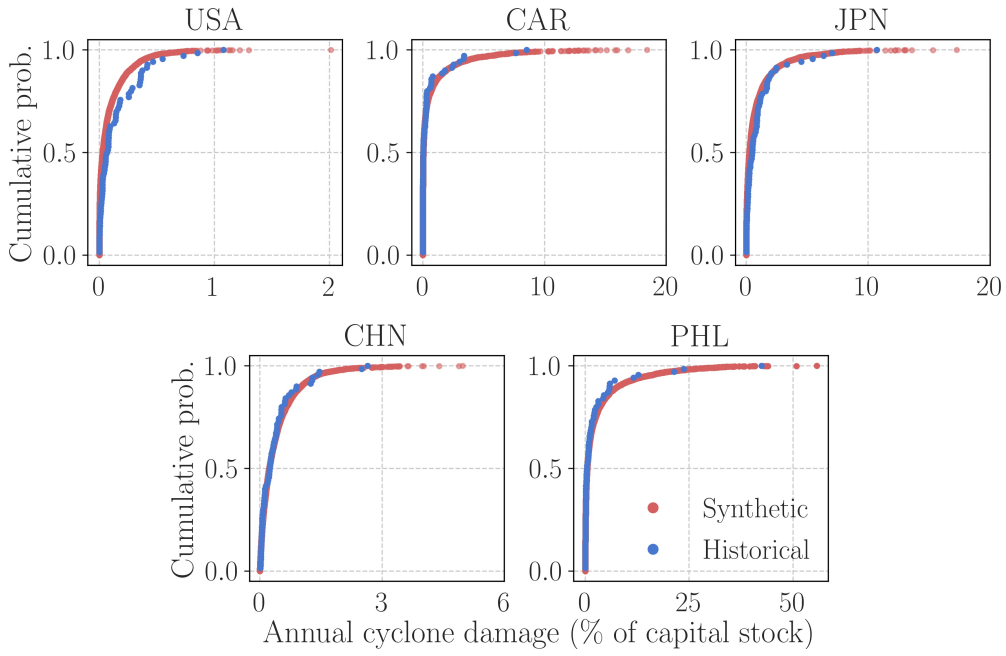

A.1.6 Cyclone simulation with climate change

The simulation of cyclones under climate change follows similar steps to the simulation without climate change. The main differences come from the fact that we need to change the occurrence rate of the cyclones (the frequency) and the damage that each cyclone may cause (the intensity).

We start from the historical tracks to again extend our sample to synthetic years. We use 2020 as a starting and reference year for climate change. We generate a new pool of 5,070 synthetic years of damages for every 10-years steps from 2025 to 2095. The pool of damages we compute for the year 2025 corresponds to our damage estimates for the 2020-2030 period. At each step, we use CLIMADA to compute the change in intensity of the cyclones. CLIMADA relies on Knutson et al. (2015) as a reference for its climate change scenario. Knutson et al. (2015) use a dynamical downscaling of models from the Coupled Model Intercomparison Project Phase 5 (CMIP5) under the RCP4.5 scenario to project tropical cyclone activity for the years 2081–2100. Knutson et al. (2015) present results only for the RCP4.5 scenario. CLIMADA interpolates other RCP scenarios from the RCP4.5 values according to the relative radiative forcing of each scenario. This interpolation allows us to get estimates of the intensity of cyclones under RCP8.5.

Similar to the simulation without climate change, we proceed to the creation of synthetic years. We need to adapt the Poisson parameter that represents the frequency of cyclones. In their late twenty-first century projections, Knutson et al. (2015) find no significant change in tropical cyclones' frequency in the North Atlantic basin. They find, however, a statistically significant change in tropical cyclones' frequency in the Northwestern Pacific basin of -34.5% on average overall cyclone categories. We use these results and do not adjust the average number of cyclones per year in the Caribbean islands and the USA. We specify, however, the -34.5% change in frequency for countries in the Northwestern Pacific basin by 2090. We interpolate the occurrence rate linearly at each decadal step from 2025 to 2095. We assume the same frequency of cyclones in 2100 as in 2095.

Since Knutson et al. (2015) have no estimates for the change in frequency for the RCP8.5 scenario, we take Emanuel (2013) as a reference. Emanuel (2013) also downscales models from CMIP5 to project tropical cyclone activity for the

late twenty-first century. Emanuel (2013) assumes an RCP8.5 scenario. His results complement the ones of Knutson et al 2015. But Emanuel (2013) reports his results globally. He finds an increase in cyclone frequency of $10 - 40\%$ globally depending on models of the CMIP5. According to Emanuel (2013), this increase is mostly concentrated in the Northwestern Pacific basin but also present in the North Atlantic basin. We take a conservative calibration of 5% and 10% increase in cyclone frequency for the North Atlantic and Northwestern Pacific basin respectively.

RCP4.5

Figure A.1.9 shows the cumulative distribution of damages from the synthetic years without climate change, with 2020 as reference climate, versus the synthetic yearly damages in 2100 under an RCP4.5 scenario. The intensity of the damages in the North Atlantic basin increases by 4.5% in 2100 compared to the present day's climate. In the Northwestern Pacific region, although the intensity of cyclones in this region increases by 5-7%, their frequency decreases by 16-30%.

Figure A.1.9: Probability estimates of cyclone damages under in 2020 versus their potential damages in 2100 under the RCP4.5 scenario

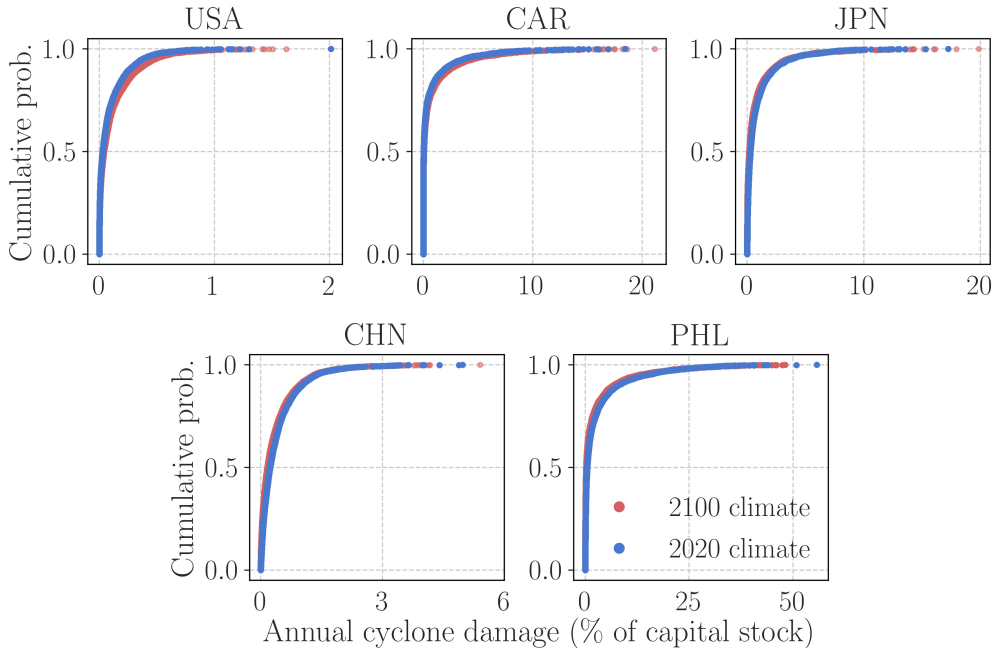

RCP8.5

Figure A.1.10 shows the cumulative distribution of damages from the synthetic years without climate change, with 2020 as reference climate, versus the synthetic yearly damages in 2100 under an RCP8.5 scenario. For all regions, we see an increase in the mean and standard deviation of damages. Under the RCP8.5, both the intensity and the frequency of the cyclone increase in both the North Atlantic and the Northwestern Pacific basin.

Figure A.1.10: Probability estimates of cyclone damages under in 2020 versus their potential damages in 2100 under the RCP8.5 scenario

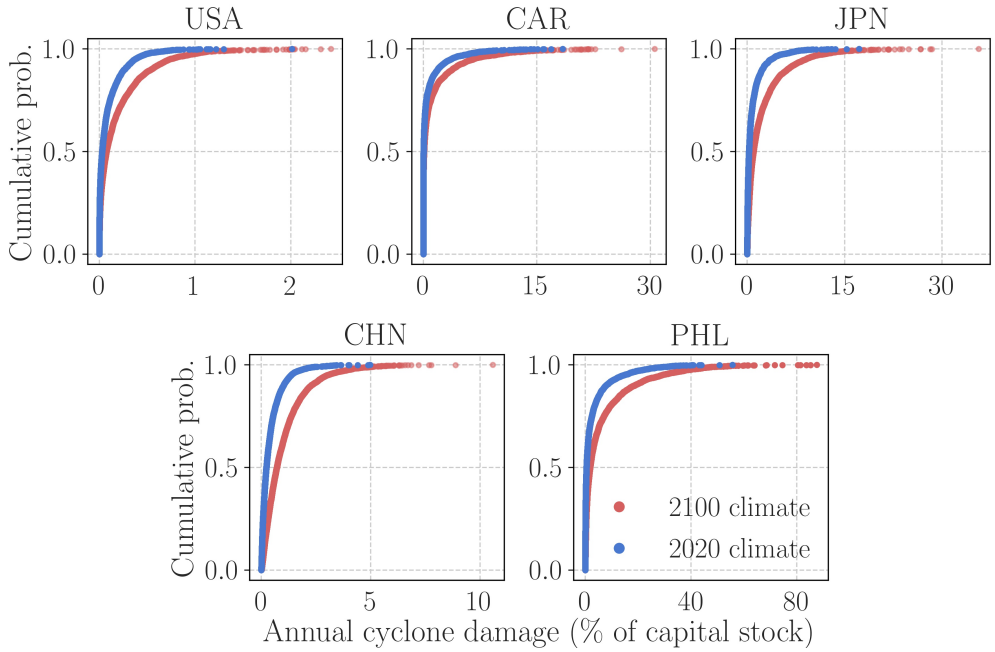

A.2 Appendices to Chapter 3

A.2.1 Summary statistics

Table A.2.1 summarizes the main variables of the analysis. Note that the most costly flood caused about 97,549 million dollars in damages (2015 $USD). It occurred in China in 1998. But, this flood caused 'only' 30,000 million dollars in the value of the year of occurrence. The biggest damage in the value of the year of occurrence is a flood that occurred in Thailand in 2011. It cost 40,000 million dollars at the time (2011 $USD), and it's the second biggest flood in my dataset (about 45,000 2015 $USD).

Table A.2.1: Summary statistics of the main variables

	N	*Min.*	Mean	*Max.*	*Std.*
Population density (population/km^2)	1,411	0.03	257	13,883	965
GDP per capita (2015 $USD)	1,411	49	8,341	116,616	14,950
Fatalities (deaths/flood)	1,411	0	63	6,054	256
Damages (mio 2015 $USD)	616	0.02	1,181	97,549	5,450
Flood magnitude (km^2)	1,411	2	111,561	2,857,000	232,702
Mean flood depth (no protection)	1,411	0	4,765	173,034	12,752
Mean flood depth (100-years protection)	1,411	0	107	3,764	281

Notes: N is the number of observations, Min. and Max. the respective minimum and maximum values over the whole dataset, and Std. the standard deviation of the variables. The Mean flood depth variables represent the average flood depth in the affected regions over the period 1971-2010. All statistics are rounded to the nearest integer except for the minimum values.

A.2.2 Region definition & Country-fixed effects regressions

In this section, I detail the grouping of countries into different regions. Regions that I use for the region fixed effects results throughout the main text. I also provide the country-fixed effect results and show that broadly, the main conclusions don't differ from the ones presented in Section 5.4.

Country-fixed effects

The notable difference between Table A.2.2 and results in the main body with region-fixed effects is that the coefficients for low- and high-intensity flooding lose their significance. But their sign stays negative and positive respectively. Results for adaptation via population density and GDP per capita don't change.

Table A.2.2: Evidence of adaptation to fatalities and damages with country-fixed effects

	Fatalities	Damages
	(1)	(2)
Ln km2 flooded	0.122***	0.202**
	(0.028)	(0.081)
Ln pop. density	0.203***	0.476***
	(0.054)	(0.154)
Ln GDP pc	−0.209**	0.372
	(0.082)	(0.255)
Ln low flood depth	−0.043	−0.080
	(0.069)	(0.155)
Ln high flood depth	0.095	0.311
	(0.070)	(0.225)
Constant	2.714***	50.646
	(0.617)	(32.481)
Observations	1,411	616
R^2	0.430	0.387

*Notes: Dependent variables: log fatalities and log damages. All specifications have robust standard errors clustered at the country level and country-fixed effects. *p<0.1; **p<0.05; ***p<0.01.*

Region definition

Table A.2.3: Aggregation of countries into regions

Regions	Countries
Afghanistan	Afghanistan
Bangladesh	Bangladesh
Brazil, Russia, and South Africa	South Africa, Russia, Brazil
Canada	Canada
Caribbean islands	Saint Vincent and the Grenadines, Puerto Rico, Cuba, Haiti, Dominican Republic
Central and South America	Suriname, El Salvador, Guatemala, Guyana, Nicaragua, Uruguay, Honduras, Ecuador, Venezuela, Chile, Panama, Paraguay, Costa-Rica, Mexico, Peru, Argentina, Bolivia, Colombia
East Africa	Somalia, Ethiopia
Eastern Europe	ex-Yugoslavia, Montenegro, Croatia, Slovenia, Bosnia and Herzegovina, North Macedonia, Serbia, Czech Republic, Hungary, Moldova, Slovakia, Romania, Poland, Belarus, Bulgaria, Ukraine, Albania, Kosovo
Greece and Turkey	Greece, Turkey
India	India
Indonesia	Indonesia
Korea and Japan	North Korea, South Korea, Japan
Mongolia, China, and Nepal	Mongolia, China, Nepal
Northern Africa	Egypt, Morocco, Algeria, Tunisia
Northern Asia	Georgia, Kyrgyzstan, Kazakhstan, Tajikistan, Azerbaijan
Oceania	Australia, New Zealand
Oceania islands	Papua New Guinea, Solomon Islands, Vanuatu, Fiji
Pakistan	Pakistan
Philippines	Philippines
Sahara	Mali, Niger, Mauritania, Burkina Faso, Chad, Sudan
South East Asia	Viet Nam, Laos, Cambodia, Myanmar, Thailand, Malaysia
Sri Lanka	Sri Lanka
Sub-Saharan Africa	Botswana, Central African Republic, Guinea, Benin, Cameroon, Burundi, Liberia, Madagascar, Togo, Congo, D.R. Congo, Namibia, Senegal, Zimbabwe, Zambia, Lesotho, Malawi, Rwanda, Uganda, Angola, Ghana, South Sudan, Tanzania, Nigeria, Mozambique, Kenya
USA	United States of America
Western Asia	Iran, Iraq, Palestine, Saudi Arabia, Yemen
Western Europe	Belgium, Switzerland, France, Germany, United Kingdom, Italy, Spain, Portugal, Austria, Finland, Norway

A.2.3 Negative binomial regression results

In this section, I present the results of the negative binomial estimator. The negative binomial estimator is a count data technique advantageous to OLS if regression outcomes are discrete, countable, and not normally distributed (Bakkensen and Mendelsohn, 2016). These results can more easily be compared to the ones by Ferreira et al. (2013), who use a similar modeling approach, and the additional results by Bakkensen and Mendelsohn (2016) for cyclone risk.

Table A.2.4: Evidence of adaptation to fatalities using negative binomial regressions

	Base	Year FE	Region FE	Year&Region FE
	(1)	(2)	(3)	(4)
Ln km2 flooded	0.161***	0.165***	0.115***	0.124***
	(0.038)	(0.032)	(0.036)	(0.030)
Ln pop. density	0.452***	0.456***	0.256***	0.258***
	(0.054)	(0.048)	(0.075)	(0.070)
Ln GDP pc	−0.553***	−0.499***	−0.337***	−0.222***
	(0.049)	(0.045)	(0.080)	(0.082)
Ln low flood depth	−0.123*	−0.113*	−0.074	−0.104
	(0.069)	(0.067)	(0.075)	(0.077)
Ln high flood depth	0.250***	0.221***	0.114	0.131
	(0.077)	(0.077)	(0.084)	(0.087)
Constant	4.368***	4.211***	4.127***	3.881***
	(0.954)	(0.770)	(0.905)	(0.793)

*Notes: Dependent variable: fatalities count. FE = fixed-effects. All specifications have standard errors clustered at the country level. *p<0.1; **p<0.05; ***p<0.01.*

A.2.4 Elasticities across income levels

In Figures A.2.1 and A.2.2, I graph the results of income elasticities in segmented bins from low- to high-income provinces. All income is in GDP per capita in 2015 $USD. The bars that pass through the points are the standard errors of the coefficient estimate.

Figure A.2.1: Income elasticities of fatalities across 5 income groups

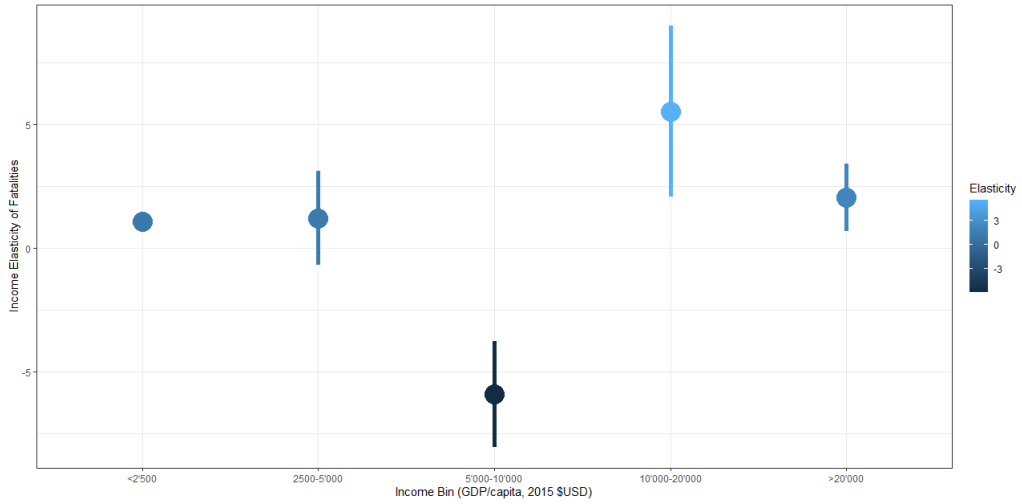

Figure A.2.2: Income elasticities of damages across 5 income groups

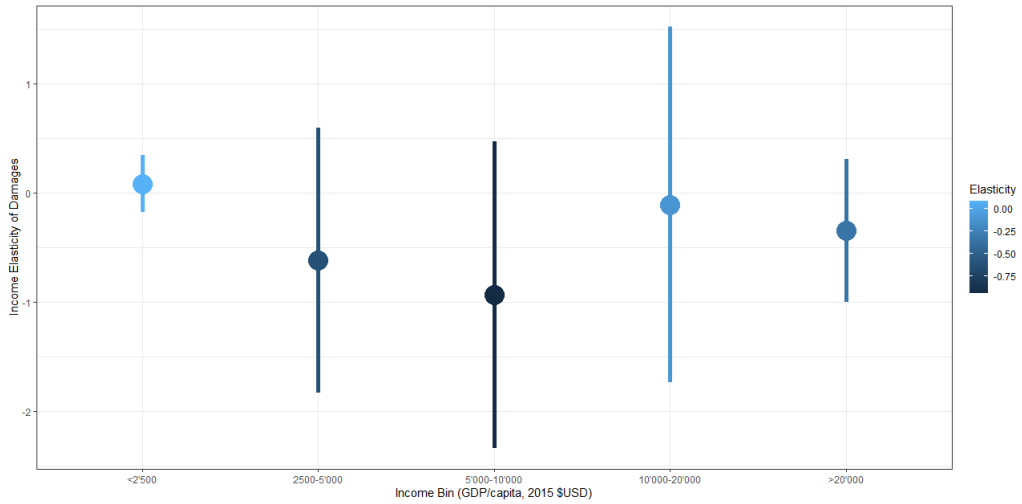

A.3 Appendices to Chapter 4

A.3.1 Exponential kernel Hawkes processes and Hawkes-diffusions

The exponential kernel Hawkes counting process N is assumed to start infinitely in the past in its stationary[21] regime and satisfies

$$\begin{cases} \mathbb{P}\Big(N_{t+h} - N_t = 1 | \mathcal{F}_t\Big) = \lambda_t h + o(h), \\ \mathbb{P}\Big(N_{t+h} - N_t > 1 | \mathcal{F}_t\Big) = o(h), \end{cases} \tag{A.3.1}$$

where the conditional intensity λ_t is given by

$$\lambda_t = \lim_{h \downarrow 0} \frac{\mathbb{E}[N_{t+h}|\mathcal{F}_t] - N_t}{h} = \bar{\lambda} + \alpha \int_{-\infty}^{t} e^{-\beta(t-s)} \mathrm{d}N_s. \tag{A.3.2}$$

Here the parameter $\beta > 0$ is an exponential decay rate driving the jump intensity back to the long-run average, while $\alpha \geq 0$ captures the scale impact of the jumps on the intensity dynamics.

In what follows, it is convenient to use the differential equation $(\lambda_t)_t$ solves. Proceeding formally, it follows from (A.3.2) that

$$\mathrm{d}(e^{\beta t}\lambda_t) = \beta e^{\beta t}\lambda_t \mathrm{d}t + e^{\beta t}\mathrm{d}\lambda_t = \beta e^{\beta t}\bar{\lambda}\mathrm{d}t + \alpha e^{\beta t}\mathrm{d}N_t \quad \Longrightarrow \quad \mathrm{d}\lambda_t = \beta[\bar{\lambda} - \lambda_t]\mathrm{d}t + \alpha \mathrm{d}N_t.$$

Lemma 1 (Infinitesimal generator)**.** *For suitably smooth functions $f : \mathbb{R} \to \mathbb{R}$, the*

[21] We use a classical definition, where Hawkes process N is assumed to start infinitely in the past in its stationary regime. This slightly differs from the alternative definition, where the intensity is initialized with some predefined value $\lambda_0 > 0$, and the dynamics are then given by the equation $\lambda(t) = e^{-\beta t}\lambda_0 + (1 - e^{-\beta t})\bar{\lambda} + \alpha \int_0^t e^{-\beta(t-s)}\mathrm{d}N_s$, $t > 0$. For t large enough, the impact of λ_0 vanishes, and the distribution of λ_t converges to some invariant distribution μ. In our exposition, we follow the classical approach, used by, e.g., Bacry et al. (2015), and assume the process starts at $-\infty$ resulting in λ_0 being sampled from μ. This approach makes the presentation of the model and results more clear.

infinitesimal generator[22] *is given by*

$$[\mathcal{A}f](\lambda) = \beta[\bar{\lambda} - \lambda]\frac{\mathrm{d}f}{\mathrm{d}\lambda}(\lambda) + \lambda[f(\lambda + \alpha) - f(\lambda)]. \tag{A.3.3}$$

Proof. Obtained directly by using Ito's lemma for semimartingales and taking conditional expectation. □

Let $\mathbb{E}^{\lambda}G(\lambda_s)$ denote the conditional expectation $\mathbb{E}[G(\lambda_s)|\lambda_0 = \lambda]$.

Lemma 2 (Feynman-Kac formula)**.** *Assume theat* $f^* : \mathbb{R} \to \mathbb{R}$ *defined by* $f^*(\lambda) = \int_0^\infty e^{-\rho s}\mathbb{E}^{\lambda}G(\lambda_s)\mathrm{d}s$ *is a differentiable function. Then* f^* *solves the integro-differential equation*

$$[\mathcal{A}f](\lambda) - \rho f(\lambda) = G(\lambda) \tag{A.3.4}$$

with a transversality condition

$$\lim_{t\to\infty} e^{-\rho t}\mathbb{E}^{\lambda}f(\lambda_t) = 0. \tag{A.3.5}$$

Proof. First, we consider an auxiliary PIDE

$$\mathcal{A}u(t,\lambda) - G(\lambda) = \rho u(t,\lambda)$$

defined on a finite interval $[0, T]$ subject to a terminal condition $u(T, x) = \psi_T(x)$.

Given a Hawkes process with intensity λ_t, the compensated stochastic process

$$\tilde{N}_t = N_t - \int_0^t \lambda_s \mathrm{d}s \tag{A.3.6}$$

is a martingale with respect to the canonical filtration of the process N_t, see, e.g., Daley and Vere-Jones (2003). Let $F(t, \lambda_t) = e^{-\rho t}u(t, \lambda_t) + \int_0^t e^{-\rho s}G(\lambda_s)\mathrm{d}s$. Applying

[22] More generally, for sufficiently smooth functions $f : \mathbb{N} \times \mathbb{R} \to \mathbb{R}$ the generator of the process (N_t, λ_t) can be expressed as $[\tilde{\mathcal{A}}f](n,\lambda) = \beta[\bar{\lambda} - \lambda]\frac{\partial f}{\partial \lambda}(n,\lambda) + \lambda[f(n+1, \lambda+\alpha) - f(n,\lambda)]$.

Ito's lemma, we get:

$$\begin{aligned}\mathrm{d}Y_t &= \mathrm{d}F(t,\lambda_t)\\ &= e^{-\rho t}\Bigg(\Big(\beta[\bar{\lambda}-\lambda]\frac{\partial u}{\partial \lambda}(t,\lambda)+\lambda[u(t,\lambda+\alpha)-u(t,\lambda)]-\rho u(t,\lambda)+G(\lambda_t)\Big)\mathrm{d}t\\ &+ [u(t,\lambda+\alpha,t)-u(t,\lambda)]\mathrm{d}\tilde{N}\Bigg).\end{aligned}$$

Now if the $\mathrm{d}t$ term is null then $u(t,\lambda_t)$ is a martingale and, thus,

$$u(t,\lambda)=F(t,\lambda_t=\lambda)=\mathbb{E}[Y_T\lambda_T=\lambda]=\mathbb{E}^{\lambda}\Bigg[e^{-\rho T}u(T,\lambda_T)+\int_0^T e^{-\rho s}G(\lambda_s)\mathrm{d}s|\,\lambda_T=\lambda\Bigg]$$

with the final condition

$$u(T,\lambda)=\psi_T(\lambda).$$

Next, we consider a set of PIDEs indexed with $T>0$ defined on time intervals $[0,T]$ with uniformly bounded terminal conditions $\{\psi_T\}_T$. Going to the limit in T results in the function f^* which satisfies (A.3.4) and (A.3.5).

□

Lemma 3 (Dynkin's formula)**.** *If the expectation*

$$\mathbb{E}\int_0^t|\lambda_s[f(\lambda_s+\alpha)-f(\lambda_s)]|\mathrm{d}s.$$

is finite for each t, then for each $\tau\leq t$ we have a Dynkin formula

$$\mathbb{E}_\tau f(\lambda_t)=f(\lambda_\tau)+\mathbb{E}_\tau\int_\tau^t\mathcal{A}f(\lambda_s)\mathrm{d}s.$$

A.3.2 Some statistics of Hawkes processes

For a different version of the process, the analog of the following result can be found, for instance, in Errais et al. (2010), and Dassios and Zhao (2011) and using an alternative approach in Cui et al. (2020).

Proposition 2 (Moments of the Hawkes process intensity λ_t)**.** *Let* $0 \leq \alpha < 1$*, then the expected intensity and its variance are given by*

$$\mathbb{E}\lambda_t = \frac{\bar{\lambda}}{1-\alpha/\beta}, \quad \textit{and} \quad \mathbf{Var}\,\lambda_t = \frac{1}{2}\frac{\bar{\lambda}\alpha^2/\beta}{(1-\alpha/\beta)^2},$$

respectively.

Proof. Let $\tau < t$. Then Dynkin's formula reads that

$$\mathbb{E}_\tau f(\lambda_t) = f(\lambda_\tau) + \mathbb{E}_\tau \int_\tau^t \mathcal{A}f(\lambda_s)\mathrm{d}s.$$

In other words, the function $t \mapsto \Lambda(t) := \mathbb{E}\lambda_t$ is a stationary solution of the ordinary differential equation (ODE) given by

$$\Lambda'(t) = \beta\bar{\lambda} + [-\beta + \alpha]\Lambda(t), \tag{A.3.7}$$

which is easy to solve and yields the first moment.

We proceed similarly for the second moment, obtaining from Dynkin's formula (with $f(\lambda) = \lambda^2$):

$$\begin{aligned}\psi(t) :=& \mathbb{E}\lambda_t^2 \\ =& \lambda_\tau^2 + 2\beta\int_\tau^t \mathbb{E}[\bar{\lambda} - \lambda_s]\lambda_s\mathrm{d}s + \int_\tau^t \mathbb{E}\lambda_s((\lambda_s+\alpha)^2 - \lambda_s^2)\mathrm{d}s \\ =& \lambda_\tau^2 + 2\beta\bar{\lambda}\int_\tau^t \Lambda(s)\mathrm{d}s - 2\beta\int_\tau^t \psi(s)\mathrm{d}s + 2\alpha\int_\tau^t \psi(s)\mathrm{d}s + (\alpha)^2\int_\tau^t \Lambda(s)\mathrm{d}s.\end{aligned}$$

It follows that $t \mapsto \psi(t)$ is a stationary solution of the ODE

$$\psi'(t) = 2\beta\bar{\lambda}\Lambda(t) - 2\beta\psi(t) + 2\alpha\psi(t) + \alpha^2\Lambda(t).$$

It yields, that $\psi(t) \equiv \frac{2\bar{\lambda}+\alpha^2/\beta}{2(1-\alpha/\beta)}\frac{\bar{\lambda}}{(1-\alpha/\beta)}$ and the variance is thus given by

$$\mathbf{Var}(\lambda_t) = \psi(t) - \Lambda(t)^2 = \frac{1}{2}\frac{\bar{\lambda}\alpha^2/\beta}{(1-\alpha/\beta)^2}.$$

□

Under our model assumptions, it implies that the process defined by (4.4) - (4.3) is a Markov decision process with state variables (K_t, λ_t) and controls $(C_t, \theta_t), t \geq 0$.

A.3.3 Derivation of the Keynes-Ramsey rule

We start with the HJB equation (4.5) of the main text:

$$\rho V(K_t, \lambda_t) = \max_{C_t, \theta_t} \{u(C_t, \lambda_t) + \frac{1}{\mathrm{d}t}\mathbb{E}_t \mathrm{d}V(K_t, \lambda_t)\},$$

where $\frac{1}{\mathrm{d}t}\mathbb{E}_t dV = V_K[(1-\theta)Y - C] + \frac{1}{2}V_{KK}\varepsilon^2 - \beta(\lambda - \bar{\lambda})V_\lambda + \lambda\mathbb{E}_Z[\tilde{V} - V]$.[23] We differentiate this HJB with respect to K_t:

$$\begin{aligned}\rho V_K = V_{KK}[(1-\theta)Y - C] + V_K(1-\theta)Y_K + \frac{1}{2}V_{KKK}\varepsilon^2 \\ + V_{KK}\varepsilon\varepsilon_K - \beta(\lambda - \bar{\lambda})V_{\lambda K} + \lambda\mathbb{E}_Z(\tilde{V}_{\tilde{K}}\tilde{K}_K - V_K),\end{aligned} \tag{A.3.8}$$

and λ_t:

$$\begin{aligned}\rho V_\lambda = U_\lambda + V_{K\lambda}[(1-\theta)Y - C] + V_\lambda(1-\theta)Y_\lambda - \beta(\lambda - \bar{\lambda})V_{\lambda\lambda} + \frac{1}{2}V_{KK\lambda}\varepsilon^2 \\ + \varepsilon V_{KK}\varepsilon_\lambda + \lambda\mathbb{E}_Z[\tilde{V}_{\tilde{\lambda}}\tilde{\lambda}_\lambda - V_\lambda] + \mathbb{E}_Z[V(\tilde{K}, \tilde{\lambda}) - V(K, \lambda)].\end{aligned} \tag{A.3.9}$$

where, as above, $\tilde{V} = V(\tilde{K}, \tilde{\lambda})$ $\tilde{K} = (1-\omega)K$, $\omega = (\varphi - \theta\upsilon)\gamma ZA$, and $\tilde{\lambda} = \lambda + \alpha$. We have $\tilde{K}_\lambda = -\omega_\lambda K = \theta\upsilon A\gamma_\lambda ZK$ and $\tilde{\lambda}_\lambda = 1$.

We can use the Ito's formula once again to express dV_K and dV_λ

$$\mathrm{d}V_K = \Big(V_{KK}[(1-\theta)Y - C] - \beta(\lambda - \bar{\lambda})V_{\lambda K} + \frac{1}{2}V_{KKK}\varepsilon^2\Big)\mathrm{d}t + [\tilde{V}_K - V_K]\mathrm{d}N + \varepsilon V_K \mathrm{d}W,$$

$$\mathrm{d}V_\lambda = \Big(V_{\lambda K}[(1-\theta)Y - C] - \beta(\lambda - \bar{\lambda})V_{\lambda\lambda} + \frac{1}{2}V_{\lambda KK}\varepsilon^2\Big)\mathrm{d}t + [\tilde{V}_\lambda - V_\lambda]\mathrm{d}N + \varepsilon V_\lambda \mathrm{d}W.$$

The latter two expressions can be simplified to the following system of the 1-st order PIDEs (from (A.3.8):

[23] The derivation of the Keynes-Ramsey rule in this Appendix is more general than the one in the main text. Here include the random jumps from assumption (4.12).

$$V_{KK}[(1-\theta)Y - C] - \beta(\lambda - \bar{\lambda})V_{\lambda K} + \frac{1}{2}V_{KKK}\varepsilon^2$$
$$= \rho V_K - V_K(1-\theta)Y_K - V_{KK}\varepsilon\varepsilon_K - \lambda\mathbb{E}_Z[\tilde{V}_{\tilde{K}}\tilde{K}_K - V_K]$$

and from (A.3.9) we have:

$$V_{\lambda K}[(1-\theta)Y - C] - \beta(\lambda - \bar{\lambda})V_{\lambda\lambda} + \frac{1}{2}V_{\lambda KK}\varepsilon^2$$
$$= (\rho+\beta)V_\lambda - U_\lambda + \beta(\lambda - \bar{\lambda})V_{\lambda\lambda} - V_\lambda(1-\theta)Y_\lambda - \lambda\mathbb{E}_Z[\tilde{V}_{\tilde{\lambda}}\tilde{\lambda}_\lambda - V_\lambda] - \mathbb{E}_Z[\tilde{V} - V],$$

such that:

$$\begin{cases} \mathrm{d}V_K = \Big(\rho V_K - V_{KK}\varepsilon\varepsilon_K - V_K(1-\theta)Y_K - \lambda\mathbb{E}_Z[\tilde{V}_{\tilde{K}}\tilde{K}_K - V_K]\Big)\mathrm{d}t \\ \qquad\quad +[\tilde{V}_K - V_K]\mathrm{d}N + \varepsilon V_K \mathrm{d}W, \\ \mathrm{d}V_\lambda = \Big((\rho+\beta)V_\lambda - U_\lambda + \beta(\lambda-\bar{\lambda})V_{\lambda\lambda} - V_\lambda(1-\theta)Y_\lambda \\ \qquad\quad -\lambda\mathbb{E}_Z[\tilde{V}_{\tilde{\lambda}}\tilde{\lambda}_\lambda - V_\lambda] - \mathbb{E}_Z[\tilde{V} - V]\Big)\mathrm{d}t \\ \qquad\quad +[\tilde{V}_\lambda - V_\lambda]\mathrm{d}N + \varepsilon V_\lambda \mathrm{d}W. \end{cases} \tag{A.3.10}$$

To obtain the Keynes-Ramsey rule describing the evolution of marginal utility U_C we divide the second equation from (A.3.10) by V_K

$$\frac{\mathrm{d}V_K}{V_K} = \left(\rho - \frac{V_{KK}}{V_K}\varepsilon\varepsilon_K - (1-\theta)Y_K - \lambda_t\mathbb{E}_Z\left[\frac{\tilde{V}_{\tilde{K}}}{V_K}\tilde{K}_K - 1\right]\right)\mathrm{d}t + \left[\frac{\tilde{V}_K}{V_K} - 1\right]\mathrm{d}N + \varepsilon\mathrm{d}W,$$

and use the first-order conditions (4.7) and (4.8) to get:

$$\frac{\mathrm{d}U_C}{U_C} = \left(\rho - (1-\theta_t)Y_K - \frac{\varepsilon_K}{\varepsilon_\theta}Y + \lambda_t\int\left[\frac{\tilde{U}_C}{U_C}\left(\frac{\varepsilon_K}{\varepsilon_\theta}\tilde{K}_\theta - \tilde{K}_K\right) + 1\right]\mathrm{d}\nu\right)\mathrm{d}t \tag{A.3.11}$$
$$+\left[\frac{\tilde{U}_C}{U_C} - 1\right]\mathrm{d}N + \varepsilon\mathrm{d}W,$$

where $\tilde{U}_C$ is the marginal value of consumption after the jump.

In the case of additive utility (i.e. when U_C uniquely defines C by expression $f(C) = U_C$ for some invertible differentiable function f) we can use the standard change of variable to get Keynes-Ramsey rule for optimal consumption

$$\frac{\mathrm{d}C}{C} = \frac{1}{\mathcal{R}(C)}\Bigg((1-\theta_t)Y_K - \rho + \frac{\varepsilon_K}{\varepsilon_\theta}Y + \lambda_t \int \Big[\frac{U_C(\tilde{C})}{U_C(C)}\Big(\tilde{K}_K - \frac{\varepsilon_K}{\varepsilon_\theta}\tilde{K}_\theta\Big) - 1\Big]\mathrm{d}\nu\Bigg)\mathrm{d}t + \Big[\frac{\tilde{C}}{C} - 1\Big]\mathrm{d}N + \varepsilon \mathrm{d}W,$$

where $\mathcal{R}(C) = -\frac{CU_{CC}}{U_C}$ stands for the Arrow-Pratt measure of relative risk-aversion. Note that the term $\frac{1}{\mathcal{R}(C)}((1-\theta)Y_K - \rho)$ corresponds to the standard deterministic Keynes-Ramsey rule.

A.3.4 Verification Theorem

The HJB equation (4.5) reads:[24]

$$\rho V(K_t, \lambda_t) = \max_{C_t, \theta_t} \Big\{ \ln(C_t) + V_K[(1-\theta)Y - C] - \beta(\lambda - \bar{\lambda})V_\lambda + \frac{1}{2}V_{KK}(\delta\Gamma)^2 + \lambda \int [V(\tilde{K}, \tilde{\lambda}) - V(K, \lambda)]\mathrm{d}\nu \Big\}, \tag{A.3.12}$$

which under the value function guess (4.16) writes:

$$\rho(\ln(K) + g(\lambda)) = \max\Big\{ \frac{\ln(C)}{X_1} + \Big((1-\theta)A - C/K\Big) - \beta(\lambda - \bar{\lambda})\frac{\mathrm{d}}{\mathrm{d}\lambda}g(\lambda) - \frac{1}{2}\delta^2\Gamma^2 + \lambda \int \ln\left(z(1-\omega)\right)\mathrm{d}\nu(z) + \lambda[g(\lambda+\alpha) - g(\lambda)] \Big\}.$$

Clearly, $X_1 = 1/\rho$, optimal consumption $C^* = \rho K$, and optimal mitigation is given by (4.17). Substituting the optimal controls into the latter expression we find that the function g must solve the following equation

$$[\mathcal{A}g](\lambda) - \rho g(\lambda) = G(\lambda), \tag{A.3.13}$$

[24] In this Appendix, we prove the verification theorem in a more general setting than they appear in the main text. We allow random jumps from equation (4.12).

where the infinitesimal operator writes $[\mathcal{A}g](\lambda) = \beta[\bar{\lambda} - \lambda]\frac{\mathrm{d}g}{\mathrm{d}\lambda}(\lambda) + \lambda[g(\lambda+\alpha) - g(\lambda)]$ and the right-hand-side is given by

$$G(\lambda) = -\ln(\rho) - R(\theta^*(\lambda), \lambda). \tag{A.3.14}$$

The following proposition generalizes the result by Aït-Sahalia and Hurd (2015) for the case when jump sizes are randomly distributed, and the coefficients of equation (4.15) depend on λ.

Proposition 3. *The solution g of the functional equation*(A.3.13) *is given by an absolutely convergent integral*

$$g(\lambda) = \int_0^\infty e^{-\rho s}\mathbb{E}^\lambda G(\lambda_s)\mathrm{d}s. \tag{A.3.15}$$

Proof. Since λ_t is a stationary semimartingale with bounded moments, it has the ergodic property. Namely for any measurable function $f(\lambda)$ that satisfies a bound[25] $|f(\lambda)| \leq M(1 + |\lambda|^2)$ for some constant M the law of large numbers holds:

$$\lim_{T\to\infty}\frac{1}{T}\int_0^T f(\lambda_t)\mathrm{d}t = \lim_{t\to\infty}\mathbb{E}f(\lambda_t) = \int_{\mathbb{R}_+} f(\lambda)\mu(\mathrm{d}\lambda).$$

where μ is the invariant distribution of λ_t.

One can verify that under our assumption on functions γ and δ the function G defined by (A.3.14) satisfies $|G(\lambda)| \leq M(1 + |\lambda|^2)$. By the ergodic property we have

$$\lim_{t\to\infty}\mathbb{E}^\lambda[G(\lambda_t)] = \int_{\mathbb{R}_+} G(\lambda)\mu(\mathrm{d}\lambda)$$

and

$$\lim_{t\to\infty}\frac{\mathrm{d}}{\mathrm{d}\lambda_t}\mathbb{E}^\lambda[G(\lambda_t)] = 0.$$

[25] see Aït-Sahalia and Hurd (2015) and Khas'minskii (1960)

These implies that both integral (A.3.15) and

$$\frac{\mathrm{d}}{\mathrm{d}\lambda}g(\lambda) = \int_0^\infty e^{-\rho s}\frac{\mathrm{d}}{\mathrm{d}\lambda}\mathbb{E}^\lambda G(\lambda_s)\mathrm{d}s$$

are absolutely convergent. Since $g(\lambda)$ is shown to be differentiable, the Feynman-Kac formula, see Lemma 2, reads it satisfies equation (A.3.13). □

In the next section (under a specific choice of parameter values and functional form of ψ), we will get an expression for the value function in elementary functions. For the general case considered here, we still need to prove the verification theorem, in particular, check that (A.3.13) satisfies the transversality conditions.

Theorem 1 (Verification theorem)**.** *Consider the optimization problem* (4.3)-(4.4) *under a general log-utility specification* (4.10)*. Under the non-explosion assumption* $\alpha < \beta$ *and that discounting rate* $0 < \rho < 1$*:*

1. *The function* $V(K, \lambda, t) = e^{-\rho t}(\ln(K) + g(\lambda))$ *with* $f(\lambda)$ *defined by* (A.3.13) *is a classical (differentiable) solution of the HJB equation* (4.5)*.*

2. *For any initial positive values of capital stock* $K_0 = k$ *and intensity* λ*, the pair* $(C^*, \theta^*), t \geq 0$*, defined by* $C_t^* = \rho K_t$ *and* (4.17) *correspondingly is an admissible control, i.e. capital stock* K_t *remains* (t, ω)*-a.s. finite and positive and solves* (4.5)*.*

3. *Let* $\mathcal{C}$ *denote the class of admissible controls* $(C_t, \theta_t), t \geq 0$*, such that the transversality condition is satisfied:*

$$\lim_{t\to\infty} \mathbb{E}^{k,\lambda}\Big[V(K_t, \lambda_t, t)\Big] = 0. \tag{A.3.16}$$

For any $(C_t, \theta_t) \in \mathcal{C}$*,*

$$\mathbb{E}^{k,\lambda}\Big[\int_0^\infty e^{-\rho s}U(C_s, \lambda_s)\mathrm{d}s\Big] \leq V(k, \lambda, 0). \tag{A.3.17}$$

4. Let $L(k,\lambda)$ denote the value function

$$L(k,\lambda) = \max_{(C,\theta)\in\mathcal{C}} \mathbb{E}^{k,\lambda}\Big[\int_0^\infty e^{-\rho s}U(C_s,\lambda_s)\mathrm{d}s\Big]. \tag{A.3.18}$$

Then the optimal controls $(C_t^*,\theta_t^*), t\geq 0$, satisfy the transversality condition:

$$\lim_{t\to\infty}\mathbb{E}^{k,\lambda}\Big[V(K_t,\lambda_t,t)\Big] = 0 \tag{A.3.19}$$

and the equality

$$\mathbb{E}^{k,\lambda}\Big[\int_0^\infty e^{-\rho s}U(C_s,\lambda_s)\mathrm{d}s\Big] \leq V(k,\lambda,0). \tag{A.3.20}$$

Hence, $V(k,\lambda,0) = L(k,\lambda)$ and (C_t^*,θ_t^*) are the optimal controls in the class $\mathcal{C}$.

Proof. Proposition 1 states that $V(K,\lambda,t) = e^{-\rho t}(\ln(K) + g(\lambda))$ is a classical (differentiable) solution of Equation (4.5). Let ξ_t denote $V(X_t,\lambda_t,t)$ and $(C,\theta)\in\mathcal{C}$. We apply the Dynkin formula to $\xi_t, t>0$, to obtain:

$$\mathbb{E}^{k,\lambda}[\xi_t] = \xi_0 + \int_0^t \mathbb{E}^{k,\lambda}\Big[\mathcal{A}^{(C,\theta)}V(X_s,\lambda_s,s)\Big]\mathrm{d}s,$$

where controlled Markov process generator is given by:

$$\begin{aligned}\Big[\mathcal{A}^{(C,\theta)}f\Big](K,\lambda,t) =& -\rho f(K,\lambda,t) + [(1-\theta)AK - C]f_K(K,\lambda,t)\\ &+\frac{1}{2}f_{KK}(K,\lambda,t)(\delta E)^2 - \beta(\lambda-\bar{\lambda})f_\lambda(K,\lambda,t)+\\ &+\lambda\int[f((1-\omega)K,\lambda+\alpha,t) - f(K,\lambda,t)]\mathrm{d}\nu(z),\end{aligned}$$

where, as above, $\omega = (\varphi-\theta\upsilon)\gamma ZA$. Since $(C,\theta)\in\mathcal{C}$, it holds

$$-\mathcal{A}^{(C,\theta)}V(K_s,\lambda_s,s) + U(C_s,\lambda_s)\geq 0.$$

resulting

$$\mathbb{E}^{k,\lambda}[\xi_t]\mathrm{d}s \leq \xi_0 - \mathbb{E}_{k,\lambda}\Big[\int_0^t e^{-\rho s}U(C_s,\lambda_s)\Big]\mathrm{d}s$$

Next, going to the limit and using transversality condition (A.3.16) we obtain the desired inequality

$$L(k,\lambda) \equiv \mathbb{E}^{k,\lambda}\Big[\int_0^\infty e^{-\rho s}U(C_s,\lambda_s)\Big]\mathrm{d}s \leq \xi_0 = V(k,\lambda,0).$$

To finalize the proof we need to check that the optimal control $(C^*,\theta^*), t \geq 0$, defined by (4.7) satisfy the transversality condition $\lim_{t\to\infty} V(k,\lambda,t) = 0$. Again, by the ergodic property $\lim_{t\to\infty} \mathbb{E}_{k,\lambda}\Big[e^{-\rho t}|g(\lambda_t)|\Big] = 0$.

The expression

$$\lim_{t\to\infty} \mathbb{E}^{K,\lambda}\Big[e^{-\rho t}|\log(K_t^*)|\Big] = 0,$$

which follows from (4.9). □

A.3.5 Pure Hawkes uncertainty

Optimization problem (4.17) writes that:

$$\theta^*(\lambda) = \mathrm{argmax}_{\theta\in[0,\theta_{max}]}\Big((1-\theta)A + \lambda\ln(1-\omega)\Big),$$

where , as above, $\omega = \omega(\theta) = \gamma(\varphi - \upsilon\theta)A$, resulting the first order condition of the form

$$A = \lambda\frac{\upsilon\gamma A}{1-\omega}.$$

The optimal mitigation policy $\theta_t^* = \theta^*(\lambda_t)$ in the baseline Hawkes uncertainty case is given by:

$$\theta^*(\lambda) = \begin{cases} 0, & \text{if} \quad \lambda \leq \lambda^{min}, \\ \theta^{max}, & \text{if} \quad \lambda \geq \lambda^{max}, \\ \frac{\varphi}{\upsilon} - \frac{1-\lambda\upsilon\gamma}{A\upsilon\gamma}, & \text{otherwise}, \end{cases} \tag{A.3.21}$$

where $\lambda^{min} = \frac{1}{\upsilon\gamma} - \frac{A\varphi}{\upsilon}$ and $\lambda^{max} = \lambda^{min} + A\theta^{max}$. The first two cases correspond to the corner solutions of the problem, while the latter (interior) solution is of our primal interest.

A.3.6 Expected growth

Under the same assumptions of Section 4.4.1 we take the expectation of both sides of identity (4.9), which results in:

$$\begin{aligned} \frac{d\mathbb{E}_t[C_t]}{dt} &= \mathbb{E}_t\Big[A\Big(1-\frac{\varphi}{\sigma}\Big) + \frac{1}{\sigma\gamma} - \rho - \lambda_t^{\#}\Big]C_t + \lambda_t\mathbb{E}_t[\tilde{C}_t - C_t] \\ &= C_t\mathbb{E}_t\Big[A\Big(1-\frac{\varphi}{\sigma}\Big) + \frac{1}{\sigma\gamma} - \rho - \lambda_t^{\#} + \lambda_t(\lambda_t^{\#}\sigma\gamma - 1)\Big]. \end{aligned}$$

The term $\mathbb{E}_t\Big[A\Big(1-\frac{\varphi}{\sigma}\Big)+\frac{1}{\sigma\gamma}-\rho-\lambda_t^{\#}\Big]$ is the expected trend growth rate, while the last term represents the expected reduction in the growth rate due to the occurrence of disasters (jumps). The latter is the expectation of the product of the arrival rate and the damage on impact (recall that $\lambda_t^{\#}\upsilon\gamma$ is the fraction of the capital stock that survives the disaster). Next, by dividing both sides of the latter identity by C_t and applying (unconditional) expectation operator we get

$$g_0^e = \mathbb{E}_0\frac{\mathrm{d}\mathbb{E}_t[C_t]/\mathrm{d}t}{C_t} = A\Big(1-\frac{\varphi}{\sigma}\Big) + \frac{1}{\sigma\gamma} - \rho - \mathbb{E}\lambda_t^{\#} - \mathbb{E}\lambda_t + \sigma\gamma\mathbb{E}\lambda_t^{\#}\lambda_t.$$

A.3.7 Mixed Hawkes-Brownian uncertainty

Now optimization problem (4.17) rewrites that:

$$\theta^*(\lambda) = \mathrm{argmax}_{\theta\in[0,\theta_{max}]}\Big((1-\theta)A + \delta^2\Gamma^2 + \lambda\ln(1-\omega)\Big),$$

where $\Gamma = (\varphi - \upsilon\theta)A$ and $\omega = \gamma\Gamma$, resulting first order condition of the form

$$-1 + \delta^2\upsilon A\Gamma + \frac{\lambda\gamma\upsilon}{1-\gamma\Gamma} = 0.$$

Solving this quadratic equation in $\Gamma = (\varphi - \theta\upsilon)A$ we obtain:

$$\Gamma^* = \frac{1}{2}\frac{A\delta^2\upsilon + \gamma - \sqrt{4\lambda_t A\delta^2\gamma^2\upsilon^2 + (\delta^2\upsilon A - \gamma)^2}}{\gamma\delta^2\upsilon}.$$

Then the resulting optimal abatement is $\theta^* = \frac{\varphi A - \Gamma^*}{A\upsilon} = \frac{\varphi}{\upsilon} - \frac{\Gamma^*}{A\upsilon}$. Further, we work out asymptotic *linear* representations for the following two special cases:

- If the Hawkes uncertainty dominates, i.e., $\delta \to 0$, then:

$$\Gamma = \Gamma^H + \lambda A\upsilon^2\Gamma^H\delta^2 + o(\delta^2), \quad \theta = \theta^H + \upsilon\lambda\Gamma^H\delta^2 + o(\delta^2),$$

  where $\Gamma^H = (1 - \lambda_t\gamma\upsilon)/\gamma$ and $\theta^H = \frac{\varphi}{\upsilon} - \frac{1-\lambda_t\upsilon\gamma}{A\upsilon\gamma}$ are the random processes for the optimal Γ and θ in the case of pure Hawkes uncertainty obtained in the previous section.

- If the Wiener uncertainty dominates, i.e., when $\gamma \to 0$, then:

$$\Gamma = \frac{1}{A\delta^2\upsilon} - \frac{\lambda}{A\delta^2}\gamma + o(\gamma), \quad \theta = \theta^W + \frac{\lambda}{\delta^2A^2\upsilon}\gamma + o(\gamma)$$

  where $\theta^W = \frac{\varphi}{\upsilon} - \frac{1}{(A\upsilon\delta)^2}$ is the (constant) value of abatement in the pure Wiener uncertainty case.

A.3.8 Random jump-size

Let Z have a Bernoulli distribution with outcomes b and s representing big and small relative loss ($b > s > 0$) taking place with probabilities $(p, 1-p)$. Optimization problem (4.17) writes that:

$$\theta^*(\lambda) = \text{argmax}_{\theta\in[0,\theta_{max}]}\Big((1-\theta)A + \lambda\Big[\ln\left(s(1-\omega)\right)(1-p) + \ln\left(b(1-\omega)\right)p\Big]\Big),$$

where, as above, $\Gamma = (\varphi - \upsilon\theta)A$ and $\omega = \gamma\Gamma$, resulting first order condition of the form

$$-A + \lambda_t\Big[\frac{b\gamma\upsilon A}{1 - b\gamma\Gamma}p + \frac{s\gamma\upsilon A}{1 - s\gamma\Gamma}(1-p)\Big] = 0.$$

This is again a quadratic equation in variable $\Gamma = (\varphi - \upsilon\theta)A$ and can be solved explicitly.

If we assume that the probability p of a big disaster is small, we can derive the following asymptotic expansion[26]:

$$\Gamma = \Gamma^H - \upsilon A\Delta_1 p + o(p), \theta = \theta_H + \Delta_1 p + o(p).$$

where $\Gamma^H = \frac{1-\lambda\gamma\upsilon s}{\gamma s}$, $\theta_H = \frac{\varphi}{\upsilon} - \frac{1-\lambda_t\upsilon\gamma s}{A\upsilon\gamma s}$ and Δ_1 stands for $\frac{\lambda(b-s)}{|A(s-b(1-\lambda\upsilon\gamma s))|}$. If $\lambda\upsilon\gamma s$ is small then $\Delta_1 \approx \frac{\lambda}{A}$.

[26]under the uniform approximation assumption $|A(s - b(1 - \lambda\upsilon\gamma s))| \geq \varepsilon$ for some $\varepsilon > 0$; if $A(s - b(1 - \lambda\upsilon\gamma s) \equiv 0$, then simply $\theta^H = \frac{\varphi}{\upsilon} + \frac{-s+\sqrt{p}(b-s)}{\gamma bs\upsilon A}$.

A.4 Appendices to Chapter 5

A.4.1 The CITE model

The version of CITE we use for our analysis is a dynamic, multi-sectoral numerical general equilibrium model of a small open economy where the growth mechanism follows Romer (1990).[27] Hence, the growth rate of the economy is determined by the expansion in the variety of intermediate goods. The broader variety of intermediate inputs increases productivity through gains from specialization. In addition to the main endogenous growth structure, it includes an energy sector. The time horizon of the theoretical model formulation is infinite but solved for a finite number of periods and goods in the numerical implementation.[28]

Household

We consider five infinitely lived, forward-looking households with perfect foresight and preferences:

$$U_h = \sum_{t=0}^{\infty} \left[\frac{1}{1+\rho}\right]^t \frac{(C_{h,t} + \theta_h L_{U_{h,t}})^{1-\zeta} - 1}{1-\zeta}, \tag{A.4.1}$$

where $C_{h,t}$ is the consumption flow at time t by household h and L_U the leisure time. Each household is representative of an income and activity category.[29] Instantaneous utility from consumption and leisure is discounted at the intertemporal discount rate ρ and $\zeta \geq 0$ is the intertemporal elasticity of substitution. We consider no population growth and normalize total labor supply to unity. Each representative household allocate its time budget between manufacturing, research , and leisure. The time allocated to leisure, θ_h, is fixed and specific to each household

[27] Bretschger et al. (2011) and Karydas and Zhang (2019) use similar version of CITE.
[28] See Section A.4.3 for a calibration to the balanced growth path.
[29] More details on households categories in Section 5.2.2.

category. Labor market clears:[30]

$$L_U + L_{X_t} + L_{J_t} = 1. \tag{A.4.2}$$

We also assume that the representative households own all the assets in this economy. Hence, they balance their income between consumption and saving for investment. Their total income consists of labor and capital income, and transfers from the government. Their expenditures are consumption expenses, tax payments, and investment:

$$\sum_i p^J_{i,t+1} J_{i,t+1} = w_t(L_{X_t} + L_{J_t}) + \sum_i (1 + r_t) p^J_{i,t} J_{i,t} - p^C_t C_t - T_t. \tag{A.4.3}$$

Through intermediate firm ownership, household own the capital J_i from sector i, r_t is the interest rate, w_t is the wage from labor, T_t are the taxes and p^C_t is the price index of aggregate consumption such that $C_t = \sum_i C_{i,t}$ according to a CES aggregation of final goods as given by:

$$C_{i,t} = \left[\sum_i \alpha_C C_{Yi,t}^{\frac{\varepsilon_C - 1}{\varepsilon_C}} + (1 - \alpha_C) C_{Egyi,t}^{\frac{\varepsilon_C - 1}{\varepsilon_C}} \right]^{\frac{\varepsilon_C}{\varepsilon_C - 1}}. \tag{A.4.4}$$

Both consumption of regular goods, $C_{Yi,t}$, and consumption of the energy composite, $C_{Egyi,t}$, also stem from CES production function with elasticities σ_Y and σ_E respectively as we describe in Figure 5.2. Maximizing (A.4.1) with respect to (A.4.3) gives the optimal consumption growth rate $g = \frac{C_{t+1}}{C_t}$ according to the standard Keynes-Ramsey rule:

$$g_C \equiv \left[\frac{1 + r_{t+1}}{1 + \rho} \frac{p^C_t}{p^C_{t+1}} \right]^{\frac{1}{\theta}}. \tag{A.4.5}$$

According to Equation (A.4.5), a higher interest rate r boosts growth by inducing more savings, whereas a higher discount rate ρ gives incentives to present consumption, therefore reducing the growth rate.

[30] From now on we ignore the household index when no confusion arises.

Production

Final good producers

The representative final good producer in sector i and time t produces an output of $Y_{i,t}$ according to the following constant elasticity of substitution (CES) production function:

$$Y_{i,t} = \left[\alpha_Y Q_{i,t}^{\frac{\varepsilon_Y - 1}{\varepsilon_Y}} + (1 - \alpha_Y) B_{i,t}^{\frac{\varepsilon_Y - 1}{\varepsilon_Y}}\right]^{\frac{\varepsilon_Y}{\varepsilon_Y - 1}}, \tag{A.4.6}$$

where $Q_{i,t}$ is the sector-specific composite of intermediate goods. $B_{i,t}$ denotes the composite output of final goods from all sectors that are needed as inputs for producing i. Outputs from different sectors are assembled into B according to a Leontief-type production function. The value shares of $Q_{i,t}$ and $B_{i,t}$ in the production function are determined by share parameters α_Y, and the elasticity of substitution between the two types of inputs are given by ε_Y. Both parameters are also sector-specific. The parameter values used in the numerical simulations are available in the Appendix A.4.3.

In each sector, the final good producer maximizes profits in a perfectly competitive market according to:

$$\max_{Q_{i,t}, B_{i,t}} p_{i,t}^Y Y_{i,t} - p_{i,t}^Q Q_{i,t} - p_{i,t}^B B_{i,t}, \text{ w.r.t (A.4.6)}, \tag{A.4.7}$$

where $p_{i,t}^Y, p_{i,t}^Q$ and $p_{i,t}^B$ denote the prices of final goods, intermediate composite, and other inputs, respectively. Solving equation (A.4.7), and combining the resulting optimal demand functions for $Q_{i,t}$ and $B_{i,t}$ yields the following condition for optimal input use:

$$\frac{Q_{i,t}}{B_{i,t}} = \left(\frac{\alpha_Y}{1 - \alpha_Y}\right)^{\varepsilon_Y} \left(\frac{p_{i,t}^B}{p_{i,t}^Q}\right)^{\varepsilon_Y}. \tag{A.4.8}$$

According to equation (A.4.8), an increase in the price of one input type increases the share of the other input in the optimal bundle.

Production of intermediate composites

In the second step of the production nest, producers of a sector-specific intermediate composite assemble their output $Q_{i,t}$ by combining different varieties of individual intermediate goods according to a standard Dixit-Stiglitz CES production function:

$$Q_{i,t} = \left[\int_{j=0}^{J_{i,t}} x_{j,i,t}^{\kappa} dj \right]^{\frac{1}{\kappa}}, \tag{A.4.9}$$

where $x_{j,i,t}$ denotes the j^{th} type of intermediate good variety that is available in sector i. $J_{i,t}$ is the sector-specific number of variety. This specification gives us two channels through which the intermediate sector can induce growth in the overall economy: either by producing a larger amount of any single variety $x_{j,i,t}$ by employing more labour and energy, or by expanding the number of available varieties through investing to the sector-specific capital stock $J_{i,t}$. The parameter κ measures the substitutability between different varieties $x_{j,i,t}$ (or equivalently, the gains from specialization), and is formally defined as $\kappa = (\sigma_Q - 1)/\sigma_Q$, where we assume $\sigma_Q > 1$ for the endogenous growth specification. Note that if we set $\kappa = 1$, the model collapses to a standard, Ramsey-type exogenous growth model.

The producer of the intermediate good composite $Q_{i,t}$ maximizes profits on a competitive market, taking all prices as given and solve:

$$\max_{x_{j,i,t}} p_{i,t}^{Q} Q_{i,t} - \int_{j=0}^{J_{i,t}} p_{j,i,t}^{x} x_{j,i,t} dj, \text{ w.r.t (A.4.9).} \tag{A.4.10}$$

Where we denote by $p_{j,i,t}^{x}$ the price of individual intermediate varieties. Solving the optimization problem in equation (A.4.10) determines the optimal demand for $x_{j,i,t}$:

$$x_{j,i,t} = \left(\frac{p_{i,t}^{Q}}{p_{j,i,t}^{x}} \right)^{\frac{1}{1-\kappa}} Q_{i,t}. \tag{A.4.11}$$

From now on, we assume that all varieties of the sector-specific intermediate good are perfectly symmetrical—each manufacturer of intermediates demands the same amount of labor and energy inputs—so we simplify the notation as $x_{j,i,t} = x_{i,t}$.

Production of intermediate goods

As described in Equation (A.4.9), what determines the expansion of each production sector i are the amount, variety, and substitutability of different intermediate goods. Moreover, we assume that each intermediate variety $x_{i,t}$ is first invented, and then produced, by a single firm that receives a perpetual patent at the moment of invention. Therefore, the growth rate of the overall economy depends on the decisions of profit-seeking intermediate firms.

i) Capital investments to new varieties

There are two types of capital in the model, as depicted in Figure 5.1, physical and non-physical, which together make up the sector-specific capital composite $J_{i,t}$. That is, we follow Karydas and Zhang (2019) and Bretschger et al. (2011) and include both a "lab equipment" approach, with I_{P_i} the direct physical investment for sector i, as well as a "scientific labor and R&D" innovation with I_{N_i}, the non-physical investments. The low of motion for the stock of sectoral capital follows:

$$J_{i,t+1} = \left[\alpha_J I_{P_{i,t}}^{\frac{\tau-1}{\tau}} + (1-\alpha_J) I_{N_{i,t}}^{\frac{\varepsilon_J-1}{\varepsilon_J}}\right]^{\frac{\varepsilon_J}{\varepsilon_J-1}} - (1-\delta_t) J_{i,t}, \tag{A.4.12}$$

with δ_t the depreciation rate of capital. The non-physical investments stems from labor in research $L_{J_{i,t}}$ and investments into R&D, $I_{J_{i,t}}$:

$$I_{N_{i,t}} = \left[\alpha_I L_{J_{i,t}}^{\frac{\omega-1}{\omega}} + (1-\alpha_I) I_{J_{i,t}}^{\frac{\omega-1}{\omega}}\right]^{\frac{\omega}{\omega-1}}, \tag{A.4.13}$$

The incentives to invest in new varieties stem from the monopoly rent, which is obtained when producing the intermediate goods $x_{i,t}$.

ii) Optimal output of new varieties

In order to produce one unit of output, the intermediate good producers combine two types of inputs, labour $L_{X_{i,t}}$ and energy $E_{i,t}$, according to the following CES technology:

$$x_{i,t} = \left[\lambda_i L_{X_{i,t}}^{\frac{\varepsilon_x-1}{\varepsilon_x}} + (1-\lambda_i) E_{i,t}^{\frac{\varepsilon_x-1}{\varepsilon_x}}\right]^{\frac{\varepsilon_x}{\varepsilon_x-1}}. \tag{A.4.14}$$

We assume labour $L_{X_{i,t}}$ to be in inelastic supply throughout the modelling horizon, perfectly mobile between sectors within the country. The energy aggregate $E_{i,t}$, on the other hand, is combined from a fossil (F) and fossil-free (G) energy sources, according to:

$$E_{i,t} = \left[\phi_i F_{i,t}^{\frac{\varepsilon_E - 1}{\varepsilon_E}} + (1 - \phi_i) G_{i,t}^{\frac{\varepsilon_E - 1}{\varepsilon_E}} \right]^{\frac{\varepsilon_E}{\varepsilon_E - 1}}, \tag{A.4.15}$$

where the fossil-sources of energy, f_k, oil, gas and heat combine into F under a CES production:

$$F_{i,t} = \left[\sum_k \phi_{i,k} f_{k,i,t}^{\frac{\varepsilon_{fos} - 1}{\varepsilon_{fos}}} \right]^{\frac{\varepsilon_{fos}}{\varepsilon_{fos} - 1}}, \tag{A.4.16}$$

the index k denotes each type of fossil energy.

The output decision of the intermediate monopoly is twofold. First, it chooses an optimal bundle of labour and energy inputs as to maximize profits in a perfectly competitive market:

$$\max_{L_{X_{i,t}}, E_{i,t}} = \psi_{i,t}^x x_{i,t} - w_t L_{X_{i,t}} - p_{i,t}^E E_{i,t}, \tag{A.4.17}$$

where $\psi_{i,t}^x$ is the price that would prevail under a perfectly competitive market. We denote the price of labor w_t and price of energy by $p_{k,t}^E$. Second, the firm exploits its monopoly power in the output market and sets the optimal output price solving:

$$\max_{p_{i,t}^x} = p_{i,t}^x x_{i,t} - \psi_{i,t}^x x_{i,t}, \tag{A.4.18}$$

taking the demand for $x_{i,t}$ in equation (A.4.11) as given. Thus, it sets prices according to:

$$p_{i,t}^x = \frac{1}{\kappa} \psi_{i,t}^x, \tag{A.4.19}$$

with profits being equal to:

$$\pi_{i,t} = (1 - \kappa) p^x_{i,t} x_{i,t}. \tag{A.4.20}$$

As the individual intermediate goods $x_{i,t}$ are imperfect substitutes, and the intermediate good producer competes in a monopolistic market with an output price $p^x_{i,t}$. The imperfect substituability among $x_{i,t}$ in (A.4.9) turns into the mark-up $\frac{1}{\kappa} - 1$. The term $1 - \kappa$ in (A.4.20) measures the share of revenues in the production of Q which is used to compensate firm owners from their investments.

International trade

The economy is open to trade on the goods' market. In each sector, a domestic and a foreign good are available for consumption and production. We model international trade assuming Armington aggregation, i.e. each sectoral good is an imperfect substitute to an imported sectoral output in consumption. For each sector i, domestic D_i and imported goods M_i are combined according to the following CET function:

$$A_{i,t} = \left[\alpha_A D_{i,t}^{\frac{\xi-1}{\xi}} + (1 - \alpha_A) M_{i,t}^{\frac{\xi-1}{\xi}} \right]^{\frac{\xi}{\xi-1}}, \tag{A.4.21}$$

where ξ is the elasticity of substitution between the domestic and the foreign good. Note that the domestic good D_i is the share of the final output Y_i that the economy keeps for domestic use. The final goods supplier i at time t maximizes profits taking prices as given according to:

$$\max_{M_{i,t}, Y_{i,t}} = p^A_{i,t} A_{i,t} - p^Y_{i,t} D_{i,t} - p^A_{i,t} M_{i,t}, \tag{A.4.22}$$

subject to (A.4.21). Trade is balanced in every period and since we model Switzerland as a small open economy, foreign prices are exogenous. The economy exports and imports regular and energy goods and also purchases crude oil and natural gas from abroad. The latter are assembled with the final good Y_i of the oil and gas sector only according to a Leontief production function.

Equilibrium

The dynamic equilibrium path using the equations derived in this Section A.4.1 is characterized by a time path of quantities and prices:

$$\{Y_{i,t}, Q_{i,t}, B_{i,t}, x_{i,t}, J_{i,t}, L_{X_{i,t}},$$
$$L_{J_{i,t}}, E_{i,t}, A_{i,t}, D_{i,t}, M_{i,t}, I_{P_{i,t}}, I_{N_{i,t}}, \Delta J_{i,t}, C_{Y_{i,t}}, C_{Egyi,t}, C_{i,t}\}_{t=0}^{\infty}$$
$$\{p_{i,t}^{Y}, p_{i,t}^{Q}, p_{i,t}^{B}, p_{i,t}^{x}, p_{i,t}^{J}, w_t, p_{i,t}^{E}, p_{i,t}^{A}, p_{P_{i,t}}^{I}, p_{N_{i,t}}^{I}, p_{Y_{i,t}}^{C}, p_{Egyi,t}^{C}, p_{i,t}^{C}, r_t\}_{t=0}^{\infty}$$

which clear goods and factors markets and satisfy the first order conditions for firms and households.

A.4.2 Sectoral aggregation

Table A.4.1: Mapping of NOGA divisions to sectors

Sector label	Description	NOGA Divisions
AGR	Agriculture	01 - 03
CHM	Chemical Industry	20 - 21
MCH	Machinery and Equipment	26 - 30, 33
EGY	Energy (Electricity, Oil, Gas, Heat)	19, 35, 38
CON	Construction	41 - 43
TRN	Transport	49 - 52
BNK	Banking and Financial Services	64
INS	Insurances	65
HEA	Health	86
OSE	Other Services	36 - 39, 45 - 47, 53 - 63, 68 - 97
OIN	Other Industries	05 - 18, 22 - 25, 31 - 32

A.4.3 Calibration parameters

Table A.4.2: Parameters used in the economic model

Model parameters		
Parameter	Description	Value
Elasticities of substitution for production activities		
ε_Y	Intermediate composite Q and inputs B from other sectors	$\star$
ε_x	Labour and energy in intermediate good production	$\star\star$
ε_E	Electricity and non-electricity for intermediate goods production	2.00
ε_{fos}	Types of Fossil energy in intermediate production	1.00
τ	Physical investment I_{P_i} and non-physical investments I_{N_i}	0.30
ω	Labor in research L_{J_i} and investments in R&D I_{J_i}	0.30
κ	Intermediate varieties	0.70
υ	Elasticity of substitution between sectoral outputs for the input B_i	0
Elasticities of substitution for consumption		
σ_C	Energy and non-energy goods in consumption	0.50
σ_E	Energy goods in consumption	2.00
σ_{fos}	Types of Fossil energy in consumption	1.00
σ_Y	Different regular goods	0.50
Elasticities of substitution for welfare		
$1/\zeta$	Intertemporal elasticity of substitution	0.85
σ_L	Consumption and leisure	0.65
Other parameters		
ξ	Trade elasticities	$\star\star\star$
$\bar{r}$	Benchmark Interest rate	0.006
g_K	Benchmark growth rate of capital	0.007
$\bar{\delta}$	Benchmark depreciation rate	0.07
θ	Leisure share in total time endowment of the households	0.40

Notes:
$\star$*: 0.392 (AGR); 0.568 (OIN); 1.264 (CON); 0.848 (Fossil, CHM); 0.518 (MCH); 0.352 (TRN); 0.100 (Electricity); 0.492 (others).*
$\star\star$*: 0.7 (AGR, MCH, Electricity, Fossil); 0.52 (CON); 0.55 (CHM, TRN, OIN); 0.4 (others).*
$\star\star\star$*: 3.52 (AGR); 5.06 (MCH); 4.18 (Electricity, OIN); 3.19 (others).*
Sources: ε_Y *Okagawa and Ban (2008);* ε_x *Van der Werf (2008), Mohler and Müller (2012);* ε_E *Papageorgiou et al. (2017);* ε_{fos} *and* σ_{fos} *Bretschger and Zhang (2017);* τ, ω, ξ *Bretschger et al. (2011);* σ_C *and* σ_Y *Vöhringer et al. (2007);*
$1/\zeta$ *Hasanov (2007);* σ_L *Imhof (2012);* ξ *Donnelly et al. (2004);* υ *Paltsev et al. (2005b).*

A.4.4 Carbon tax effects on consumption and investment

Figure A.4.1: The effect of carbon reductions on the aggregate consumption growth and investments growth

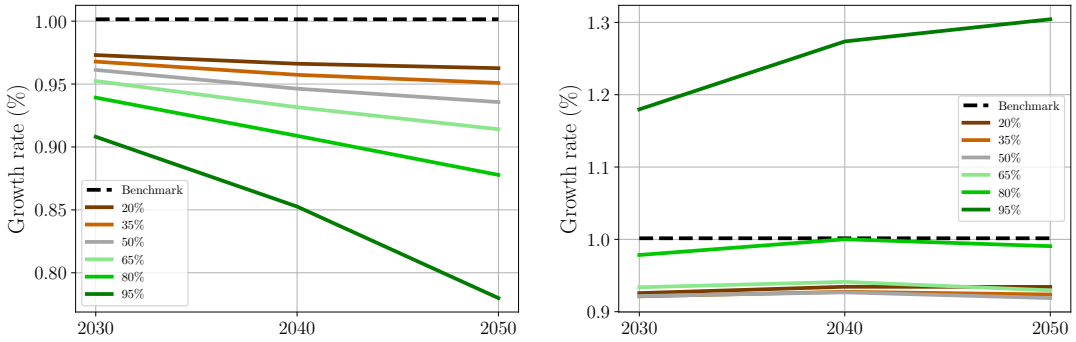

(a) Consumption growth **(b)** Investments growth

Notes: The figure shows the results for various policy targets under the anticipation of future policies. For example, a 65% policy implies a 65% reduction in CO_2 emissions in comparison to the benchmark year.

A.4.5 Anticipation effect on energy use

Figure A.4.2: Anticipation effect on the use of energy from different sources

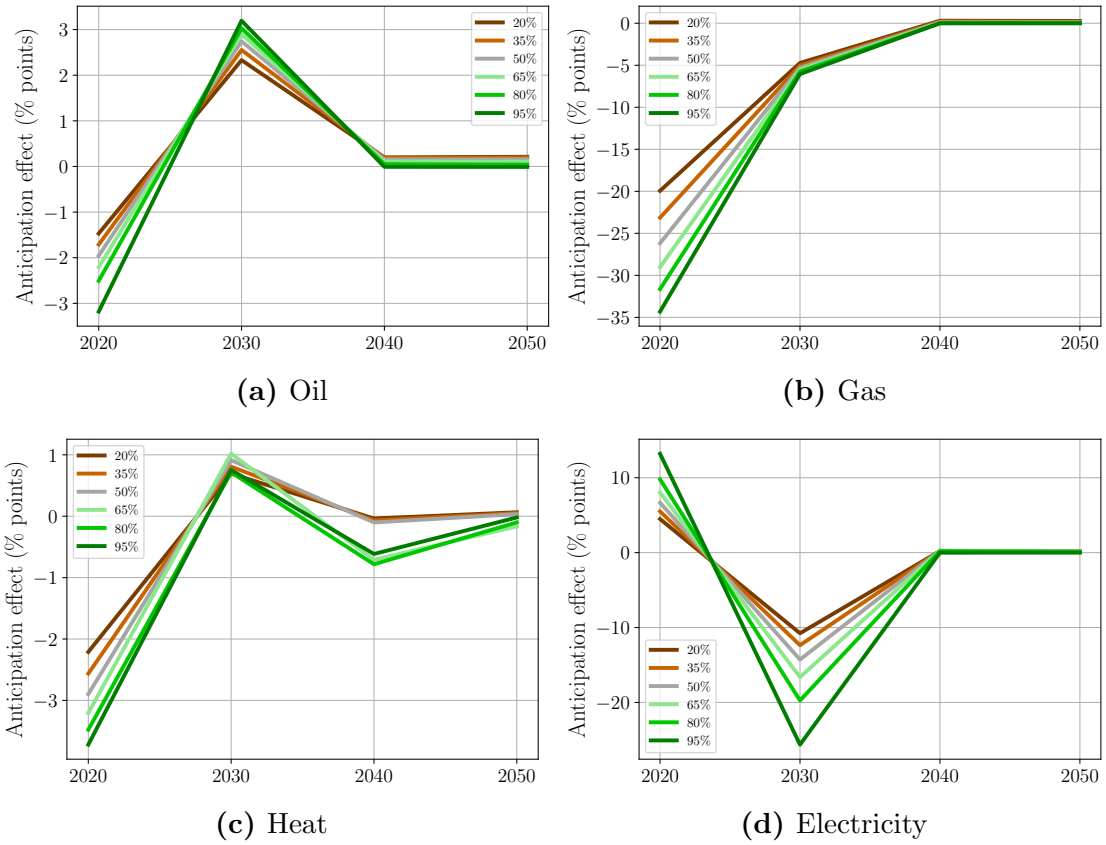

(a) Oil **(b)** Gas

(c) Heat **(d)** Electricity

A.4.6 Anticipation effect on consumption and leisure

For both graphs, we show the effect of anticipation at various levels of the carbon tax such that the total carbon emissions decrease by 20-95%.

Figure A.4.3: Anticipation effect on labor supply by household

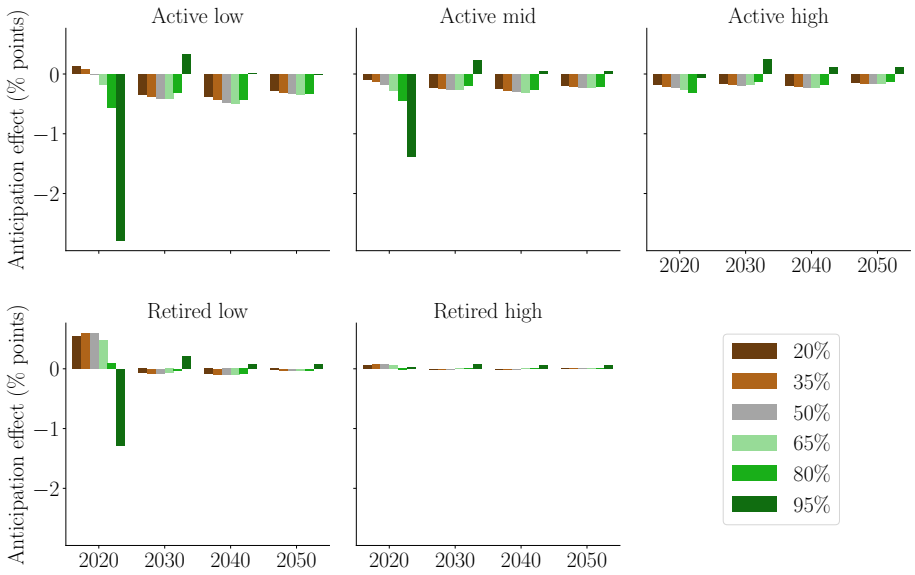

Figure A.4.4: Anticipation effect on consumption index by household

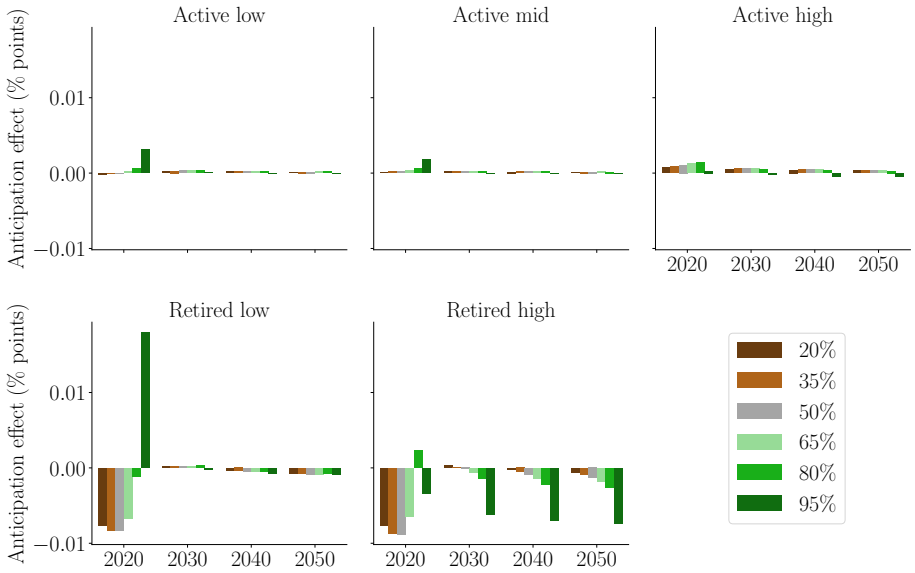

A.4.7 Inverse-proportional redistribution

Figure A.4.5: The difference in welfare between the inverse-proportional and lump-sum redistribution schemes across household groups, the anticipation case

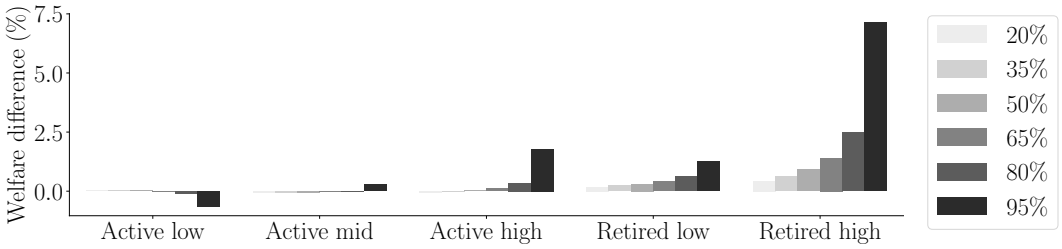

Notes: We show the results for scenarios that go from 20% to 95% reduction of carbon emissions. As the graph reads, for a 95% carbon reduction policy, the welfare of the "Retired high" household group increases by about 7.5% when the tax revenues are redistributed inversely proportional to total income compared to the lump-sum redistribution scheme.

References

Acemoglu, D. (2009). *Introduction to Modern Economic Growth*. Princeton University Press.

Acemoglu, D., Aghion, P., Bursztyn, L., and Hemous, D. (2012). The environment and directed technical change. *American economic review*, 102(1):131–66.

Acemoglu, D., and V. Chernozhukov and I. Werning and M. Whinston (2021). Optimal targeted lockdowns in a multigroup sir model. *American Economic Review: Insights*, 3(4):487–502.

Aït-Sahalia, Y. and Hurd, T. R. (2015). Portfolio choice in markets with contagion. *Journal of Financial Econometrics*, 14(1):1–28.

Akao, K.-I. and Sakamoto, H. (2018). A theory of disasters and long-run growth. *Journal of Economic Dynamics and Control*, 95:89–109.

Allen, M., Dube, O., Solecki, W., Aragón-Durand, F., Cramer, W., Humphreys, S., Kainuma, M., Kala, J., Mahowald, N., Mulugetta, Y., Perez, R., Wairiu, M., and Zickfeld, K. (2018). Framing and context. In *Global Warming of 1.5°C. An IPCC Special Report on the impacts of global warming of 1.5°C above pre-industrial levels and related global greenhouse gas emission pathways, in the context of strengthening the global response to the threat of climate change, sustainable development, and efforts to eradicate poverty [Masson-Delmotte, V., P. Zhai, H.-O. Pörtner, D. Roberts, J. Skea, P.R. Shukla, A. Pirani, W. Moufouma-Okia, C. Péan, R. Pidcock, S. Connors, J.B.R. Matthews, Y. Chen, X. Zhou, M.I. Gomis, E. Lonnoy, T. Maycock, M. Tignor, and T. Waterfield (eds.)]*. In Press.

Almond, R., Grooten, M., Juffe Bignoli, D., and Petersen, T. (2022). Living planet report 2022–building a nature-positive society. *World Wildlife Fund*.

Andre, F. E., Booy, R., Bock, H. L., Clemens, J., Datta, S. K., John, T. J., Lee, B. W., Lolekha, S., Peltola, H., Ruff, T., et al. (2008). Vaccination greatly reduces disease, disability, death and inequity worldwide. *Bulletin of the World health organization*, 86:140–146.

Anttila-Hughes, J. and Hsiang, S. (2013). Destruction, disinvestment, and death: Economic and human losses following environmental disaster. *Available at SSRN 2220501*.

Armington, P. (1969). A theory of demand for products distinguished by place of production. *IMF staff working papers*.

Arnell, N. W. and Gosling, S. N. (2016). The impacts of climate change on river flood risk at the global scale. *Climatic Change*, 134:387–401.

Aznar Siguan, G. and Bresch, D. N. (2019). Climada v1: a global weather and climate risk assessment platform. *Geoscientific Model Development*, 12:3085–3097.

Bacry, E., Mastromatteo, I., and Muzy, J.-F. (2015). Hawkes Processes in Finance. *Market Microstructure and Liquidity*, 01(01):1550005.

Bakkensen, L. and Barrage, L. (2018). Climate Shocks, Cyclones, and Economic Growth: Bridging the Micro-Macro Gap. *NBER Wroking Paper*.

Bakkensen, L. A. and Mendelsohn, R. O. (2016). Risk and adaptation: Evidence from global hurricane damages and fatalities. *Journal of the Association of Environmental and Resource Economists*, 3(3):555–587.

Baldwin, E., Cai, Y., and Kuralbayeva, K. (2020). To build or not to build? Capital stocks and climate policy. *Journal of Environmental Economics and Management*, 100:102235.

Barro, R. J. (2006). Rare disasters and asset markets in the twentieth century. *The Quarterly Journal of Economics*, 121(3):823–866.

Barro, R. J. (2009). Rare disasters, asset prices, and welfare costs. *American Economic Review*, 99(1):2543–264.

Bauer, N., McGlade, C., Hilaire, J., and Ekins, P. (2018). Divestment prevails over the green paradox when anticipating strong future climate policies. *Nature Climate Change*, 8(2):130–134.

Beck, M., Rivers, N., Wigle, R., and Yonezawa, H. (2015). Carbon tax and revenue recycling: Impacts on households in british columbia. *Resource and Energy Economics*, 41:40–69.

Benedictow, O. J. (2004). *The Black Death, 1346-1353: the complete history*. Boydell & Brewer.

Bernstein, L., Bosch, P., Canziani, O., Chen, Z., Christ, R., and Riahi, K. (2008). Ipcc, 2007: climate change 2007: synthesis report.

Bloom, N. (2009). The impact of uncertainty shocks. *Econometrica*, 77(3):623–685.

Bosetti, V., Carraro, C., Galeotti, M., Massetti, E., and Tavoni, M. (2006). A world induced technical change hybrid model. *The Energy Journal*, 27(Special Issue# 2).

Bosetti, V., Carraro, C., and Tavoni, M. (2009). Climate change mitigation strategies in fast-growing countries: The benefits of early action. *Energy Economics*, 31(7):S144–S151.

Bosetti, V. and Victor, D. G. (2011). Politics and economics of second-best regulation of greenhouse gases: the importance of regulatory credibility. *The Energy Journal*, 32(1).

Bresch, D. N. and Aznar-Siguan, G. (2021). Climada v1.4.1: towards a globally consistent adaptation options appraisal tool. *Geoscientific Model Development*, 14(1):351–363.

Bretschger, L. (2020). Malthus in the light of climate change. *European Economic Review*, 127:103477.

Bretschger, L., Lechthaler, F., Rausch, S., and Zhang, L. (2017). Knowledge diffusion, endogenous growth, and the costs of global climate policy. *European Economic Review*, 93:47–72.

Bretschger, L., Ramer, R., and Schwark, F. (2011). Growth effects of carbon policies: applying a fully dynamic CGE model with heterogeneous capital. *Resource and Energy Economics*, 33(4):963–980.

Bretschger, L. and Schaefer, A. (2017). Dirty history versus clean expectations: Can energy policies provide momentum for growth? *European Economic Review*, 99:170–190.

Bretschger, L. and Vinogradova, A. (2018). Escaping damocles' sword: endogenous climate shocks in a growing economy. *CER-ETH–Center of Economic Research at ETH Zurich, Working Paper*, 18:291.

Bretschger, L. and Vinogradova, A. (2019). Best policy response to environmental shocks: Applying a stochastic framework. *Journal of Environmental Economics and Management*, 97:23–41.

Bretschger, L. and Zhang, L. (2017). Nuclear phase-out under stringent climate policies: A dynamic macroeconomic analysis. *The Energy Journal*, 38(1).

Brock, W. and Xepapadeas, A. (2020). The economy, climate change and infectious diseases: links and policy implications. *Environmental and Resource Economics*, 76(4):811–824.

Brock, W. and Xepapadeas, A. (2021). Regional climate policy under deep uncertainty: robust control and distributional concerns. *Environment and Development Economics*, 26(3):211–238.

Brock, W. A. and Mirman, L. J. (1972). Optimal economic growth and uncertainty: the discounted case. *Journal of Economic Theory*, 4(3):479–513.

Callaghan, C. T., Nakagawa, S., and Cornwell, W. K. (2021). Global abundance estimates for 9,700 bird species. *Proceedings of the National Academy of Sciences*, 118(21):e2023170118.

Carrera, L., Standardi, G., Bosello, F., and Mysiak, J. (2015). Assessing direct and indirect economic impacts of a flood event through the integration of spatial and computable general equilibrium modelling. *Environmental Modelling & Software*, 63:109–122.

CBO (2016). Potential increases in hurricane damage in the united states: Implications for the federal budget.

Chen, X. and Nordhaus, W. D. (2011). Using luminosity data as a proxy for economic statistics. *Proceedings of the National Academy of Sciences*, 108(21):8589–8594.

Cheng, V. C., Lau, S. K., Woo, P. C., and Yuen, K. Y. (2007). Severe acute respiratory syndrome coronavirus as an agent of emerging and reemerging infection. *Clinical microbiology reviews*, 20(4):660–694.

CIESIN (2016). Gridded population of the world, version 4 (gpwv4): Administrative unit center points with population estimates. Center for International Earth Science Information Network. Palisades, NY: NASA Socioeconomic Data and Applications Center (SEDAC).

Clarke, H. R. and Reed, W. J. (1994). Consumption/pollution tradeoffs in an environment vulnerable to pollution-related catastrophic collapse. *Journal of Economic Dynamics and Control*, 18(5):991–1010.

Cornélis, D., Melletti, M., Korte, L., Ryan, S. J., Mirabile, M., Prin, T., Prins, H. H., et al. (2014). African buffalo syncerus caffer (sparrman, 1779). *Ecology, evolution and behaviour of wild cattle: implications for conservation*, pages 326–372.

Crespo Cuaresma, J., Hlouskova, J., and Obersteiner, M. (2008). Natural disasters as creative destruction? Evidence from developing countries. *Economic Inquiry*, 46(2):214–226.

Cropper, M. L. (1976). Regulating activities with catastrophic environmental effects. *Journal of environmental Economics and Management*, 3(1):1–15.

Crosby, A. W. (2003). *The Columbian exchange: biological and cultural consequences of 1492*, volume 2. Greenwood Publishing Group.

Cui, L., Hawkes, A., and Yi, H. (2020). An elementary derivation of moments of Hawkes processes. *Advances in Applied Probability*, 52(1):102–137.

Daley, D. J. and Vere-Jones, D. (2003). *An introduction to the theory of point processes. Vol. I, II.* Probability and its Applications (New York). Springer-Verlag, New York, second edition.

Daniell, J. E., Schaefer, A. M., and Wenzel, F. (2017). Losses associated with secondary effects in earthquakes. *Frontiers in Built Environment*, 3(30).

Dassios, A. and Zhao, H. (2011). A dynamic contagion process. *Advances in Applied Probability*, 43(3):814–846.

De Zeeuw, A. and Zemel, A. (2012). Regime shifts and uncertainty in pollution control. *Journal of Economic Dynamics and Control*, 36(7):939–950.

Deryugina, T. (2017). The fiscal cost of hurricanes: Disaster aid versus social insurance. *American Economic Journal: Economic Policy*, 9(3):168–98.

Deryugina, T., Kawano, L., and Levitt, S. (2018). The economic impact of hurricane katrina on its victims: Evidence from individual tax returns. *American Economic Journal: Applied Economics*, 10(2):202–33.

Devereux, S. (2009). Why does famine persist in africa? *Food security*, 1:25–35.

Di Maria, C., Smulders, S., and van der Werf, E. (2012). Absolute abundance and relative scarcity: Environmental policy with implementation lags. *Ecological Economics*, 74:104–119.

Di Maria, C., Smulders, S., and van der Werf, E. (2017). Climate policy with tied hands: Optimal resource taxation under implementation lags. *Environmental and Resource Economics*, 66(3):537–551.

Di Maria, C. and van der Werf, E. (2008). Carbon leakage revisited: unilateral climate policy with directed technical change. *Environmental and Resource Economics*, 39(2):55–74.

Dietz, S., Rising, J., Stoerk, T., and Wagner, G. (2021). Economic impacts of tipping points in the climate system. *PNAS*, 118(34):e2103081118.

Dirkse, S. P. and Ferris, M. C. (1995). The path solver: a nommonotone stabilization scheme for mixed complementarity problems. *Optimization Methods and Software*, 5(2):123–156.

Donnelly, W. A., Johnson, K., Tsigas, M. E., and Ingersoll, D. L. (2004). Revised armington elasticities of substitution usitc model and the concordance for constructing consistent set for the gtap model. *Available at SSRN 970539*.

Douenne, T. (2020). Disaster risks, disaster strikes, and economic growth: The role of preferences. *Review of Economics Dynamics*, 38:251–272.

Eberenz, S., Lüthi, S., and Bresch, D. N. (2021). Regional tropical cyclone impact functions for globally consistent risk assessments. *Natural Hazards and Earth System Sciences*, 21(1):393–415.

Eberenz, S., Stocker, D., Röösli, T., and Bresch, D. N. (2019). Exposure data for global physical risk assessment. *Earth System Science Data Discussions*, 2019:1–19.

Ehrlich, P. R. (2008). Key issues for attention from ecological economists. *Environment and Development Economics*, 13:1–20.

EM-DAT (2020). EM-DAT: The emergency events database - Université Catholique de Louvain (UCL) - CRED, D. Guha-Sapir - www.emdat.be, Brussels, Belgium. Accessed on 21/03/2021.

Emanuel, K. (2011). Global warming effects on us hurricane damage. *Weather, Climate, and Society*, 3(4):261–268.

Emanuel, K. (2013). Downscaling CMIP5 climate models shows increased tropical cyclone activity over the 21st century. *Proceedings of the National Academy of Sciences*, 110(30):12219–12224.

Embrechts, P. and Kirchner, M. (2018). Hawkes graphs. *Theory of Probability & Its Applications*, 62(1):132–156.

Errais, E., Giesecke, K., and Goldberg, L. R. (2010). Affine point processes and portfolio credit risk. *SIAM Journal on Financial Mathematics*, 1(1):642–665.

Fankhauser, S. and McDermott, T. K. (2014). Understanding the adaptation deficit: why are poor countries more vulnerable to climate events than rich countries? *Global Environmental Change*, 27:9–18.

Favero, C. and Giavazzi, F. (2012). Measuring tax multipliers: The narrative method in fiscal vars. *American Economic Journal: Economic Policy*, 4(2):69–94.

Felbermayr, G. and Gröschl, J. (2013). Natural disasters and the effect of trade on income: A new panel IV approach. *European Economic Review*, 58:18–30.

Felbermayr, G. and Gröschl, J. (2014). Naturally negative: The growth effects of natural disasters. *Journal of development economics*, 111:92–106.

Fenner, F., Henderson, D., Arita, I., Ježek, Z., and Ladnyi, I. (1988). The incidence and control of smallpox between 1900 and 1958. *Smallpox and its Eradication; World Health Organization: Geneva, Switzerland*, 330.

Ferraro, D. and Peretto, P. F. (2020). Market size, innovation, and the economic effects of an epidemic. *Innovation, and the Economic Effects of an Epidemic (October 12, 2020)*.

Ferreira, S., Hamilton, K., and Vincent, J. R. (2013). Does development reduce fatalities from natural disasters? New evidence for floods. *Environment and Development Economics*, 18(6):649–679.

Ferris, M. C. and Munson, T. S. (2000). Complementarity problems in gams and the path solver. *Journal of Economic Dynamics and Control*, 24(2):165–188.

Filimonov, V. and Sornette, D. (2012). Quantifying reflexivity in financial markets: Toward a prediction of flash crashes. *Phys. Rev. E*, 85:056108.

Fremstad, A. and Paul, M. (2019). The impact of a carbon tax on inequality. *Ecological Economics*, 163(1):88–97.

Galor, O. (2005a). The demographic transition and the emergence of sustained economic growth. *Journal of the European Economic Association*, 3(2-3):494–504.

Galor, O. (2005b). From stagnation to growth: unified growth theory. *Handbook of economic growth*, 1:171–293.

Galor, O. and Moav, O. (2002). Natural selection and the origin of economic growth. *The Quarterly Journal of Economics*, 117(4):1133–1191.

Galor, O. and Weil, D. N. (1999). From malthusian stagnation to modern growth. *American Economic Review*, 89(2):150–154.

Galor, O. and Weil, D. N. (2000). Population, technology, and growth: From malthusian stagnation to the demographic transition and beyond. *American economic review*, 90(4):806–828.

Geiger, T., Gütschow, J., Bresch, D. N., Emanuel, K., and Frieler, K. (2021). Double benefit of limiting global warming for tropical cyclone exposure. *Nature Climate Change*, 11(10):861–866.

Gertz, A. B., Davies, J. B., and Black, S. L. (2019). A CGE framework for modeling the economics of flooding and recovery in a major urban area. *Risk Analysis*, 39(6):1314–1341.

Gettelman, A., Bresch, D. N., Chen, C. C., Truesdale, J. E., and Bacmeister, J. T. (2018). Projections of future tropical cyclone damage with a high-resolution global climate model. *Climatic Change*, 146(3-4):575–585.

Golosov, M., Hassler, J., Krusell, P., and Tsyvinski, A. (2014). Optimal taxes on fossil fuels in general equilibrium. *Econometrica*, 82(1):41–88.

Gompper, M. E. (2014). The dog-human-wildlife interface: assessing the scope of the problem. *Free-ranging dogs and wildlife conservation*, pages 9–54.

Gosling, S., Müller Schmied, H., Betts, R., Chang, J., Ciais, P., Dankers, R., Döll, P., Eisner, S., Flörke, M., Gerten, D., et al. (2017). ISIMIP2a simulation data from water (global) sector. *GFZ Data Services*, 10.

Greene, W. H. (2007). Fixed and random effects models for count data. *Leonard N. Stern School of Business Paper No. ISSN*, pages 1547–3651.

Greenlaw, R. W. (1958). *The economic origins of the French Revolution : poverty or prosperity?* Problems in European civilization. Heath and Co., Boston.

Guiteras, R., Jina, A., and Mobarak, A. M. (2015). Satellites, self-reports, and submersion: exposure to floods in Bangladesh. *American Economic Review*, 105(5):232–236.

Gupta, J. (2010). A history of international climate change policy. *Wiley Interdisciplinary Reviews: Climate Change*, 1(5):636–653.

Hallegatte, S. (2007). The use of synthetic hurricane tracks in risk analysis and climate change damage assessment. *Journal of applied meteorology and climatology*, 46(11):1956–1966.

Hallegatte, S. and Dumas, P. (2009). Can natural disasters have positive consequences? Investigating the role of embodied technical change. *Ecological Economics*, 68(3):777–786.

Hallegatte, S. and Przyluski, V. (2010). *The economics of natural disasters: Concepts and methods*. The World Bank.

Hallegatte, S. and Vogt-Schilb, A. (2016). Are losses from natural disasters more than just asset losses? The role of capital aggregation, sector interactions, and investment behaviors. Policy Research Working Paper;No. 7885. World Bank, Washington, DC.

Harari, Y. N. (2016). *Homo Deus: A brief history of tomorrow*. Random House.

Hasanov, F. (2007). Housing, household portfolio, and intertemporal elasticity of substitution. *Available at SSRN 825324*.

Hasegawa, T., Fujimori, S., Havlík, P., Valin, H., Bodirsky, B. L., Doelman, J. C., Fellmann, T., Kyle, P., Koopman, J. F., Lotze-Campen, H., et al. (2018). Risk of increased food insecurity under stringent global climate change mitigation policy. *Nature Climate Change*, 8(8):699–703.

Héran, F. (2014). Générations sacrifiées: le bilan démographique de la grande guerre. *Population & sociétés*, 510(4):1–4.

Hsiang, S. M. and Jina, A. S. (2014). The causal effect of environmental catastrophe on long-run economic growth: Evidence from 6,700 cyclones. Technical report, National Bureau of Economic Research.

Hsiang, S. M. and Narita, D. (2012). Adaptation to cyclone risk: Evidence from the global cross-section. *Climate Change Economics*, 3(02):1250011.

Ikefuji, M. and Horii, R. (2012). Natural disasters in a two-sector model of endogenous growth. *Journal of Public Economics*, 96(9-10):784–796.

Imhof, J. (2012). Fuel exemptions, revenue recycling, equity and efficiency: evaluating post-Kyoto policies for Switzerland. *Swiss Journal of Economics and Statistics*, 148(2):197–227.

IPCC (2023). Climate Change 2023: Synthesis Report. Contribution of Working Groups I, II and III to the Sixth Assessment Report of the Intergovernmental Panel on Climate Change [Core Writing Team, H. Lee and J. Romero (eds.)]. IPCC Geneva, Switzerland, pp. 35-115.

Jacod, J. and Protter, P. (2004). *Probability essentials*. Springer Science & Business Media.

Jensen, S., Mohlin, K., Pittel, K., and Sterner, T. (2015). An introduction to the green paradox: the unintended consequences of climate policies. *Review of Environmental Economics and Policy*, 9(2):246–265.

Jo, A. (2020). The elasticity of substitution between clean and dirty energy with technological bias. *Economics Working Paper Series*, 20.

Jones, R. L., Guha-Sapir, D., and Tubeuf, S. (2022). Human and economic impacts of natural disasters: can we trust the global data? *Scientific data*, 9(1):572.

Jongman, B., Winsemius, H. C., Aerts, J. C., Coughlan de Perez, E., Van Aalst, M. K., Kron, W., and Ward, P. J. (2015). Declining vulnerability to river floods

and the global benefits of adaptation. *Proceedings of the National Academy of Sciences*, 112(18):E2271–E2280.

Kahn, M. E. (2005). The death toll from natural disasters: the role of income, geography, and institutions. *Review of economics and statistics*, 87(2):271–284.

Kam, P. M., Aznar-Siguan, G., Schewe, J., Milano, L., Ginnetti, J., Willner, S., McCaughey, J. W., and Bresch, D. N. (2021). Global warming and population change both heighten future risk of human displacement due to river floods. *Environmental Research Letters*, 16(4):044026.

Karydas, C. and Zhang, L. (2019). Green tax reform, endogenous innovation and the growth dividend. *Journal of Environmental Economics and Management*, 97:158–181.

Kellenberg, D. K. and Mobarak, A. M. (2008). Does rising income increase or decrease damage risk from natural disasters? *Journal of urban economics*, 63(3):788–802.

Keppo, I., Butnar, I., Bauer, N., Caspani, M., Edelenbosch, O., Emmerling, J., Fragkos, P., Guivarch, C., Harmsen, M., Lefèvre, J., Le Gallic, T., Leimbach, M., McDowall, W., Mercure, J.-F., Schaeffer, R., Trutnevyte, E., and Wagner, F. (2021). Exploring the possibility space: taking stock of the diverse capabilities and gaps in integrated assessment models. *Environmental Research Letters*, 16(5):053006.

Khas'minskii, R. Z. (1960). Ergodic properties of recurrent diffusion processes and stabilization of the solution to the cauchy problem for parabolic equations. *Theory of Probability & Its Applications*, 5(2):179–196.

Kirchner, M. (2017). An estimation procedure for the Hawkes process. *Quantitative Finance*, 17(4):571–595.

Kirchner, M. and Bercher, A. (2018). A nonparametric estimation procedure for the Hawkes process: comparison with maximum likelihood estimation. *Journal of Statistical Computation and Simulation*, 88(6):1106–1116.

Knapp, K. R., Kruk, M. C., Levinson, D. H., Diamond, H. J., and Neumann, C. J. (2010). The international best track archive for climate stewardship (IBTrACS) unifying tropical cyclone data. *Bulletin of the American Meteorological Society*, 91(3):363–376.

Knutson, T. R., Sirutis, J. J., Zhao, M., Tuleya, R. E., Bender, M., Vecchi, G. A., Villarini, G., and Chavas, D. (2015). Global projections of intense tropical cyclone activity for the late twenty-first century from dynamical downscaling of CMIP5/RCP4.5 scenarios. *Journal of Climate*, 28(18):7203–7224.

Koch, N., Grosjean, G., Fuss, S., and Edenhofer, O. (2016). Politics matters: Regulatory events as catalysts for price formation under cap-and-trade. *Journal of Environmental Economics and Management*, 78:121–139.

Kocornik-Mina, A., McDermott, T. K., Michaels, G., and Rauch, F. (2020). Flooded cities. *American Economic Journal: Applied Economics*, 12(2):35–66.

Krugman, P. (1991). History versus expectations. *Quarterly Journal of Economics*, 106(2):651–667.

Kummu, M., Taka, M., and Guillaume, J. H. (2018). Gridded global datasets for gross domestic product and human development index over 1990–2015. *Scientific data*, 5(1):1–15.

Kydland, F. E. and Prescott, E. C. (1977). Rules rather than discretion: The inconsistency of optimal plans. *Journal of political economy*, 85(3):473–491.

Landis, F., Marcucci, A., Rausch, S., Kannan, R., and Bretschger, L. (2019). Multi-model comparison of swiss decarbonization scenarios. *Swiss Journal of Economics and Statistics*, 155(1):173.

Lau, M. I., Pahlke, A., and Rutherford, T. F. (2002a). Approximating infinite-horizon models in a complementarity format: A primer in dynamic general equilibrium analysis. *Journal of Economic Dynamics and Control*, 26(4):577–609.

Lau, M. I., Pahlke, A., and Rutherford, T. F. (2002b). Approximating infinite-horizon models in a complementarity format: A primer in dynamic general equilibrium analysis. *Journal of Economic Dynamics and Control*, 26(4):577 – 609.

Lehtomaa, J. and Renoir, C. (2022). Catastrophes naturelles et dynamiques économiques: application aux cyclones tropicaux. *Revue française d'économie*, 37(2):11–41.

Lehtomaa, J. and Renoir, C. (2023). The economic impact of tropical cyclones: Case studies in general equilibrium. *Economics Working Paper Series*, 23/382.

Lemoine, D. and Traeger, C. (2014). Watch your step: Optimal policy in a tipping climate. *American Economic Journal: Economic Policy*, 6(1):137–166.

Lescureux, N. and Linnell, J. D. (2014). Warring brothers: The complex interactions between wolves (canis lupus) and dogs (canis familiaris) in a conservation context. *Biological conservation*, 171:232–245.

Lewis, S. L. and Maslin, M. A. (2015). Defining the anthropocene. *Nature*, 519(7542):171–180.

Ljungqvist, L. and Sargent, T. J. (2018). *Recursive macroeconomic theory*. MIT press.

Loayza, N. V., Olaberria, E., Rigolini, J., and Christiaensen, L. (2012). Natural disasters and growth: Going beyond the averages. *World Development*, 40(7):1317–1336.

Lucas, R. E. and Lucas (1987). *Models of business cycles*, volume 26. Basil Blackwell Oxford.

Macrae, J. and Zwi, A. B. (1992). Food as an instrument of war in contemporary african famines: a review of the evidence. *Disasters*, 16(4):299–321.

Maddison, A. (2001). *A millennial perspective*. OECD.

Malthus, T. R. (1798). *An Essay on the Principle of Population*. J. Johnson, London.

Manne, A., Mendelsohn, R., and Richels, R. (1995). Merge: A model for evaluating regional and global effects of ghg reduction policies. *Energy policy*, 23(1):17–34.

Marani, M., Katul, G. G., Pan, W. K., and Parolari, A. J. (2021). Intensity and frequency of extreme novel epidemics. *Proceedings of the National Academy of Sciences*, 118(35):e2105482118.

Martin, I. W. and Pindyck, R. S. (2015). Averting catastrophes: The strange economics of Scylla and Charybdis. *American Economic Review*, 105(10):2947–85.

Martin, I. W. R. (2008). Disasters and the welfare cost of uncertainty. *American Economic Review*, 98(2):74–78.

Masson-Delmotte, V., Zhai, P., Pirani, A., Connors, S. L., Péan, C., Berger, S., Caud, N., Chen, Y., Goldfarb, L., Gomis, M., et al. (2021). Climate change 2021: the physical science basis. *Contribution of working group I to the sixth assessment report of the intergovernmental panel on climate change*, 2.

Mathiesen, L. (1985). Computation of economic equilibria by a sequence of linear complementarity problems. In Manne, A. S., editor, *Economic Equilibrium: Model Formulation and Solution*, pages 144–162, Berlin, Heidelberg. Springer Berlin Heidelberg.

Mendelsohn, R., Emanuel, K., Chonabayashi, S., and Bakkensen, L. (2012). The impact of climate change on global tropical cyclone damage. *Nature climate change*, 2(3):205–209.

Mendelsohn, R., Nordhaus, W. D., and Shaw, D. (1994). The impact of global warming on agriculture: a Ricardian analysis. *The American economic review*, pages 753–771.

Mertens, K. and Ravn, M. O. (2011). Understanding the aggregate effects of anticipated and unanticipated tax policy shocks. *Review of Economic dynamics*, 14(1):27–54.

Mertens, K. and Ravn, M. O. (2012). Empirical evidence on the aggregate effects of anticipated and unanticipated us tax policy shocks. *American Economic Journal: Economic Policy*, 4(2):145–81.

Miftakhova, A. and Renoir, C. (2021). Economic growth and equity in anticipation of climate policy. *Economics Working Paper Series*, 21/355.

Mohan, P. S., Ouattara, B., and Strobl, E. (2018). Decomposing the macroeconomic effects of natural disasters: A national income accounting perspective. *Ecological Economics*, 146:1–9.

Mohler, L. and Müller, D. (2012). Substitution elasticities in Swiss manufacturing. *Report for the Swiss Federal Office of Energy (SFOE)*.

Morand, S. (2022). The role of agriculture in human infectious disease outbreaks. *CABI Reviews*.

Müller-Fürstenberger, G. and Schumacher, I. (2015). Insurance and climate-driven extreme events. *Journal of Economic Dynamics and Control*, 54:59–73.

Nachtigall, D. and Rübbelke, D. (2016). The green paradox and learning-by-doing in the renewable energy sector. *Resource and Energy Economics*, 43:74–92.

Narayanan, B., Aguiar, A., and McDougall, R. (2012). Global trade, assistance, and production: The GTAP 8 data base.

Narita, D., Tol, R. S., and Anthoff, D. (2009). Damage costs of climate change through intensification of tropical cyclone activities: an application of FUND. *Climate Research*, 39(2):87–97.

Nathani, C., Zandonella, R., van Nieuwkoop, R., Brandes, J., Schwehr, T., Killer, M., and Sutter, D. (2019). Energie-und verkehrsbezogene differenzierung der schweizerischen input-output-tabelle 2014. Technical report, Bundesamt für Energie. Bern.

Nemet, G. F., Jakob, M., Steckel, J. C., and Edenhofer, O. (2017). Addressing policy credibility problems for low-carbon investment. *Global Environmental Change*, 42:47–57.

Neumann, J. (1977). Great historical events that were significantly affected by the weather: 2, the year leading to the revolution of 1789 in france. *Bulletin of the American Meteorological Society*, 58(2):163–168.

Neumann, J. and Lindgrén, S. (1979). Great historical events that were significantly affected by the weather: 4, the great famines in finland and estonia, 1695–97. *Bulletin of the American Meteorological Society*, 60(7):775–787.

Nordhaus, W. D. (2010). The economics of hurricanes and implications of global warming. *Climate Change Economics*, 1(01):1–20.

Noy, I. (2009). The macroeconomic consequences of disasters. *Journal of Development economics*, 88(2):221–231.

Nunn, N. and Qian, N. (2010). The columbian exchange: A history of disease, food, and ideas. *Journal of Economic Perspectives*, 24(2):163–188.

Ohlendorf, N., Jakob, M., Minx, J. C., Schröder, C., and Steckel, J. C. (2021). Distributional impacts of carbon pricing: A meta-analysis. *Environmental and Resource Economics*, 78(1):1–42.

Okagawa, A. and Ban, K. (2008). Estimation of substitution elasticities for CGE models. *Discussion Papers in Economics and Business*, 16.

Okullo, S. J., Reynès, F., and Hofkes, M. W. (2020). (Bio-)Fuel mandating and the green paradox. *Energy Economics*, 72(1):105014.

Okuyama, Y., Hewings, G. J., and Sonis, M. (2004). Measuring economic impacts of disasters: interregional input-output analysis using sequential interindustry model. In *Modeling spatial and economic impacts of disasters*, pages 77–101. Springer.

Pachauri, R. K., Allen, M. R., Barros, V. R., Broome, J., Cramer, W., Christ, R., Church, J. A., Clarke, L., Dahe, Q., Dasgupta, P., et al. (2014). *Climate change 2014: synthesis report. Contribution of Working Groups I, II and III to the fifth assessment report of the Intergovernmental Panel on Climate Change*. Ipcc.

Paltsev, S. (2004). Moving from static to dynamic general equilibrium economic models. *MIT Joint Program on the Science and Policy of Global Change, Technical note No. 4*.

Paltsev, S., Reilly, J., Jacoby, H., Eckaus, R., McFarland, J., Sarofim, M., Asadoorian, M., and Babiker, M. (2005a). The mit emissions prediction and policy analysis (EPPA) model: Version 4. *Joint Program Report Series Report 125*.

Paltsev, S., Reilly, J. M., Jacoby, H. D., Eckaus, R. S., McFarland, J. R., Sarofim, M. C., Asadoorian, M. O., and Babiker, M. H. (2005b). The MIT emissions prediction and policy analysis (EPPA) model: version 4. Technical report, MIT Joint Program on the Science and Policy of Global Change.

Papageorgiou, C., Saam, M., and Schulte, P. (2017). Substitution between clean and dirty energy inputs: A macroeconomic perspective. *Review of Economics and Statistics*, 99(2):281–290.

Patterson, K. D. and Pyle, G. F. (1991). The geography and mortality of the 1918 influenza pandemic. *Bulletin of the History of Medicine*, 65(1):4–21.

Peretto, P. F. (2021). Through scarcity to prosperity: Toward a theory of sustainable growth. *Journal of Monetary Economics*, 117:243–257.

Pielke Jr., R. A. (2007). Future economic damage from tropical cyclones: sensitivities to societal and climate changes. *Philosophical Transactions of the Royal Society A: Mathematical, Physical and Engineering Sciences*, 365(1860):2717–2729.

Piketty, T. (2020). *Capital and ideology*. Harvard University Press.

Pörtner, H.-O., Roberts, D. C., Adams, H., Adler, C., Aldunce, P., Ali, E., Begum, R. A., Betts, R., Kerr, R. B., Biesbroek, R., et al. (2022). *Climate change 2022: Impacts, adaptation and vulnerability*. IPCC Geneva, Switzerland.

Potter, C. W. (2001). A history of influenza. *Journal of applied microbiology*, 91(4):572–579.

Pye, S., Broad, O., Bataille, C., Brockway, P., Daly, H. E., Freeman, R., Gambhir, A., Geden, O., Rogan, F., Sanghvi, S., Tomei, J., Vorushylo, I., and Watson, J. (2021). Modelling net-zero emissions energy systems requires a change in approach. *Climate Policy*, 21(2):222–231.

Rao, N. D., van Ruijven, B. J., Riahi, K., and Bosetti, V. (2017). Improving poverty and inequality modelling in climate research. *Nature Climate Change*, 7(12):857–862.

Rausch, S., Metcalf, G. E., and Reilly, J. M. (2011). Distributional impacts of carbon pricing: A general equilibrium approach with micro-data for households. *Energy Economics*, 33:S20–S33.

Reed, W. J. (1984). The effects of the risk of fire on the optimal rotation of a forest. *Journal of Environmental Economics and Management*, 11(2):180–190.

Reed, W. J. and Heras, H. E. (1992). The conservation and exploitation of vulnerable resources. *Bulletin of Mathematical Biology*, 54(2-3):185–207.

Riekhof, M.-C. and Bröcker, J. (2017). Does The Adverse Announcement Effect of Climate Policy Matter? — A Dynamic General Equilibrium Analysis. *Climate Change Economics*, 08(02):1750007.

Ripple, W. J., Estes, J. A., Beschta, R. L., Wilmers, C. C., Ritchie, E. G., Hebblewhite, M., Berger, J., Elmhagen, B., Letnic, M., Nelson, M. P., et al. (2014). Status and ecological effects of the world's largest carnivores. *Science*, 343(6167):1241484.

Romer, P. M. (1990). Endogenous technological change. *Journal of political Economy*, 98(5, Part 2):S71–S102.

Román, M. O., Wang, Z., Sun, Q., Kalb, V., Miller, S. D., Molthan, A., Schultz, L., Bell, J., Stokes, E. C., Pandey, B., Seto, K. C., Hall, D., Oda, T., Wolfe, R. E., Lin, G., Golpayegani, N., Devadiga, S., Davidson, C., Sarkar, S., Praderas, C., Schmaltz, J., Boller, R., Stevens, J., González, O. M. R., Padilla, E., Alonso, J., Detrés, Y., Armstrong, R., Miranda, I., Conte, Y., Marrero, N., MacManus, K., Esch, T., and Masuoka, E. J. (2018). Nasa's black marble nighttime lights product suite. *Remote Sensing of Environment*, 210:113 – 143.

Roush, S. W., Murphy, T. V., Group, V.-P. D. T. W., et al. (2007). Historical comparisons of morbidity and mortality for vaccine-preventable diseases in the united states. *Jama*, 298(18):2155–2163.

Rutherford, T. F. (1999a). Applied general equilibrium modeling with MPSGE as a GAMS subsystem: An overview of the modeling framework and syntax. *Computational economics*, 14(1-2):1–46.

Rutherford, T. F. (1999b). Applied general equilibrium modeling with mpsge as a gams subsystem: An overview of the modeling framework and syntax. *Computational Economics*, 14:1–46.

Ryan, S. J., Carlson, C. J., Tesla, B., Bonds, M. H., Ngonghala, C. N., Mordecai, E. A., Johnson, L. R., and Murdock, C. C. (2021). Warming temperatures could expose more than 1.3 billion new people to zika virus risk by 2050. *Global Change Biology*, 27(1):84–93.

Ryan, S. J., Lippi, C. A., and Zermoglio, F. (2020). Shifting transmission risk for malaria in africa with climate change: a framework for planning and intervention. *Malaria Journal*, 19:1–14.

Sauer, I. J., Reese, R., Otto, C., Geiger, T., Willner, S. N., Guillod, B. P., Bresch, D. N., and Frieler, K. (2021). Climate signals in river flood damages emerge under sound regional disaggregation. *Nature Communications*, 12(1):2128.

Schäfer, A. and Stünzi, A. (2019). The impact of green preferences on the relevance of history versus expectations. *Environment and Development Economics*, 24(6):583–607.

Sealy, K. S. and Strobl, E. (2017). A hurricane loss risk assessment of coastal properties in the caribbean: Evidence from the bahamas. *Ocean & coastal management*, 149:42–51.

Sen, A. (1982). *Poverty and famines: an essay on entitlement and deprivation*. Oxford university press.

Sen, S. and von Schickfus, M.-T. (2020). Climate policy, stranded assets, and investors' expectations. *Journal of Environmental Economics and Management*, 100(1):102277.

Sennewald, K. and Wälde, K. (2006). "Itô's Lemma" and the Bellman Equation for Poisson Processes: An Applied View. *Journal of Economics*, 89(1):1–36.

Sinn, H.-W. (2008). Public policies against global warming: a supply side approach. *International Tax and Public Finance*, 15(4):360–394.

Skidmore, M. and Toya, H. (2002). Do natural disasters promote long-run growth? *Economic inquiry*, 40(4):664–687.

Smulders, S., Tsur, Y., and Zemel, A. (2012). Announcing climate policy: Can a green paradox arise without scarcity? *Journal of Environmental Economics and Management*, 64(3):364–376.

Solomon, S., Qin, D., Manning, M., Averyt, K., and Marquis, M. (2007). *Climate change 2007-the physical science basis: Working group I contribution to the fourth assessment report of the IPCC*, volume 4. Cambridge university press.

Strobl, E. (2012). The economic growth impact of natural disasters in developing countries: Evidence from hurricane strikes in the central american and caribbean regions. *Journal of Development economics*, 97(1):130–141.

Strulik, H. and Trimborn, T. (2019). Natural disasters and macroeconomic performance. *Environmental and resource economics*, 72(4):1069–1098.

Tanoue, M., Hirabayashi, Y., and Ikeuchi, H. (2016). Global-scale river flood vulnerability in the last 50 years. *Scientific reports*, 6(1):1–9.

Taubenberger, J. K. and Morens, D. M. (2006). 1918 influenza: the mother of all pandemics. *Revista Biomedica*, 17(1):69–79.

Toya, H. and Skidmore, M. (2007). Economic development and the impacts of natural disasters. *Economics letters*, 94(1):20–25.

Tsur, Y. and Zemel, A. (1996). Accounting for global warming risks: Resource management under event uncertainty. *Journal of Economic Dynamics and Control*, 20(6-7):1289–1305.

Tsur, Y. and Zemel, A. (1998). Pollution control in an uncertain environment. *Journal of Economic Dynamics and Control*, 22(6):967–975.

Tsur, Y. and Zemel, A. (2008). Regulating environmental threats. *Environmental and Resource Economics*, 39(3):297–310.

Tsur, Y. and Zemel, A. (2009). Endogenous discounting and climate policy. *Environmental and Resource Economics*, 44(4):507.

Tsur, Y. and Zemel, A. (2017). Coping with multiple catastrophic threats. *Environmental and Resource Economics*, 68(1):175–196.

United Nations (2022). *The Sustainable Development Goals Report 2022*. The Sustainable Development Goals Report. United Nations Publications.

van der Meijden, G. and Smulders, S. (2017). Carbon lock-in: the role of expectations. *International Economic Review*, 58(4):1371–1415.

van der Ploeg, F. and de Zeeuw, A. (2018). Climate tipping and economic growth: Precautionary capital and the price of carbon. *Journal of the European Economic Association*, 16(5):1577–1617.

van der Ploeg, F. and Withagen, C. (2015). Global warming and the green paradox: A review of adverse effects of climate policies. *Review of Environmental Economics and Policy*, 9(2):285–303.

Van der Werf, E. (2008). Production functions for climate policy modeling: An empirical analysis. *Energy economics*, 30(6):2964–2979.

van der Wielen, W. (2020). The macroeconomic effects of tax changes: Evidence using real-time data for the european union. *Economic Modelling*, 90:302–321.

Van Long, N. (1975). Resource extraction under the uncertainty about possible nationalization. *Journal of Economic Theory*, 10(1):42–53.

van Wijhe, M., McDonald, S. A., de Melker, H. E., Postma, M. J., and Wallinga, J. (2016). Effect of vaccination programmes on mortality burden among children and young adults in the netherlands during the 20th century: a historical analysis. *The Lancet Infectious Diseases*, 16(5):592–598.

Vikash Ramiah, Belinda Martin, and Imad Moosa (2013). How does the stock market react to the announcement of green policies? *Journal of Banking and Finance*, 37:1747–1758.

Vöhringer, F., Müller, A., Böhringer, C., and Strubegger, M. (2007). Auswirkungen langfristig hoher ölpreise. Technical report, Bundesamt für Energie BFE.

Wälde, K. (2011). *Applied Intertemporal Optimization, Edition 1.1.* Mainz University Gutenberg Press, Available at www.waelde.com/aio.

Wang, Q., Hubacek, K., Feng, K., Wei, Y.-M., and Liang, Q.-M. (2016). Distributional effects of carbon taxation. *Applied Energy*, 184:1123–1131.

White, G. F. (1975). *Flood hazard in the United States : a research assessment.* Monograph - Program on Technology, Environment and Man, University of Colorado ; NSF-RA-E-75-006. Institute of Behavioral Science, University of Colorado, Boulder.

Williams III, R. C. (2011). Setting the initial time-profile of climate policy: The economics of environmental policy phase-ins. In *The design and implementation of US Climate Policy*, pages 245–254. University of Chicago Press.

Williams III, R. C. (2016). Environmental taxation. Technical report, National Bureau of Economic Research.

Winsemius, H. C., Aerts, J. C., Van Beek, L. P., Bierkens, M. F., Bouwman, A., Jongman, B., Kwadijk, J. C., Ligtvoet, W., Lucas, P. L., Van Vuuren, D. P., and Ward, P. J. (2016). Global drivers of future river flood risk. *Nature Climate Change*, 6(4):381–385.

World Bank (2018). Building the world bank's wealth accounts: Methods and data. Environment and Natural Resources Global Practice, World Bank.

Zhou, K., Zha, H., and Song, L. (2013). Learning triggering kernels for multi-dimensional Hawkes processes. In *International conference on machine learning*, pages 1301–1309. PMLR.